

Converging Chemical and Biological Sciences for a Sustainable Era

Edited by

Hari Shankar Biswas

Sandeep Poddar

Sheikh Ahmad Izaddin Sheikh Mohd Ghazali

Amiya Bhaumik

Published by :

Lincoln University College
Malaysia

www.lucp.net

Converging Chemical and Biological Sciences for a Sustainable Era

Dr. Hari Shankar Biswas

Department of Chemistry
Surendranath College, India

Dr. Sandeep Poddar

Deputy Vice Chancellor (Research & Innovation)
Lincoln University College, Malaysia

Dr. Sheikh Ahmad Izaddin Sheikh Mohd Ghazali

School of Chemistry and Environmental Sciences
Univcity Teknologi MARA, Malaysia

Dr. Amiya Bhaumik

Founder and President
Lincoln University College, Malaysia

Published by :

Lincoln University College, Malaysia

www.lucp.net

Copyright © 2025

Lincoln University College, Malaysia

All rights reserved

No part of this book can be reproduced or transmitted by any means, electronic or mechanical, including photocopying recording or by any information storage and retrieval system without prior written permission from the publisher.

Published on: 27th June, 2025

Published by:

Lincoln University College

Wisma Lincoln

No. 12-18, Off Jalan, Perbandaran SS 6/12

47301 Petaling Jaya

Selangor Darul Ehsan

Malaysia

Tel.: +603-7806 3478

Fax: +603-7806 3479

Toll Free: 1-300-880-111

E-mail: lucp@lincoln.edu.my

Web.: www.lucp.net

ISBN: 978-967-2819-48-6

eISBN: 978-967-2819-49-3

doi: 10.31674/book.2025ccbsse

Price: USD 100



Dato (Amb) Dr. Mohd Yusoff Bin A. Bakar

Vice Chancellor & CEO

Lincoln University College, Malaysia

Foreword

In an age where sustainability is no longer an option but a necessity, the convergence of chemical and biological sciences offers a powerful platform for transformative innovation. This book, *Converging Chemical and Biological Sciences for a Sustainable Era*, is a timely and vital contribution to the scientific literature that addresses one of the most pressing challenges of our time – how to reconcile human progress with environmental stewardship.

Bridging the molecular precision of chemistry with the dynamic complexity of biological systems, this interdisciplinary volume underscores the potential of integrated approaches to drive sustainable development. From green chemistry and bio-based materials to novel biotechnological applications and environmental remediation, the chapters herein explore cutting-edge research and practical strategies that illuminate the path forward.

The editors and contributors, drawn from diverse academic and research backgrounds, present a carefully curated selection of studies and perspectives that emphasise innovation, collaboration, and ecological responsibility. This work not only advances academic understanding but also serves as an inspiration for policymakers, educators, and industry leaders committed to shaping a more sustainable future.

As we stand at the intersection of scientific discovery and global necessity, this book exemplifies the collaborative spirit required to build resilient, science-driven solutions for the world ahead. I commend the authors for their vision and dedication in producing this important work.

Dato (Amb) Dr. Mohd Yusoff Bin A. Bakar

Vice Chancellor & CEO

Lincoln University College, Malaysia

Contents	Pages
Preface	i-iii
Micellar Effects on the Chromium (VI) Oxidation on Various Substrates: Exploring Different Kinetic Models in Micellar System <i>Monirul Islam, Debraj Roy</i>	1-18
Blue Flower Extract: An Antioxidant-Rich Beverage, Mediated Bio-Synthesis of Metal, Metal Oxide Nanoparticles for Anti-Bacterial and Anti-Cancer Applications <i>Amit Kumar Dutta</i>	19-33
Metal-Free and Sustainable Strategies in the Synthesis of Substituted Furans: A Contemporary Review <i>Harisadhan Ghosh, Anupam Jana</i>	34-52
Clerodendrum: A Useful Beneficial Phytomedicinal Plant <i>Dora Das, Sirshendu Chatterjee, Shamba Chatterjee, Sucheta Das</i>	53-59
Investigating Materials for Green Hydrogen Generation with Potential and Challenges in Biological Hydrogen Production <i>Aniruddha Mondal, Prasenjit Mandal, Amit Kumar Kundu, Shib Shankar Biswas</i>	60-81
Dynamics of Micelle-Vesicle Interconversion: Mechanisms and Modulation <i>Shrabani Sen</i>	82-87
Breast Milk: A Free Radical Scavenger and Role of Mother's Diet <i>Pritha Mondal</i>	88-98
Study of Synthesis, Crystal Structure, Magnetic Properties, EPR, Cyclic Voltammetric Analysis and Zigzag Chain Coordination of Polymer Prepared through Copper Catalysed Hemiacetal Synthesis <i>Piu Dhal</i>	99-107
KOtBu Promoted Transformation of Nitriles to Amides <i>Ganesh Chandra Midya</i>	108-127
Association of Insect Fauna with the Flowers of the Zea mays (Sweet corn variety AKSH4) in Southern Part of West Bengal <i>Biswanath Bhowmik</i>	128-137
Multireference Perturbation Based Quantum Chemical Investigation on Isomerization Alley of Diphosphorous Compounds <i>Suvonil Sinha Ray</i>	138-145
Non-Adiabatic Escape Rate of a Quantum Dissipative System from a Rapidly Oscillating Periodic Potential <i>Anindita Shit</i>	146-164
Exploring the Catalytic Potential of Ionanofluids in Green Chemistry <i>Prasenjit Mandal, Aniruddha Mondal, Shib Shankar Biswas, Amit Kumar Kundu</i>	165-188
A Review on the Spectroscopic Studies of the Binding Interactions between Serum Albumins and Quercetin <i>Sugata Samanta</i>	189-194
From Fossil Fuels to Blue-Green Energy: A New Era for Sustainability <i>Suchandra Chatterjee</i>	195-210
Mnemonic of Carbohydrates Structure with Proper Stereochemistry <i>Sisir Debnath</i>	211-216
A Brief Review on Recent Developments in C(Sp²)-H and C(Sp³)-H Activation Protocols through Cobalt-catalysis <i>Rupankar Paira</i>	217-231

Preface

In an era defined by complex global challenges, the need for innovative and integrated solutions has never been more persistent. This book entitled “Converging Chemical and Biological Sciences for a Sustainable Era”, delves into the critical intersection of chemistry and biology, showcasing interdisciplinary fusion is essential in addressing the multifaceted sustainability issues confronting our planet. From pioneering green technologies to advancements in environmental protection and healthcare, the book explores the transformative power of scientific integration in fostering a truly sustainable future.

The first article explores the kinetic behavior of Chromium (VI) oxidation in the presence of micellar systems, offering a detailed comparative analysis of various kinetic models. It emphasises the role of micelles in modulating redox reactions, which has implications for environmental chemistry and biochemical applications. By examining substrate-specific responses and surfactant interactions, the study contributes valuable insights into micellar catalysis and the mechanisms underpinning electron transfer in heterogeneous systems.

The article by Amit Kumar Dutta presents an innovative approach to the green synthesis of metal and metal oxide nanoparticles using blue flower extract, a beverage rich in antioxidants. Highlighting its significant antibacterial and anticancer potential, the study demonstrates eco-friendly routes to nanoparticle development. The work offers valuable insight into sustainable nanotechnology and opens new avenues for biomedical and therapeutic applications rooted in plant-based green chemistry.

Metal-Free and Sustainable Strategies in the Synthesis of Substituted Furans by Harisadhan Ghosh and Anupam Jana, offers a comprehensive review of recent eco-friendly synthetic methodologies. Emphasizing green chemistry principles, this work highlights metal-free catalytic, multicomponent, and cycloaddition approaches. The study serves as a vital resource for researchers pursuing sustainable solutions in organic synthesis and showcases the growing relevance of environmentally benign pathways in chemical science.

Sucheta Das's *Clerodendrum – One Useful Beneficial Phytomedicinal Plant* offers a comprehensive review of the therapeutic potential of various *Clerodendrum* species. Highlighting their traditional uses, phytochemical composition, and diverse pharmacological effects, this work underscores the genus's significance in ethnomedicine and modern drug discovery. It serves as a valuable resource for researchers in herbal medicine, pharmacology, and botanical sciences.

Anirudha Mondal *et al.* in their article explore innovative materials for green hydrogen generation, focusing on the potential and challenges in biological hydrogen production. The study examines key biomaterials, catalytic systems, and environmental considerations critical to advancing sustainable hydrogen technologies. This research offers valuable insights for scientists and engineers working toward eco-friendly energy solutions and contributes to the growing discourse on renewable and bio-based hydrogen production.

Another article by Shrabani Sen investigates the dynamic transition between micelles and vesicles in surfactant systems, emphasizing the role of pH oscillators. Using a two-state model and numerical simulations, the study explores the rhythmic interconversion of self-assembled structures. The research offers valuable insights into the mechanisms governing surfactant phase behavior and contributes to advancements in drug delivery and nanostructure design.

Pritha Mondal in her article explores the antioxidant properties of breast milk and the critical role of maternal diet in enhancing its protective function. Highlighting key enzymes like CAT, SOD, and GPx, the study emphasises how nutrients, trace elements, and lifestyle factors influence infant development. The work underscores the importance of tailored maternal nutrition during lactation for optimal oxidative stress defence in newborns.

The article by Piu Dhal presents a detailed investigation into the synthesis, structure, and magnetic properties of a 1D polymeric copper complex. Employing copper-catalysed hemiacetal synthesis, the study explores zigzag chain coordination and antiferromagnetic interactions through alkoxo and thiocyanato bridges. Combining spectroscopic,

electrochemical, and magnetic analyses, the work contributes significantly to the field of coordination chemistry and offers insights into designing novel metal-organic frameworks.

This article by Ganesh Chandra Midya explores the KOTBu-promoted transformation of nitriles into amides, offering a mild, efficient, and environmentally friendly synthetic approach. The study highlights the mechanistic aspects and broad substrate applicability of this base-mediated conversion. Contributing to the development of sustainable organic synthesis, this work provides valuable insight for researchers in synthetic chemistry seeking greener and more versatile methods for functional group transformations.

The study by Biswanath Bhowmik shows the association of insect fauna with the flowers of *Zea mays* (sweet corn variety AKSH4) in southern West Bengal. Highlighting both diurnal and nocturnal pollinators, the work insect-plant interactions, particularly in relation to environmental factors like temperature and humidity. As a pioneering effort in the Indian context, this research offers essential baseline data on insect-mediated pollination in maize and underscores its ecological and agricultural importance.

The article, *Multireference Perturbation Based Quantum Chemical Investigation on Isomerisation Alley of Diphosphorous Compounds* by Suvonil Sinha Ray, presents an in-depth study using IVO-SSMRPT methodology to explore isomerisation pathways in P=P bonded systems. Emphasizing computational efficiency and accuracy, the research bridges theoretical chemistry with practical insight into molecular behavior. It offers significant contributions to multireference electronic structure theory and is a valuable resource for researchers in quantum chemistry and phosphorus-based molecular systems.

The article *Non-Adiabatic Escape Rate of a Quantum Dissipative System from a Rapidly Oscillating Periodic Potential* explores quantum tunnelling phenomena in non-equilibrium conditions. Focusing on the non-adiabatic escape dynamics, it examines the periodic potentials and dissipation influence particle transitions. This study adds valuable theoretical insights to quantum mechanics, particularly in the fields of quantum transport, condensed matter physics, and the modelling of dynamic quantum systems under time-dependent perturbations.

The article, *Exploring the Catalytic Potential of Ionanofluids in Green Chemistry*, presents a comprehensive evaluation of ionanofluids as efficient and sustainable catalysts. Highlighting their unique physicochemical properties and environmentally friendly nature, the study emphasises their applications in promoting greener chemical processes. This work contributes significantly to the advancement of eco-conscious catalysis, aligning with global efforts toward cleaner production technologies and sustainable chemical innovation.

The article by Sugata Samanta provides a comprehensive review of the spectroscopic studies on the binding interactions between serum albumins and quercetin. Highlighting fluorescence quenching, energy transfer, and time-resolved emission techniques, the study reveals critical insights into protein-flavonoid interactions. The work contributes significantly to understanding the therapeutic potential of quercetin and its molecular association with serum albumins in biomedical and pharmaceutical contexts.

The book chapter, "From Fossil Fuels to Blue-Green Energy: A New Era for Sustainability", delves into the transformative shift from traditional fossil fuels to sustainable energy solutions like green hydrogen and blue ammonia. Through comprehensive analysis, it explores their production, advancements, and environmental benefits. Addressing the technological, economic, and policy challenges, this work provides valuable insights into how these energy carriers can drive the global transition toward a cleaner, more sustainable energy future.

This article authored by Sisir Debnath presents a simple and effective mnemonic technique to help students quickly and accurately recall the stereochemistry of D-aldohehexoses and aldopentoses. Designed to reduce the complexity and memorization burden, this method enables learners to draw Fischer projections with ease, enhancing long-term retention and interest in carbohydrate chemistry.

Rupankar Paira explores emerging advances in cobalt-catalysed C–H activation protocols, focusing on both C(Sp²)–H and C(Sp³)–H bonds in his article. The study highlights cobalt's growing significance as a cost-effective and sustainable alternative to noble metals, offering valuable insights into synthetic methodologies, functionalisation strategies, and enantioselective transformations in modern organic chemistry.

The diverse articles compiled in *Converging Chemical and Biological Sciences for a Sustainable Era* collectively underscore the immense power of interdisciplinary collaboration in tackling the complex challenges of our time. Each article highlights innovative solutions linking chemistry and biology. This volume serves as a powerful testament to the transformative potential of combining chemical and biological insights, offering valuable resources for researchers, practitioners, and students committed to building a sustainable era. Ultimately, *Converging Chemical and Biological Sciences for a Sustainable Era* it is a testament to the power of collaborative science. We hope this book inspires interdisciplinary approaches, fostering a new generation of solutions that will pave the way for a healthier planet and a more sustainable tomorrow.

Hari Shankar Biswas
Sandeep Poddar
Sheikh Ahmad Izaddin Sheikh Mohd Ghazali
Amiya Bhaumik

Micellar Effects on the Chromium (VI) Oxidation on Various Substrates: Exploring Different Kinetic Models in Micellar System

Monirul Islam^{1*}, Debraj Roy^{2*}

¹Seth Anandram Jaipuria College, Kolkata, West Bengal 700005, India

²Sripat Singh College, Jiaganj, Murshidabad, West Bengal 742123, India

*Corresponding Author's E-mail: roydebraj29@gmail.com, michem989@gmail.com

Abstract

Chromium(VI), a potent and mighty oxidising agent, undergoes reduction to chromium(III) through various redox reactions. This process is significantly influenced by the choice of students and experimental parameters and often involves intermediate oxidation states such as Cr(V) and Cr(IV). The redox behaviour of Cr(VI) is highly relevant due to its carcinogenic and mutagenic activities, as well as its interaction with biologically active molecules during reduction. Cr(VI) typically exists as CrO_4^{2-} at neutral pH and can invade the cells, leading to toxicity associated with the intermediate state during the reduction to Cr(III). Electron transfer reactions in organised assemblies like micelles vesicles, and polyelectrolytes have been extensively studied, highlighting the role of hydrophobic and electrostatic interactions in reaction kinetics. Micellar systems, which emulate cellular membranes, provide insights into electron transfer mechanisms in heterogeneous environments. These systems are crucial for understanding biochemical processes, including drug-membrane interactions and photochemical energy storage. In pharmaceutical applications, micelles enhance drug bioavailability, prevent degradation and enable targeted delivery to regions with leaky blood vessels, highlighting their importance in therapeutic and biomedical research.

Keywords: Chromate Toxicity; Electron Transfer Kinetics; Micelles; Vesicular Structure

Introduction

Chromium(VI) as a powerful oxidising agent serves in various redox reactions, during which it is reduced to Cr(III). The Cr(VI) is reduced to Cr(III) significantly depending on the type of reductant used and the choice of specific experimental parameters (Codd *et al*, 2001; Das, 2004; Mahanti & Banerji, 2002; Mitewa & Bontchev, 1985). Sometimes Cr(V) and Cr(IV) are determined and explained as intermediates within many reactions. Understanding these subtle variations, the researchers have thoroughly studied Cr(VI) in the context of redox kinetics. Cr(VI) appeared as a hazardous one because of its carcinogenic and mutagenic activity (Arslan, Beltrame & Tomasi, 1987; Costa, 1997; De Flora, 2000; Katz, Ballantyne & Salem, 2005.; Rossi & Wetterhahn, 1989). The kinetics and mechanism of Cr(VI) oxidation are biologically relevant as a reducing agent, making them relevant for the biochemists and inorganic chemists (Codd *et al*, 2001; Das, 2004). In its intermediate oxidation states, chromium, i.e., $\text{Cr(VI)} \rightarrow \text{Cr(III)}$, could potentially engage with bioactive compounds and lead

Micellar Effects on Chromium (VI) Oxidation Kinetics

to harmful effects. Considering chromate toxicity, it's reasonable to suggest that reducing agents significantly influence and modulate its various effects Codd *et al* (2001). At neutral pH, via non-specific anion carriers, Cr(VI) predominantly exists as CrO_4^{2-} . It can enter inside the cells (Arslan, Beltrame & Tomasi, 1987), where it gains an electron to Cr(III), producing various states of transition in chromium during the $\text{Cr(VI)} \rightarrow \text{Cr(III)}$ electron acceptance process. The intermediates of DNA bases are very often kinetically labile (Köster & Beyersmann, 1985), which can induce chromate toxicity.

The organised structures or assemblies influence electron transfer rate, and reactions have been explored by different research workers (Bhalekar & Engberts, 1978; Cavasino, 1985). The influence of structured gatherings on the reaction rate is thought to arise as a consequence of their interactions (Bhalekar & Engberts, 1978; Cavasino, 1985) from hydrophobic and electrostatic forces of interactions, which attribute reactants within the system. Many redox reactions in the biochemical model, which involve the transfer of electrons, take place in systems that contain both a water-based (aqueous) part and a fat-like (lipophilic) part. Studies have documented occurrences of electron transfer processes (Bhalekar & Engberts, 1978; Cavasino, 1985) at polyelectrolytes, cell vesicles, and micellar surfaces. In a simulated system, the micelle-based structures are considered to emulate the cellular membranes. These studies help us to comprehend the electron transfer mechanism in a partially mixed, small-scale, heterogeneous environment. Kinetic equilibria on electron transfer reactions in micellar systems are very crucial (Minero *et al*, 1983) for understanding various events; phenothiazine derivatives exhibit diverse therapeutic activities, including antitumor, antibacterial, and antioxidant effects. They interact with cellular surface membranes, altering lipid composition and tri-layered membrane integrity, which can disrupt cancer cell functions. Additionally, compounds with photo-redox properties are utilised in photochemical energy storage systems, often within micellar structures, enhancing their efficiency and stability. Micelles have potent utility in pharmacy and act as a tool for numerous applications (Rangel-Yagui *et al*, 2005), like in drug delivery, drug degradation and loss, and preventing harmful side effects by solubilising the poorly soluble drugs to enhance their bioavailability. Micelles can house in the bloodstream for a long period of time, allowing them up slowly and sequentially in the target area. The size also enables them to gather in regions with leaky blood vessels.

Attributions of Micelles in Aqueous Solutions

Surfactants possess diphilic moieties, with the head region constituted from a hydrophilic or polar moiety and the tail region from a hydrophobic component. Surfactant head can be charged, anionic or cationic, dipolar (zwitter ionic) or charge-less (non-ionic). Ionic surfactants are represented as RX , where "R" denotes a hydrocarbon chain consisting of 8 to 18 carbon atoms. This "R" group may be part of an alkyl or aromatic radical, or it could be another form of hydrophobic structure (Hait & Moulik, 2002; Im *et al*, 2003). Therefore, the moiety, that is, ionic X taking both anionic and cationic parts. The surfactants are cation-active and anion-active, contingent upon the nature of Charge on "X", and hydrophilic anion-active surfactants have phosphate, sulphonate, carboxylate or sulphate groups. For example, $(\text{CH}_3)(\text{CH}_2)_n\text{SO}_3^-\text{M}^+$, $(\text{CH}_3)(\text{CH}_2)_n\text{SO}_3^-\text{M}^+$, $(\text{CH}_3)(\text{CH}_2)_n\text{CO}_2^-\text{M}^+$ (where, $\text{M}^+ = \text{Li}^+$,

Na^+ , K^+ , and MMe^{4+} etc. Here, $n = 8-18$ carbon chain number) and many more are listed. One can relay that the best example is sodium dodecyl sulphate (SDS) $\text{C}_{12}\text{H}_{25}\text{OSO}_3\text{Na}^+$ in all experimental cases, whereas for the surfactants that are cation active parts, attract water (hydrophilic moiety), made up either of a quaternary ammonium, pyridinium, or phosphonium group (Montalvo & Khan, 2002). Few lists are provided herewith: $(\text{CH}_3)(\text{CH}_2)_n\text{N}(\text{CH}_3)_3\text{B}^-$, $(\text{CH}_3)(\text{CH}_2)_n\text{N}(\text{CH}_3)_3\text{B}^-$, $(\text{CH}_3)(\text{CH}_2)_n\text{N}(\text{C}_2\text{H}_5)_3\text{B}^-$, etc. (Here, $\text{B}^- = \text{Cl}^-$, Br^- , OH^- , etc.; and $n = 8-18$). Various studies support the best example of cetyltrimethylammonium bromide (CTAB), $\text{C}_{16}\text{H}_{33}\text{N}^+\text{Me}_3\text{Br}^-$; cetylpyridinium chloride (CPC) $\text{C}_{16}\text{H}_{33}\text{N}^+(\text{C}_5\text{H}_5)\text{Cl}^-$ for their best activity and less chemical jargon (Im *et al*, 2003). Non-ionic surfactants can often be represented as RX, where the component X, which is electrically neutral, typically signifies a polyoxyethylene group (Dwars, Paetzold & Oehme, 2005).

When any surfactants act as solutes, taken into solution, the solute particles naturally aggregate on their own, forming thermodynamically stable particles that fall within the colloidal size range. At lower concentrations, the surfactant acts like an ordinary solute; when the concentration reaches a certain threshold, they come together, with an aggregation number, denoted as N , ranging from twenty to a hundred depending on the conditions, to create micelles (Figure 1). Micelles are like cellular membranes, and the minimum concentration that starts micellisation is called the critical micelle concentration (CMC). Aggregation of surfactant molecules occurs among the hydrocarbon chains due to their hydrophobic interaction. The enlargement of micelles and the separation of surfactants into a micro-phase depend on factors like hydrophilic group hydration, electrostatic repulsion for ionic reactants, steric hindrance, and entropy losses, which prevent the formation of a micellar pseudo-phase.

The transformation between micelles and surfactant molecules that occurs quickly and can easily reverse itself takes place within milliseconds. As long as the surfactant concentration drops below the CMC, the resultant micelles can be broken down to a basic surfactant solution by simple dilution.

At a given temperature, all surfactants have a definite CMC. The value of CMC depends on the length of the hydrocarbon chains. For the shorter hydrocarbon chain, higher is its CMC value due to a small decrease in free energy during the micellisation process. Any CMC value of a particular surfactant depends on the chemical composition of the solution in which micellisation is carried out. For the ionic surfactants, the factors that minimise the electrostatic repulsion among the hydrophilic moieties favour micellisation. An increase in the concentration of counterions lowers the CMC value. Essentially, more counterions make micelle formation easier, so it requires a low surfactant concentration. Counterions reduce the electrostatic repulsion among the head groups, thereby stabilising a micelle formation. The higher alcohols, which can reduce the surface charge density, diminish the CMC of ionic surfactants. Micellisation of non-ionic surfactants is promoted by the increase in the temperature, as it reduces the hydration of their hydrophilic groups. Micellisation occurs within a specific concentration range near the critical CMC, where solution properties like viscosity, electrical conductivity, surface tension, light scattering, etc. change significantly. Micelles can take various shapes, like spheres or rods, but they all share a common

Micellar Effects on Chromium (VI) Oxidation Kinetics

structure: their hydrophobic hydrocarbon ends cluster inside, while their hydrophilic ends extend outward, interacting with the surrounding solvent.

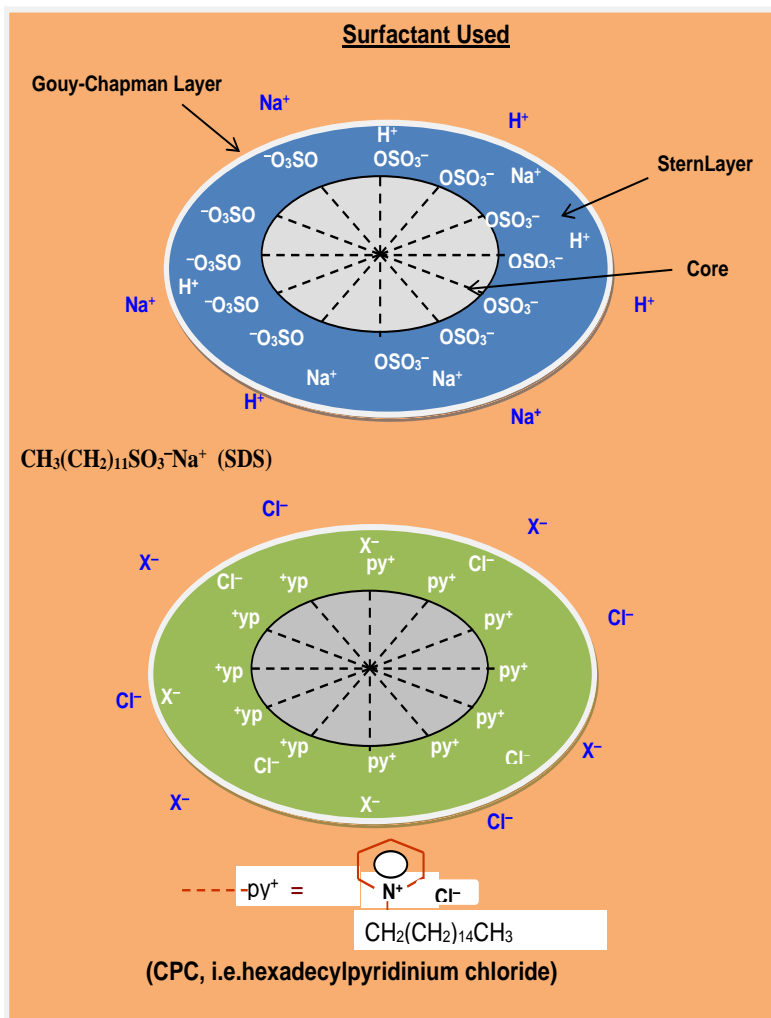


Figure 1: Schematic Representation of the Micellar System Involving Cationic Surfactant CPC and Anionic Surfactant SDS (Source: Author)

The Stern layer contains the ionic head groups of surfactants, neutralising 60-70 per cent of the micellar charge along with some gegenions. The leftover counterions from a diffuse (Bhalekar & Engberts, 1978; Cavasino, 1985) layer balance the remaining charge. Counterions that attach to neutralise the micellar head group charge, creating electrical double layers. The micelles create electrical double layers that influence the stability, particularly in colloidal and interfacial systems.

Dwars, Paetzold and Oehme (2005) have explained the amphiphile aggregates' shape and formation in water that balance the two forces in opposite directions: the hydrophobic

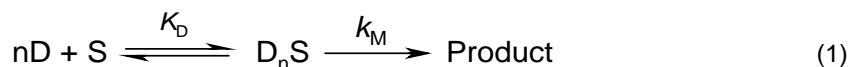
Converging Chemical and Biological Sciences for a Sustainable Era

attraction between the alkyl chains and the polar repulsion of head groups. The alkyl chain attraction is mainly driven by entropy. Over an extensive span of temperatures, the Gibbs energy (free energy) associated with the formation process displays negligible fluctuation, reflecting a sharp and precise equilibrium between enthalpic and entropic contributions. Aggregates of amphiphilic molecules, such as micelles, have the capability to assemble within solvents exhibiting polar characteristics and hydrogen-bonding tendencies akin to those of water.

Different Kinetic Models of Micellar Effect

(A) Cooperative Model

Surfactants influence the reaction rates, and such reactions are very much similar to the models of enzyme-catalysed interactions. Piskiewicz (1977) used a mechanistic model, very nearly a similar Hill model, to explain how micelles influence bimolecular reactions. Micelles, which are aggregates formed by surfactants, can alter reaction rates by creating unique microenvironments. This model helps explain the cooperative behaviour observed in such systems. to explain the micellar effect on bimolecular reactions. In Scheme 1, the model proposes that S (Substrate) and D (Detergent) molecules combine to form active micelles (D_nS).



Scheme 1

The dissociation constant, K_D expresses the equilibrium between the micelle and its free components. The above scheme helps to explain the expression for the observed rate constant (k_{obs}).

$$k_{obs} = (k_M[D]^n + k_W K_D) / (K_D + [D]^n) \quad (3)$$

$$\text{or, } \log(k_{obs} - k_W) / (k_M - k_{obs}) = \log(G) = n \log[D] - \log K_D \quad (4)$$

$$[\text{Where } G = (k_{obs} - k_W) / (k_M - k_{obs})]$$

The constants, K_D , n (measure of cooperativity), and $\log[D]_{50} = (\log K_D) / n$ (= The logarithmic value of the detergent concentration required to achieve half of the maximum velocity) are determined graphically. For analysing the data, k_W refers to the observed rate constants without detergents, while k_M proposed the rate constant if the detergent is present. The analysis mainly focused on the detergent concentration range, showing an initial sigmoid relevance of k_{obs} (the observed constant of the rate) on the detergent concentration. It didn't account for higher detergent concentrations where k_{obs} tends to decrease in bimolecular reactions due to the reactants getting diluted in the micellar phase. The Piskiewicz model is advantageous because it does not rely on knowing the CMC of the detergent, which can be difficult to determine under experimental conditions. The value of n typically ranges from 1 to 3, which is much smaller than the aggregation number of micelles, usually between 20

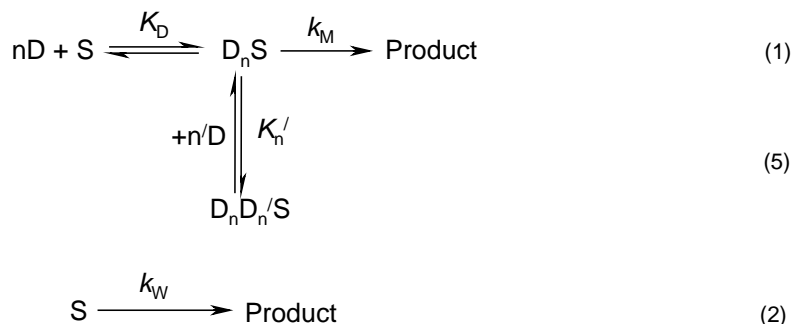
Micellar Effects on Chromium (VI) Oxidation Kinetics

and 100. Low values of n suggest that catalytically active micelles begin to form even at low concentrations, in the permicellar range. The non-integral nature of n implies that multiple equilibria might be involved in the formation of these active premicelles. From analogy with the enzyme-catalysed reactions, a value of $n > 1$ indicates positive cooperativity.

Piszkiewicz model (Matos & Gehlen, 2004) has been extended to explain: In bimolecular reactions, detergents can act as catalysts, speeding up the reaction by helping the reactants interact more effectively. However, when the concentration of detergent becomes very high, it starts to interfere with the reaction instead of helping it. This is called the “rate retarding effect”. Essentially, the detergent molecules crowd the system, making it harder for the reactants to collide and react.

In Scheme 2, n' gives the additional number of detergent molecules which are associated with the catalytically active micelle (D_nS) to form the completely inactive species ($D_nD_{n'}S$); $K_{n'}$ is the corresponding binding constant.

The proposed model is outlined below (Scheme 2).



Scheme 2

The k_2 is the second-order rate constant of a bimolecular reaction: obtained from the above scheme, it is as follows:

$$k_2 = (k_M[D]^n + k_W K_D) / (K_D + [D]^n + K_{n'}[D]^n[D]^{n'}) \quad (6)$$

At low concentration of detergent, Eqn. 6 reduces to Eqn. 3, while at higher concentration of detergent, Eqn. 6 reduces to:

$$k_2 = k_M / (1 + K_{n'}[D]^{n'}) \quad (7)$$

$$\text{or, } \log[(k_M/k_2) - 1] = \log K_{n'} + n' \log [D] \quad (8)$$

(B) Ion Exchange Model (Pseudo-phase):

The model called as pseudo-phase ion exchange (PIE) (Bunton *et al*, 1991; Das *et al*, 2001a), surface of the micelles is assumed to be the selectively saturated counter ions exchangers. If the reactant is a species with a +2 charge (such as R^{2+}), then when sodium dodecyl sulphate (SDS) micelles are present, both the R^{2+} ions and Na^+ ions will exhibit behaviour influenced by the micellar environment.



Scheme 3

The observed pseudo-first-order rate constant (k_ψ) is given by:

$$k_\psi = (k_W + k_M K_{ex} / YF) / (1 + K_{ex} / YF) \quad (11)$$

The pseudo-phase ion exchange equilibrium constant (K_{ex}) is given by:

$$K_{ex} = [R_M^{2+}] YF / [R_W^{2+}] \quad (12)$$

$$\text{Where, } Y = ([Na_W^+] / [Na_M^+])^2 \quad (13)$$

$$F = \gamma_W^2(Na^+) / \gamma_W(R^{2+}) \quad (14)$$

For the micellar pseudo-phase, the ratio of activity denoted as $\gamma_W^2(Na^+) / \gamma_M(R^{2+})$, reasonably be regarded as constant and equal to one. The activity coefficient factor, F, is determined using the Davies equation (Davies & Waing, 1950), considering the total micellar surface charge to be compensated by the bound ions, *i.e.*, Na^+ and R^{2+} , the binding parameter (β refers to the proportion of the micellar surface charge that is balanced by the ions attached to it) is given by:

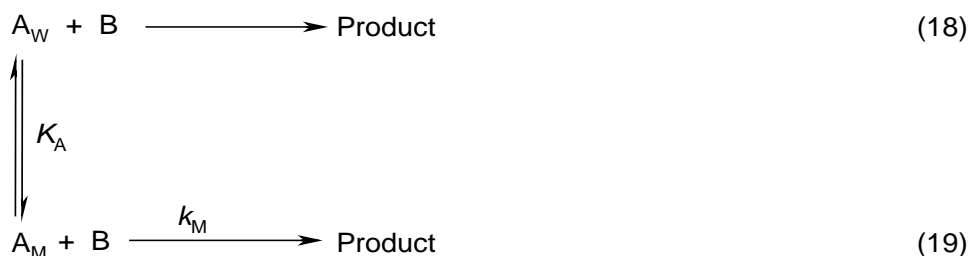
$$\beta = ([Na_M^+] / [D_n]) + (2[R_M^{2+}] / [D_n]) = m_{Na} + 2m_R \quad (15)$$

$$\text{Where } [D_n] = [SDS]_T - CMC \quad (16)$$

$$Y = [(\beta - 2m_R)[D_n] / \{[Na^+]_T - (\beta - 2m_R)[D_n]\}]^2 \quad (17)$$

(C) Menger-Portnoy Model

The Menger-Portnoy model (Menger & Portnoy, 1967) focuses on the distribution of a single reactant, such as A, between the micellar phase and an aqueous phase (as depicted in Scheme 4).



Scheme 4

Scheme 4 derived the following rate law;

$$k = \frac{k_M K_A C + k_W}{1 + K_A C} \quad (20)$$

Here, K_A represents the binding constant for the micellized surfactant. k_m and k_w are the first-order rate constants in the micellar and aqueous phases, respectively, incorporating the concentration of reactant 'B' in these pseudo-phases. C denotes the concentration of the micelle.

(D) Berezin's Model

Berezin model (Berezin, Martinek & Yatsimirskii, 1973) suggests the system consists of two phases: one for the aqueous and the other for the micellar pseudo-phase at the above CMC. The quantitative rate equation for a bimolecular reaction involving the reactants A and B is as follows:

$$\text{rate} = k_M[A]_M[B]_M CV + k_M'[A]_M[B]_W CV + k_M''[A]_W[B]_M CV + k_W[A]_W[B]_W(1 - CV) \quad (21)$$

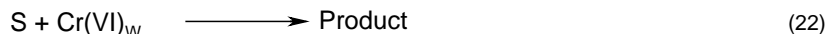
Here, $C = [D]_T - \text{CMC}$; where $[D]_T$ represents the total surfactant concentration (molarity), some authors have defined $C = ([D]_T - \text{CMC})/N$ where N gives the aggregation number. V is the partial molar volume of the surfactant in the micelle ($\approx 0.3 \text{ mol dm}^{-3}$) (Berezin, Martinek & Yatsimirskii, 1973); CV and $(1 - CV)$ represent the fractions by volume of micellar phase and aqueous phase, respectively; the subscripts M and W stand for the quantities relating to the micellar phase and aqueous phase, respectively; k_M and k_W are the rate constants for the reaction occurring in the micellar phase and the aqueous phase respectively; k_M' stands for the rate constant of the reaction due to the encounter between the reactant A in the micellar phase and the reactant B in the aqueous phase; k_M'' refers to the exactly reverse situation.

Effects of Surfactants on the Kinetic Studies of Substrates by Hexavalent Chromium

Oxidation of malonic acid by Cr(VI), when exposed to the anionic surfactant SDS, the rate of the reaction is retarded. The slowing down of the reaction rate has been attributed to the partitioning behaviour of Cr(VI) species and the acid concentration across the aqueous and micellar phases. Findings suggest that the reaction takes place in the aqueous phase, where the H^+ concentration is significantly diminished.

To analyse the binding of one reactant (i.e. H_2CrO_4) to the micelle, the kinetic data has been interpreted using Berezin model (Berezin, Martinek & Yatsimirskii, 1973) (as depicted in Scheme 5).

The suggested reaction steps are shown in Scheme 5 is as follows:



Scheme 5

In the above Scheme Cr(VI) is H_2CrO_4 and 'S' is the organic substrate present at the interface. This rate law is given by

$$k_\psi = (k_W + k_M K_{Cr} C) / (1 + K_{Cr} C) \quad (24)$$

The plot of $1/k_\psi$ vs C gives that $k_W \gg k_M K_{Cr} C$. Using Menger-Portnoy model (Menger & Portnoy, 1967), a proposed type of conclusion could be drawn. It is noted that the affinity of binding constant value of Cr(VI) is increased for the upscale value increase of H^+ concentrations. The Cr(VI) oxidation of cyclohexanol (Acharjee *et al*, 2019) in water acidic media was found to be catalysed by SDS.

The rate enhancement phenomenon likely arises from the solubilisation of both the oxidant and substrate within the micellar phase of both the oxidant and substrate within the micellar phase, where the reaction predominantly occurs. The catalytic effect can be attributed to the increased solubilisation of the protonated Cr(VI)-cyclohexanol complex, positively charged micellar pseudo-phase through electrostatic attraction.

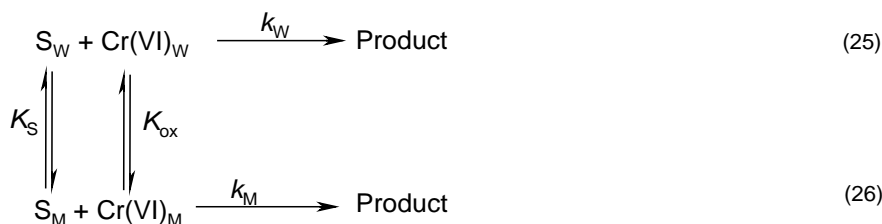
The kinetic data has been interpreted using Berezin's phase separation model, which is relevant when both reactants- H_3CrO_4^+ (consider kinetically active) and cyclohexanol- are strongly associated with the micellar phase. Graphical methods were used to estimate binding and rate constants. High binding constants and partition coefficients suggest that the substrate and oxidant bind to the micelle through hydrophobic and electrostatic interactions. However, the existence of H_3CrO_4^+ as a species is debatable.

In a water acid media kinetic analysis for Cr(VI) oxidation on lactic acid (Saha, Islam & Das, 2006) and dl-mandelic acid are performed by Sahu and Panigrahi (1996) with an anionic surfactant of Sodium dodecyl sulphate (SDS).

At CMC, oxidation rate is increased with the increase of surfactant concentration and decreased if further surfactant concentration is increased. The experimental findings indicate that the Menger-Portnoy model (Menger & Portnoy, 1967) fails to provide an adequate explanation.

Instead, by taking into account the distribution of the reactants- namely the organic substrates and H_2CrO_4 , which are considered kinetically active-between the bulk aqueous phase and the micellar pseudo-phase, the kinetic data has been interpreted using Berezin's model. The proposed reaction mechanism is outlined below.

Micellar Effects on Chromium (VI) Oxidation Kinetics



Scheme 6

In Scheme 6, the organic substrate 'S' represents lactic acid or *dl*-mandelic acid respectively and the active species H_2CrO_4 is represented by Cr(VI) . According to Berezin's approach, the rate equation is given by

$$k_\psi = (k_W + k_M K_S K_{\text{Ox}} C) / \{(1 + K_S C)(1 + K_{\text{Ox}} C)\} \quad (27)$$

The symbols maintain their conventional meanings. Various rates and binding constants can be determined using Equation 27. The observed reduction in the rate at high concentrations has been analysed for compatibility with Piskiewicz model (Piskiewicz, 1977), which is linked to Hill model commonly used in enzyme catalysis studies.

The anionic surfactant, sodium dodecyl sulphate (SDS), is progressive for Cr(VI) oxidation on dialkyl sulphides (Ganesan, Rajagopal & Bharathy, 2000), while the cationic surfactant, cetyltrimethylammonium chloride (CTAC), slows down the rate of activity. This type of finding is explained by considering the fact that the reaction occurs in water as well as in the micellar phase simultaneously. The enhancement of reaction rate of sodium dodecyl sulphate (SDS) occurs through enhanced concentration of the local reactants in the micellar phase. In an acid-catalysed reaction H^+ ions are preferred to concentrate around the anionic micellar phase. The cationic surfactant, CTAC, slowly reacts because the approach of H^+ ions on the cationic micellar surface (both the reactants are concentrated) is unfavoured. The oxidation of an organic sulphide is because the electron transfer from sulphide to Cr(VI) to buildup positive charge on sulphur is not favoured for interaction with the cationic micellar top edge groups. The picolinic acid and bipyridine catalysed Cr(VI) oxidation of dimethyl sulfoxide have been found to be accelerated by sodium dodecyl sulphate (SDS, an anionic surfactant), and the rate is retarded by *N*-cetylpyridinium chloride (CPC, cationic surfactant). A similar micellar effect has been found in the Cr(VI) oxidation of formic acid (Das, 1999) in the presence of picolinic acid catalyst. In the presence of surfactant the rate retardation has been explained by considering the applicability of Piskiewicz model (Piskiewicz, 1977). The rate of Cr(VI) oxidation of cyclopentanol (Sahu & Panigrahi, 1996) with sodium dodecyl sulphate (SDS) is found to be decreased monotonically with increasing SDS concentration after the CMC. This observation is explained correctly with the Menger-Portnoy model (Menger & Portnoy, 1967) and its modified form (Bunton & Robinson, 1969), which considers solubilisation of one reactant only into the micellar phase. This modified Menger-Portnoy equation, which neglects the k_M -path (reaction in the micellar phase), is:

$$1/k_\psi = 1/k_W + KC/k_W \quad (28)$$

Here, K is a binding constant of the species that is partitioned between the two phases, that is, aqueous and micellar. This is identified as H_3CrO_4^+ . By using Berezin's equation (the k_M is not considered, and the relationship with other micellar phases is considered) for the determination of the binding constant, it nicely agreed with that obtained from Eqn. 28. The k_ψ decreases exponentially with increasing K_2SO_4 concentration. The presence of K^+ and SO_4^{2-} ions around the Stern layer may result in an increase of surface potential of the micelle, which in turn facilitates the preferential accumulation of the active chromium species (*i.e.* H_3CrO_4^+) in the micellar pseudo phase. The rate of retardation with increase of K_2SO_4 concentration is due to depletion of the active chromium species. However, the existence of the species, H_3CrO_4^+ is questioned.

Scientists have studied how a chemical called sodium dodecyl sulphate (SDS), which forms tiny structures called micelles, affects the speed of a reaction where Cr(VI) is involved in breaking down different alcohols. They found that for alcohols that dissolve in water (like butan-1-ol, propan-2-ol, benzyl alcohol), the reaction speed increases as $[\text{SDS}]_T$ is added but only up to certain point-after that, adding more SDS slows it down. This happens because of a balance between charged particles (ions) in the reaction and how they interact with the SDS micelles. Rodenas and Perez-Benito (1991) conducted a study on alcohols that do not mix well with water, and for the same alcohols, such as hexan-1-ol and octan-1-ol, the pattern may differ. These reactions need an acidic environment to work. Additionally, other studies have looked at how different types of surfactants (Chemicals that help liquids mix) affect the same kind of reactions with various compounds like sugars, acids, and alcohols. They observed that a negatively charged surfactant like SDS speeds up the reaction, while a positively charged surfactant, such as *N*-cetylpyridinium chloride (CPC), slows it down. Adding certain helpers (chelating agents) can also speed up these reactions.

The reactions are acid catalysed. Recently, the effects of both anionic (*i.e.* sodium dodecyl sulphate, SDS) and cationic (*i.e.* *N*-cetylpyridinium chloride, CPC) surfactants have been studied for the Cr(VI) oxidation of different substrates, *e.g.* hexitols (Saha *et al*, 2004), diols (Das *et al*, 2001b), D-glucose (Bayen *et al*, 2005), D-fructose (Das, Roy & Saha, 2001; Islam, Saha & Das, 2005), L-sorbose (Islam & Das, 2008b; Saha *et al*, 2004), maleic acid (Islam, Saha & Das, 2007), *dl*-mandelic acid (Islam & Das, 2008a), *etc.*, in aqueous acid media in absence and presence of different chelating agents like 2,2'-bipyridyl (bipy), 1,10-phenanthroline (phen) and picolinic acid (PA). It has been observed that the cationic surfactant *N*-cetylpyridinium chloride (CPC) retards the reaction rate, while the anionic surfactant sodium dodecyl sulphate (SDS) accelerates the reaction rate.

Rodenas and Perez-Benito (1991) have investigated that anionic surfactant sodium dodecyl sulphate (SDS) reverse micelles in hexan-1-ol, octan-1-ol or butan-1-ol on the oxidation of corresponding alcohol by Cr(VI) in water-perchloric acid medium. To explain the experimental findings, it was required to consider the intermicellar exchange of the reactants. The interaction is influenced by the thickness of the layer containing the surfactant and alcohol, which was determined using fluorescence quenching techniques.

Kabir-ud-Din, Iqbal and Khan (2005) and Kabir-ud-Din, Morshed and Khan (2002) have studied the micellar effects on the Cr(VI) oxidation of sugars. They observed that the

Micellar Effects on Chromium (VI) Oxidation Kinetics

increase in concentration of anionic surfactants, sodium dodecyl sulphate (SDS), and non-ionic surfactant, octylphenoxypolyethoxy ethanol (TX-100), the oxidation rate increases. Rate enhancement in SDS micelles is decreased in the presence of Li^+ , Na^+ , NH_4^+ ions. Rate inhibition due to the presence of those ions can be explained by electrostatic considerations.

Effect of ionic micelles that propel the oxidation of citric acid by chromium(VI) continued with some workers (Hartani & Khan, 2000). They have proposed a one-step, three-electron oxidation mechanism. The rate decreases with the increase in concentration of the cationic surfactants cetyl trimethylammonium bromide (CTAB) and cetyl pyridinium bromide (CPB), while the anionic surfactant, sodium dodecyl sulphate (SDS) has no effect on the rate. The activation parameters (ΔH^\ddagger , ΔS^\ddagger) are significantly affected in the presence of CTAB or CPB.

Interpretation for the effects of surfactants on the kinetic studies of some organic substrates by hexavalent chromium.

It has been observed that different natures of graphs for the kinetic studies of some organic substrates by hexavalent chromium in the presence of surfactants. These works have already been published in a reputed journal (Islam, Saha & Das, 2005). Some of these research works have been presented here for interpretation of the effects of surfactants on the kinetic studies.

(A) Interpretation cationic surfactant (N-cetylpyridinium chloride) CPC concentration variation over organic substrates-a kinetic study:

The compound N-cetylpyridinium chloride exhibits inhibitory effects on the catalysed pathways. Observations of k_{obs} plotted against $[\text{CPC}]_{\text{T}}$ (Figure 2) reveal a progressive decline, eventually plateauing at higher concentrations of CPC. This behaviour mirrors findings reported by Bunton and Cerichelli (1980) and documents similar effects during the electron release of ferrocene by ferric salts in the presence of the cationic surfactant cetyl trimethyl ammonium bromide (CTAB).

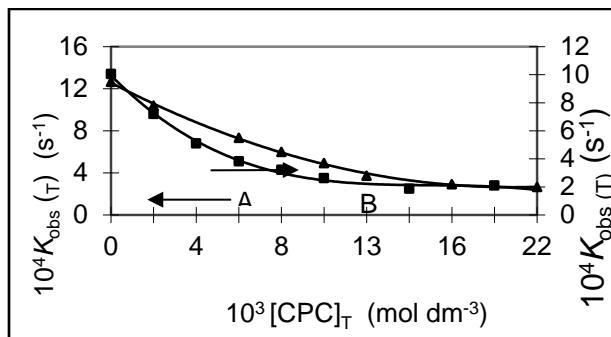
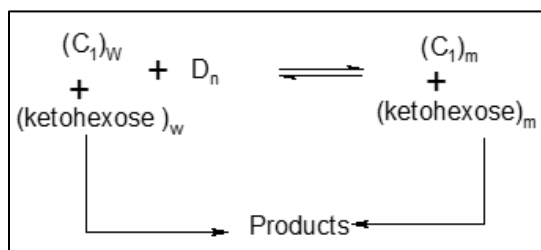


Figure 2: Effect of $[\text{CPC}]_{\text{T}}$ on $k_{\text{obs}}(\text{T})$ for the Cr(VI) oxidation of D-fructose in the presence of bipy and phen in aqueous H_2SO_4 media (Islam, Saha & Das, 2005)

Experimental conditions:- $[\text{Cr(VI)}]_{\text{T}} = 4 \times 10^{-4} \text{ mol dm}^{-3}$, $[\text{H}_2\text{SO}_4] = 0.5 \text{ mol dm}^{-3}$. (A) : $[\text{phen}]_{\text{T}} = 50 \times 10^{-4} \text{ mol dm}^{-3}$, $[\text{D-fructose}]_{\text{T}} = 140 \times 10^{-4} \text{ mol dm}^{-3}$, $T = 40^\circ\text{C}$. (B) : $[\text{bipy}]_{\text{T}} = 120 \times 10^{-4} \text{ mol dm}^{-3}$, $[\text{D-fructose}]_{\text{T}} = 60 \times 10^{-4} \text{ mol dm}^{-3}$, $T = 50^\circ\text{C}$.

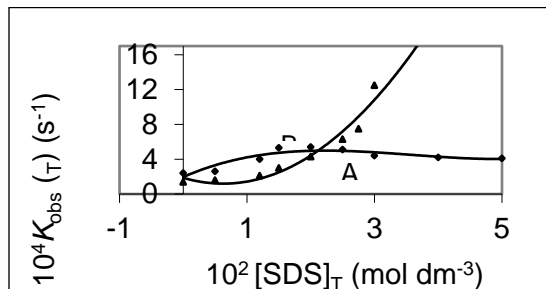
The findings align with the observations made by Sahu and Panigrahi (1996) regarding the oxidation of acetophenone by Ce(IV) in the presence of *N*-dodecyl pyridinium chloride (NDPC). In this process, cetylpyridinium chloride (CPC) limits the activity of the positively charged Cr(VI) catalyst complex, the active oxidising agent, in the water phase.

Consequently, the neutral substrate accumulated in the micellar phase (specifically, the Stern layer) does not contribute to the reaction. Therefore, the catalysed reaction is predominantly confined to the aqueous phase, where the substrate concentration diminishes due to its portioning into the Stern layer of the micelle. The portioning behaviour of the reactants between the aqueous phase and the micellar phase is illustrated in Scheme 7, where D_n signifies micellises surfactants, with 'n' denoting the aggregation number.



Scheme 7: Partitioning of the Reactive Species between the Aqueous and Micellar Phases

(B) Interpretation for the concentration variation of anionic surfactant, Sodium dodecyl sulfate (SDS) for the kinetic studies of organic substrates:



Source: Islam, Saha & Das, 2005

Figure 3: Effect of $[\text{SDS}]_{\text{T}}$ on $k_{\text{obs}(T)}$ for the Cr(VI) oxidation of D-fructose in the presence of bipy and phen in aqueous H_2SO_4 media

Experimental conditions:- $[\text{Cr(VI)}]_{\text{T}} = 4 \times 10^{-4} \text{ mol dm}^{-3}$, $[\text{H}_2\text{SO}_4] = 0.25 \text{ mol dm}^{-3}$, $T = 35^\circ\text{C}$. (A) : $[\text{D-fructose}]_{\text{T}} = 50 \times 10^{-4} \text{ mol dm}^{-3}$, $[\text{phen}]_{\text{T}} = 40 \times 10^{-4} \text{ mol dm}^{-3}$. (B): $[\text{D-fructose}]_{\text{T}} = 60 \times 10^{-4} \text{ mol dm}^{-3}$, $[\text{bipy}]_{\text{T}} = 40 \times 10^{-4} \text{ mol dm}^{-3}$.

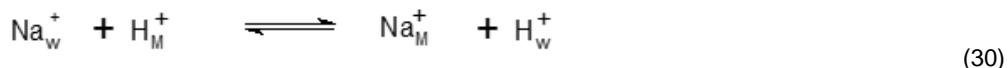
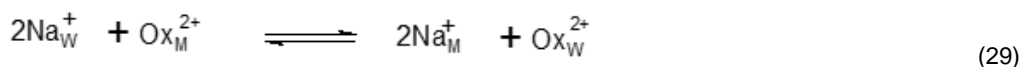
Sodium dodecyl sulphate (SDS) enhances the catalysed pathway by facilitating interactions between reactants and oxidants. The Cr(VI)-catalyst complex, a cationic species, is

Micellar Effects on Chromium (VI) Oxidation Kinetics

considered the active oxidant, preferentially distributed in the micellar pseudo-phase of SDS due to electrostatic attraction. The presence of SDS starts a reaction for both micellar pseudo-phases for an increase of reactants, and the water phase promotes the rate of the observed reaction.

The plot of k_{obs} versus $[SDS]_T$ (c.f. Figs. 3) indicates continuous rate improvement for bipy-catalysed reactions with increasing SDS concentration. For phen-catalysed reactions, the rate initially rises with higher $[SDS]_T$, then reaches a limit followed by slight retardation. Rate acceleration is driven by preferential portioning of positively charged oxidants and neutral substrates into the Stern layer of micelles.

Conversely, at very high $[SDS]_T$ levels, rate retardation occurs due to reactant dilution within the micellar phase. Increased SDS concentration also raises micellar counterion (e.g., Na^+) levels, which could displace H^+ and Ox^{2+} ions from the micellar surface, affecting the reaction dynamics.



The equilibria mentioned causes a reduction in the concentrations of $[HM]^+$ and $[OxM]^{2+}$, which in turn slows the reaction rate. These opposing effects influence the reaction rate in different ways. For the phen-catalysed pathway, the two effects essentially cancel each other out at higher surfactant concentrations, leading to rate saturation. However, in the bpy-catalyzed pathway, the solubilisation effect (first effect) dominates over the counterion effect (second effect) up to the maximum SDS concentration used.

Conclusion

The redox behaviour of chromium(VI) and its reduction to chromium(III), along with intermediate states, emphasises its biological significance and environmental impact. Understanding these reactions and their toxicological effects is essential for advancing safety measures and biochemical applications.

Furthermore, micellar systems and organised assemblies provide a valuable platform for studying electron transfer and reaction kinetics in heterogeneous environments. Their ability to emulate cellular membranes has profound implications for pharmaceutical science, enhancing drug delivery, bioavailability, and targeted therapy. Together, these fields underscore the importance of interdisciplinary research in chemistry, biology, and medical science to address pressing challenges and develop innovative solutions.

Acknowledgement

The cooperation of Dr. Debabrata Singha, a research scholar in the Chemistry Department at Visva-Bharati University, Santiniketan, West Bengal, India, is thankfully acknowledged.

References

- Acharjee, A., Rakshit, A., Chowdhury, S., Malik, S., Barman, M. K., Ali, M. A., & Saha, B. (2019). Micellar catalysed and heteroaromatic base promoted rate enhancement of oxidation of an alicyclic alcohol in aqueous medium. *Journal of Molecular Liquids*, 277, 360–371. <https://doi.org/10.1016/j.molliq.2018.12.082>
- Arslan, P., Beltrame, M., & Tomasi, A. (1987). Intracellular chromium reduction. *Biochimica et Biophysica Acta (BBA) - Molecular Cell Research*, 931(1), 10–15. [https://doi.org/10.1016/0167-4889\(87\)90044-9](https://doi.org/10.1016/0167-4889(87)90044-9)
- Bayen, R., Islam, M., Saha, B., & Das, A. K. (2005). Oxidation of d-glucose in the presence of 2,2'-bipyridine by CrVI in aqueous micellar media: a kinetic study. *Carbohydrate Research*, 340(13), 2163–2170. <https://doi.org/10.1016/j.carres.2005.07.002>
- Berezin, I. V., Martinek, K., & Yatsimirskii, A. K. (1973). Physicochemical foundations of micellar catalysis. *Russian Chemical Reviews*, 42(10), 787. <https://doi.org/10.1070/RC1973v042n10ABEH002744>
- Bhalekar, A. A., & Engberts, J. B. F. N. (1978). Electron transfer reactions of transition metal aminocarboxylates in the presence of micelle-forming surfactants. Catalysis by cetyltrimethylammonium bromide of the reduction of Mn(cydt)- by Co(edta)2- and Co(cydt)2-. *Journal of the American Chemical Society*, 100(18), 5914–5920. <https://doi.org/10.1021/ja00486a051>
- Bunton, C. A., & Cerichelli, G. (1980). Micellar effects upon electron transfer from ferrocenes. *International Journal of Chemical Kinetics*, 12(8), 519–533. <https://doi.org/10.1002/kin.550120803>
- Bunton, C. A., & Robinson, L. B. (1969). Micellar effects upon the reaction of P-nitrophenyl diphenyl phosphate with hydroxide and fluoride ions. *The Journal of Organic Chemistry*, 34(4), 773–780. <https://doi.org/10.1021/jo01256a002>
- Bunton, C. A., Nome, F., Quina, F. H., & Romsted, L. S. (1991). Ion binding and reactivity at charged aqueous interfaces. *Accounts of Chemical Research*, 24(12), 357–364. <https://doi.org/10.1021/ar00012a001>
- Cavasino, F. P. (1985). Equilibrium and kinetic studies of the electron-transfer reactions involving ferrocene and cobalt(III) complexes in micellar solutions. *The Journal of Physical Chemistry*, 89(16), 3578–3582. <https://doi.org/10.1021/j100262a031>
- Codd, R., Dillon, C. T., Levina, A., & Lay, P. A. (2001). Studies on the genotoxicity of chromium: from the test tube to the cell. *Coordination Chemistry Reviews*, 216, 537–582. [https://doi.org/10.1016/S0010-8545\(00\)00408-2](https://doi.org/10.1016/S0010-8545(00)00408-2)
- Costa, M. (1997). Toxicity and Carcinogenicity of Cr(VI) in Animal Models and Humans. *Critical Reviews in Toxicology*, 27(5), 431–442. <https://doi.org/10.3109/10408449709078442>
- Das, A. K., Roy, A., & Saha, B. (2001). Kinetics and mechanism of the picolinic acid catalysed chromium (VI) oxidation of ethane-1, 2-diol in the presence and absence of surfactants. *Transition Metal Chemistry*, 26(6), 630–637. <https://doi.org/10.1023/A:1012058409538>
- Das, A. K. (1999). Kinetics and mechanism of the chromium (VI) oxidation of formic acid in the presence of picolinic acid and in the presence and absence of surfactants. *BioInorganic Reaction Mechanisms*, 1(2), 161–168. <https://doi.org/10.1515/irm-1999-0210>

Micellar Effects on Chromium (VI) Oxidation Kinetics

- Das, A. K. (2004). Micellar effect on the kinetics and mechanism of chromium(VI) oxidation of organic substrates. *Coordination Chemistry Reviews*, 248(1–2), 81–99. <https://doi.org/10.1016/j.cct.2003.10.012>
- Das, A. K., Mondal, S. K., Kar, D., & Das, M. (2001a). Micellar effect on the reaction of picolinic acid catalyzed chromium (VI) oxidation of dimethyl sulfoxide in aqueous acidic media: a kinetic study. *International Journal of Chemical Kinetics*, 33(3), 173–181. [https://doi.org/10.1002/1097-4601\(200103\)33:3%3C173::AID-KIN1011%3E3.0.CO;2-I](https://doi.org/10.1002/1097-4601(200103)33:3%3C173::AID-KIN1011%3E3.0.CO;2-I)
- Das, A. K., Roy, A., Saha, B., Mohanty, R. K., & Das, M. (2001b). Micellar effect on the reaction of chromium(VI) oxidation of α -fructose in the presence and absence of picolinic acid in aqueous media: a kinetic study. *Journal of Physical Organic Chemistry*, 14(6), 333–342. <https://doi.org/10.1002/poc.374>
- Davies, C. W., & Waite, G. M. (1950). 65. The extent of dissociation of salts in water. Part XII. Calcium salts of some amino-acids and dipeptides. *Journal of the Chemical Society (Resumed)*, 301. <https://doi.org/10.1039/jr9500000301>
- De Flora, S. (2000). Threshold mechanisms and site specificity in chromium(VI) carcinogenesis. *Carcinogenesis*, 21(4), 533–541. <https://doi.org/10.1093/carcin/21.4.533>
- Dwars, T., Paetzold, E., & Oehme, G. (2005). Reactions in Micellar Systems. *Angewandte Chemie International Edition*, 44(44), 7174–7199. <https://doi.org/10.1002/anie.200501365>
- Ganesan, T. K., Rajagopal, S., & Bharathy, J. B. (2000). Comparative Study of Chromium(V) and Chromium(VI) Oxidation of Dialkyl Sulfides. *Tetrahedron*, 56(32), 5885–5892. [https://doi.org/10.1016/S0040-4020\(00\)00431-2](https://doi.org/10.1016/S0040-4020(00)00431-2)
- Hait, S. K., & Moulik, S. P. (2002). Interfacial Composition and Thermodynamics of Formation of Water/Isopropyl Myristate Water-in-Oil Microemulsions Stabilized by Butan-1-ol and Surfactants Like Cetyl Pyridinium Chloride, Cetyl Trimethyl Ammonium Bromide, and Sodium Dodecyl Sulfate. *Langmuir*, 18(18), 6736–6744. <https://doi.org/10.1021/la011504t>
- Hartani, K., & Khan, Z. (2000). Unusual rate inhibition of manganese (II) assisted oxidation of citric acid by chromium (VI) in the presence of ionic micelles. *Transition Metal Chemistry*, 25, 478–484. <https://doi.org/10.1023/A:1007010306107>
- Im, J.-Y., Kim, D.-B., Lee, S. H., & Lee, Y.-S. (2003). Porous Vesicles Dispersible in Organic Solvents. *Langmuir*, 19(16), 6392–6396. <https://doi.org/10.1021/la034189e>
- Islam, M., & Das, A. K. (2008a). Picolinic Acid Assisted Three-Electron Transfer Chromic Acid Oxidation of dl -Mandelic Acid in Aqueous Micellar Media: A Kinetic Study. *Progress in Reaction Kinetics and Mechanism*, 33(3), 219–240. <https://doi.org/10.3184/146867808X339296>
- Islam, M., & Das, A. K. (2008b). Heteroaromatic N-base ligands in 1,10-phenanthroline- and 2,2'-bipyridyl-assisted chromic acid oxidation of (–)-l-sorbose in aqueous micellar acid media: a kinetic study. *Carbohydrate Research*, 343(13), 2308–2314. <https://doi.org/10.1016/j.carres.2008.05.017>
- Islam, M., Saha, B., & Das, A. K. (2005). Kinetics and mechanism of 2,2'-bipyridyl and 1,10-phenanthroline-catalysed chromium(VI) oxidation of d-fructose in aqueous micellar media. *Journal of Molecular Catalysis A: Chemical*, 236(1–2), 260–266. <https://doi.org/10.1016/j.molcata.2005.04.019>

- Islam, M., Saha, B., & Das, A. K. (2007). Kinetics and mechanism of picolinic acid promoted chromic acid oxidation of maleic acid in aqueous micellar media. *Journal of Molecular Catalysis A: Chemical*, 266(1–2), 21–30. <https://doi.org/10.1016/j.molcata.2006.10.042>
- Kabir-ud-Din, Iqbal, S. M. S., & Khan, Z. (2005). Effect of ionic and non-ionic surfactants on the reduction of water soluble colloidal MnO₂ by glycolic acid. *Colloid and Polymer Science*, 284(3), 276–283. <https://doi.org/10.1007/s00396-005-1373-7>
- Kabir-ud-Din, Morshed, A. M. A., & Khan, Z. (2002). Influence of sodium dodecyl sulfate/TritonX-100 micelles on the oxidation of d-fructose by chromic acid in presence of HClO₄. *Carbohydrate Research*, 337(17), 1573–1583. [https://doi.org/10.1016/S0008-6215\(02\)00167-2](https://doi.org/10.1016/S0008-6215(02)00167-2)
- Katz, S.A.; Ballantyne, B.; Salem, H. (2005). The inhalation toxicity of chromium compounds. In *Inhalation Toxicity*, 2nd ed.; Salem, H., Katz, S.A., Eds.; CRC Press: Boca Raton, FL, USA, 2006; pp. 543–564.
- Köster, A., & Beyersmann, D. (1985). Chromium binding by calf thymus nuclei and effects on chromatin. *Toxicological & Environmental Chemistry*, 10(4), 307–313. <https://doi.org/10.1080/02772248509360968>
- Mahanti, M. K., & Banerji, K. K. (2002). Synthetic and mechanistic aspects of reactions of complexed chromium (VI) compounds. *Journal of the Indian Chemical Society*, 79(1), 31–44. <https://doi.org/10.5281/zenodo.5840096>
- Matos, M. S., & Gehlen, M. H. (2004). Charge transfer complexes of 9-vinyl-carbazole with π acceptors in homogeneous and in micellar solutions. *Spectrochimica Acta Part A: Molecular and Biomolecular Spectroscopy*, 60(7), 1421–1426. <https://doi.org/10.1016/j.saa.2003.08.006>
- Menger, F. M., & Portnoy, C. E. (1967). Chemistry of reactions proceeding inside molecular aggregates. *Journal of the American Chemical Society*, 89(18), 4698–4703. <https://doi.org/10.1021/ja00994a023>
- Minero, C., Pramauro, E., Pelizzetti, E., & Meisel, D. (1983). One-electron transfer equilibria and kinetics of N-methylphenothiazine in micellar systems. *The Journal of Physical Chemistry*, 87(3), 399–407. <https://doi.org/10.1021/j100226a009>
- Mitewa, M., & Bontchev, P. R. (1985). Chromium(V) coordination chemistry. *Coordination Chemistry Reviews*, 61, 241–272. [https://doi.org/10.1016/0010-8545\(85\)80006-0](https://doi.org/10.1016/0010-8545(85)80006-0)
- Montalvo, G., & Khan, A. (2002). Self-Assembly of Mixed Ionic and Zwitterionic Amphiphiles: Associative and Dissociative Interactions between Lamellar Phases. *Langmuir*, 18(22), 8330–8339. <https://doi.org/10.1021/la0204489>
- Piszkiwicz, D. (1977). Cooperativity in bimolecular micelle-catalyzed reactions. Inhibition of catalysis by high concentrations of detergent. *Journal of the American Chemical Society*, 99(23), 7695–7697. <https://doi.org/10.1021/ja00465a046>
- Rangel-Yagui, C. de O., Pessoa, A., & Tavares, L. C. (2005). Micellar solubilization of drugs. *Journal of Pharmacy and Pharmaceutical Sciences*, 8(2), 147–163. Retrieved from: [https://sites.ualberta.ca/~csps/JPPS8\(2\)/C.Rangel-Yagui/solubilization.pdf](https://sites.ualberta.ca/~csps/JPPS8(2)/C.Rangel-Yagui/solubilization.pdf), Accessed on 5th January 2025.
- Rodenas, E., & Perez-Benito, E. (1991). Chromium(VI) oxidation of alkanol components of sodium

Micellar Effects on Chromium (VI) Oxidation Kinetics

- dodecyl sulfate reverse micelles. *The Journal of Physical Chemistry*, 95(23), 9496–9500. <https://doi.org/10.1021/j100176a084>
- Rossi, S. C., & Wetterhahn, K. E. (1989). Chromium(V) is produced upon reduction of chromate by mitochondrial electron transport chain complexes. *Carcinogenesis*, 10(5), 913–920. <https://doi.org/10.1093/carcin/10.5.913>
- Saha, B., Das, M., Mohanty, R. K., & Das, A. K. (2004). Micellar Effect on the Reaction of Chromium(VI) Oxidation of L-Sorbose in the Presence and Absence of Picolinic Acid in Aqueous Acid Media: A Kinetic Study. *Journal of the Chinese Chemical Society*, 51(2), 399–408. <https://doi.org/10.1002/jccs.200400062>
- Saha, B., Islam, M., & Das, A. K. (2006). Micellar Effects on the Reactions of Chromium(VI) Oxidation of Lactic Acid and Malic Acid in the Presence and Absence of Picolinic Acid in Aqueous Acid Media. *Bioinorganic Reaction Mechanisms*, 6(2), 141–149. <https://doi.org/10.1515/IRM.2006.6.2.141>
- Sahu, S. K., & Panigrahi, G. P. (1996). Micellar catalysis-Effect of sodium lauryl sulphate in the oxidation of cyclopentanol by chromic acid. *Journal-Indian Chemical Society*, 73, 576–579. Retrieved from: https://hero.epa.gov/hero/index.cfm/reference/details/reference_id/1578254. Accessed on 5th January 2025.

Blue Flower Extract: An Antioxidant-Rich Beverage, Mediated Bio-Synthesis of Metal, Metal Oxide Nanoparticles for Anti-Bacterial and Anti-Cancer Applications

Amit Kumar Dutta

Department of Chemistry, Bangabasi Morning College, Kolkata 700009, West Bengal, India

Corresponding Author's E-mail: amitkumardutta@bangabasimorning.edu.in

Abstract

This research emphasises the development of nanomedicine for cancer treatment through the exploration of the antibacterial and anticancer activities of different metallic nanoparticles (NPs) [Ag(0), Au(0) NPs] and metal oxides such as CuO, Fe₂O₃, ZnO, and NiO NPs. Through the green biosynthesis process, these NPs have been synthesised using an antioxidant-rich beverage, blue tea [blue flower, *Clitoria Ternatea* (CT), extract]. The surface functionalization with the high level of polyphenolic compounds, anthocyanin, catechin, etc., present in the blue flower extract, which resists the body from free-radical damage, has been confirmed through FTIR (Fourier Transform Infrared Spectroscopy) and EDX (Energy Dispersive X-ray Spectroscopy) analysis, which can enhance their stability and impart bio-compatibility, anti-bacterial, anti-microbial and anti-cancer activity. The antioxidant activities of both bare blue flower extract and CT-incorporated nanomaterials have been investigated using radical inhibition through the 2,2-diphenyl-1-picrylhydrazyl (DPPH) free-radical scavenging assay, and the corresponding antioxidant abilities have been compared using median inhibition concentration (IC₅₀) parameters. Furthermore, the anti-bacterial activity of the synthesised nanomaterials against various pathogenic organisms (gram-positive and gram-negative bacterial strains) has been evaluated by determining the Minimum Inhibitory Concentration (MIC) and Minimum Bactericidal Concentration (MBC). Finally, dose-dependent cytotoxicity analysis and anti-cancer activity in both in vitro and in vivo settings have established the anti-proliferative properties of the NPs against different cancer cell lines. In this chapter, it has been elaborated on how the antioxidant-incorporated nanomaterials can be used as potential antioxidants, antibacterials, and anticancer agents for commercial applications.

Keywords: *Anti-Cancer; Anti-Microbial; Apoptosis; Bio-Synthesis; Carcinogenesis; Clitoria-Ternatea; DPPH Free Radical; Nano-Materials*

Introduction

Blue butterfly-pea flower extract, commonly known as Blue-Tea, becomes a very popular beverage nowadays for daily intake. It is a caffeine-free herbal tea made from flower petals or whole flower extracts of *Clitoria ternatea* (butterfly-pea) plant and is high in antioxidants that resist the body from free-radical damage. *Clitoria ternatea*, also known as 'Aparajita' in Indian Ayurveda, and various parts of this plant, i.e., roots, leaves, flowers, seeds, etc., are

Blue Flower Extract: Antioxidants and Nanoparticles for Health Applications

important herbs in the Ayurvedic system with great medicinal values. These flower plants are mainly grown automatically in the tropical belt of India, Sri Lanka, Malaysia, Burma, and the Philippine Islands (Lakshan *et al.*, 2019). It has already been used since very old days as traditional ayurvedic-medicine as a memory enhancer, nootropic, anti-stress, anxiolytic, anti-depressant, anti-convulsant, tranquilizing and sedative agent for several neurological disorders. Such types of medicinal plants generally possess a wide range of chemical constituents (bio-active phytochemicals) such as flavonoids, polyphenols, terpenoids, alkaloids, quinines, tannins, etc. which exhibit high antioxidant, antimicrobial, antibacterial, antidiabetic, anti-inflammatory, anti-obesity, and anti-cancer actions and actually can decrease the risk of developing different chronic non-communicable diseases (Ullah *et al.*, 2020) and prevent different health issues and even the risk of cancer. The flower extract contains a significant amount of anthocyanin, a polyphenolic flavonoids compound, which is the main responsible for blue or purple colour and acts as a good anti-oxidant, playing a vital role in the prevention and management of a range of oxidative stress-related chronic diseases (Jeyaraj, Lim & Choo, 2022). The Blue-tea also contains catechin, particularly Epigallocatechin-3-gallate (EGCG), another important component of the human diet for daily intake with strong anti-cancer and anti-inflammatory behavior (Yoshizawa *et al.*, 1987). Koskei (2019) explored the effect of blue flower extract on human cancer cells, especially on breast cancer (J1NT1), cervical (HeLa), prostate (A2780), liver (HepG2), etc. (Koskei, 2019). After that, the blue flower extract becomes more attentive to modern anti-cancer research groups to implement as an anti-cancer agent to inhibit the growth of various cancerous cells and to reduce other chronic diseases, oxidation, DNA damage, cell cycle arrest, and low-grade inflammation.

Bio-synthesis of nanoparticles is a laboratory synthesis process where different biological resources, such as parts of plants (leaves, flowers, barks, seeds, etc.) and micro-organisms, have been used to prepare different nano-sized inorganic materials, especially metal and metal oxide nanomaterials (Vidana-Gamage, Lim & Choo, 2021). In recent years, this bio-synthesis process has been extensively studied for the development of more eco-friendly, non-toxic, most sustainable, cost-effective, and environmentally friendly ease of production, which can be extensively applicable in the biomedical field. In blue flower extract the antioxidant-rich phytochemicals act as good chelating/reducing agent where electrons have been transferred from anthocyanin to inorganic compounds, enabling the production of stable bulk metallic nano-materials with controlled sizes and shapes as well as capping/stabilizing agents, preventing the nano-particles from agglomerating with each other (Chatterjee *et al.*, 2022; Demirbas *et al.*, 2019). In addition, the bio-active phytochemical components have automatically been incorporated onto the surface of the nano-materials, i.e., surface functionalization, during bio-synthesis process. As a result, the potent antioxidant activity of the plant extract has been transmitted into the nano-particles, making them more bio-compatible and have been widely employed as more effective, cheaper, and lower-toxicity new therapeutic agents and nano-carriers for nano-delivery (Kumar *et al.*, 2020). So many in vitro and in vivo experiments have been carried out in the treatment or management of chronic diseases (Gonçalves *et al.*, 2022). It has been proved that antioxidant functionalised nano-materials exhibit higher free-radical scavenging activity

Converging Chemical and Biological Sciences for a Sustainable Era

(lower IC₅₀ value) than bare antioxidant-containing natural extracts and have been widely used as potential antioxidants, anti-bacterial, and anti-cancer agent for commercial applications (Kumar *et al.*, 2020).

Recently, in cancer research, nano-materials have been designed through bio-synthesis process in such a way that they can bind to specific sites on cancer cells or tumours to deliver drugs more effectively. After that the antioxidant functionalised nano-materials efficiently aggregate at the target location, releasing their surface-loaded anti-cancer agents to particular targeted sites during cancer therapy. Different metallic(0) nano-materials especially silver (0) and gold (0) nano-materials, iron oxide, and copper oxide nano-materials are the most popular and acceptable bio-synthesised and bio-compatible material in the medical sector (Fatimah *et al.*, 2020; George, Rajasekar & Rajeshkumar, 2021). Antioxidant-functionalised Au(0) NPs have been found to be excellent cancer preventives in both in vitro and in vivo settings, which could help to improve the effectiveness of cancer therapy. Also, Au(0) NPs possess superior photophysical and optical properties which make them interesting for cell imaging (Hosny *et al.*, 2022). Again, Silver possesses well-known potential to inhibit microorganisms, and its effect has been shown to further increase after transformation into nano-sized metallic Ag(0), becoming a popular anti-microbial, anti-fungal, anti-viral and anti-inflammation agent and having been extensively utilised in ointments/creams for burns and wounds to inhibit bacterial infections (Urnuksaikhani *et al.*, 2021). Another research group has explored the potency of CuO and ZnO NPs for the treatment of bacterial infections and anti-cancer effects (Prabhu, Thangadurai & Bharathy, 2021).

With this evidence, this chapter focused on bio-synthesis of different metal and metal oxide nanomaterials using antioxidant-rich blue flower extract and assessed their anti-oxidant, cytotoxic activities. The antioxidant activities of both bare blue flower extract and CT-incorporated nano-materials have been investigated through the 2,2-diphenyl-1-picrylhydrazyl (DPPH) free-radical scavenging assay, and the corresponding IC₅₀ values have been determined. Furthermore, the bacterial activity of the synthesised nano-materials against various pathogenic organisms (gram-positive and gram-negative bacterial strains) has been compared and discussed. Finally, dose-dependent cytotoxicity analysis and anti-cancer activity in both in vitro and in vivo settings have been elaborated.

Nano-Scaled Metal, Metal Oxides

At first, the antioxidant-rich blue flower extracts have been prepared by following a standard methodology, starting from grinding about 25 g of fresh flower followed by maceration using 50 mL of water, followed by centrifugation at 600 rpm for 5min. The clear extracts have been collected into a sterilised bottle and preserved at 4°C until further use.

Silver (0) NPs has been synthesised by Neciosup-Puican *et al.* (2024) using antioxidant-rich blue flower extract, which acts as both a reducing and stabilizing agent for the reduction of silver ions. In this process, a 5 mM silver nitrate (AgNO₃) solution has been used as an optimisation condition at PH 10, with a reaction time of 30 min. Hosny *et al.* (2022) prepared Au(0) NPs by suspending varied volumes of 1 mM auric chloride (HAuCl₄.3H₂O) with 2 mL

Blue Flower Extract: Antioxidants and Nanoparticles for Health Applications

of blue flower extract. The reduction of Au^{3+} to $\text{Au}(0)$ NPs has been performed by mixing varied volumes of 10 mM with 2 mL of blue flower extract, where the colour of the solution was changed from blue into light pink. Fatimah *et al.* (2020) used the ultrasound probe Delta DH68H (Taiwan) with a frequency of 40 kHz and power of 68 W to synthesize Gold(0) nanoparticles under blue flower extract (ultrasound-assisted method).

During CuO NPs preparation, 10 ml of the blue flower extract has been mixed with 100 ml of 1 mM $\text{Cu}(\text{CH}_3\text{COO})_2$ solution, and the mixture has been heated at 80°C for 100 min. the colour of the solution changes to dark brown, which confirmed the formation of CuO NPs (George, Rajasekar & Rajeshkumar, 2021).

For the synthesis of iron oxide nanoparticles, 10 ml of 0.1 M FeCl_3 has been added dropwise to 100 ml of the blue flower extract under gentle but continuous agitation. Afterward, the pH of the solution has been adjusted to 8 by using 1 M NaOH. The change in the color of the resultant solution from violet to black indicated the successful formation of iron-oxide nanoparticles (Kachhawaha *et al.*, 2025).

In another study, ZnO and NiO NPs has been prepared through an eco-friendly biosynthesis process using aqueous flower extract of *Clitoria ternatea* under constant stirring at 60°C for 2 h, followed by pH adjustment to 8 by using 1 M NaOH. The colour of the solution changed from violet to yellow or black, followed by precipitation (Prabhu, Thangadurai & Bharathy, 2021; Chatterjee *et al.*, 2022).

Results and Discussion

The bio-synthesis of gold and silver nanoparticles [$\text{Au}(0)$ and $\text{Ag}(0)$ NPs] has been carried out through the reduction of aqueous gold metal ions, gold(III) chloride salt ($\text{HAuCl}_4 \cdot 3\text{H}_2\text{O}$)

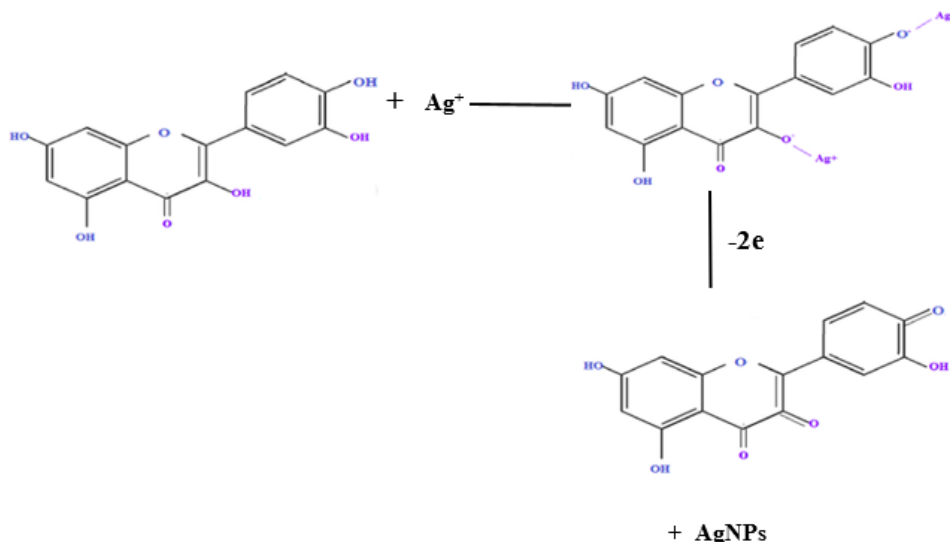


Figure 1: Proposed Mechanism of Bio-Synthesis Reduction of Metal Ion in Presence of Anthocyanin Flavonoids

Converging Chemical and Biological Sciences for a Sustainable Era

and silver nitrate (AgNO_3), respectively, by antioxidant-rich phytochemicals that are present in blue flower extracts. During this reaction, the metal ions are converted from their mono/di/trivalent state to a zero-valent state followed by nucleation and growth to form metal nanoparticles (Figure 1). Numerous research groups have demonstrated that the presence of functional groups, such as hydroxyl and carboxyl, in a plant's phytochemicals (anthocyanin) primarily acts as reducing, capping, and stabilising agents (Chatterjee *et al.*, 2022). Similarly, when those antioxidant-rich blue flower extracts have been added to the aqueous metal salt solution, followed by pH adjustment to an alkaline medium using NaOH or NH_4OH , the colour of the solution changes from light blue to dark, indicating the formation of metal oxide nano-particles. The pH of the reaction medium is one of the most important factors for nano-material synthesis, which has generally been adjusted to alkaline medium.

During bio-synthesis process, the bioactive phytochemical components, anthocyanin, have automatically been incorporated onto the surface of the nano-materials. Several research groups have confirmed the presence of anthocyanin functional groups on the surface of nano-materials through FTIR analysis (Figure 2a), where the main peak at 3387 cm^{-1} is present in the FTIR spectrum of synthesised Ag(0) NPs corresponding to the involvement of anthocyanin's hydroxyl groups (free O-H stretching band). The involvement of methyl and carbonyl groups of anthocyanin has also been located at 2931 and 1603 cm^{-1} , respectively.

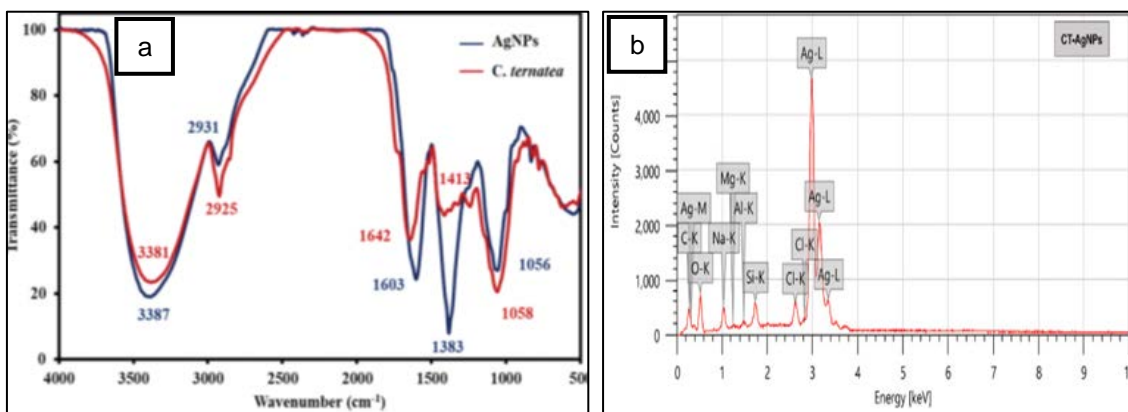


Figure 2 (a): IR Spectra of CT-Ag NPs and Blue Flower Extract; (b) EDX Analysis of CT-Ag NPs (Chatterjee *et al.*, 2022; Singh *et al.*, 2025)

Very recently, Singh *et al.* (2025) has verified the presence of bio-active compounds on the surface of the synthesised NPs through EDX analysis (Figure 2b), where some data for carbon (21.63%) and oxygen (4.54%) have been visualised in addition to predominant silver (66.49%) elemental composition.

Characterisation of the Green Synthesised Nano-Materials

During the biosynthesis process, the colour change was obtained from light blue to dark brown (Figure 3) for Ag(0) NPs and from light blue to very intense pink for AuNPs, which are the primary indicator of the formation of corresponding nano-materials. UV-visible spectrophotometer has primarily been used to monitor the formation of the nano-materials

by recording the spectrum of the reaction mixture from 200-900 nm, and the product formation was further confirmed by the development of an absorption peak at ~400 nm (Figure 3a) for Ag(0) NPs, ~530 nm (Figure 3b) for Au(0) NPs, which is associated with the surface plasmon resonance (SPR) band, as metals have free electrons and exhibits excitation of longitudinal plasmon vibrations and formation of quasi-linear superstructures of nanoparticles (Neciosup-Puican *et al.*, 2024).

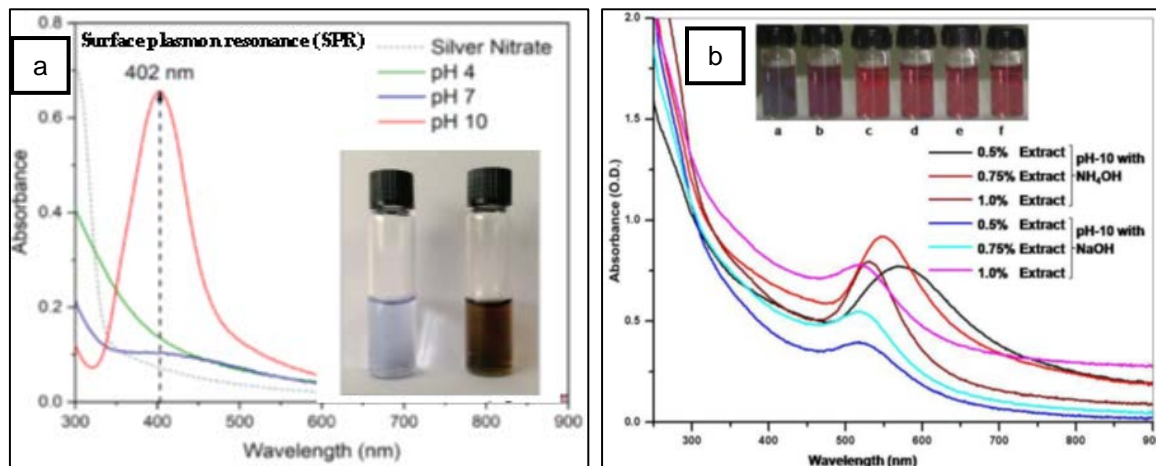


Figure 3: UV-Vis Spectra of (a) Ag(0) NPs; and (b) Au (0) NPs at Different pH Medium, Inset: Corresponding Photography of Reaction System (Neciosup-Puican *et al.*, 2024; Fatimah *et al.*, 2020)

Again, the pH of the reaction medium is one of the most important factors for nano-material synthesis, which has generally been adjusted by 0.1 M NaOH or NH_4OH to obtain different pH-containing solutions having acidic, neutral and alkaline medium. But only in alkaline medium, maximum metal, metal oxide nano-particle formation has occurred, and corresponding dark colouration and UV-visible spectra have been developed. Chatterjee *et al.* (2022) have investigated the synthesis of Ag(0) NPs at different PH medium and obtained brown-coloured NPs of 15 to 50 nm at only PH 10 medium (with a UV absorbance peak at 402 nm) (Figure 3a). Spherical gold nanoparticles (7-29 nm) synthesised using flower extract of *Clitoria ternatea* (CT) have been reported by Neciosup-Puican *et al.* (2024). Such flower extract has been further reported to be an effective bio-reductant and stabilizing agent for Au (0) NPs. The size of the synthesised Au (0) NPs has been found to decrease (56.5 ± 13.6 to 24.7 ± 8.2) with increasing extract concentration (0.5%-1.0%) in an alkaline medium. The reaction time has also been optimised through the development of UV-vis spectral bands at different times ranging from 0 to 90 minutes and reveals that the synthesis of Au (0) NPs with an average particle size of 5.5 ± 2.7 requires 20 minutes to complete. In the case of metal oxide synthesis, various phytochemicals present in blue flower extract have also been shown to play a significant role in the bio-reduction of metal ions into metal oxides.

The crystalline structure, purity, and average size have generally been determined by the powder X-ray diffraction (XRD) pattern, where sharp peaks corresponding to specific crystal

planes confirm the presence of the metal and metal oxide nanoparticles and their crystalline nature. Pure maghemite (Fe_2O_3) (JCPDS ID. 39 1346) phase of iron oxide with one major orientation along the (311) plane (Figure 4) has been successfully synthesised by Dutta *et al.* (2012). In transmission electron microscopy (TEM) and high-resolution transmission electron microscopy (HRTEM), the surface modification has also been visualised which confirms the formation of hetero-nanostructure with an average size of about 40 nm.

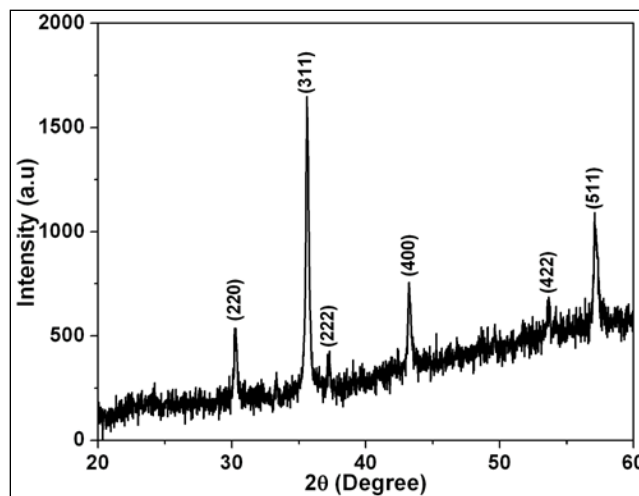


Figure 4: XRD Pattern of the Fe_2O_3 Nanoparticles (Dutta *et al.*, 2012)

Determination of the Antioxidant Activity

Numerous studies showed that the foods or beverages rich in antioxidant components anthocyanins and anthocyanidins mainly possess the ability to act as free radical scavengers against harmful oxidants such as reactive oxygen (ROS) and nitrogen species (RNS) generated inside biological systems during electron transfer reactions by losing or accepting electrons. When the antioxidant functionalised nano-materials has been synthesised through the biosynthesis process, it exhibits superior free-radical scavenging activity compared to bare antioxidant-containing natural extract. From the chemical point of view, the compounds containing dibenzopyran or pyrone ring structure (Figure 5) and so many conjugated double bonds and phenolic hydroxyl groups can accommodate the unpaired electrons through extensively delocalizing over the conjugated system or Hydrogen Atom Transfer (HAT) or Single Electron Transfer (SET) mechanism and effectively scavenge peroxy ($\text{ROO}\cdot$), alkoxy ($\text{RO}\cdot$), $\text{OH}\cdot$, O_2^- , $\text{NO}\cdot$ and other nitrogen or sulphur-containing free radicals.

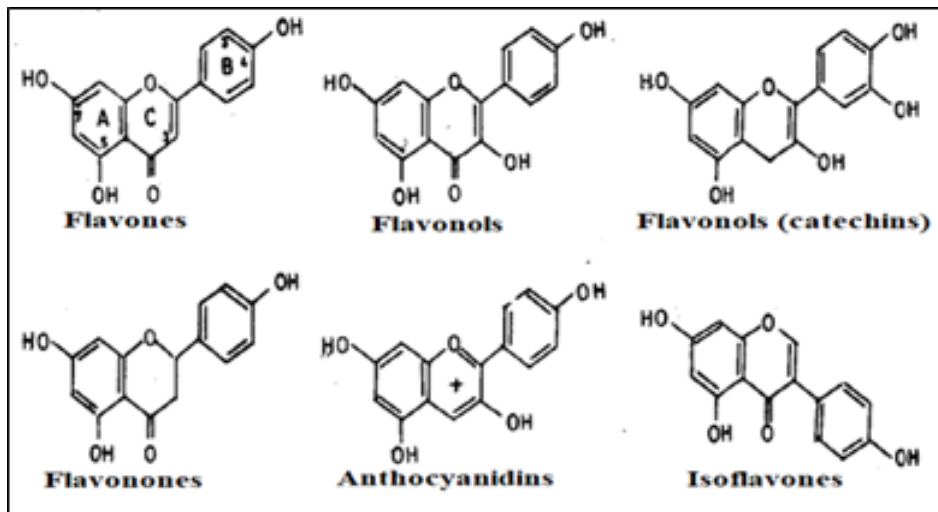


Figure 5: Chemical Structure of Different Natural Flavonoids Compounds

The 2,2-diphenyl-1-picrylhydrazyl (DPPH) free radicals scavenging assay has been generally used in antioxidant research to determine the antioxidant properties of both tea extract and synthesised nano-materials. DPPH is commercially available as a stable free radical, an organic nitrogen free radical, representing any kind of free radical within the body, which is used to test antioxidant capabilities. A compound is considered a good antioxidant if it can readily donate an electron to the electron-deficient DPPH radicals, thereby terminating the chain reaction of electron transfer between molecules. This action helps prevent oxidative damage to healthy cells and vital biomolecules such as DNA, proteins, and cellular membranes.

During radical scavenging experiments, when the antioxidant anthocyanine, EGCG molecules react with DPPH free radicals, electron transfer occurs, the antioxidant molecules are oxidised and the DPPH is reduced. The investigation has generally been carried out spectrophotometrically because DPPH has an absorption band at 515 nm which disappears gradually upon reduction by an antioxidant compound. Lower absorbance of the reaction mixture indicates higher DPPH free radical scavenging activity (Fang *et al.*, 2017; Baygar & Ugur, 2017). Ascorbic acid has been used as a reference antioxidant because it can react with DPPH, quickly reaching a steady state immediately. Free radical scavenging activity has generally been expressed as the % of inhibition; the higher the percentage inhibition, the more antioxidant the particular compound is. The percentage of inhibition has been calculated by the following equation:

$$\% \text{ DPPH scavenging effect} = [(\text{OD}_{\text{control}} - \text{OD}_{\text{sample}}) / \text{OD}_{\text{control}}] \times 100,$$

where 'control' has been prepared without a tested antioxidant tea sample or nano-material sample. A strong antioxidant, ascorbic acid, has been used as a reference sample.

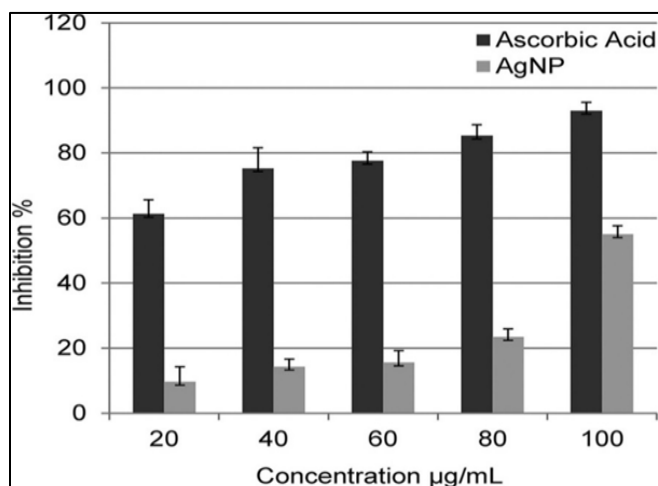


Figure 6: Antioxidant Activity of Bio-synthesised Ag NPs and Reference Ascorbic Acid (Baygar & Ugur, 2017)

During the experiment, when the tested antioxidant sample has added to Control DPPH solution, the absorbance value, i.e., OD_{control}, gradually decreased owing to the inhibition effect of the antioxidant sample, making it decompose some harmful free DPPH radicals, and hence the amount of total DPPH radicals decreased. Baygar and Ugur (2017) have reported that various concentrations of 20, 40, 60, 80 and 100 µg/ml of biosynthesised AgNPs exhibited 9.66%, 14.27%, 15.59%, 23.46% and 54.99% free radical scavenging capability, respectively (Figure 6). When compared with standard ascorbic acid, the antioxidant activity of the biosynthesised NPs was found to increase gradually with the increase in the treatment dose (dose-dependent matter).

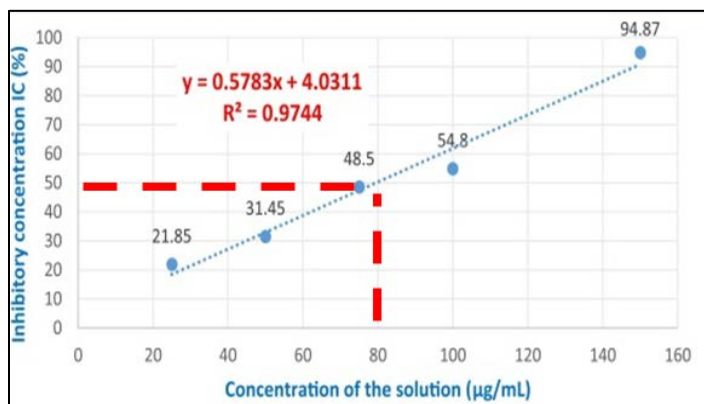


Figure 7: Calibration Curve for Determination of IC₅₀ Value (Fatimah et al., 2020)

Furthermore, Median inhibition concentration (IC₅₀) calculations are widely used to determine the concentration of antioxidant molecules that can do 50% inhibition, i.e., how much of an antioxidant molecule or drug is needed to inhibit a biological process by half

(50%). High IC₅₀ values mean that a relatively high amount (concentration) of a drug or compound is needed to inhibit 50% of a biological process; that compound is less potent and requires a larger amount to achieve the desired effect, whereas the lower IC₅₀ value in microg/ml is more acceptable to us, and the compound is more potent because a small amount of the compound can produce significant inhibitory effects. The IC₅₀ calculation has been carried out graphically using a calibration curve in the linear range by plotting the antioxidant concentration vs the corresponding scavenging effect.

From the experimental data (Figure 7), the more preferable low IC₅₀ value in the range of 50-200 µg/ml of Ag(0) NPs has been determined through constructing calibration curves which exhibit increasing % DPPH radical scavenging ability, but a concentration of 140 µg/ml of Ag(0) NPs exhibits the highest antioxidant activity (~80%). Furthermore, the IC₅₀ value of Ag NPs is around 80.37 µg/ml, comparable with the IC₅₀ value of standard ascorbic acid, 44.10 µg/ml (Fatimah *et al.*, 2020). Kumar *et al.* (2020) have reported that Ag(0) NPs synthesised using tea extract show a significantly lower IC₅₀ value, i.e., 55.86 µg/ml, compared to tea extract alone (IC₅₀ 1920 µg/ml), indicating its strong anti-oxidant potential relevant to that of standard ascorbic acid.

Anti-bacterial Activity

Nano-materials especially metal-based ones, can inhibit bacterial growth through various mechanisms such as bacterial cell-membrane damage, production of reactive oxygen species (ROS) inside the bacterial cell or interference with bacterial metabolism and DNA replication. When high levels of polyphenolic compounds, anthocyanins, catechins, etc., have been functionalised on the surface of the NPs, the anti-microbial and anti-inflammatory effect has been increasing much more. Silver possesses famous potential to inhibit micro-organisms and their effect has been shown to further increase after transformation into nano-sized material. The Ag(0) and Au(0) NPs are also well-known anti-bacterial agents because they can interact very easily with bacterial cell walls through attraction between the microbial cell wall's negative charge and NPs' positive charge (owing to possessing negative zeta potential). After interaction, the permeability function of the bacteria cell membrane changes, and hence bacterial integrity has been disrupted and caused cell death (Yamanaka, Hara & Kudo, 2005). Again, after interaction of the NPs with bacterial cells, the thiol group in the electron transport chain enzyme has been disrupted because of the affinity of Ag(0) NPs to Sulphur and Phosphorus elements, which are abundantly found in bacterial cell wall, main responsible for anti-bacterial properties of the NPs. The capability of NPs to enter and accumulate inside the wall of a bacterial cell increases with decreasing the size of the NPs.

The synthesised NPs have been evaluated for anti-bacterial capabilities towards gram-positive and gram-negative bacterial stains through calculation of the inhibition zones and Minimum Inhibitory Concentration (MIC) in µg/ml of the nano-antibiotics i.e., quantitative measurement of the lowest concentration of the NPs that inhibits the growth of a given strain of bacteria. Different bacterial stains show different diameters of inhibition zone (DIZ) in mm units (Figure 8) in the disc diffusion assay experiment. But Minimum inhibitory concentration (MIC) and Minimal Bactericidal Concentration (MBC) have generally been determined with different bacteria in µg/ml units during anti-bacterial activity testing (Wintachai *et al.*, 2019).

In the case of CT-Ag(0) NPs, the MIC has been evaluated as 0.5 mM (0.05 mg/mL) and the corresponding MBC, the lowest concentration, as 4.5 mM, which kills 99% of the initial bacterial population against *E. Coli* bacteria (Wintachai *et al.*, 2019). Again, Antioxidant functionalised Gold(0) NPs have been found to be excellent anti-bacterial agents, and using a special ultra-sound assisted synthesis method, smaller and more uniform Au(0) particles illustrated enhanced anti-bacterial activity through providing more surface contact with micro-organisms. *S. aureus* bacteria have been found to be most resistant to Au(0) NPs with a minimum inhibition zone of ~20 mm (Figure 8b) (Fatimah *et al.*, 2020).

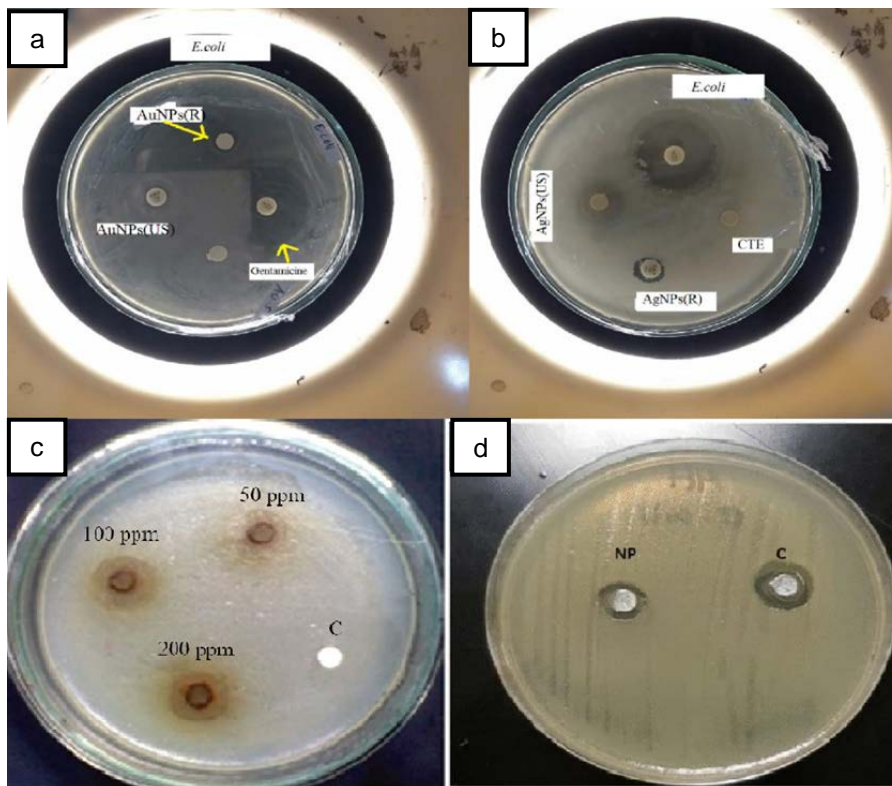


Figure 8: Photography of Disc-Diffusion Assay of (a) Au(0) NPs; (b) Ag(0) NPs; (c) Fe₂O₃ NPs; and (d) ZnO NPs Against *E.coli* Bacteria (Wintachai *et al.*, 2019; Fatimah *et al.*, 2020; Naiel *et al.*, 2022)

Among the metal oxide NPs, ZnO and TiO₂ NPs are very popular for their characteristic ultraviolet ray scattering properties and wound-healing applications. Naiel *et al.* (2022) have reported that phyto-synthesised ZnO NPs exhibit potent anti-microbial, anti-fungal activity against gram-negative bacteria *E. Coli*. The anti-bacterial capabilities of those ZnO NPs have been investigated against various pathogenic organisms with different concentrations of ZnO NPs using the agar well diffusion method, which exhibits different sizes of the inhibition zone based on the concentration of the NPs. In another study, bio-synthesised ZnO NPs exhibits anti-bacterial activity against both *Escherichia Coli* and *Staphylococcus*

Blue Flower Extract: Antioxidants and Nanoparticles for Health Applications

aureus bacteria after 24 hours incubation with an 11 mm and 10 mm diameter bacterial growth inhibition zone, respectively (Figure 8d) (Naiel *et al.*, 2022). Again, Fe₂O₃ NPs showed a higher zone of inhibition of E. Coli in the range of 18-26 mm (Figure 8c) (at a concentration of 10 mg/ml). Using the very popular Fenton mechanism, iron can easily generate ROS inside the bacterial cell; that ROS could completely inhibit the function of protein and mitochondria and cause DNA damage and cell lysis.

Anti-cancer Activity

In the case of cancer cells, the good antioxidant can oxidize itself and attack cysteine residues of proteins in cancerous cells, inhibit their growth, and induce apoptosis (programmed cell death). In this way, strong antioxidant-containing materials can inhibit the development of various cancer cells and metabolic pathways that enhance apoptosis, suppress cell proliferation, and inhibit angiogenesis, resulting in cancer cell growth and carcinogenesis. With the help of nano-biotechnology, engineered NPs have been synthesised in such a way that highly porous morphology and a high surface-to-volume ratio of the NPs can enhance the anti-cancer effects. Again, when a high level of polyphenolic compounds, anthocyanins, catechins, etc., has been functionalised on the surface of the NPs, the anti-tumour and anti-cancer effects have been increasing much more, which could help to improve the effectiveness of cancer therapy, cancer cell imaging and prevention methods. Actually, anthocyanin and catechin (EGCG) from tea extract possess high levels of cancer prevention action; they have been widely used in the manufacture of medicine capsules and are prescribed to cancer patients undergoing treatment with radiotherapy. Again, tea catechin (EGCG) shows additional health benefits as a cancer preventive and can-do anti-tumour activity through inhibition of metallo-proteinase activity, inducing the formation of ROS in the mitochondria of cancer cell lines. According to Hsu *et al.* (2012), anthocyanin in blue tea plays a role in cancer prevention through suppressing cell proliferation of COLO 320 DM (IC₅₀ = 64.9 µg/ml) and HT-29 (IC₅₀ = 55.2 µg/ml) by blocking cell cycle progression at the G₀/G₁ phase inducing apoptotic cell death.

Ag(0) and Au(0) NPs have already been widely used for cancer cell imaging owing to possessing superior photophysical and optical properties. Antioxidant-functionalised gold (0) NPs have been found to be excellent cancer preventives, suppress cell proliferation, have minimum toxicity and can be used to deliver drugs to cancer cells. Again, iron oxide (Fe₂O₃) NPs have already been investigated in cancer research due to holding unique magnetic properties which enable various applications like magnetic targeting and drug delivery, cancer hyperthermia, and magnetic resonance imaging (MRI). The Fe₂O₃ has been designed and utilised to target specific cancer cells, and their magnetic properties allow for precise control of therapeutic agents using an external magnetic field.

The anti-cancer activity of bio synthesised NPs has been investigated by Ansar *et al.* (2020) through the reduction of 3-(4,5-dimethyl thiazole-2-yl)2,5-diphenyl Tetrazolium bromide dye (MTT), and that MTT assay has been generally utilised to explore cytotoxic effects and apoptosis. It has been demonstrated that CT-Ag(0) NPs are potent anti-cancer agents, which exhibits cytotoxic activity against MCF-7 breast cancer cell lines with a very low IC₅₀ value of 17 µg/ml and also exhibit cell death at higher concentrations of nanoparticles i.e.,

cytotoxicity increases proportionately with increasing concentrations of Ag(0) NPs with a maximum effect at 100 µg/ml with an IC 50 of 55 µg/ml (Ansar *et al.*, 2020). In another study revealed that CT-Ag(0) NPs are able to kill almost all lung cancer cells (A549 and L-132) at 30 µg/ml concentration. Among the metal oxide NPs, ZnO NPs have been investigated for their anti-skin cancer and cytotoxic effect against cancer cell lines, where dose-dependent cytotoxicity analysis reveals that higher concentrations of 500 or 250 µg/ml ZnO can significantly reduce cell viability at 22% and 38%, respectively and the IC50 of skin cancer has been reported as 409.7 µg/ml (Naiel *et al.*, 2022).

Conclusion

The proposed nano-scaled materials have been successfully produced through a green bio-synthesis route using antioxidant-rich blue Aparajita flower aqueous extract. Using flower extract as reducing and stabilizing agents for synthesis offers advantages, such as the fact that flower extract is readily available, sustainable, eco-friendly, cost-effective, and non-hazardous. The synthesised nano-materials has been widely explored as efficient anti-bacterial and anti-cancer agents owing to their possessing superior anti-oxidant activity. They exhibit different anti-oxidant efficiencies based on different size, shape and morphology. The anti-oxidant performances have also been improved by tuning the size and morphology through the ultrasound-assisted synthesis way. The prepared NPs exhibited efficient antimicrobial activities against both Gram-positive and Gram-negative bacteria. Moreover, a low amount of NPs can produce significant inhibitory effects against the development of cancer cells. Therefore, the antioxidant-incorporated nano-materials can be used as potential anti-oxidant, anti-bacterial, anti-cancer agent for commercial applications.

Acknowledgement

The Author is grateful to Prof. Bibhotosh Adhikary, Department of Chemistry, Indian Institute of Engineering Science and Technology (IIST), Shibpur, for constructive discussions. The Author is indebted to UGC, India, for financial support through the MRP [PSW-066/15-16 (ERO)]. The author also acknowledges the MHRD (India) for providing instrumental facilities to the Department of Chemistry, IIST Shibpur and the RUSA Scheme of the Department of Higher Education, Government of West Bengal, for providing instrumental facilities to the Department of Chemistry, Bangabasi Morning College, Kolkata, India.

References

- Ansar, S., Tabassum, H., Aladwan, N. S., Naiman Ali, M., Almaarik, B., AlMahrouqi, S., ... & Alsubki, R. (2020). Eco friendly silver nanoparticles synthesis by Brassica oleracea and its antibacterial, anticancer and antioxidant properties. *Scientific Reports*, 10(1). <https://doi.org/10.1038/s41598-020-74371-8>
- Baygar, T., & Ugur, A. (2017). Biosynthesis of silver nanoparticles by Streptomyces griseorubens isolated from soil and their antioxidant activity. *IET Nanobiotechnology*, 11(3), 286-291. <https://doi.org/10.1049/iet-nbt.2015.0127>
- Chatterjee, R., Sarkar, S., Dutta, A. K., Akinay, Y., Dasgupta, S., & Mukhopadhyay, M. (2022). Scope and challenges for green synthesis of functional nanoparticles. In *Novel Applications of Carbon Based Nano-Materials* (pp. 274-318). CRC Press.

Blue Flower Extract: Antioxidants and Nanoparticles for Health Applications

- Demirbas, A., Büyükbezirci, K., Celik, C., Kislakci, E., Karaagac, Z., Gokturk, E., ... & Ocsoy, I. (2019). Synthesis of long-term stable gold nanoparticles benefiting from red raspberry (*Rubus idaeus*), strawberry (*Fragaria ananassa*), and blackberry (*Rubus fruticosus*) extracts–gold ion complexation and investigation of reaction conditions. *ACS Omega*, 4(20), 18637-18644. <https://doi.org/10.1021/acsomega.9b02469>
- Dutta, A. K., Maji, S. K., Srivastava, D. N., Mondal, A., Biswas, P., Paul, P., & Adhikary, B. (2012). Synthesis of FeS and FeSe nanoparticles from a single source precursor: a study of their photocatalytic activity, peroxidase-like behavior, and electrochemical sensing of H₂O₂. *ACS Applied Materials & Interfaces*, 4(4), 1919-1927. <https://doi.org/10.1021/am300408r>
- Fang, Y. T., Li, Q., Cao, A. C., Li, Y., & Wei, Y. (2017). Isolation and purification of phenolic acids from sugarcane (*Saccharum officinarum* L.) rinds by pH-zone-refining counter-current chromatography and their antioxidant activity evaluation. *Food Analytical Methods*, 10(7), 2576-2584. <https://doi.org/10.1007/s12161-017-0824-3>
- Fatimah, I., Hidayat, H., Nugroho, B. H., & Husein, S. (2020). Ultrasound-assisted biosynthesis of silver and gold nanoparticles using *Clitoria ternatea* flower. *South African Journal of Chemical Engineering*, 34, 97-106. <https://doi.org/10.1016/j.sajce.2020.06.007>
- George, R. S., Rajasekar, A., & Rajeshkumar, S. Blue Tea Mediated Synthesis and Characterisation of Copper Nanoparticles: An In-vitro Study. <https://doi.org/10.9734/JPRI/2021/v33i63B35646>
- Gonçalves, A. C., Falcão, A., Alves, G., Lopes, J. A., & Silva, L. R. (2022). Employ of anthocyanins in Nanocarriers for Nano delivery: in vitro and in vivo experimental approaches for chronic diseases. *Pharmaceutics*, 14(11), 2272. <https://doi.org/10.3390/pharmaceutics14112272>
- Hosny, M., Fawzy, M., El-Badry, Y. A., Hussein, E. E., & Eltaweil, A. S. (2022). Plant-assisted synthesis of gold nanoparticles for photocatalytic, anticancer, and antioxidant applications. *Journal of Saudi Chemical Society*, 26(2), 101419. <https://doi.org/10.1016/j.jscs.2022.101419>
- Hsu, C. P., Shih, Y. T., Lin, B. R., Chiu, C. F., & Lin, C. C. (2012). Inhibitory effect and mechanisms of an anthocyanins-and anthocyanidins-rich extract from purple-shoot tea on colorectal carcinoma cell proliferation. *Journal of Agricultural and Food Chemistry*, 60(14), 3686-3692. <https://doi.org/10.1021/jf204619n>
- Jeyaraj, E. J., Lim, Y. Y., & Choo, W. S. (2022). Antioxidant, cytotoxic, and antibacterial activities of *Clitoria ternatea* flower extracts and anthocyanin-rich fraction. *Scientific Reports*, 12(1), 14890. <https://doi.org/10.1038/s41598-022-19146-z>
- Kachhawaha A. S., Elizabeth M, Hari, P., Rajan A., & Verma N. (2025). Green Synthesis and Antibacterial Evaluation of Iron Oxide Nanoparticles Using *Clitoria Ternatea* Flowers. *Biomedical and Pharmacology Journal*, 18(1), 749-759. <https://dx.doi.org/10.13005/bpj/3125>
- Koskei, L. C. (2019). *In Vitro Studies of the Effects of Purple Tea (Camellia Sinensis) Extracts on Selected Human Cancer Cell Lines and Multi-drug Resistant Bacteria* (Doctoral dissertation, University of Nairobi). Retrieved from: <http://erepository.uonbi.ac.ke/handle/11295/152829>, Accessed on 13th February 2025.
- Kumar, H., Bhardwaj, K., Nepovimova, E., Kuča, K., Singh Dhanjal, D., Bhardwaj, S., ... & Kumar, D. (2020). Antioxidant functionalised nanoparticles: A combat against oxidative stress. *Nanomaterials*, 10(7), 1334. <https://doi.org/10.3390/nano10071334>

- Lakshan, S. A. T., Jayanath, N. Y., Abeysekera, W. P. K. M., & Abeysekera, W. K. S. M. (2019). A commercial potential blue pea (*Clitoria ternatea* L.) flower extract incorporated beverage having functional properties. *Evidence-Based Complementary and Alternative Medicine*, 2019(1). <https://doi.org/10.1155/2019/2916914>
- Naïel, B., Fawzy, M., Halmy, M. W. A., & Mahmoud, A. E. D. (2022). Green synthesis of zinc oxide nanoparticles using Sea Lavender (*Limonium pruinosum* L. Chaz.) extract: characterization, evaluation of anti-skin cancer, antimicrobial and antioxidant potentials. *Scientific Reports*, 12(1), 20370. <https://doi.org/10.1038/s41598-022-24805-2>
- Neciosup-Puican, A. A., Pérez-Tulich, L., Trujillo, W., & Parada-Quinayá, C. (2024). Green Synthesis of Silver Nanoparticles from Anthocyanin Extracts of Peruvian Purple Potato INIA 328—Kullipapa. *Nanomaterials*, 14(13), 1147. <https://doi.org/10.3390/nano14131147>
- Prabhu, S., Thangadurai, T. D., & Bharathy, P. V. (2021). Greenbased Biosynthesis of Zinc Oxide Nanoparticles Using *Clitoria ternatea* Flower Extract and Its Antibacterial Activity. *Nano Biomedicine and Engineering*, 13(4), 394-400. <https://doi.org/10.5101/nbe.v13i4.p394-400>
- Singh, S. R., Kittur, B., Bhavi, S. M., Thokchom, B., Padti, A. C., Bhat, S. S., ... & Yara Jarla, R. B. (2025). The effect of *Clitoria ternatea* L. flowers-derived silver nanoparticles on A549 and L-132 human cell lines and their antibacterial efficacy in *Caenorhabditis elegans* in vivo. *Hybrid Advances*, 8. <https://doi.org/10.1016/j.hybadv.2024.100359>
- Ullah, A., Munir, S., Badshah, S.L., Khan, N., Ghani, L., Poulson, B.G., Emwas, A.H., Jaremko, M. (2020). Important Flavonoids and Their Role as a Therapeutic Agent. *Molecules*, 25(22), 5243-5263. <https://doi.org/10.3390/molecules25225243>
- Urnuksaïkhan, E., Bold, B. E., Gunbileg, A., Sukhbaatar, N., & Mishig-Ochir, T. (2021). Antibacterial activity and characteristics of silver nanoparticles biosynthesised from *Carduus crispus*. *Scientific Reports*, 11(1). <https://doi.org/10.1038/s41598-021-00520-2>
- Vidana Gamage, G. C., Lim, Y. Y., & Choo, W. S. (2021). Anthocyanins from *Clitoria ternatea* flower: Biosynthesis, extraction, stability, antioxidant activity, and applications. *Frontiers in Plant Science*, 12. <https://doi.org/10.3389/fpls.2021.792303>
- Wintachai, P., Paosen, S., Yupanqui, C. T., & Voravuthikunchai, S. P. (2019). Silver nanoparticles synthesised with *Eucalyptus critriodora* ethanol leaf extract stimulate antibacterial activity against clinically multidrug-resistant *Acinetobacter baumannii* isolated from pneumonia patients. *Microbial Pathogenesis*, 126, 245-257. <https://doi.org/10.1016/j.micpath.2018.11.018>
- Yamanaka, M., Hara, K., & Kudo, J. (2005). Bactericidal actions of a silver ion solution on *Escherichia coli*, studied by energy-filtering transmission electron microscopy and proteomic analysis. *Applied and Environmental Microbiology*, 71(11), 7589-7593. <https://doi.org/10.1128/AEM.71.11.7589-7593.2005>
- Yoshizawa, S., Horiuchi, T., Fujiki, H., Yoshida, T., Okuda, T., & Sugimura, T. (1987). Antitumor promoting activity of (–)-epigallocatechin gallate, the main constituent of “Tannin” in green tea. *Phytotherapy Research*, 1(1), 44-47. <https://doi.org/10.1002/ptr.2650010110>

Metal-Free and Sustainable Strategies in the Synthesis of Substituted Furans: A Contemporary Review

Harisadhan Ghosh^{1*}, Anupam Jana²

¹Department of Chemistry, Surendranath College, Kolkata 700009, West Bengal, India

²National Institute of Pharmaceutical Education and Research (NIPER) Hajipur 844102, Bihar, India

*Corresponding Author's E-mail: ghosh.harisadhan@gmail.com

Abstract

Furans and their derivatives play an important role in synthetic organic chemistry and biological chemistry, and they serve as key structural units in numerous natural products. In recent times, environmentally benign synthetic processes have emerged as a vital strategy for the production of fine organic chemicals. This review article summarises recent advances in various transition metal-free, sustainable synthetic methodologies for the synthesis of substituted furans. The focus is placed on literature reports published during the past five years (2020–2025). Various synthetically important methodologies—such as catalytic methods, cycloaddition reactions, and multicomponent reactions—used to prepare substituted furan scaffolds have been critically reviewed. Particular emphasis has been placed on metal-free methods that adhere to the principles of Green Chemistry.

Keywords: *Biological Activities; Cycloaddition Reaction; Green Chemistry; Metal-Free Synthesis; Multicomponent Reaction; Substituted Furans*

Introduction

Furan and its derivatives are heterocyclic organic compounds featuring a five-membered aromatic ring composed of four carbon atoms and one oxygen atom. Furan itself is a colourless, highly volatile, and flammable liquid with a boiling point close to room temperature (Joule & Mills, 2010). It exhibits aromatic properties (Resonance energy= 16 kcal/mol or 67 kJ/mol) due to the delocalisation of π -electrons within the ring (Figure 1).

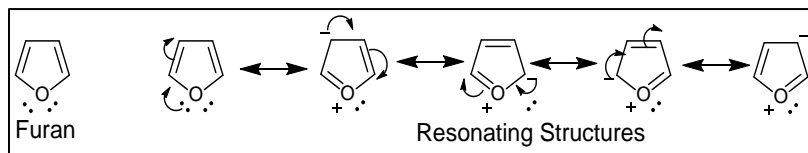


Figure 1: Furan and its resonating structures

It is an important class of organic compound because it acts as a key structural unit in numerous natural products and also has been found to exhibit several biological activities, such as anti-inflammatory, anticancer, antioxidant, antifungal, antibacterial, antispasmodic and herbicidal activities (Saeid, Al-sayed & Bader, 2023). Compounds comprising the furan ring are biologically active and are existent in a number of pharmaceutical products (Figure 2).

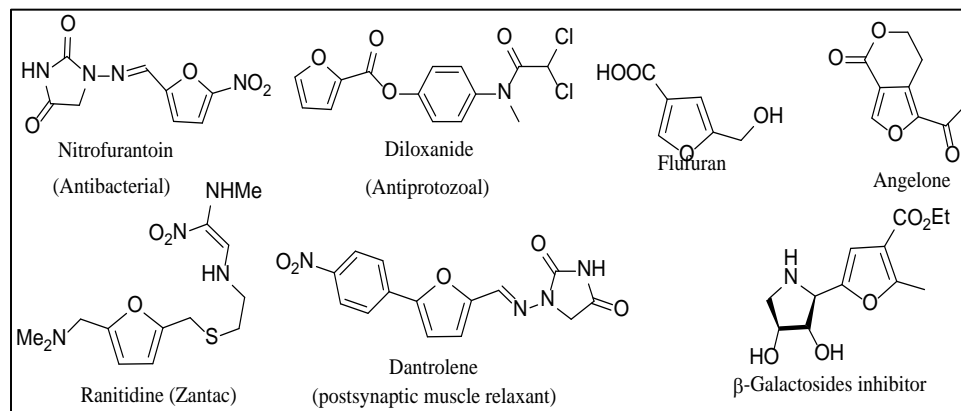


Figure 2: Biologically active furans

Furan rings act as unique synthetic intermediates because of the low resonance energy value of the furan scaffold (Gubina & Kharchenko, 1995). They undergo a number of synthetically useful transformations, such as addition reactions, metalations, cycloadditions, Ring-opening reactions, and electrophilic substitutions (Eicher, Hauptmann & Speicher, 2003).

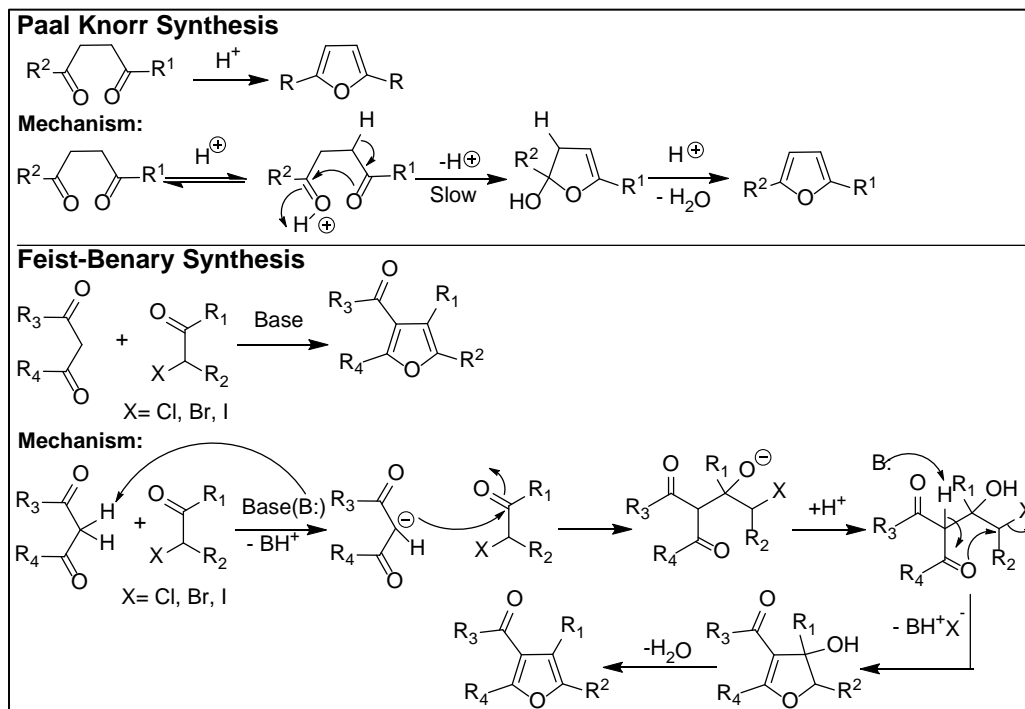
Due to the wide range of biological and synthetic importance, various synthetic methodologies have been developed for the synthesis of the furan moiety over the years (Deepthi, Babu & Balachandran, 2019). This book chapter discusses the metal-free, green, and sustainable synthetic methodologies that have been explored for the construction of substituted furan scaffolds over the past five years (2020–2025).

Literature Review

Many synthetic approaches have been followed for the construction of furan scaffolds. The most classic synthetic route to achieve poly-substituted furan is Paal-Knorr synthesis, which is basically an acid-catalysed cyclisation of 1,4-dicarbonyl compounds (Khaghaninejad & Heravi, 2014; Li, 2009) (Scheme 1).

Another classical synthetic method is the Feist–Benary synthesis which is an organic reaction between β -dicarbonyl compounds and α -halo ketones which leads to substituted furan compounds. Contrary to the Paal-Knorr synthesis, this cyclocondensation reaction is catalysed by a base (Scheme 1) (Peng *et al.*, 2016).

Recently, a diverse array of advanced methodologies has been developed for the construction of furan scaffolds, including (a) transition metal-catalysed construction of furan skeletons (Gulevich *et al.*, 2013) (b) direct functionalisation of the furan core to achieve substituted furan moieties (Karlinskii & Ananikov, 2021) (c) catalytic methods for the preparation of substituted furans from sugar and biomass (Romo *et al.*, 2018) facilitating the rapid and efficient synthesis of structurally diverse furan frameworks.



Scheme 1: Paal-Knorr and Feist-Benary Synthesis of Poly-substituted Furan

Although these methods have demonstrated efficiency in synthesising substituted furan derivatives, they exhibit certain limitations, including the reliance on costly metal catalysts, the use of environmentally hazardous solvents, and the requirement for harsh reaction conditions. Consequently, there is a strong impetus to develop straightforward, cost-effective, and, most importantly, metal-free green and sustainable methodologies for the synthesis of densely functionalised furan derivatives from readily available starting material. This book chapter will primarily focus on metal-free, sustainable, and environmentally benign synthetic strategies for the construction of substituted furans, as highlighted in recent advancements.

Discussion

A recent literature survey covering the last five years (2020–2025) reveals that numerous efforts have been made to develop non-metallic synthetic routes for the construction of poly-substituted furan scaffolds. The synthetic reports have been documented as follows:

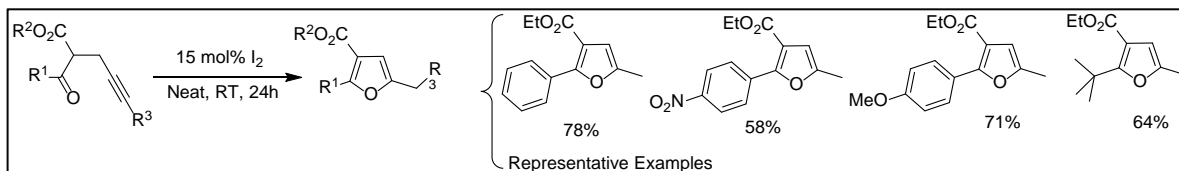
Synthesis of Substituted Furans via Various Metal-Free Catalytic Methods:

Iodine Catalysed Synthesis of Substituted Furan:

Pace *et al.* (2021) introduced an efficient and practical approach for synthesising 3-carboxy-2,5-disubstituted furans. Their method utilises α -propargyl- β -ketoester substrates and

Sustainable Synthesis of Substituted Furans

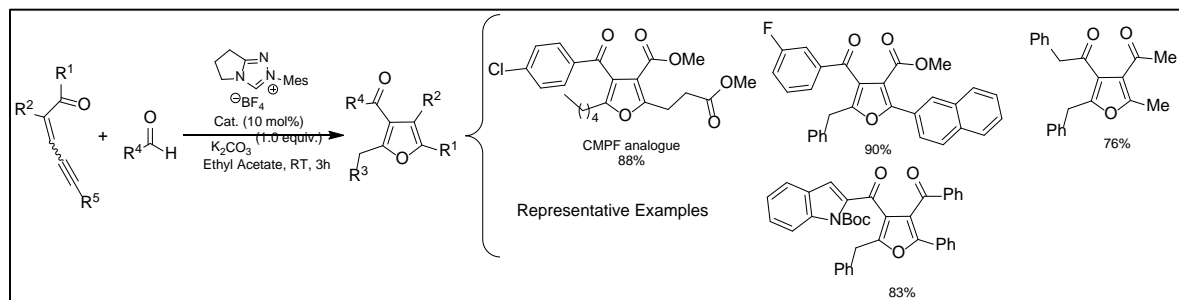
employs molecular iodine as a catalyst under mild conditions. This protocol accommodates a wide variety of functional groups and provides an environmentally friendly alternative to existing methods for obtaining furan derivatives. After conducting DFT (Density Functional Theory) calculations, the authors determined that the reaction mechanism is complex and may involve multiple competing pathways occurring simultaneously (Scheme-2).



Scheme 2: Synthesis of 3-carboxy-2,5-disubstituted Furans

NHC Catalysed Synthesis of Substituted Furan:

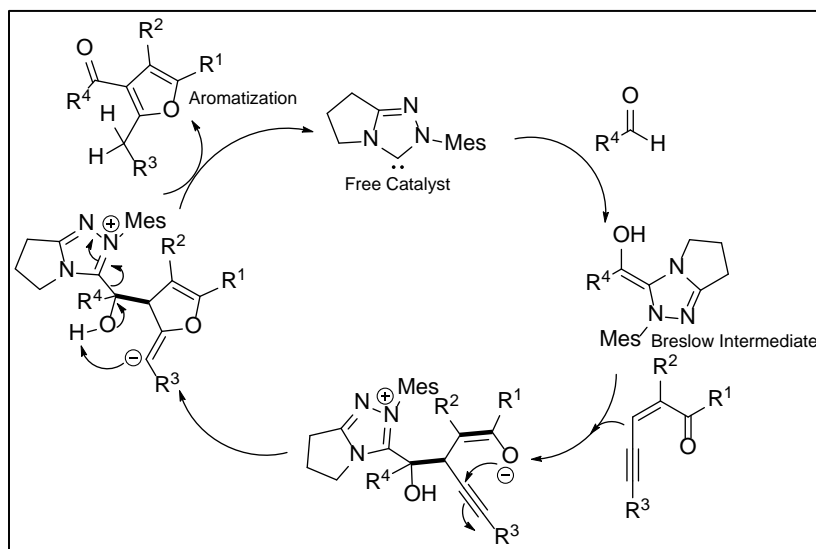
A recent study by the research group of Wang (2024) presents an efficient and selective approach for synthesising highly substituted furans. They have demonstrated an innovative *N*-heterocyclic carbene (NHC)-catalysed strategy that enables the cross-coupling and cyclisation of readily available ynones with various aldehydes (Scheme 3). This method is characterised by high atom economy, mild reaction conditions, broad substrate compatibility, and excellent functional group tolerance.



Scheme 3: Synthesis of Tetra-Substituted Furans from Enynone Catalysed by NHCs

The proposed reaction mechanism, illustrated in Scheme 4, begins with the base activating the catalyst. This active catalyst then interacts with the aldehyde, leading to the Breslow intermediate.

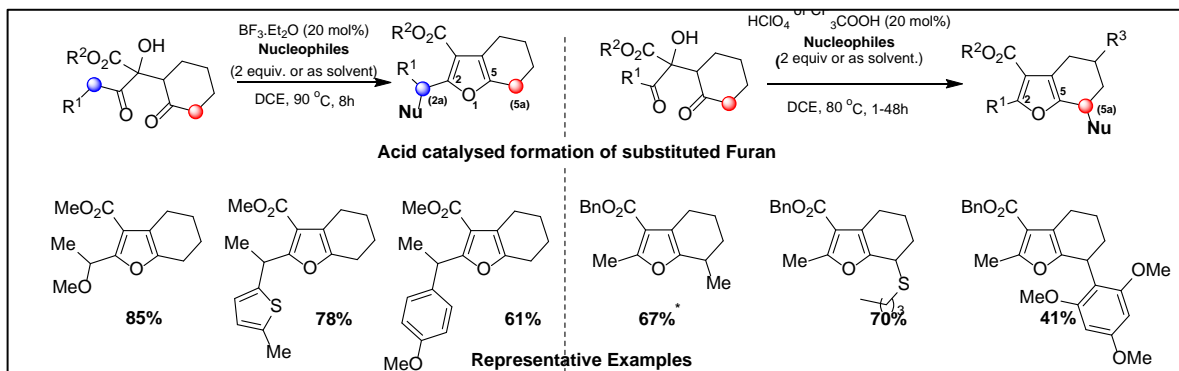
Subsequently, the Breslow intermediate undergoes a reaction with the alkenyl group of enynone, generating intermediate I. This intermediate then proceeds through a 5-exo-dig cyclisation, yielding intermediate II. Finally, the aromatisation step results in the desired product (Scheme 4).



Scheme 4: Plausible Mechanism of NHC Catalysed Tetra-substituted Furans Formation

Acid Catalysed Synthesis of Substituted Furan:

Liu's research group (2021) developed a novel divergent approach for synthesising substituted furan derivatives from 2-hydroxy-1,4-diones *via* an acid-catalysed method. The reaction enables selective functionalisation at either the 2a or 5a position of the resulting product, determined by the structure of the starting material (Scheme 5).

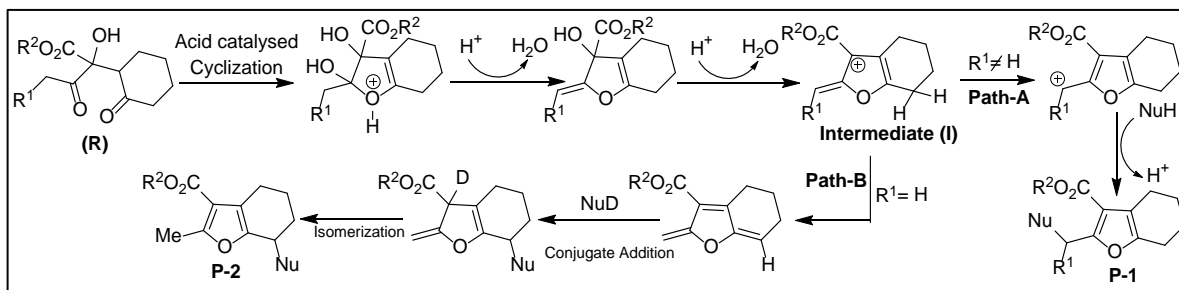


Scheme 5: Synthesis of Substituted Furan by Cascade Reactions

The authors proposed a plausible reaction mechanism that accounts for the formation of different products based on the structure of the starting materials (Scheme 6). When the R¹ group is a hydrogen atom, a 1,4-hydrogen elimination proceeds *via* the Path-B mechanism, generating a 1,3,5-triene intermediate. A subsequent 1,6-conjugate addition by a nucleophile, followed by isomerisation, leads to the formation of the product P-2. In contrast, when R¹ is an alkyl group, the reaction follows Path-A, involving a carbocation

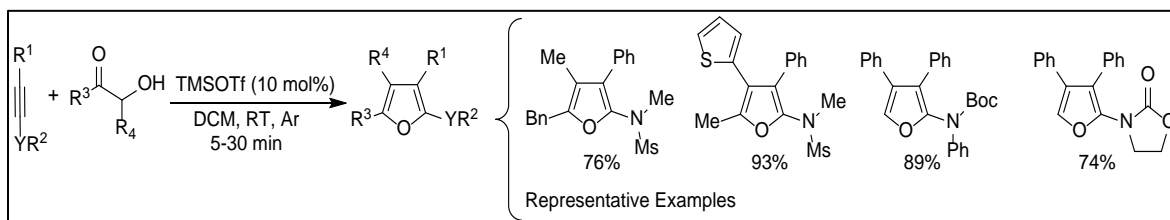
Sustainable Synthesis of Substituted Furans

rearrangement that is quickly intercepted by a nucleophile through a Friedel–Crafts-type reaction, yielding the functionalised product P-1 (Scheme 6).



Scheme 6: Proposed Reaction Mechanism

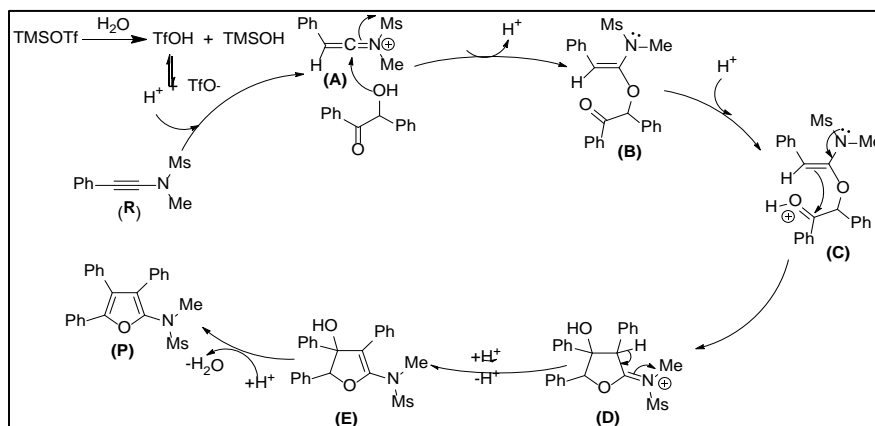
Chen and colleagues (2021) developed a metal-free method for synthesising poly-substituted furans through a TMSOTf-catalysed formal [3+2] cycloaddition between electron-rich alkynes and α -hydroxy ketones. This approach is an atom economic method that generates water as the primary by-product (Scheme 7).



Scheme 7: TMSOTf-catalysed Synthesis of Substituted Furans

Mechanistic investigations indicate that the reaction likely follows an acid-catalysed sequence involving syn-addition, cyclisation, and aromatisation steps (Scheme-8). In the initial stage, TMSOTf may react with trace water present in the system to generate TfOH. The resulting TfOH then activates the ynamide (R), leading to the formation of a reactive keteniminium ion intermediate (A). This intermediate is intercepted by the hydroxyl group of benzoin, resulting in the formation of the enamide intermediate (B).

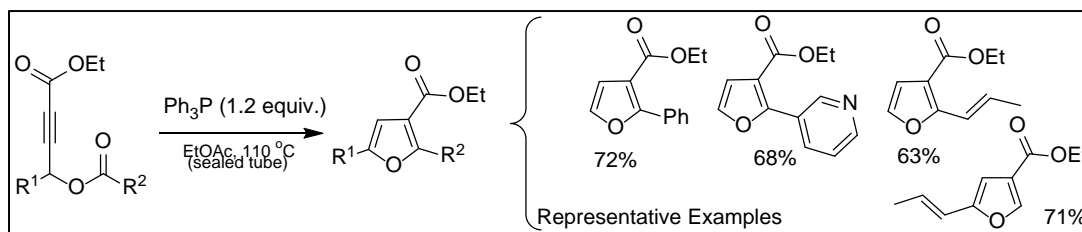
A subsequent intramolecular nucleophilic attack on the acid-activated carbonyl group produces iminium ion (D). This species undergoes enamide–iminium tautomerisation to form another enamide intermediate (E), which then undergoes acid-catalysed dehydration to furnish the final product (P) (Scheme 8).



Scheme 8: Proposed Reaction Mechanism of Furan Synthesis through Acid Catalysis

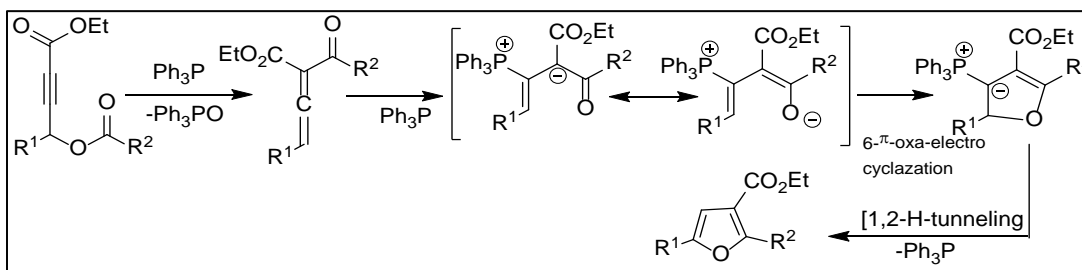
Phosphine Mediated Synthesis of Substituted Furan:

The phosphine-mediated synthesis of substituted furan moieties has been the subject of extensive study for many years (Kuroda, Hanaki & Kawakami, 1999; Wang *et al.*, 2011). In 2004, Jung, Wang and Krische reported phosphine-mediated reductive condensation of *g*-acyloxy butynoates to form furans (Krische furan Synthesis) (Scheme-9).



Scheme 9: Krische Furan Synthesis

Very recently, Wang *et al.* (2024) reinvestigated the Krische furan synthesis method. It is accepted that Ph_3P -mediated formation of the acyl allenolate intermediates is a crucial step for this reaction (Scheme-9). The ketene intermediate subsequently undergoes 6π oxa-1,5-electrocyclisation catalysed by organophosphine. The final step is a cascading [1, 2]-H shifts followed by eliminative aromatisation to give rise to the substituted furans.

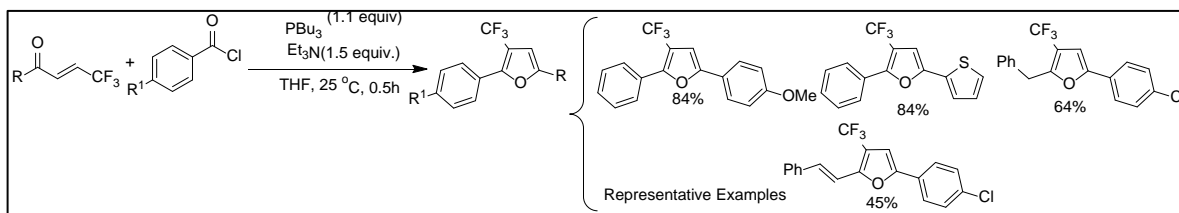


Scheme 10: Mechanistic Pathway of the Krische Furan Synthesis

Converging Chemical and Biological Sciences for a Sustainable Era

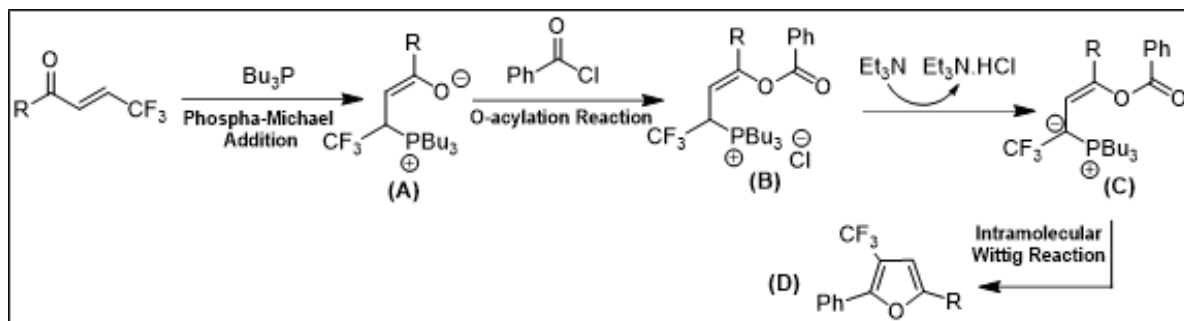
Sustainable Synthesis of Substituted Furans

Recently, Li and Zhou (2020) have effectively developed a highly efficient method involving nucleophilic addition, O-acylation, and an intramolecular Wittig reaction of β -trifluoromethyl α,β -enones, enabling the synthesis of trifluoromethyl-functionalised, multi-substituted furan compounds (Scheme 11).



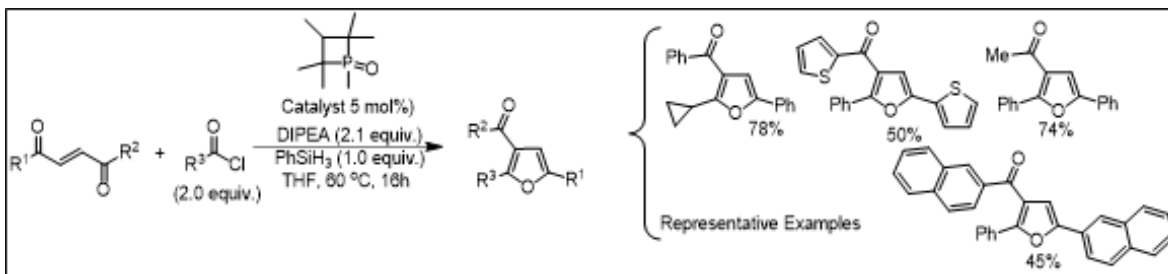
Scheme 11: Synthesis of Substituted Furans via Tandem Acylation–Wittig Reaction

A proposed mechanism for this phospho-Michael addition, followed by O-acylation and an intramolecular Wittig reaction, is illustrated in Scheme 12. The process begins with the regioselective nucleophilic addition of Bu_3P to β -trifluoromethyl α,β -enones, forming the zwitterionic intermediate (A). Subsequently, intermediate (A) undergoes acylation with acyl chloride, yielding intermediate (B). This intermediate is then deprotonated by Et_3N , generating ylide (C). Finally, an intramolecular Wittig reaction involving ylide (C) results in the formation of trifluoromethylated furan (D).



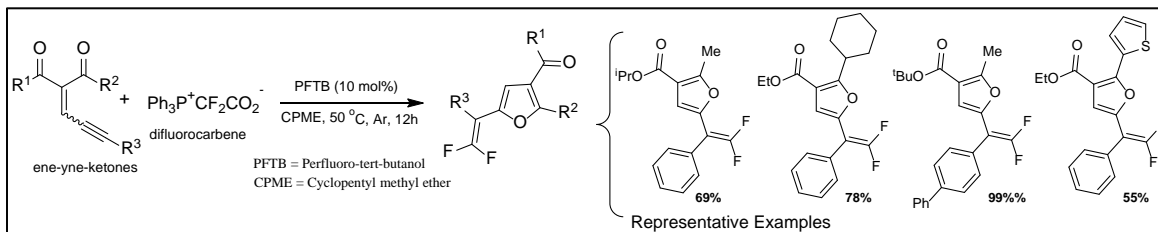
Scheme 12: Plausible Reaction Mechanism

Tönjes, Medvarić and Werner (2024) reported the synthesis of tri-tetrasubstituted furans starting from activated alkenes and acyl chlorides using a phospholene or phosphetane P(III)/P(V) redox cycling catalytic system (Scheme 13). In this transformation, Phenylsilane (PhSiH_3) is used as a terminal reductant, which reduces the formed phosphine oxides in the catalytic cycle.



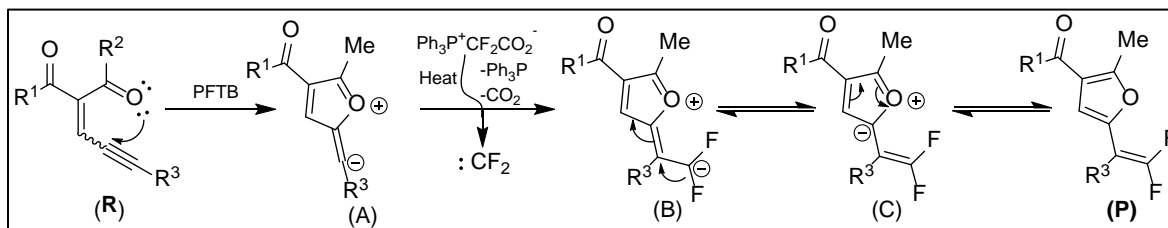
Scheme 13: Synthesis of Tri-substituted Furan by P(III)/P(V) Redox Cycling Catalysis

Very recently, Li *et al.* (2025) demonstrated a facile synthesis of furan-substituted gem difluoroalkenes using conjugated ene-yne-ketones as the furan source and Ph₃P⁺CF₂CO₂⁻ as an efficient difluoro carbene (:CF₂) source mediated by PFTB-promoted cross-coupling strategy (Scheme-14). It is worth noting that furan-substituted gem-difluoroalkenes serve as bioisosteres of the α-carbonyl furan framework, a key structural motif commonly found in natural products and potential drug candidates.



Scheme 14: Synthesis of Substituted Furan with Gem Difluoroalkenes

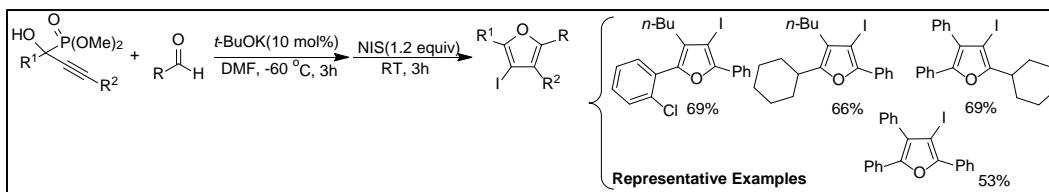
The authors proposed a most probable reaction mechanism based on their controlled experiment results (Scheme 15). The conjugated eneyne ketone (1) is initially activated by (CF₃)₃COH (PFTB). This promotes an intramolecular nucleophilic attack by the carbonyl oxygen, forming a stabilised zwitterionic intermediate A. The vinyl anion in A then rapidly traps a difluorocarbene (:CF₂) which is generated from thermal decomposition of Ph₃P⁺CF₂CO₂⁻, yielding intermediate B/C. Tautomerisation of B/C ultimately gives the desired furan-substituted gem-difluoroalkene -P.



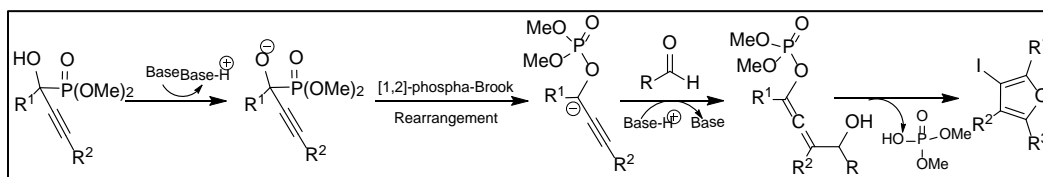
Scheme 15: Proposed Reaction Mechanism for the Formation of Furan-Substituted Gem-Difluoroalkene

Synthesis of Substituted Furan through Cyclo-Addition Reaction

Kondoh and colleagues (2020) developed an efficient approach for synthesising tetrasubstituted furans *via* a [3 + 2] cycloaddition strategy, utilising the [1,2]-phospha-Brook rearrangement under Brønsted base catalysis (Scheme-16). This two-step, one-pot formal cycloaddition involves the nucleophilic attack of an α -oxygenated propargyl anion—generated in situ through the [1,2]-phospha-Brook rearrangement—on an aldehyde at the γ -position, followed by NIS-mediated intramolecular cyclisation (Scheme-17). The process selectively yields 2,4,5-trisubstituted-3-iodofurans bearing diverse substituents. This methodology, employing readily accessible starting materials, offers a valuable route to structurally diverse tetrasubstituted furan.

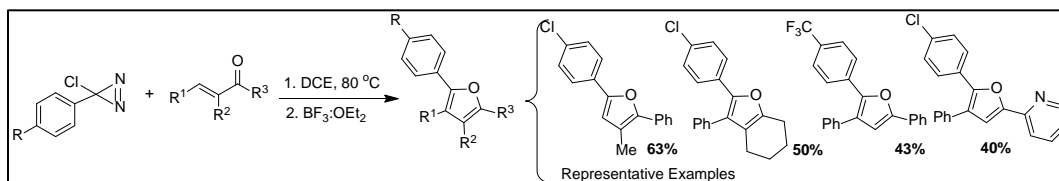


Scheme 16: Synthesis of Tetrasubstituted Furans Utilising [1,2]-Phospha-Brook Rearrangement



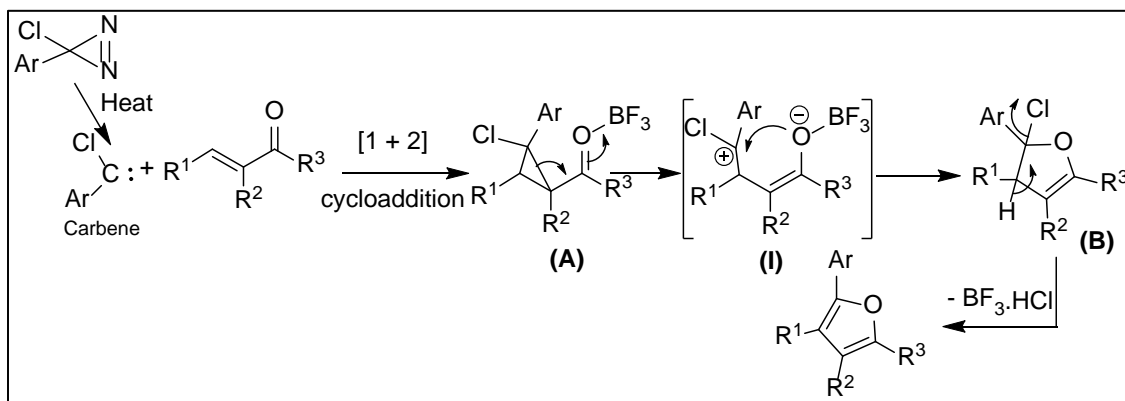
Scheme 17: Proposed Reaction Mechanism

Zhang *et al.* (2022) have recently introduced a convenient one-pot strategy for synthesising di-, tri-, and even tetra-substituted furans in moderate to good yields. This method utilises readily accessible starting materials and employs cost-effective boron trifluoride as a catalyst (Scheme-18). Notably, the process is both metal- and oxidant-free. It involves the cyclopropanation of α,β -alkenyl ketones with phenylchlorocarbene, followed by a BF_3 -mediated ring-opening and cyclo-isomerisation *via* a Cloke–Wilson rearrangement, culminating in HCl elimination to form multi-substituted furans. This protocol offers operational simplicity, mild reaction conditions, and broad substrate compatibility, making it an efficient route to synthetically and biologically valuable furan derivatives.



Scheme 18: Synthesis of Substituted Furan through $\text{BF}_3\cdot\text{Et}_2\text{O}$ Mediated Formal [4 + 1] Reaction

To gain insight into the reaction mechanism, the authors conducted a series of control experiments. A simplified representation is provided in Scheme-19. Upon thermolysis, the precursor 3-halo-3-phenyldiazirine undergoes decomposition to generate the electrophilic singlet phenyl-halo-carbene (PhClC:). This reactive carbene rapidly engages in a [1 + 2] cycloaddition with the α,β -alkenyl ketone, yielding a halocyclopropyl ketone intermediate (A). The introduction of $\text{BF}_3 \cdot \text{Et}_2\text{O}$ facilitates the Cloke–Wilson rearrangement of intermediate A, producing a key zwitterionic species (I). Intramolecular cyclisation of intermediate I then furnish dihydrofuran B, which undergoes elimination of HX in the presence of BF_3 to afford the final furan product (Scheme-19).

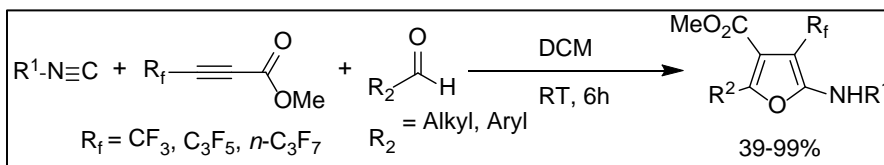


Scheme 19: A Plausible Reaction Mechanism

Synthesis of Substituted Furan through Multicomponent Reaction

The synthesis of fluorine-containing furan scaffolds presents a significant challenge due to their structural complexity. However, these fluorinated furan derivatives are of great interest because they exhibit valuable pharmacological activities, including anti-HIV, antibacterial, and antiparasitic effects.

In 2019, 2-amino-3-perfluoroalkylfurans were successfully synthesised *via* a multicomponent reaction involving aldehydes, isocyanides, and methyl perfluoroalk-2-ynoates as the starting materials (Wang *et al.*, 2019) (Scheme 20).

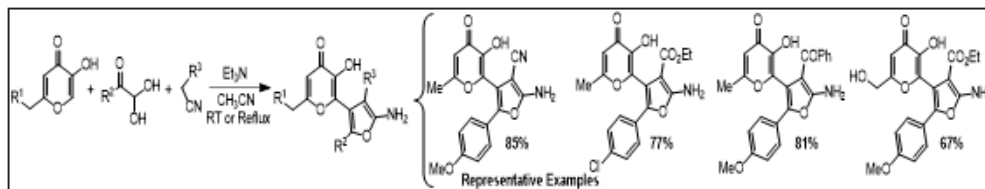


Scheme 20: Synthesis of 2-amino-3-perfluoroalkylfurans through Multicomponent Reaction

Komogortsev and colleagues (2020) developed an efficient one-pot method for synthesising a variety of substituted 2-aminofurans. This strategy involves a multicomponent reaction between 3-hydroxy-4H-pyran-4-ones, α -ketoaldehydes, and methylene-active nitriles (Scheme 21). The approach stands out for its operational simplicity and effectiveness, offering a straightforward route to access the 2-aminofuran framework. Key advantages of

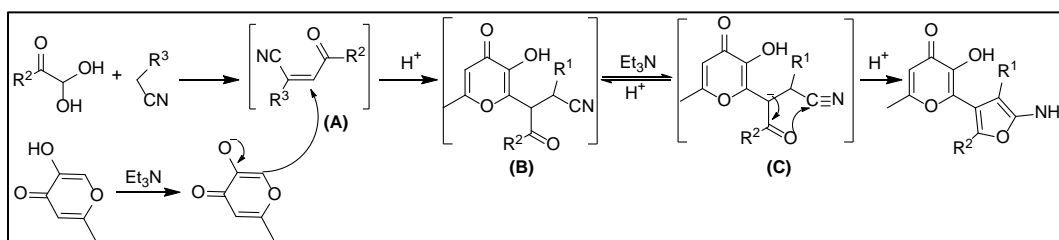
Sustainable Synthesis of Substituted Furans

the method include high product yields, mild reaction conditions, good atom economy, and a straightforward purification process.



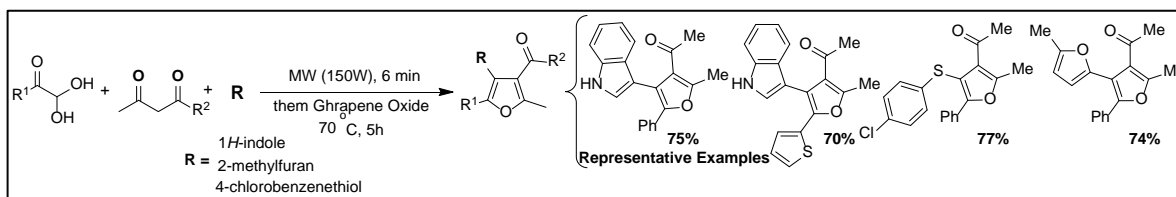
Scheme 21: Synthesis of 2-aminofuran Derivatives via Multicomponent Reaction

A plausible mechanism for this transformation as suggested by the authors has been presented below (Scheme 22)-



Scheme 22: Proposed Reaction Mechanism for the Formation of 2-aminofurans

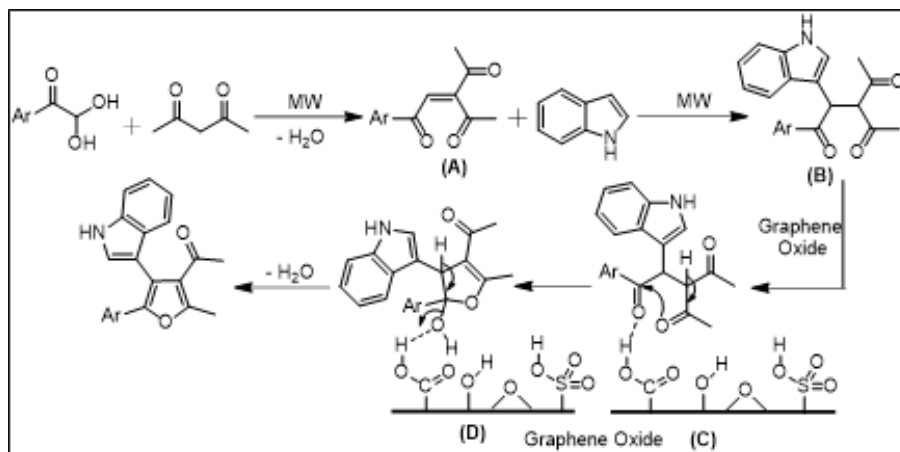
In 2020, Jana, Adhikary and Pramanik introduced a highly effective method utilising graphene oxide as a catalyst in a microwave-assisted, one-pot process for synthesising densely substituted furan derivatives. This approach, which started with basic compounds like 1,3-diketones, arylglyoxal and indole or benzothiophenol, etc., demonstrated a broad reaction scope. The team successfully synthesised various multi-substituted indole–furan conjugates, achieving excellent compatibility with a range of functional groups (Scheme 23).



Scheme 23: Graphene Oxide Catalysed MW-assisted One-pot Synthesis of Densely Substituted Furan

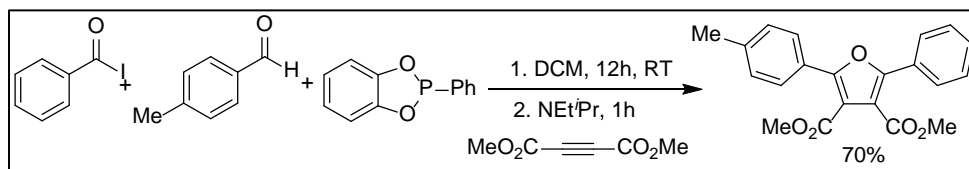
The proposed mechanism for the multicomponent reaction is depicted in Scheme 24. Initially, arylglyoxal participates in an aldol-type condensation with a 1,3-diketone, which is subsequently followed by a Michael addition with indole, resulting in the formation of intermediate A. This is followed by a Paal–Knorr cyclisation, facilitated by graphene oxide (GO), leading to the formation of intermediate B and ultimately yielding the desired furan-based product. The oxygen-rich surface of GO—featuring groups like epoxy, hydroxyl,

carboxyl, and sulfonic acid—provides both hydrophilic and acidic conditions that are crucial for driving the reaction forward.



Scheme 24: Proposed Reaction Mechanism of Graphene Oxide Catalysed Furan Synthesis

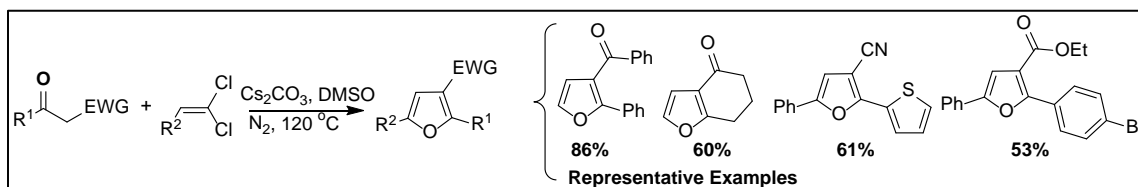
Very recently, Erguven, Zhou and Arndtsen (2021) have described a modular method to construct furans from aldehydes, acyl chlorides and alkynes (Scheme 25).



Scheme 25: Synthesis of Substituted Furan through Multicomponent Reaction

Base Mediated Synthesis of Substituted Furans:

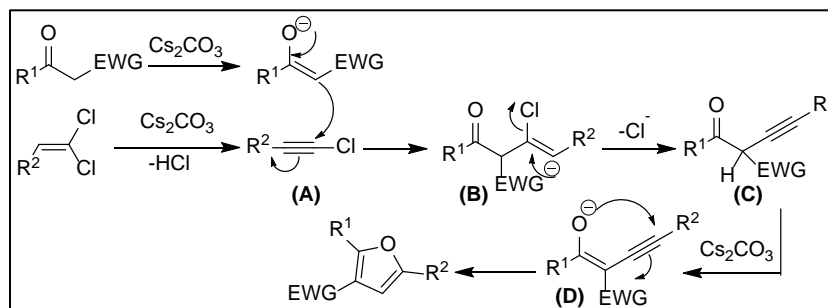
In 2020, You and colleagues introduced an innovative, transition-metal-free approach for synthesising polysubstituted furans using inexpensive and readily accessible starting materials. This base-mediated method effectively accommodates a wide range of β -keto substrates—such as β -diketones, β -ketoesters, β -ketosulfonyls, and β -ketonitriles—along with vinyl dichlorides, enabling the efficient formation of 2,3-disubstituted and 2,3,5-trisubstituted furans with moderate to excellent yields (Scheme-26).



Scheme 26: Transition-metal-free Approach to Polysubstituted Furans

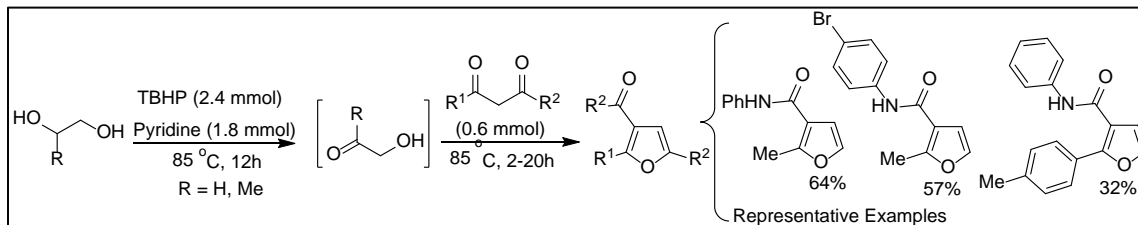
Sustainable Synthesis of Substituted Furans

The proposed reaction mechanism is illustrated in Scheme 27. Under basic conditions, the elimination of 1,1-dichloroalkene leads to the formation of the key intermediate, alkynyl chloride (A). This intermediate then undergoes a nucleophilic α -addition by the anionic species generated from deprotonation of the β -keto compound, resulting in intermediate (B). A subsequent elimination from (B) gives rise to the β -ketoalkyne intermediate (C). Finally, an intramolecular cycloisomerisation of intermediate (C) through the enolate form (D), promoted by the basic environment, yields the desired polysubstituted furan products (Scheme 27).



Scheme 27: Proposed Reaction Mechanism of Base Mediated Furan Synthesis

An oxidative synthetic route that excludes the use of transition metals has been developed for producing substituted furans from β -ketoanilides and vicinal diols (Maity & Panda, 2025). This methodology is compatible with a diverse array of functional groups, including halogens, methoxy, methyl, and nitro, and allows for the regioselective synthesis of 2,3-disubstituted and 2,3,5-trisubstituted furans through base-induced oxidative C–C and C–O bond formation (Scheme 28). Furthermore, the approach has been extended to the regioselective construction of substituted pyrroles from β -ketoenamines, utilising ethylene glycol as a two-carbon source. Key benefits of this strategy include straightforward execution, gentle reaction conditions, broad functional group compatibility, and notably, the elimination of both solvents and hazardous transition metal catalysts.

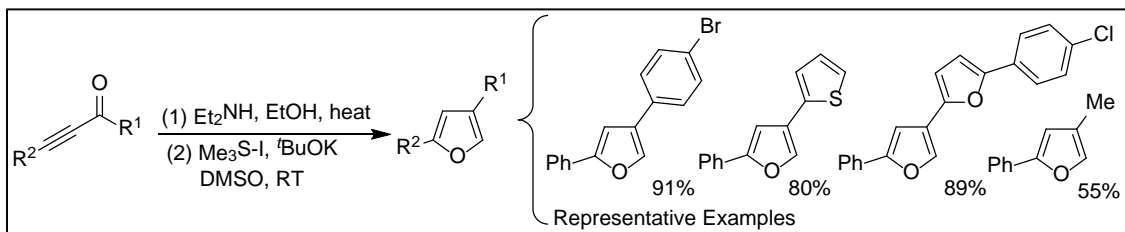


Scheme 28: Synthesis of Substituted Furan from β -ketoanilides and Vicinal Diols

Synthesis of Substituted Furans Using Various Green Methodologies

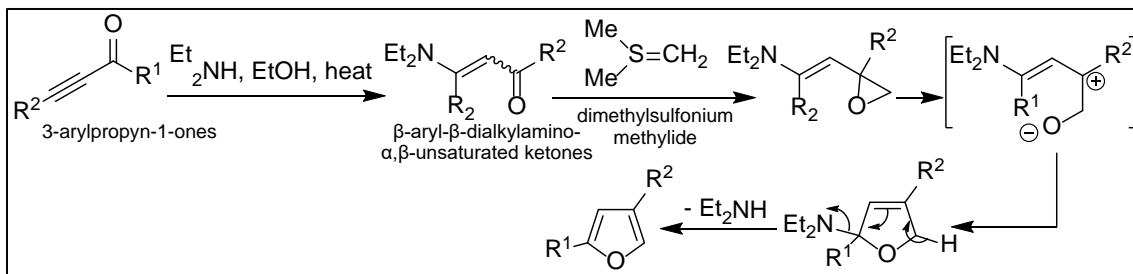
Very recently in 2023, a method for the synthesis of unsymmetrically substituted furans based on the extended Corey–Chaykovsky reaction has been developed (Shcherbakov et

et al., 2023). The method is characterised by simple reaction conditions and reagents, high yields, and a wide range of formed products (Scheme-29).



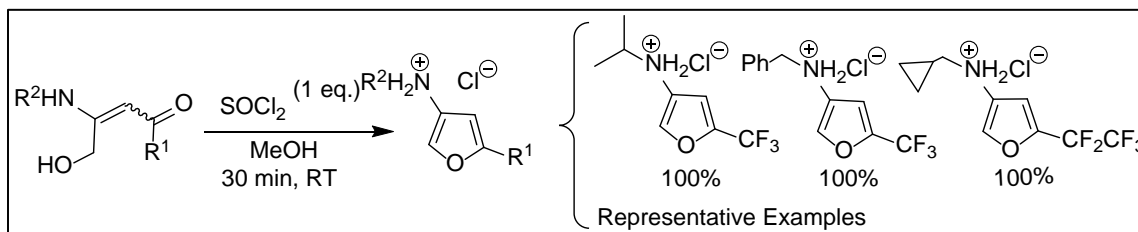
Scheme 29: Synthesis of Substituted Furan via Extended Corey–Chaykovsky Reaction

The initial compounds used are β -aryl- β -dialkylamino- α,β -unsaturated ketones, which can be readily synthesised through the Michael addition of diethylamine to 3-arylpropyn-1-ones (Scheme-30). When these resulting enamines react with dimethylsulfonium methylide, a cascade reaction occurs, resulting in the formation of 2,4-disubstituted furans.



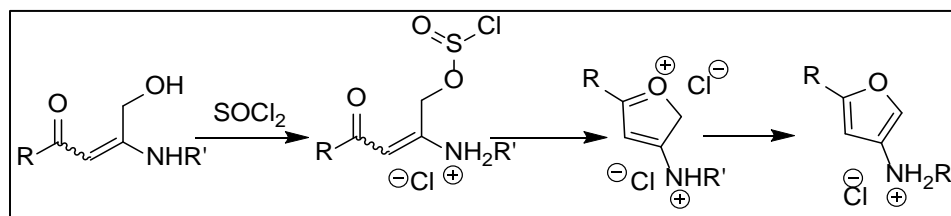
Scheme 30: Proposed Reaction Mechanism

A straightforward methodology has been recently developed for the synthesis of 3-amino-5-fluoroalkylfurans in quantitative or nearly quantitative yields starting from fluoroenones (Plaçais *et al.*, 2021) (Scheme-31).



Scheme 31: Synthesis of Substituted Furan via Intramolecular Cyclisation Reaction

In terms of the cyclisation mechanism, the authors propose that the reaction begins with the activation of alcohol by thionyl chloride (see Scheme 32). This is followed by a nucleophilic attack from the oxygen lone pair of the enone onto the α -carbon of the activated alcohol, leading to the formation of a five-membered ring. Subsequent aromatisation then yields the furan product.



Scheme 32: Proposed Reaction Mechanism of Synthesis of 3-Amino-5-fluoroalkylfurans

Conclusion

In summary, this book chapter documents various metal-free approaches developed over the past five years for the synthesis of poly-substituted furans. Several attractive catalytic methodologies – such as those involving iodine, *N*-heterocyclic carbenes (NHCs), and acids – have been reviewed, along with representative examples of substituted furans synthesised *via* these methods.

The corresponding mechanistic pathways for these transformations are also presented. Additional metal-free approaches, including phosphine-mediated synthesis, cycloaddition reactions, and multicomponent reactions, are discussed with relevant examples and mechanisms. Finally, two noteworthy methodologies based on the extended Corey–Chaykovsky reaction and thionyl chloride-mediated synthesis of substituted furans are explored. In conclusion, this chapter offers helpful information regarding the importance and recent advancements in the sustainable synthesis of substituted furan scaffolds, which serve as crucial building blocks in both synthetic and biological chemistry.

Acknowledgement

The author sincerely acknowledges Principal of Surendranath College and all the faculties of Department of Chemistry for extending their valuable help whenever needed. He also greatly acknowledges the generous financial support from the National Institute of Pharmaceutical Education and Research (NIPER)-Hajipur, Department of Pharmaceuticals, Ministry of Chemicals and Fertilizers, Govt. of India and Science and Engineering Research Board, Govt. of India for financial support (SERB Start-up Research Grant No. SRG/2023/001403).

References

- Chen, P., Cao, W., Li, X., & Shi, D. (2021). A Unified Approach for Divergent Synthesis of Heterocycles *via* TMSOTf-Catalyzed Formal [3+ 2] Cycloaddition of Electron-Rich Alkynes. *Advanced Synthesis & Catalysis*, 363(20), 4789-4794. <https://doi.org/10.1002/adsc.202100769>
- Deepthi, A., Babu, B. P., & Balachandran, A. L. (2019). Synthesis of furans—recent advances. *Organic Preparations and Procedures International*, 51(5), 409-442. <https://doi.org/10.1080/00304948.2019.1633228>

- Eicher, T., Hauptmann, S. & Speicher, A. (2003). *The Chemistry of Heterocycles: Structure, Reactions, Syntheses, and Applications*. 3rd Edn. Wiley-VCH. 215-254. <https://doi.org/10.1002/352760183Xed>
- Erguven, H., Zhou, C., & Arndtsen, B. A. (2021). Multicomponent formation route to a new class of oxygen-based 1, 3-dipoles and the modular synthesis of furans. *Chemical Science*, 12(45), 15077-15083. <https://doi.org/10.1039/D1SC04088J>
- Gubina, T. I., & Kharchenko, V. G. (1995). Furan and its derivatives in the synthesis of other heterocycles. *Chemistry of Heterocyclic Compounds*, 31(8), 900-916. <https://doi.org/10.1007/BF01170318>.
- Gulevich, A. V., Dudnik, A. S., Chernyak, N., & Gevorgyan, V. (2013). Transition metal-mediated synthesis of monocyclic aromatic heterocycles. *Chemical Reviews*, 113(5), 3084-3213. <https://doi.org/10.1021/cr300333u>
- Jana, A., Adhikary, N. D., & Pramanik, A. (2020). Graphene oxide (GO) catalysed MW-assisted one-pot synthesis of densely substituted furan. *Green Chemistry*, 22(13), 4304-4310. <https://doi.org/10.1039/D0GC00723D>
- Joule, J. A., & Mills, K. (2010). *Heterocyclic Chemistry*. (5th Edn), John Wiley & Sons. Retrieved from: <https://tech.chemistrydocs.com/Books/Organic/Heterocyclic-Chemistry-by-J-A-Joule-and-K-Mills-5th-Edition.pdf>. Accessed on 8th January 2025.
- Jung, C. K., Wang, J. C., & Krische, M. J. (2004). Phosphine-mediated reductive condensation of γ -acyloxy butynoates: A diversity-oriented strategy for the construction of substituted furans. *Journal of the American Chemical Society*, 126(13), 4118-4119. <https://doi.org/10.1021/ja049377l>
- Karlinskii, B. Y., & Ananikov, V. P. (2021). Catalytic C–H Functionalization of Unreactive Furan Cores in Bio-Derived Platform Chemicals. *ChemSusChem*, 14(2), 558-568. <https://doi.org/10.1002/cssc.202002397>
- Khaghaninejad, S., & Heravi, M. M. (2014). Paal–Knorr reaction in the synthesis of heterocyclic compounds. In *Advances in Heterocyclic Chemistry*, 111, 95-146. Academic Press. <https://doi.org/10.1016/B978-0-12-420160-6.00003-3>
- Komogortsev, A. N., Melekhina, V. G., Lichitsky, B. V., & Minyaev, M. E. (2020). Novel one-pot approach to 2-aminofuran derivatives via multicomponent reaction of 3-hydroxy-4H-pyran-4-ones, α -ketoaldehydes and methylene active nitriles. *Tetrahedron Letters*, 61(41), 152384. <https://doi.org/10.1016/j.tetlet.2020.152384>
- Kondoh, A., Aita, K., Ishikawa, S., & Terada, M. (2020). Synthesis of tetrasubstituted furans through one-pot formal [3+ 2] cycloaddition utilizing [1, 2]-phospha-Brook rearrangement. *Organic Letters*, 22(5), 2105-2110. <https://dx.doi.org/10.1021/acs.orglett.0c00619>
- Kuroda, H., Hanaki, E., & Kawakami, M. (1999). A convenient method for the preparation of furans by the phosphine-initiated reactions of enynes bearing a carbonyl group. *Tetrahedron Letters*, 40(19), 3753-3756. [https://doi.org/10.1016/S0040-4039\(99\)00601-2](https://doi.org/10.1016/S0040-4039(99)00601-2)
- Li, J. J. (2009). Paal–Knorr furan synthesis. In *Name Reactions*. Springer, Berlin, Heidelberg. 440-441. https://doi.org/10.1007/978-3-642-01053-8_188

Sustainable Synthesis of Substituted Furans

- Li, M., & Zhou, W. (2020). Transition-Metal-Free Synthesis of Trifluoromethylated Furans via a Bu₃P-Mediated Tandem Acylation–Wittig Reaction. *Synlett*, 31(20), 2035-2038. <https://doi.org/10.1055/s-0040-1707263>
- Li, N., Li, C., Zhou, Q., Zhang, X., Deng, Z., Jiang, Z. X., & Yang, Z. (2025). General access to furan-substituted gem-difluoroalkenes enabled by PFTB-promoted cross-coupling of ene-yne-ketones and difluorocarbene. *Chemical Science*, 16(3), 1455-1464. <https://doi.org/10.1039/D4SC08247H>
- Liu, H. X., Ji, F., Chen, Y., Gao, Y., Wang, J. K., Zhang, M. Z., ... & Sha, Q. (2021). De Novo and Divergent Synthesis of Highly Functionalized Furans by Cascade Reactions of 2-Hydroxy-1, 4-diones with Nucleophiles. *Chemistry–A European Journal*, 27(16), 5225-5229. <https://doi.org/10.1002/chem.202005098>
- Maity, S., & Panda, N. (2025). Synthesis of Substituted Furans from β -Ketoanilides Using Ethylene Glycol as C2-Precursor. *Asian Journal of Organic Chemistry*. <https://doi.org/10.1002/ajoc.202400706>
- Pace, D. P., Robidas, R., Tran, U. P., Legault, C. Y., & Nguyen, T. V. (2021). Iodine-catalyzed synthesis of substituted furans and pyrans: reaction scope and mechanistic insights. *The Journal of Organic Chemistry*, 86(12), 8154-8171. <https://doi.org/10.1021/acs.joc.1c00608>
- Peng, Y., Luo, J., Feng, Q., & Tang, Q. (2016). Understanding the Scope of Feist–Bénary Furan Synthesis: Chemoselectivity and Diastereoselectivity of the Reaction Between α -Halo Ketones and β -Dicarbonyl Compounds. *European Journal of Organic Chemistry*, 2016(30), 5169-5179. <https://doi.org/10.1002/ejoc.201600975>
- Plaçais, C., Donnard, M., Panossian, A., Vors, J. P., Bernier, D., Pazenok, S., & Leroux, F. R. (2021). Synthesis of 3-amino-5-fluoroalkylfurans by intramolecular cyclization. *Organic Letters*, 23(12), 4915-4919. <https://doi.org/10.1021/acs.orglett.1c01672>
- Romo, J. E., Bollar, N. V., Zimmermann, C. J., & Wettstein, S. G. (2018). Conversion of sugars and biomass to furans using heterogeneous catalysts in biphasic solvent systems. *ChemCatChem*, 10(21), 4805-4816. <https://doi.org/10.1002/cctc.201800926>
- Saeid, H., Al-sayed, H., & Bader, M. (2023). A review on biological and medicinal significance of furan. *AlQalam Journal of Medical and Applied Sciences*, 44-58. <https://doi.org/10.5281/zenodo.7650255>
- Shcherbakov, R. O., Myasnikov, D. A., Trushkov, I. V., & Uchuskin, M. G. (2023). Extended Version of the Corey–Chaykovsky Reaction: Synthesis of 2, 4-Substituted Furans by the Treatment of β -Dialkylamino Chalcones with Dimethylsulfonium Methylide. *The Journal of Organic Chemistry*, 88(13), 8227-8235. <https://doi.org/10.1021/acs.joc.3c00203>
- Tönjes, J., Medvarić, V., & Werner, T. (2024). Synthesis of trisubstituted furans from activated alkenes by P (III)/P (V) redox cycling catalysis. *The Journal of Organic Chemistry*, 89(15), 10729-10735. <https://doi.org/10.1021/acs.joc.4c00985>
- Wang, J., Zheng, M., Jia, Q., Ren, Q., & Wu, J. (2024). Synthesis of Highly Substituted Furans via Intermolecular Enynone-Aldehyde Cross-Coupling/Cyclization Catalyzed by N-Heterocyclic Carbenes. *Organic Letters*, 26(23), 4868-4872. <https://doi.org/10.1021/acs.orglett.4c01253>
- Wang, X., Peng, Y., Zheng, J., & Li, W. D. Z. (2024). Diversified Reactivity of Triphenylphosphine: Reinvestigation of the Phosphine-Mediated Reductive Condensation Approach for the

- Synthesis of Substituted Furans. *The Journal of Organic Chemistry*, 89(17), 12795-12799. <https://doi.org/10.1021/acs.joc.4c01336>
- Wang, Y., Luo, Y. C., Hu, X. Q., & Xu, P. F. (2011). A powerful cascade approach for expeditious synthesis of trifluoromethylated furans. *Organic Letters*, 13(19), 5346-5349. <https://doi.org/10.1021/ol2022092>
- Wang, Y., Tao, L., Chen, J., He, W., Deng, H., Shao, M., ... & Cao, W. (2019). Isocyanide-Based Multicomponent Reactions: A Concise Approach to 2-Amino-3-perfluoroalkylfurans Using Methyl Perfluoroalk-2-ynoates as Fluorinated Building Blocks. *Asian Journal of Organic Chemistry*, 8(5), 710-715. <https://doi.org/10.1002/ajoc.201900010>
- You, C., Zhang, Z., Tu, Y., Tang, H., Wang, Y., Long, D., & Zhao, J. (2020). Transition-metal-free approach to polysubstituted furans. *The Journal of Organic Chemistry*, 85(5), 3902-3910. <https://dx.doi.org/10.1021/acs.joc.9b03006>
- Zhang, Z., Huang, A., Ma, L., Xu, J. H., & Zhang, M. (2022). A facile metal-free one-flask synthesis of multi-substituted furans via a BF₃·Et₂O mediated formal [4+ 1] reaction of 3-chloro-3-phenyldiazirines and α , β -alkenyl ketones. *RSC Advances*, 12(24), 15190-15195. <https://doi.org/10.1039/D2RA01472F>

Clerodendrum: A Useful Beneficial Phytomedicinal Plant

Dora Das¹, Sirshendu Chatterjee², Shamba Chatterjee¹, Sucheta Das^{1*}

¹Department of Biotechnology, Haldia Institute of Technology, ICARE Complex, Hatiberia, Haldia, East Midnapur, West Bengal 721657, India

²Department of Biotechnology, Techno India University, Saltlake, Kolkata, West Bengal 700091, India

*Corresponding author: sucheta.bt@gmail.com

Abstract

The genus *Clerodendrum* belongs to the Lamiaceae (Verbenaceae) family of flowering plants. It is indigenous to both tropical and warm temperate regions of the planet. The majority of the species are found in tropical Africa and southern Asia. To date, numerous species of this genus have been documented in indigenous medical systems and are utilised to make traditional remedies for a range of serious illnesses. More than 11 species of the *Clerodendrum* genus, ranging in number from 150 to 500, have had their chemical composition and biological activities thoroughly examined. Of these, 283 compounds have been isolated and identified, including monoterpene and its derivatives, sesquiterpene, diterpenoids, triterpenoids, flavonoid and flavonoid glycosides, phenylethanoid glycosides, steroids and steroid glycosides, cyclohexylethanoids, anthraquinones, cyanogenic glycosides, and others. In many parts of the world, including India, China, Korea, Japan, Thailand, and Africa, it is used as folk and traditional medicine to treat a wide range of illnesses, including colds, hyperpyrexia, asthma, furunculosis, hypertension, rheumatism, dysentery, mastitis, toothaches, anorexia, leucoderma, leprosy, arthrophlogosis, and other inflammatory diseases. The majority of the isolated phytochemicals of the genus were reported from *C. serratum*, *C. inerme*, *C. bungei*, *C. incisum*, *C. infortunatum*, and *C. trichotomum*. Aerial parts, roots, and leaves were the most often investigated targets for bioactive principles. In this review article we have tried to summarise the medicinal benefits obtained from different parts of different species of this useful medicinal plant so far.

Keywords: Antimicrobial Properties; Antioxidant Activity; *Clerodendrum*; Medicinal Plants; Phytochemicals; Phytomedicine

Introduction

Around 80% of people worldwide, particularly in developing nations, rely on herbal medicines to address their healthcare needs, according to the World Health Organisation (WHO). Folk medicine, which is based on bioactive substances found in plants and animals and used by many ethnic groups, especially those who (indigenous peoples) don't have easy access to western medicine is studied and compared in ethnomedicine. Ancestral Hindu books like the Shushrut Samhita, the Atharva Veda, and the Charak Samhita all talk about a lot of plants that are used for medicine. Despite the fact that medicinal herbs have been utilised for thousands of years, only in the last few decades has scientific research on their positive benefits become more prominent. Numerous therapeutic phytomolecules found in these plants have been shown to have therapeutic use (Khushali *et al.*, 2020). Flowering plants in

Converging Chemical and Biological Sciences for a Sustainable Era

Clerodendrum as a Phytomedicinal Plant

the genus *Clerodendrum* belong to the Lamiaceae (Verbenaceae) family. Glorybower, bleeding-heart, and bag flower are some of its common names. The world's tropical and warm temperate zones are home to *Clerodendrum*. Estimates of its species range widely, from roughly 150 (Sharma, Verma & Jha, 2022) to 500 (Wang *et al.*, 2018). The vast majority of the species are located in tropical Africa, Eastern and southern Asia and northern Australia.

Linnaeus first defined this genus in 1753, using the Indian species *Clerodendrum infortunatum*. Around 1763, Adanson modified the Latinised name "*Clerodendrum*" to its Greek equivalent, "*Clerodendron*". After over two centuries, in 1942, Moldenke readopted the Latinised word "*Clerodendrum*," which is now widely employed by taxonomists for genus classification and description. According to progressive studies the genus *Clerodendrum*, which was once categorised in the Verbenaceae, is now considered to be part of the Lamiaceae. The species is commonly known by its scientific synonym, *Rotheca serrata* (L.) (Harley *et al.*, 2004; Mabberley, 2008), *Clerodendrum* species exhibit a great deal of variety in their morphology, cytology, and chemistry. Approximately eighteen formulas, including the Ayurvedic Pharmacopoeia of India and conventional texts, were the very initial sources that searched for *C. serratum* roots as one of the ingredients (estimated from 0.14%w/w to 7.69%w/w) for therapy of multiple medical conditions. The most prevalent titles for the roots of *C. serratum* are Blue Glory or Beetle Killer in English and Bharangi (meaning glorious) in Hindi. Asthma, chronic inflammation, and viral diseases have traditionally been treated using *C. serratum* as conventional medicine. The shoot sample of *C. colebrookianum* yielded a total of forty-four phytoconstituents, the majority of which are beneficial substances for normal growth and development (Yuan *et al.*, 2010). Considerable antibacterial efficacy against microorganisms which have become resistant to medication, especially *E. coli* and *S. aureus*, is demonstrated by the extract of dried leaf powder of *Clerodendrum infortunatum* in several solvents. In Northeast Indian communities and Chinese traditional medicine, *Clerodendrum glandulosum* Lindl is well-known for its traditional herbal medicines and medicinal qualities. A wide range of illnesses are treated including hypertension, diabetes, and other metabolic disorders, due to its numerous pharmacological qualities, which include antihypertensive, hypolipidaemic, hepatoprotective, anti-inflammatory, and neuroprotective effects. Most of the genus's isolated phytochemicals have been discovered from *C. trichotomum*, *C. serratum*, *C. inerme*, *C. bungei*, *C. indium*, and *C. infortunatum*.

In this review article we have tried to summarise the medicinal benefits obtained from different parts of different species of this useful medicinal plant so far.

Pharmacological Effects

A growing number of investigations revealed that active compounds or extracts derived from *Clerodendrum* species demonstrated a broad spectrum of pharmacological actions (Harley *et al.*, 2004). Numerous clinical applications of the genus *Clerodendrum* in traditional Chinese medicine have motivated scientists to look into its pharmacological characteristics and confirm the usage of several species as medicinal remedies (Mabberley, 2008).

Antimicrobial Activity

i) Antibacterial effect

Bacillus subtilis, *Salmonella typhi*, *Staphylococcus aureus*, *Escherichia coli*, *Proteus mirabilis* and *Klebsiella pneumoniae* are all inhibited by the methanolic extract of *C. siphonanthus*. Both the water extract and n-butyl extracts from *C. bungei* demonstrated strong antibacterial activity against *Fusarium graminearum*, *Micrococcus pyogenes*, and *Staphylococcus aureus* respectively (Chae *et al.*, 2006).

ii) Anti-fungal effect

The majority of fungi were inhibited in their growth by *C. inerm* ethyl acetate extract (Kim *et al.*, 2009). Extracts of *C. infortunatum* in ethyl acetate and chloroform inhibited the growth of *K. pneumonia*, *S. aureus*, *E. coli*, and *B. subtilis*.

iii) Anti-plasmodial activity

Aqueous extracts, methanol and ethyl acetate extracts from *C. rotundifolium* prevented *Plasmodium falciparum* strains NF54 and FCR3 from growing.

iv) Anti-viral activity

The bioactive phytochemicals that were isolated from various *Clerodendrum* species showed potential in combatting some of the most pathogenically relevant viruses, including the Chikungunya Virus (CHIKV), Japanese Encephalitis Virus (JEV), Influenza Virus, Hepatitis C Virus (HCV), Herpes Simplex Virus (HSV), Human Immunodeficiency Virus (HIV) and Severe Acute Respiratory Syndrome-Corona Virus-2 (SARS-CoV-CoV-2).

Anti-Inflammatory and Anti-Nociceptive Activities

Numerous investigations have illustrated the anti-inflammatory qualities of extracts of aerial parts, roots, leaves, and stems from *C. laevifolium*, *C. phlomidis*, *C. petasites*, *C. inerme*, *C. bungei*, and *C. serratum*. Methanolic extract of *C. indicum* has strong antiulcer properties that prevent stomach ulceration when used to treat aspirin-induced ulcers (Sinha *et al.*, 1981). Significant decreases in acid secretory measures, including total acidity, total acid production, and gastric secretion volume, were also noted. According to a histopathological analysis. *C. indicum* extract eliminated *H. pylori* infections and decreased stomach damage (Wang *et al.*, 2018)

Activity against Diarrhoea

Methanolic extract and chloroform fraction from the *C. indicum* and Methanolic extract from the leaves of *C. phlomidis* inhibited defecation in castor oil-induced diarrhoea (Xu *et al.*, 2014). It has been suggested that the antidiarrheal effect of *C. wallichii*'s hydroalcohol extract and its chloroform fraction among other things, is caused by the flavonoid concentration (Kundan & Mahamedha, 2020). The preliminary phytochemical screening of methanolic root extracts of *Clerodendrum viscosum* showed the presence of flavonoids, phenolic compounds, alkaloids, tannin, steroids, glycosides and coumarins. it can be said that the root of *Clerodendrum viscosum* is a potential source of drugs for antidiarrheal activity.

Anti-Obesity Activity

Clerodendron glandulosum. Coleb. confirming its long-standing therapeutic application in the management of obesity by downregulation of PPAR γ -2 related genes and Lep expression. Due to the inhibition of pancreatic lipase activity, which postpones the intestinal absorption of dietary fat, methanolic extract of *Clerodendrum phlomidis* has demonstrated a potent anti-obesity action (Blackadar, 2016). In vitro investigations verified that pancreatic lipase function was inhibited (Jadeja *et al.*, 2011). SGOT, SGPT, TG, TC, LDL-c, glucose, insulin, pancreatic lipase activity, adiposity diameter, food consumption, body weight, and adiposity index were all reduced by the methanolic extract of *C. phlomidis*.

Memory Boosting Effects

Methanolic extract from *C. infortunatum* leaves demonstrated promising memory-enhancing qualities. It is likely that the extract will be used to create a potential nootropic to prevent dementia senilis. The pharmacological analyses of *Clerodendrum serratum*'s methanolic extract demonstrated its anti-amnesic properties (Akihisa *et al.*, 1990). The high flavonoid content of *Clerodendrum serratum*'s ethanol extract, particularly its luteolin and apigenin, gives it strong antioxidant potential and may have neuroprotective benefits. It stops the development of many illnesses brought on by oxidative stress or slows its progression. For the treatment of neurological conditions, ethanol extracts from the *C. serratum* plant may be suggested as a supplement to synthetic antidepressant medications (Jadeja *et al.*, 2011).

Activity Against Free Radicals and Antioxidant

By-products like free radicals and reactive oxygen species (ROS) are continuously produced *in vivo* for both specific metabolic processes and "accidents of chemistry". *C. serratum* aerial parts ethanol extract show strong antioxidant activity against 1,1 diphenyl, 2 picryl hydrazyl (DPPH) and nitric oxide radical, whereas *Clerodendrum serratum* root extract demonstrated significant antioxidant activity against DPPH. Comparing the ethanol extract of *Clerodendrum phlomidis* roots to petroleum ether, chloroform & ethyl acetate the former had the highest level of free radical scavenging activity (Muthu *et al.*, 2013). Higher levels of free radical and antioxidant activity were demonstrated by the methanolic extract of *Clerodendrum inerme* leaves. In addition to damaging biological molecules like DNA, lipids and proteins, ROS has a high reactive potential and is the cause of numerous human diseases, including diabetes, cancer, viral infections, cardiovascular disorders, and infections (Aung *et al.*, 2017).

Anticancerous Activity

A condition known as cancer occurs when cells in the body multiply unchecked. It can appear anywhere in the human body. With a 49.9% incidence and the second-highest crude death rate of 12.9% among the 36 cancer forms, breast cancer is the most common type (Wang *et al.*, 2018). Though variety of anticancer drugs have been created to target the molecular processes that cause cancer, there hasn't been any appreciable rise in cancer patients' overall survival rate (Shrivastava & Patel, 2007). Advancements in cancer treatment, including surgery, radiotherapy, chemotherapy, immunotherapy, targeted

therapy, vaccines, combination therapy and stem cell transformation therapy, have been significant but not fully curable due to their high costs and adverse effects. The WHO estimates that one-third of the world's population lacks regular access to modern, necessary medical care (Cao *et al.*, 2024). It has been shown that many cancer patients are receiving their primary treatment from traditional drugs. The National Cancer Institute (NCI) conducted research on medicinal plants and ethno medicine for cancer treatment, analysing 114,000 extracts from 35,000 plant samples from 20 nations. Anticancer drugs can cause adverse effects like heart disease, immunosuppression, mental disorders, decreased blood production, gastrointestinal tract inflammation, and hair loss due to their targeting of both malignant and fast-proliferating cells. Certain natural and manufactured chemicals are effective in cancer chemoprevention. Radiation therapy and chemotherapy are currently used to treat cancer, but they are very costly and can have serious negative effects on patients (Blackadar, 2016). Natural products have been utilised significantly in cancer treatments in recent years to minimise the expense and harmful consequences of radiation and chemotherapy (Cao *et al.*, 2024). There are many distinct phytochemicals found in plants, and more than 75% of drugs used to treat various diseases come from plants. The behaviour of cancer cells and the microenvironment may be altered by natural antioxidants derived from plants. The hill glory bower, *C. viscosum* also known as *Clerodendrum infortunatum*, has long been used as a key Ayurvedic medicinal plant material. Based on some reports, *C. viscosum* can help with intestinal infections, renal failure, snake bites, scorpion stings, and a variety of skin-related issues. *C. serratum* extract in methanol inhibited tumour development. Flavonoids in total from *C. bungi* suppressed the HepG2 cell (Kyaw *et al.*, 2022).

Other Activities

The prospective neurological protective properties of acetin, a flavonoid that is derived from *C. inerme* were evaluated. The ethanolic extract of *C. petasite* showed a substantial relaxing effect on the tracheal smooth muscle. Acacetin was found to suppress the cytosolic free Ca^{2+} concentration and glutamate release triggered by depolarisation in the hippocampus nerve terminals. Methanolic extracts of *C. philmidis* leaves are responsible for a reduction in spontaneous activity. It also decreased exploratory behavioural characteristics. On being separated, the active ingredient was found to be the flavonoid hispidulin. The finding suggested that hispidulin might help treat conditions linked to asthma. For the first time, Huang *et al.* (2015), showed that hispidulin extracted from the dichloromethane and n-hexane fractions of *C. inerme* ethanol extract dramatically decreased hyperdopaminergic diseases.

Conclusion

Safety, effectiveness, and herbal supplement quality supervision have become crucial issues due to the massive global growth in the use of traditional medicine. The chemical components of the genus *Clerodendrum* have been identified and isolated in the current review. Pharmacological studies have shown that the genus's crude extracts and some unique monomer compounds have a variety of biological activities, including anti-inflammatory and antinociceptive, antioxidant, anticancer, antimicrobial, antihypertensive, anti-obesity,

Clerodendrum as a Phytomedicinal Plant

antidiarrheal, hepatoprotective, memory-enhancing and neuroprotective properties. This plant has the capacity to produce antioxidants, which could result in the creation of innovative phytomedicine. This study proposes that the compound of the plant *Clerodendrum indicum* could be employed as a lead compound in the development of powerful pills for the treatment of a variety of ailments. Only a small number of the more than 400 species of the genus *Clerodendrum* have been thoroughly examined and researched to date. Phytochemically and physiologically, many additional species are completely unknown. Keeping an eye on these species could be crucial to finding novel bioactive substances.

Acknowledgment

Authors express their appreciation to the Department of Biotechnology, Haldia Institute of Technology, India for providing access to the resources and research facilities that made this work possible.

References

- Akihisa, T., Ghosh, P., Thakur, S., Nagata, H., Tamura, T., & Matsumoto, T. (1990). 24, 24-Dimethyl-25-dehydrolophenol, a 4 α -methylsterol from *Clerodendrum inerme*. *Phytochemistry*, 29(5), 1639-1641. [https://doi.org/10.1016/0031-9422\(90\)80137-6](https://doi.org/10.1016/0031-9422(90)80137-6)
- Aung, T. N., Qu, Z., Kortschak, R. D., & Adelson, D. L. (2017). Understanding the effectiveness of natural compound mixtures in cancer through their molecular mode of action. *International Journal of Molecular Sciences*, 18(3). <https://doi.org/10.3390/ijms18030656>
- Blackadar, C. B. (2016). Historical review of the causes of cancer. *World Journal of Clinical Oncology*, 7(1). <https://doi.org/10.5306/wjco.v7.i1.54>
- Cao, W., Qin, K., Li, F., & Chen, W. (2024). Comparative study of cancer profiles between 2020 and 2022 using global cancer statistics (GLOBOCAN). *Journal of the National Cancer Center*, 4(2), 128-134. <https://doi.org/10.1016/j.jncc.2024.05.001>
- Chae, S., Kang, K. A., Kim, J. S., Hyun, J. W., & Kang, S. S. (2006). Trichotomoside: a new antioxidative phenylpropanoid glycoside from *Clerodendron trichotomum*. *Chemistry & biodiversity*, 3(1), 41-48. <https://doi.org/10.1002/cbdv.200690005>
- Harley, R. M., Atkins, S., Budantsev, A. L., Cantino, P. D., Conn, B. J., Grayer, R., *et al.* (2004). Labiatae. In J. W. Kadereit (Ed.), *The Families and Genera of Vascular Plants: Volume VII. Flowering Plants: Dicotyledons. Lamiales (except Acanthaceae including Avicenniaceae)* (pp. 167–275). Springer. https://doi.org/10.1007/978-3-642-18617-2_11
- Huang, W. J., Lee, H. J., Chen, H. L., Fan, P. C., Ku, Y. L., & Chiou, L. C. (2015). Hispidulin, a constituent of *Clerodendrum inerme* that remitted motor tics, alleviated methamphetamine-induced hyperlocomotion without motor impairment in mice. *Journal of Ethnopharmacology*, 166, 18-22. <https://doi.org/10.1016/j.jep.2015.03.001>
- Jadeja, R. N., Thounaojam, M. C., Ramani, U. V., Devkar, R. V., & Ramachandran, A. V. (2011). Anti-obesity potential of *Clerodendron glandulosum*. Coleb leaf aqueous extract. *Journal of Ethnopharmacology*, 135(2), 338-343. <https://doi.org/10.1016/j.jep.2011.03.020>

- Khushali U., Elizabeth R., Denni M., & Darshee B. (2020) Recent Scenario of Medicinal Plants of India in Cancer Therapeutics. *Interwoven: An Interdisciplinary Journal of Navrachana University*, 3(2), 25-42. Retrieved from: https://nuv.ac.in/wp-content/uploads/pdf/interwoven/issue/Volume3_12.pdf, Accessed on 16th August 2024.
- Kim, K. H., Kim, S., Jung, M. Y., Ham, I. H., & Whang, W. K. (2009). Anti-inflammatory phenylpropanoid glycosides from *Clerodendron trichotomum* leaves. *Archives of pharmacal research*, 32, 7-13. <https://doi.org/10.1007/s12272-009-1112-6>
- Kundan, S. B., & Mahamedha, D. (2020) Evaluation of Anti-Diarrheal Potential of *Clerodendrum Wallichii* (Merr.) Leaves. *Open Access Journal of Pharmaceutical Research (OAJPR)*, 4(1), <https://doi.org/10.23880/oajpr-16000193>
- Kyaw, E. H., Iwasaki, A., Suenaga, K., & Kato-Noguchi, H. (2021). Phytotoxic activity of *Clerodendrum indicum* (L.) Kuntze and its potential phytotoxic substance. *Emirates Journal of Food and Agriculture*, 33(10), 884-892. <https://doi.org/10.9755/ejfa.2021.v33.i10.2779>
- Mabberley, D. J. (2008). *Mabberley's Plant-Book: A Portable Dictionary of Plants, Their Classifications and Uses* (3rd ed.). CABI. Retrieved from: <https://www.cabidigitallibrary.org/doi/full/10.5555/20083188502>, Accessed on 18th August 2024.
- Muthu, C., Baskar, K., Ignacimuthu, S., & Al-Khaliel, A. S. (2013). Ovicidal and oviposition deterrent activities of the flavonoid pectolinarigenin from *Clerodendrum phlomis* against *Earias vittella*. *Phytoparasitica*, 41, 365-372. <https://doi.org/10.1007/s12600-013-0296-y>
- Sharma, H., Verma, A. K., & Jha, K. P. (2022). A Brief Study on Medicinal Plant *Clerodendrum* Species: A Review Article. *International Journal of Pharmaceutical Research and Applications*, 7(3), 440-442. Retrieved from: https://ijprajournal.com/issue_dcp/A%20Brief%20Study%20on%20Medicinal%20Plant%20Clerodendrum%20Species%20A%20Review%20Article.pdf, Accessed on 16th August 2024.
- Shrivastava, N., & Patel, T. (2007). *Clerodendrum* and healthcare: an overview. *Medicinal and Aromatic Plant Science and Biotechnology*, 1(1), 142-150. Retrieved from: <https://shorturl.at/o9iZC>, Accessed on 18th August 2024.
- Sinha, N. K., Seth, K. K., Pandey, V. B., Dasgupta, B., & Shah, A. H. (1981). Flavonoids from the flowers of *Clerodendron infortunatum*. *Planta Medica*, 42(07), 296-298. <https://doi.org/10.1055/s-2007-971645>
- Wang, J. H., Luan, F., He, X. D., Wang, Y., & Li, M. X. (2018). Traditional uses and pharmacological properties of *Clerodendrum* phytochemicals. *Journal of Traditional and Complementary Medicine*, 8(1), 24-38. <https://doi.org/10.1016/j.jtcme.2017.04.001>
- Xu, R. L., Wang, R., Ha, W., & Shi, Y. P. (2014). New cyclohexylethanoids from the leaves of *Clerodendrum trichotomum*. *Phytochemistry Letters*, 7, 111-113. <https://doi.org/10.1016/j.phytol.2013.10.010>
- Yuan, Y. W., Mabberley, D. J., Steane, D. A., & Olmstead, R. G. (2010). Further disintegration and redefinition of *Clerodendrum* (Lamiaceae): implications for the understanding of the evolution of an intriguing breeding strategy. *Taxon*, 59(1), 125-133. <https://doi.org/10.1002/tax.591013>

Investigating Materials for Green Hydrogen Generation with Potential and Challenges in Biological Hydrogen Production

Aniruddha Mondal^{1*}, Prasenjit Mandal², Amit Kumar Kundu³, Shib Shankar Biswas⁴

¹Department of Chemistry, Harindanga High School, Harindanga, Falta, West Bengal, 743504 India

²Department of Chemistry, Santipur College, Nadia, West Bengal, 741404 India

³Department of Chemistry, Sripat Singh College, Jiaganj, Murshidabad, West Bengal, 742123 India

⁴Department of Physics, Surendranath College, 24/2, Mahatma Gandhi Road, Kolkata, West Bengal, 700009 India

*Corresponding Author's E-mail: aniruddha.chem007@gmail.com

Abstract

The global pursuit of sustainable and clean energy sources has intensified interest in green hydrogen production, particularly through biological methods that offer eco-friendly alternatives to conventional technologies. This review investigates the potential of various materials and strategies used in biological hydrogen production, including phototrophic and fermentative pathways involving algae, cyanobacteria, and photosynthetic bacteria. Special emphasis is placed on the role of advanced nanomaterials and bio-catalysts that enhance the efficiency and scalability of hydrogen generation processes. Key materials such as metal-based catalysts, semiconductor photocatalysts, and carbon-based nanostructures are explored for their roles in optimising biological pathways and improving electron transfer mechanisms. Additionally, the paper discusses integrated systems that couple biological processes with engineered materials to boost hydrogen yields. Despite promising advancements, several challenges hinder large-scale application, including low production rates, oxygen sensitivity of hydrogenase enzymes, and difficulties in reactor design and process optimisation. Addressing these barriers requires multidisciplinary efforts involving material science, microbiology, and process engineering. This review provides a comprehensive overview of the state-of-the-art materials and methodologies, offering insights into their potential and limitations, and proposes future research directions to overcome existing challenges for viable, sustainable hydrogen production from biological sources.

Keywords: *Bio-catalysts; Biological Hydrogen Production; Green Hydrogen; Photocatalysis; Sustainable Energy; Waste-to-Energy*

Introduction

As the global demand for clean and renewable energy grows, hydrogen has emerged as a key player in the transition to a sustainable energy future (Hassan *et al.*, 2024). Hydrogen, the most abundant element in the universe, can be utilised as a clean energy carrier due to its high energy density and versatility (Zhang *et al.*, 2024a). When used as a fuel, hydrogen

Converging Chemical and Biological Sciences for a Sustainable Era

Green Hydrogen Generation: Materials, Potential, and Challenges

emits only water as a byproduct, making it an attractive alternative to fossil fuels. The potential of hydrogen as a clean energy source extends across multiple sectors, including transportation, power generation, and industrial processes, offering a pathway to significant reductions in carbon emissions and air pollution (Hassan *et al.*, 2024, Ofélia de Queiroz *et al.*, 2024).

Among various forms of hydrogen, "green hydrogen" is produced using renewable energy sources, such as solar, wind, or hydropower, ensuring minimal environmental impact (Figure 1) (Nnabuife *et al.*, 2024). Unlike "gray hydrogen," which is produced from natural gas and results in substantial carbon emissions, and "blue hydrogen," which relies on carbon capture technologies, green hydrogen is considered a truly sustainable solution (Saha *et al.*, 2024). It aligns with the global efforts to achieve carbon neutrality and mitigate climate change, particularly as nations set ambitious targets for reducing their reliance on fossil fuels. Green hydrogen has the potential to revolutionise energy systems by enabling long-term energy storage, decarbonizing heavy industries such as steel and cement production, and facilitating the widespread adoption of hydrogen fuel cells in transportation (Zaiter *et al.*, 2024). Additionally, hydrogen can play a crucial role in balancing electricity grids by storing excess renewable energy and releasing it during periods of high demand. As the world transitions to a low-carbon economy, green hydrogen is expected to become an integral component of future energy infrastructures, supporting both energy security and environmental sustainability.

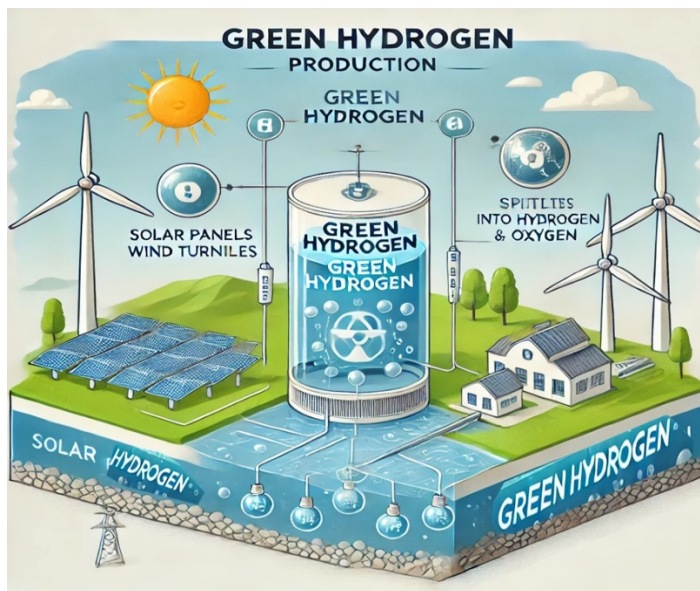


Figure 1: Schematic Diagram of Green Hydrogen Production (Source: Author)

The production of green hydrogen can be achieved through various methods, each utilising renewable energy to split water molecules (H_2O) into hydrogen (H_2) and oxygen (O_2) (Worku *et al.*, 2024). Electrolysis process involves the use of electricity generated from renewable

sources to split water into hydrogen and oxygen in an electrolyser (Akyüz, Telli & Farsak, 2024). There are different types of electrolysis, including alkaline electrolysis, proton exchange membrane (PEM) electrolysis, and solid oxide electrolysis (Sebbahi *et al.*, 2024). Among these, PEM electrolysis is widely researched due to its high efficiency and compatibility with intermittent renewable energy sources like solar and wind power (Kumar & Samuel, 2024). Photocatalytic water splitting sunlight leverages to drive the reaction that separates water into hydrogen and oxygen. This method relies on the development of efficient photocatalysts, such as semiconductors, that can absorb sunlight and convert it into chemical energy. Although still in the research and development phase, photocatalysis represents a promising route for large-scale, low-cost hydrogen production in the future (Ahmed *et al.*, 2024). Biological hydrogen production is gaining attention as a green and sustainable alternative to conventional methods (Ahmad *et al.*, 2024a). This approach harnesses the natural abilities of microorganisms to produce hydrogen through various biological processes. The key biological methods for hydrogen production include biophotolysis, dark fermentation, and microbial electrolysis.

Biological hydrogen production offers several advantages, such as the use of renewable feedstocks, low energy requirements, and minimal environmental impact (Jain *et al.*, 2024). Unlike electrolysis, which requires significant amounts of electricity, or photocatalysis, which depends on advanced materials, biological methods utilise naturally occurring biological systems, making them inherently sustainable. Furthermore, these methods align with circular economy principles by utilising waste materials, such as agricultural residues or wastewater, as feedstocks for hydrogen production. Biophotolysis is a process where photosynthetic microorganisms, such as cyanobacteria and green algae, use sunlight to split water molecules, producing hydrogen and oxygen (Kossalbayev *et al.*, 2024). This method mimics natural photosynthesis but redirects the energy to produce hydrogen instead of biomass. However, the efficiency of biophotolysis is currently limited by the low hydrogen yield and the oxygen sensitivity of the hydrogen-producing enzymes (hydrogenases) involved in the process (Ram, Rani & Kumar, 2024). Dark fermentation involves the anaerobic digestion of organic matter by microorganisms to produce hydrogen (Srivastava *et al.*, 2024). This process can occur in the absence of light, making it more flexible than biophotolysis. Various organic substrates, such as food waste, agricultural residues, and industrial effluents, can be used as feedstock. Although dark fermentation has shown potential for large-scale applications (Ahmad *et al.*, 2024b), the hydrogen yield is often limited, and additional treatment of byproducts, such as organic acids, is required. Microbial electrolysis cells (MECs) represent a hybrid approach that combines biological activity with electrochemical processes (Arun *et al.*, 2024). In MECs, microorganisms oxidise organic matter and release electrons, which are used to reduce protons and produce hydrogen at the cathode. MECs offer a promising route for integrating biological and electrochemical methods, but challenges such as the need for external power inputs and low hydrogen production rates still need to be addressed.

Biological hydrogen production holds great promise for contributing to a sustainable energy future, particularly by enabling the conversion of organic waste into clean energy. The simplicity and potential cost-effectiveness of biological systems make them attractive for

both developed and developing regions. Moreover, advances in synthetic biology and metabolic engineering have opened new avenues for optimising microorganisms for hydrogen production, enhancing their efficiency, and overcoming the limitations of traditional biological methods. However, several challenges remain in the widespread adoption of biological hydrogen production (Jiao *et al.*, 2024). These include the low efficiency of natural processes, the complexity of scaling up laboratory systems to industrial levels, and the economic feasibility of large-scale implementation. Additionally, maintaining optimal conditions for microbial growth and hydrogen production, such as temperature, pH, and nutrient availability, can be challenging in real-world environments. Hydrogen has the potential to play a transformative role in achieving global sustainability goals, and biological hydrogen production offers a promising and environmentally friendly pathway for green hydrogen generation. However, further research and development are essential to overcome the existing obstacles and unlock the full potential of this technology. This paper will explore the opportunities and challenges in biological hydrogen production, highlighting innovative approaches and future directions for this field.

Literature Review

The growing urgency to transition towards a low-carbon economy has prompted a surge in research focused on sustainable hydrogen production. Green hydrogen, produced through methods that utilise renewable resources and have minimal environmental impact, stands at the forefront of these efforts. Various materials and processes have been developed for green hydrogen production, including advanced photocatalysts, electrochemical materials, enzymes, and biological systems (Alinejad *et al.*, 2024). This section provides an in-depth overview of the key materials and methods used in green hydrogen production, focusing on the role of biological hydrogen production processes and recent technological advances.

The materials used in hydrogen production play a critical role in determining the efficiency, scalability, and environmental impact of the process (Chelvam *et al.*, 2024). These materials can be broadly categorised based on the hydrogen production method they support—photocatalysis, electrochemical water splitting, or biological processes. Photocatalysts are materials that can absorb sunlight and convert it into chemical energy to drive reactions, such as water splitting, that produce hydrogen. Semiconductor materials, such as titanium dioxide (TiO₂), cadmium sulphide (CdS), and zinc oxide (ZnO), have been extensively studied for their photocatalytic properties (Ghamarpour, Fallah & Jamshidi, 2024). The efficiency of a photocatalyst depends on its ability to harvest light across a broad spectrum, its stability under irradiation, and its ability to facilitate charge separation and transfer. TiO₂ is one of the most widely studied photocatalysts due to its abundance, chemical stability, and non-toxicity (AlMohamadi *et al.*, 2024). However, it can only absorb ultraviolet light, which limits its overall efficiency. Researchers are exploring ways to enhance TiO₂'s performance by doping it with metal ions or nonmetals to extend its light absorption into the visible spectrum. Cadmium Sulphide (CdS) can absorb visible light, making it a promising candidate for photocatalytic hydrogen production. However, its application is limited by its toxicity and photocorrosion (Jie *et al.*, 2024). Recent research has focused on stabilising

CdS by coupling it with other materials, such as carbon nanotubes or reduced graphene oxide, to improve its durability and efficiency.

Perovskite materials, with their tunable band gaps and excellent light absorption properties, have recently garnered attention for photocatalytic (Figure 2) hydrogen production (Khan *et al.*, 2024). The challenge with perovskites lies in their stability, as many perovskites degrade quickly under exposure to moisture and heat. The ongoing research is aimed at developing more stable perovskite structures for hydrogen production. Electrochemical Materials water splitting, also known as electrolysis, involves the use of an electrolyser that splits water molecules into hydrogen and oxygen using electricity. The materials used for the electrodes and electrolytes in electrolysers are crucial for determining the efficiency of this process. Platinum (Pt) and Iridium (Ir) are benchmark materials for hydrogen and oxygen evolution reactions (HER and OER), respectively, due to their high catalytic activity (Guo *et al.*, 2024). However, their high cost and scarcity limit their widespread application in commercial electrolysers. Researchers are actively seeking alternative materials that can match the performance of Pt and Ir while being more cost-effective and abundant. Nickel-Based Catalysts a more abundant and less expensive alternatives to platinum, making them a popular choice for alkaline electrolysis (Emam *et al.*, 2024). Nickel-based catalysts, such as nickel-iron (NiFe) and nickel-molybdenum (NiMo) alloys, have shown promise for both the HER and OER in alkaline media. These materials are being further optimised to enhance their catalytic efficiency and durability under operating conditions. Solid Oxide Electrolysis Cells (SOECs) use solid oxide materials, such as yttria-stabilised zirconia (YSZ), as the electrolyte, allowing for water splitting at high temperatures (700-1,000°C). These high temperatures improve the efficiency of the electrolysis process, but the development of robust materials that can withstand such conditions remains a challenge.

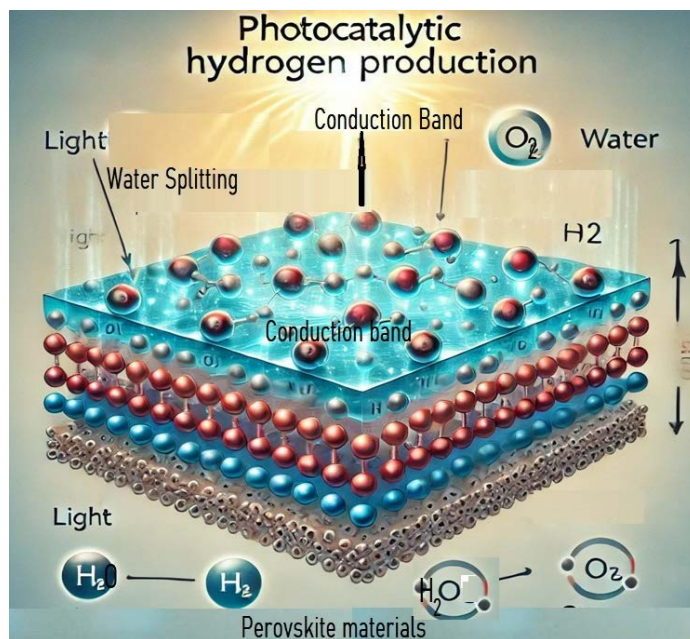


Figure 2: Schematic Image of Photocatalytic Hydrogen Production Using Perovskite Materials (Source: Author)

Enzymes play a central role in biological hydrogen production methods. In particular, hydrogenases and nitrogenases are the key enzymes involved in microbial hydrogen production (Cui *et al.*, 2024). Hydrogenases are enzymes that catalyse the reversible conversion of protons into hydrogen gas. These enzymes are found in a wide variety of microorganisms, including bacteria and algae. Hydrogenases are classified into three major types based on their metal active sites: [FeFe] hydrogenases, [NiFe] hydrogenases, and [Fe] hydrogenases (Lachmann *et al.*, 2024). [FeFe] hydrogenases are generally more efficient at hydrogen production but are sensitive to oxygen, which limits their application in oxygenic photosynthesis. Efforts to engineer oxygen-tolerant hydrogenases are underway to enhance their utility in green hydrogen production. Nitrogenases are enzymes primarily responsible for nitrogen fixation but can also produce hydrogen as a byproduct (Happe & Marx, 2024). These enzymes are less efficient at hydrogen production than hydrogenases but are more tolerant of oxygen. Recent research has focused on manipulating nitrogenase pathways to increase hydrogen yield and make them more viable for industrial-scale hydrogen production.

Biological hydrogen production harnesses the natural metabolic pathways of microorganisms to produce hydrogen. The key processes involved in biological hydrogen production include biophotolysis, dark fermentation, and microbial electrolysis (Rathi *et al.*, 2024). These methods offer unique advantages, such as the use of renewable feedstock (e.g., water, organic waste) and low energy requirements, making them attractive for sustainable hydrogen production. Biophotolysis refers to the production of hydrogen through the action of photosynthetic microorganisms, such as cyanobacteria and green algae. These microorganisms use sunlight to split water into hydrogen and oxygen through the process of photosynthesis. Biophotolysis can be further divided into two types: direct and indirect biophotolysis.

Direct Biophotolysis is when photosynthetic organisms directly split water molecules into hydrogen and oxygen using sunlight. This process occurs in the thylakoid membranes of microorganisms, where the absorbed light energy drives the water-splitting reaction (Akram *et al.*, 2024). However, the efficiency of direct biophotolysis is limited by the oxygen sensitivity of hydrogenase enzymes and the competition between oxygen and hydrogen production pathways (Kumar & Fiori, 2024). Indirect biophotolysis separates the stages of photosynthesis and hydrogen production. For example, in some cyanobacteria, photosynthesis is used to produce organic compounds, such as carbohydrates, which are then metabolised under anaerobic conditions to generate hydrogen (Ananthi *et al.*, 2024). This separation helps mitigate the inhibitory effects of oxygen on hydrogen production, but it also adds complexity to the process. Dark fermentation is a process in which microorganisms degrade organic matter to produce hydrogen in the absence of light. This process typically involves anaerobic bacteria that convert carbohydrates, proteins, and lipids into hydrogen, carbon dioxide, and organic acids. The simplicity of dark fermentation, along with its ability to utilise a wide range of feedstocks, makes it one of the most promising

methods for biological hydrogen production (Rathi *et al.*, 2024). Dark fermentation can utilise various substrates, including food waste, agricultural residues, and industrial effluents. The choice of substrates significantly affects the hydrogen yield, with carbohydrates typically producing higher yields than proteins or lipids. The diversity of potential feedstock makes dark fermentation adaptable to different waste management systems supporting the circular economy. Despite its potential, dark fermentation faces several challenges, including low hydrogen yields and the production of organic acid byproducts, which require further treatment (Jain *et al.*, 2024). Research is ongoing to optimise microbial communities, metabolic pathways, and process conditions to enhance hydrogen production and minimise byproduct formation.

Microbial electrolysis cells (MECs) represent a hybrid approach that combines biological activity with electrochemical processes (Figure 3) to produce hydrogen (Swaminathan *et al.*, 2024). In MECs, microorganisms oxidise organic matter, releasing electrons that are used to reduce protons and produce hydrogen at the cathode. Unlike conventional electrolysis, MECs operate at lower voltages, making them more energy efficient. MECs consist of an anode, where microbial oxidation of organic matter occurs, and a cathode, where hydrogen is produced. The electrons generated at the anode are transferred to the cathode through an external circuit, driving the hydrogen production reaction. MECs can be powered by renewable energy sources, further enhancing their sustainability. MECs offer several advantages, such as the ability to convert organic waste into hydrogen, lower energy requirements compared to traditional electrolysis, and the potential for integrating with renewable energy systems (Arun *et al.*, 2024). However, challenges remain, including the need for external power inputs, low hydrogen production rates, and the development of stable and efficient electrode materials.

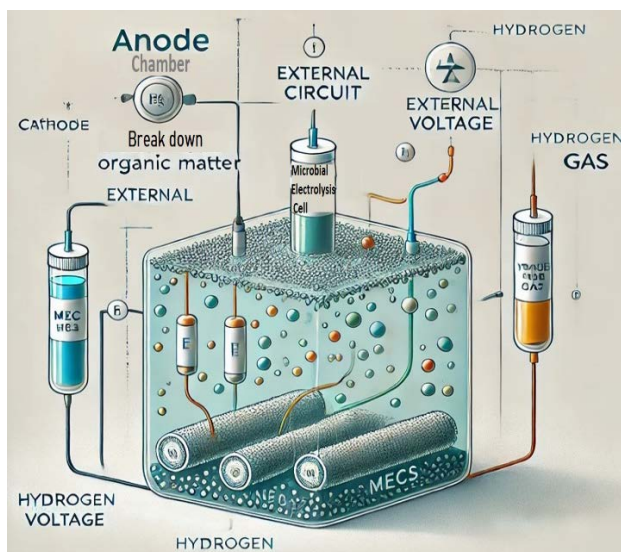


Figure 3: Schematic Drawings of Microbial Electrolysis Cells (MECs) Represent a Hybrid Approach that Combines Biological Activity with Electrochemical Processes to Produce Hydrogen (Source: Author)

Converging Chemical and Biological Sciences for a Sustainable Era

Recent advances in materials science and technology have significantly enhanced the efficiency and viability of green hydrogen production methods, including biological processes. Innovations in synthetic biology, metabolic engineering, and materials science are helping to overcome the limitations of traditional biological hydrogen production systems. Synthetic biology and metabolic engineering have opened new avenues for optimising microorganisms for hydrogen production (Zhang *et al.*, 2024b). Researchers are engineering microorganisms to enhance their hydrogen production pathways, improve enzyme stability, and increase tolerance to environmental conditions. For example, the introduction of oxygen-tolerant hydrogenases into photosynthetic organisms has shown promise in improving the efficiency of biophotolysis (Rady, Ali & El-Sheekh, 2024). Genetic engineering techniques are being used to create genetically modified strains of bacteria and algae with enhanced hydrogen production capabilities. By manipulating the genes responsible for hydrogenase expression, researchers can increase hydrogen yield and reduce the inhibition.

Opportunities in Biological Hydrogen Production

Biological hydrogen production offers a range of opportunities in the pursuit of sustainable energy, with the potential for large-scale deployment and unique advantages over conventional methods (Bhandari & Adhikari., 2024). The adaptability of biological processes, the ability to use renewable feedstocks, and the alignment with circular economy principles make biological hydrogen production an appealing avenue for green hydrogen generation. This section explores the opportunities for large-scale production, the advantages of biological methods, and case studies demonstrating successful implementation.

Potential for Large-Scale Production

The scalability of biological hydrogen production methods is a crucial factor in determining their viability as a major contributor to global hydrogen supply (Teke *et al.*, 2024). Biological hydrogen production can utilise a wide range of renewable feedstocks, including water, organic waste, agricultural residues, and wastewater. This flexibility in feedstock selection is a significant advantage, as it allows for the integration of hydrogen production into existing waste management systems. For example, agricultural waste and food waste, which are often disposed of in landfills, can be diverted to bioreactors for hydrogen production, reducing both waste and emissions. The use of renewable feedstocks not only contributes to environmental sustainability but also provides opportunities for decentralised hydrogen production (Chelvam *et al.*, 2024). In rural and agricultural regions, local waste streams can be converted into hydrogen, reducing the need for transportation and distribution of energy resources. This decentralised approach can help reduce energy poverty and increase energy security in remote or underdeveloped areas. Biological hydrogen production processes, such as dark fermentation and microbial electrolysis cells (MECs), can be integrated with existing industrial and agricultural systems to create synergies between waste management, energy production, and resource recovery. For example, wastewater treatment plants can implement dark fermentation processes to convert organic waste into hydrogen while simultaneously treating wastewater (Martínez-Fraile *et al.*, 2024). This approach not only produces clean energy but also enhances the sustainability of wastewater treatment systems. Similarly, agricultural operations that generate large quantities of organic

waste can incorporate biological hydrogen production into their processes, creating a closed-loop system where waste is converted into energy (Kazmi *et al.*, 2024). This type of integration reduces the environmental footprint of agriculture and enhances the overall efficiency of resource use.

Scaling up biological hydrogen production requires the development of efficient bioreactor systems that can accommodate large volumes of feedstock and optimise microbial activity. Recent advances in bioreactor design have focused on improving mass transfer, maintaining optimal conditions for microbial growth, and enhancing hydrogen production rates (Zarei *et al.*, 2024). Continuous-flow reactors, which allow for the constant input of feedstock and output of hydrogen, have shown promise for large-scale applications. These reactors can operate for extended periods without the need for frequent shutdowns or cleaning, increasing their overall efficiency. The design of continuous-flow systems also allows for better control of process conditions, such as temperature and pH, which are critical for maximising hydrogen production. Membrane bioreactors (MBRs) have been explored as a means of enhancing the separation of hydrogen gas from the liquid phase, reducing the loss of hydrogen and improving overall efficiency (Tran *et al.*, 2024). In MBRs, a semi-permeable membrane separates the microbial culture from the hydrogen gas, allowing for more efficient gas collection. This technology is particularly useful in processes like microbial electrolysis, where hydrogen must be efficiently harvested from the bioreactor. Hybrid systems that combine biological and electrochemical methods, such as microbial electrolysis cells, offer potential for scaling up. These systems can utilise both biological activity and electrical inputs to produce hydrogen more efficiently than either method alone. Advances in electrode materials and cell design are helping to make these systems more viable for large-scale deployment. The flexibility of biological hydrogen production systems allows for the potential development of large-scale production facilities. These facilities could be located near sources of renewable feedstock, such as agricultural regions, food processing plants, or wastewater treatment facilities. The ability to co-locate hydrogen production with feedstock sources reduces transportation costs and emissions, making the overall process more sustainable. Large-scale biological hydrogen production facilities could also benefit from economies of scale, reducing the cost of hydrogen production and making it more competitive with conventional methods. As technology continues to advance and the cost of bioreactor systems decreases, the economic feasibility of large-scale biological hydrogen production will improve.

Advantages of Conventional Methods

Biological hydrogen production offers several distinct advantages over conventional hydrogen production methods, such as steam methane reforming (SMR) and traditional electrolysis (Nemitallah *et al.*, 2024). These advantages position biological methods as a key component of future green hydrogen production systems. One of the most significant advantages of biological hydrogen production is its alignment with sustainability and environmental goals (Martins *et al.*, 2024). Unlike conventional methods, which often rely on fossil fuels and generate carbon emissions, biological processes utilise renewable resources and produce minimal environmental impact. For example, dark fermentation uses organic

waste as a feedstock, transforming waste products into clean energy rather than contributing to landfills or pollution. Biological hydrogen production also has the potential to contribute to carbon sequestration efforts. Some microorganisms involved in hydrogen production, such as algae, can absorb carbon dioxide during photosynthesis, further reducing the carbon footprint of the process. Additionally, integrating biological hydrogen production with carbon capture and utilisation (CCU) technologies could create a closed-loop system where carbon emissions are captured and reused in the production process (Zhang *et al.*, 2024c). Biological methods generally have lower energy requirements than conventional electrolysis or thermochemical processes. For example, dark fermentation and microbial electrolysis cells operate at ambient temperatures and do not require the high temperatures or pressures needed for processes like steam methane reforming. This reduces overall energy consumption and makes biological methods more energy efficient. In addition, the ability to use sunlight as a direct energy source in biophotolysis offers a unique advantage over conventional methods, which often rely on electricity generated from renewable sources. By directly harnessing solar energy, biophotolysis bypasses the need for intermediate energy conversion steps, potentially increasing the overall efficiency of hydrogen production.

Biological hydrogen production methods are highly adaptable to a wide range of feedstocks, from water and organic waste to agricultural residues and industrial effluents (Garg *et al.*, 2024). This adaptability provides flexibility in choosing the most appropriate feedstock for a given region or application, allowing for the optimisation of hydrogen production based on local resources. The use of diverse feedstocks also enables biological hydrogen production to contribute to waste management efforts. By converting waste materials into hydrogen, biological processes can help reduce the environmental impact of waste disposal and promote the circular economy. This is particularly important in regions with large agricultural or industrial sectors, where waste management is a significant challenge. The ability to implement biological hydrogen production systems on a smaller scale compared to conventional methods offers the potential for decentralised production. Decentralised systems can be deployed in remote or rural areas where access to centralised energy infrastructure is limited. This decentralisation can increase energy access, reduce reliance on fossil fuels, and promote energy independence in these regions. Decentralised biological hydrogen production systems can also be integrated with local renewable energy sources, such as solar or wind power, further enhancing their sustainability. For example, a rural community with access to both agricultural waste and solar energy could implement a combined biological and solar hydrogen production system, providing clean energy for local use without relying on external energy supplies.

Case Studies of Successful Implementation

Several successful case studies have demonstrated the potential of biological hydrogen production on both small and large scales. These case studies highlight the versatility of biological methods and their ability to contribute to green hydrogen production in various contexts.

In 2015, researchers at the University of California, Berkeley, developed a strain of cyanobacteria that could produce hydrogen through biophotolysis using sunlight and water

as inputs (Pereira *et al.*, 2024, Barry *et al.*, 2016). By introducing mutations that enhanced the efficiency of the hydrogenase enzyme, the researchers were able to increase hydrogen production rates while reducing the inhibitory effects of oxygen. This work represents a significant step forward in the development of biophotolysis for large-scale hydrogen production. The success of this project highlights the potential of genetic engineering and synthetic biology in optimising biological systems for hydrogen production. The engineered cyanobacteria demonstrated the feasibility of using biophotolysis as a sustainable hydrogen production method, particularly in regions with abundant sunlight. Further development of these systems could lead to commercial scale biophotolysis facilities that produce hydrogen using only sunlight and water. In 2019, a wastewater treatment plant in Seoul, South Korea, implemented a dark fermentation system to convert organic waste from wastewater into hydrogen (Gebreslassie *et al.*, 2021). The system used a continuous-flow reactor that allowed for the constant input of organic waste and output of hydrogen, reducing the need for frequent maintenance. The plant successfully produced hydrogen while simultaneously treating wastewater, demonstrating the potential for integrating hydrogen production with waste management.

This case study highlights the scalability and practicality of dark fermentation for hydrogen production. By using waste materials as feedstock, the plant reduced its overall environmental impact and created a new revenue stream through the sale of hydrogen. Similar systems could be implemented in other wastewater treatment facilities around the world, contributing to the circular economy and reducing the environmental footprint of waste treatment. In 2020, a pilot project in the Netherlands tested the use of microbial electrolysis cells (MECs) to produce hydrogen from agricultural waste (Kadier *et al.*, 2020). The project involved a dairy farm that generated large quantities of manure, which was fed into the MEC system to produce hydrogen. The hydrogen was then used to power farm equipment and vehicles, reducing the farm's reliance on fossil fuels.

Obstacles in Biological Hydrogen Production

Despite the numerous opportunities and advantages, biological hydrogen production faces significant challenges that must be addressed before it can be adopted on a large scale (Emetere *et al.*, 2024). These challenges include technical limitations, economic barriers, and environmental and sustainability issues. Each of these obstacles presents unique difficulties in scaling up and optimising biological hydrogen production, but ongoing research and technological advancements continue to seek solutions. In this section, the key obstacles that hinder the widespread implementation of biological hydrogen production will be discussed.

Technical Challenges

Efficiency Limitations: One of the primary technical challenges in biological hydrogen production is the low efficiency of the processes. Compared to conventional methods like steam methane reforming (SMR) and electrolysis, biological methods generally produce lower yields of hydrogen (Nemitallah *et al.*, 2024). Several factors contribute to these efficiency limitations, including the intrinsic metabolic constraints of microorganisms,

competition between metabolic pathways, and the sensitivity of enzymes involved in hydrogen production.

Microorganisms, such as bacteria, cyanobacteria, and algae, are not naturally optimised for large-scale hydrogen production. Their metabolic pathways often prioritise other cellular functions, such as growth, reproduction, and the synthesis of organic molecules (Zhang *et al.*, 2024b). As a result, the proportion of energy dedicated to hydrogen production is limited. Genetic engineering and metabolic optimisation can help address these constraints, but these approaches are still in the developmental stage. In photosynthetic microorganisms, hydrogen production often competes with other metabolic pathways, such as oxygenic photosynthesis. For example, in biophotolysis, the oxygen produced during water splitting can inhibit the activity of hydrogenases, reducing hydrogen yield. Overcoming this competition requires innovative approaches to either separate or optimise these pathways (Goveas *et al.*, 2024). Enzymes like hydrogenases and nitrogenases play a critical role in biological hydrogen production. However, these enzymes are often sensitive to environmental conditions, particularly oxygen levels (Chen *et al.*, 2024). [FeFe] hydrogenases, for instance, are highly efficient at producing hydrogen but are also highly sensitive to oxygen, which can inactivate them. This sensitivity poses a significant challenge in developing robust and reliable biological hydrogen production systems, particularly in aerobic environments.

While biological hydrogen production shows promise at the laboratory scale, scaling up these processes to industrial levels presents several challenges. Biological systems are inherently complex, and scaling up often introduces new variables that can affect performance. Effective scaling requires the development of bioreactor systems that can maintain optimal conditions for microbial growth and hydrogen production over large volumes. Achieving uniform mixing, mass transfer, and temperature control in large bioreactors is challenging. In addition, maintaining the viability and activity of microbial cultures over extended periods can be difficult, especially in continuous-flow systems where microbes are exposed to changing conditions (Sarkar *et al.*, 2024). Biological systems are often sensitive to fluctuations in environmental conditions, such as pH, temperature, and substrate concentration. These fluctuations can affect microbial activity and reduce hydrogen production efficiency. Maintaining stable process conditions at scale requires advanced monitoring and control systems, which can add complexity and cost to the production process.

Efficient separation and collection of hydrogen gas from the bioreactor is another scalability challenge. In many biological processes, hydrogen is produced in a gaseous form that must be separated from the liquid phase and other gases, such as carbon dioxide. This separation process can be energy-intensive and reduce the overall efficiency of hydrogen production. Biological hydrogen production often relies on organic waste or biomass as feedstock, which can vary widely in composition. The variability in feedstock can affect the efficiency and consistency of hydrogen production, as different substrates can produce different yields of hydrogen (Perat *et al.*, 2024). The composition of organic waste can vary depending on its source, seasonal changes, and processing methods. For example, food waste from different

regions or industries may have different ratios of carbohydrates, proteins, and fats, which can influence microbial metabolism and hydrogen yield. This variability makes it difficult to standardise biological hydrogen production processes (Economou *et al.*, 2024). Organic waste streams can contain contaminants, such as heavy metals, antibiotics, or toxic compounds, which can inhibit microbial activity and reduce hydrogen production efficiency. Managing these contaminants requires pre-treatment steps, which can add complexity and cost to the process.

Economic Challenges

High Cost of Materials and Production: The economic viability of biological hydrogen production is currently limited by the high cost of materials and production methods (Singla *et al.*, 2024). Biological processes generally require specialised materials, such as enzymes, catalysts, and bioreactors, which can be expensive to produce and maintain.

The production of enzymes, such as hydrogenases and nitrogenases, can be costly, particularly when these enzymes are used in large quantities (Happe & Marx, 2024). Enzyme production often requires complex fermentation processes, purification steps, and stabilisation techniques, all of which add to the overall cost of hydrogen production. Additionally, the sensitivity of enzymes to environmental conditions means that they may need to be replaced frequently, further increasing costs. In microbial electrolysis cells (MECs), the electrodes play a crucial role in facilitating hydrogen production. However, the materials commonly used for electrodes, such as platinum and other precious metals, are expensive and limited in supply (Swaminathan *et al.*, 2024).

Developing cost-effective and durable electrode materials is essential for reducing the overall cost of MEC-based hydrogen production. The construction and operation of large-scale bioreactors represent a significant capital investment. Bioreactors must be designed to maintain optimal conditions for microbial growth and hydrogen production, which often requires advanced control systems, monitoring equipment, and specialised materials (Jiao *et al.*, 2024). Operating costs can also be high, particularly if energy inputs, such as heating or mixing, are required to maintain process stability. Biological hydrogen production is currently less economically competitive than conventional methods, such as steam methane reforming (SMR) and electrolysis (Nemitallah *et al.*, 2024). The cost of producing hydrogen through biological methods is generally higher due to the lower efficiency of the processes and the higher cost of materials.

Cost of Hydrogen Production: The cost of producing hydrogen through biological methods is often measured in terms of dollars per kilogram of hydrogen produced (Ghasemi, Nikafshan & Akrami, 2024). Biological processes typically produce lower yields of hydrogen compared to SMR or electrolysis, which means that more feedstock and larger production facilities are needed to achieve the same output. This increases the overall cost of production, making biological hydrogen less competitive in the market.

The market for green hydrogen is still in its early stages, and demand for hydrogen produced through biological methods is relatively low. Most current hydrogen demand is met by conventional methods, which are cheaper and more widely available (Singla *et al.*, 2024).

As a result, biological hydrogen producers may struggle to compete in a market dominated by lower-cost alternatives. The development and scaling of biological hydrogen production systems require significant investment in research, development, and infrastructure. Securing funding for these projects can be challenging, particularly in a market where conventional hydrogen production methods are more established and cost-effective. Developing new biological hydrogen production technologies, such as genetically engineered microorganisms or advanced bioreactors, requires substantial investment in research and development (R&D) (Zhang *et al.*, 2024a). These R&D costs can be high, and the return on investment may not be immediate, making it difficult to attract private investment. Scaling up biological hydrogen production to commercial levels requires significant infrastructure investment, including the construction of production facilities, bioreactors, and distribution networks. Securing funding for these large-scale projects can be challenging, particularly in regions where hydrogen infrastructure is still underdeveloped.

Environmental and Sustainability Issues

While biological hydrogen production is generally more sustainable than conventional methods, it is not without its environmental impacts. The use of resources, such as water, land, and energy, must be carefully managed to ensure that biological hydrogen production remains environmentally sustainable (Jeje *et al.*, 2024). Some biological hydrogen production processes, such as biophotolysis, require large amounts of water as a feedstock. In regions where water resources are scarce, the high-water consumption of these processes could pose a sustainability challenge. Developing water-efficient processes and recycling water within the production system could help mitigate this issue. Large-scale biological hydrogen production facilities, particularly those that rely on biomass or algae, may require significant amounts of land. This could compete with other land uses, such as agriculture or conservation, particularly in densely populated regions. Ensuring that land use for biological hydrogen production does not contribute to deforestation, habitat loss, or food insecurity is essential for maintaining sustainability. Biological hydrogen production processes often generate waste products, such as organic acids, carbon dioxide, and other metabolites. Managing these byproducts in an environmentally responsible manner is essential for ensuring the sustainability of the process.

Organic Waste: Dark fermentation, for example, produces organic acids and other byproducts that must be treated or disposed of properly. Failing to manage these byproducts could result in environmental pollution or contribute to greenhouse gas emissions (Tiwari & Nakamura, 2024). Developing integrated systems that convert byproducts into useful products, such as biofuels or fertilisers, could enhance the sustainability of biological hydrogen production. While biological hydrogen production generally produces fewer carbon emissions than conventional methods, some processes, such as dark fermentation, still generate carbon dioxide as a byproduct (E Silva *et al.*, 2024). Capturing and utilising this carbon dioxide, either through carbon capture and utilisation (CCU) technologies or by integrating the process with carbon-sequestering microorganisms, could help reduce the overall carbon footprint of biological hydrogen production. The large-scale deployment of biological hydrogen production systems could have unintended impacts on biodiversity and

ecosystems. For example, the cultivation of algae for hydrogen production could disrupt aquatic life.

Discussion

A Comparative Look at Biological Hydrogen Production

Biological hydrogen production methods, particularly biophotolysis (Figure 4), dark fermentation, and microbial electrolysis cells (MECs), offer promising alternatives to conventional techniques like steam methane reforming and water electrolysis (Swaminathan *et al.*, 2024). However, each method comes with its own set of advantages and challenges. Biophotolysis harnesses the natural photosynthetic abilities of organisms such as algae and cyanobacteria to split water into hydrogen and oxygen using sunlight. While it promises high energy efficiency by directly tapping solar energy, the method is hampered by the sensitivity of hydrogenases to oxygen and the competition between photosynthetic and hydrogen-producing pathways. Scalability is another challenge due to the requirement for extensive areas for cultivation, and the high costs of constructing and maintaining photobioreactors can further complicate large-scale deployment (Kumar, Mishra & Singh, 2024). Nonetheless, biophotolysis stands out as a relatively low-cost method in terms of energy input and has the potential to minimise environmental impact by relying on water as a feedstock, provided water consumption and land use are managed effectively.

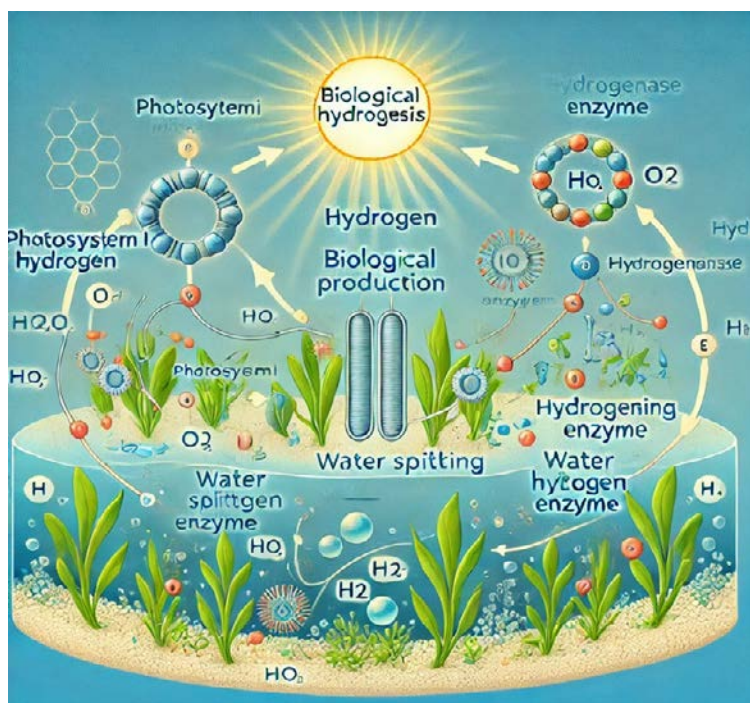


Figure 4: Schematic Illustration of Biological Hydrogen Production Methods, Focusing on Biophotolysis (Source: Author)

Green Hydrogen Generation: Materials, Potential, and Challenges

The diagram includes sunlight interacting with photosynthetic microorganisms, highlighting key components like Photosystem I and II, the water-splitting enzyme, and hydrogenase, leading to hydrogen gas production.

Dark fermentation, on the other hand, operates in anaerobic conditions, breaking down organic substrates such as agricultural waste and biomass to produce hydrogen. This method is less dependent on light and can be integrated into existing waste management infrastructures, making it more scalable than biophotolysis. However, dark fermentation struggles with lower efficiency as only a fraction of the substrate's energy is converted into hydrogen, with the rest dissipating as byproducts like organic acids (Srinadh & Neelancherry, 2024). The process's economic viability largely depends on feedstock availability and cost, with waste materials offering a promising route to cost reduction. However, scalability is limited by challenges like process stability and feedstock variability, and the management of byproducts is essential to prevent environmental contamination. Despite these hurdles, dark fermentation holds significant potential in waste-to-energy applications, particularly with optimised feedstock processing and microbial consortia.

Microbial electrolysis cells (MECs) combine biological and electrochemical processes to convert organic substrates into hydrogen, utilising an external voltage to drive the electrochemical reaction (Srivastava *et al.*, 2024). This hybrid approach can achieve higher hydrogen yields than dark fermentation, but its efficiency is closely tied to the materials used for electrodes and the energy required for the reaction. While MECs are scalable and can be integrated into waste treatment systems, they are hindered by the high cost of electrode materials, such as platinum, and the need for external energy input. Advances in non-precious metal catalysts and renewable energy integration could improve both cost-effectiveness and sustainability. MECs offer significant environmental benefits by converting waste into hydrogen, though their full potential can only be realised if the external energy used is derived from renewable sources. As a result, MECs present a compelling case for further research and development in the pursuit of scalable, cost-effective, and environmentally sustainable hydrogen production.

Conclusion

Biological hydrogen production presents a promising alternative to conventional methods of hydrogen generation, offering a sustainable and environmentally friendly solution. This review has explored various biological methods, including biophotolysis, dark fermentation, and microbial electrolysis cells (MECs), highlighting their respective advantages and challenges. While biological methods provide opportunities for utilising renewable resources and waste materials, they currently face technical challenges related to efficiency, scalability, and economic viability. Key findings suggest that each method has unique strengths: biophotolysis leverages solar energy but struggles with low efficiency due to enzyme sensitivity; dark fermentation is well-suited for waste-to-energy applications but requires better process optimisation; and MECs offer high hydrogen yields by combining biological and electrochemical processes, though they are hindered by the high cost of electrode materials. Addressing these challenges requires a multi-faceted approach. Advances in genetic engineering and synthetic biology can optimise microbial metabolic pathways, while

Converging Chemical and Biological Sciences for a Sustainable Era

innovations in bioreactor design and hybrid systems can improve scalability and stability. Furthermore, reducing the cost of key materials, such as enzymes and catalysts, is crucial for enhancing the economic viability of these processes. Looking ahead, future research must focus on enhancing microbial efficiency, developing cost-effective and sustainable production systems, and scaling up processes for industrial applications. Exploring hybrid systems that integrate biological and electrochemical methods, as well as valorising waste byproducts, will be pivotal in overcoming current limitations. The importance of further research in biological hydrogen production cannot be overstated. As the global demand for green hydrogen grows, advancing biological methods will play a critical role in meeting this demand sustainably. By addressing technical, economic, and environmental challenges, biological hydrogen production can contribute significantly to the transition toward a low-carbon, renewable energy future. Continued investment in research, innovation, and infrastructure is essential for realising the full potential of biological hydrogen production and achieving large-scale implementation.

Acknowledgment

One of the authors, Aniruddha Mondal extends his gratitude to Dr. Indranil Kar, Principal of Surendranath College, as well as Mr. Arpan Kanthal and Mr. Nabendu Mondal, assistant teachers of Harrindanga High School for their invaluable suggestions and support.

References

- Ahmad, A., Khan, S., Chhabra, T., Tariq, S., Javed, M. S., Li, H., ... & Ahmad, I. (2024a). Synergic impact of renewable resources and advanced technologies for green hydrogen production: Trends and perspectives. *International Journal of Hydrogen Energy*, 67, 788-806. <https://doi.org/10.1016/j.ijhydene.2023.06.337>
- Ahmad, A., Rambabu, K., Hasan, S. W., Show, P. L., & Banat, F. (2024b). Biohydrogen production through dark fermentation: Recent trends and advances in transition to a circular bioeconomy. *International Journal of Hydrogen Energy*, 52, 335-357. <https://doi.org/10.1016/j.ijhydene.2023.05.161>
- Ahmed, S. F., Kumar, P. S., Ahmed, B., Mehnaz, T., Shafiullah, G. M., Nguyen, V. N., ... & Kamangar, S. (2024). Carbon-based nanomaterials: characteristics, dimensions, advances and challenges in enhancing photocatalytic hydrogen production. *International Journal of Hydrogen Energy*, 52, 424-442. <https://doi.org/10.1016/j.ijhydene.2023.03.185>
- Akram, F., Fatima, T., Ibrar, R., & ul Haq, I. (2024). Biohydrogen: Production, promising progressions and challenges of a green carbon-free energy. *Sustainable Energy Technologies and Assessments*, 69, 103893. <https://doi.org/10.1016/j.seta.2024.103893>
- Akyüz, E. S., Telli, E., & Farsak, M. (2024). Hydrogen generation electrolyzers: paving the way for sustainable energy. *International Journal of Hydrogen Energy*, 81, 1338-1362. <https://doi.org/10.1016/j.ijhydene.2024.07.175>
- Alinejad, Z., Parham, N., Tawalbeh, M., Al-Othman, A., & Almomani, F. (2024). Progress in green hydrogen production and innovative materials for fuel cells: A pathway towards sustainable energy solutions. *International Journal of Hydrogen Energy*. <https://doi.org/10.1016/j.ijhydene.2024.09.153>

Green Hydrogen Generation: Materials, Potential, and Challenges

- AlMohamadi, H., Awad, S. A., Sharma, A. K., Fayzullaev, N., Távara-Aponte, A., Chiguala-Contreras, L., ... & Esmaili, H. (2024). Photocatalytic activity of metal-and non-metal-anchored ZnO and TiO₂ nanocatalysts for advanced photocatalysis: comparative study. *Catalysts*, 14(7), 420. <https://doi.org/10.3390/catal14070420>
- Ananthi, V., Bora, A., Ramesh, U., Yuvakkumar, R., Raja, K., Ponnuchamy, K., ... & Arun, A. (2024). A review on the technologies for sustainable biohydrogen production. *Process Safety and Environmental Protection*. <https://doi.org/10.1016/j.psep.2024.04.034>
- Arun, J., SundarRajan, P., Pavithra, K. G., Priyadharsini, P., Shyam, S., Goutham, R., ... & Pugazhendhi, A. (2024). New insights into microbial electrolysis cells (MEC) and microbial fuel cells (MFC) for simultaneous wastewater treatment and green fuel (hydrogen) generation. *Fuel*, 355, 129530. <https://doi.org/10.1016/j.fuel.2023.129530>
- Barry, A., Wolfe, A., English, C., Ruddick, C., & Lambert, D. (2016). 2016 National Algal Biofuels Technology Review. <https://doi.org/10.2172/1259407>
- Bhandari, R., & Adhikari, N. (2024). A comprehensive review on the role of hydrogen in renewable energy systems. *International Journal of Hydrogen Energy*, 82, 923-951. <https://doi.org/10.1016/j.ijhydene.2024.08.004>
- Chelvam, K., Hanafiah, M. M., Woon, K. S., & Al Ali, K. (2024). A review on the environmental performance of various hydrogen production technologies: An approach towards hydrogen economy. *Energy Reports*, 11, 369-383. <https://doi.org/10.1016/j.egyr.2023.11.060>
- Chen, Q. K., Xiang, X. H., Yan, P., & Liu, S. Y. (2024). Enhancing strategies of photosynthetic hydrogen production from microalgae: Differences in hydrogen production between prokaryotic and eukaryotic algae. *Bioresource Technology*, 406, 131029. <https://doi.org/10.1016/j.biortech.2024.131029>
- Cui, P., Wang, D., Wang, S., Su, H., & Wang, Y. (2024). Regulatory mechanism of antioxidant enzymes on microbial metabolism and NADH in anaerobic fermentation of food waste for hydrogen production. *Journal of Cleaner Production*, 474, 143607. <https://doi.org/10.1016/j.jclepro.2024.143607>
- e Silva, G. O. R., Carpanez, T. G., Dos Santos, C. R., Casella, G. S., Moreira, V. R., de Paula, E. C., & Amaral, M. C. S. (2024). Biohydrogen production from wastewater: production technologies, environmental and economic aspects. *Journal of Environmental Chemical Engineering*, 114104. <https://doi.org/10.1016/j.jece.2024.114104>
- Economou, F., Voukkali, I., Papamichael, I., Phinikettou, V., Loizia, P., Naddeo, V., ... & Zorpas, A. A. (2024). Turning food loss and food waste into Watts: A review of food waste as an energy source. *Energies*, 17(13), 3191. <https://doi.org/10.3390/en17133191>
- Emam, A. S., Hamdan, M. O., Abu-Nabah, B. A., & Elnajjar, E. (2024). A review on recent trends, challenges, and innovations in alkaline water electrolysis. *International Journal of Hydrogen Energy*, 64, 599-625. <https://doi.org/10.1016/j.ijhydene.2024.03.238>
- Emetere, M. E., Oniha, M. I., Akinyosoye, D. A., Elughi, G. N., & Afolalu, S. A. (2024). Progress and challenges of green hydrogen gas production: Leveraging on the successes of biogas. *International Journal of Hydrogen Energy*, 79, 1071-1085. <https://doi.org/10.1016/j.ijhydene.2024.07.115>

- Garg, A., Basu, S., Malode, S. J., & Shetti, N. P. (2024). Potential Organic Waste Materials for Green Hydrogen: A Route for Environmental Sustainability. *Green Hydrogen Economy for Environmental Sustainability. Fundamentals and Feedstocks*, 249-286. <https://doi.org/10.1021/bk-2024-1473.ch012>
- Gebreslassie, T. R., Nguyen, P. K. T., Yoon, H. H., & Kim, J. (2021). Co-production of hydrogen and electricity from macroalgae by simultaneous dark fermentation and microbial fuel cell. *Bioresource Technology*, 336, 125269. <https://doi.org/10.1016/j.biortech.2021.125269>
- Ghamarpoor, R., Fallah, A., & Jamshidi, M. (2024). A review of synthesis methods, modifications, and mechanisms of ZnO/TiO₂-based photocatalysts for photodegradation of contaminants. *ACS Omega*, 9(24), 25457-25492. <https://doi.org/10.1021/acsomega.3c08717>
- Ghasemi, A., Nikafshan Rad, H., & Akrami, M. (2024). Biomass-to-green hydrogen: a review of techno-economic-enviro assessment of various production methods. *Hydrogen*, 5(3), 474-493. <https://doi.org/10.3390/hydrogen5030027>
- Goveas, L. C., Nayak, S., Kumar, P. S., Vinayagam, R., Selvaraj, R., & Rangasamy, G. (2024). Recent advances in fermentative biohydrogen production. *International Journal of Hydrogen Energy*, 54, 200-217. <https://doi.org/10.1016/j.ijhydene.2023.04.208>
- Guo, R., Wang, J., Li, J., Li, H., Wang, H., Cao, Y., ... & Sheng, M. (2024). Regulating the oxygen vacancy of 3R-phase iridium oxide by loading platinum nanoparticles for efficient hydrogen evolution. *ACS Catalysis*, 14(15), 11164-11171. <https://doi.org/10.1021/acscatal.4c02062>
- Happe, T., & Marx, C. (2024). Alternative Biological and Biotechnological Processes for Hydrogen Production. *CO₂ and CO as Feedstock: Sustainable Carbon Sources for the Circular Economy*, 41-61. 10.1007/978-3-031-27811-2_4
- Hassan, Q., Algburi, S., Sameen, A. Z., Salman, H. M., & Jaszczur, M. (2024). Green hydrogen: A pathway to a sustainable energy future. *International Journal of Hydrogen Energy*, 50, 310-333. <https://doi.org/10.1016/j.ijhydene.2023.08.321>
- Jain, R., Panwar, N. L., Jain, S. K., Gupta, T., Agarwal, C., & Meena, S. S. (2024). Bio-hydrogen production through dark fermentation: an overview. *Biomass Conversion and Biorefinery*, 14(12), 12699-12724. 10.1007/s13399-022-03282-7
- Jeje, S. O., Marazani, T., Obiko, J. O., & Shongwe, M. B. (2024). Advancing the hydrogen production economy: A comprehensive review of technologies, sustainability, and future prospects. *International Journal of Hydrogen Energy*, 78, 642-661. <https://doi.org/10.1016/j.ijhydene.2024.06.344>
- Jiao, H., Tsigkou, K., Elsamahy, T., Pispas, K., Sun, J., Manthos, G., ... & Ali, S. S. (2024). Recent advances in sustainable hydrogen production from microalgae: Mechanisms, challenges, and future perspectives. *Ecotoxicology and Environmental Safety*, 270, 115908. <https://doi.org/10.1016/j.ecoenv.2023.115908>
- Jie, L., Gao, X., Cao, X., Wu, S., Long, X., Ma, Q., & Su, J. (2024). A review of CdS photocatalytic nanomaterials: Morphology, synthesis methods, and applications. *Materials Science in Semiconductor Processing*, 176, 108288. <https://doi.org/10.1016/j.mssp.2024.108288>
- Kadier, A., Al-Shorgani, N. K., Jadhav, D. A., Sonawane, J. M., Mathuriya, A. S., Kalil, M. S., ... & Alabbosh, K. F. S. (2020). Microbial Electrolysis Cell (MEC) an innovative Waste to Bioenergy

Green Hydrogen Generation: Materials, Potential, and Challenges

- and Value-added By-product technology. *Bioelectrosynthesis: Principles and Technologies for Value-Added Products*, 95-128. <https://doi.org/10.1002/9783527343829.ch4>
- Kazmi, B., Sadiq, T., Taqvi, S. A. A., Nasir, S., Khan, M. M., Naqvi, S. R., & AlMohamadi, H. (2024). Towards a sustainable future: Bio-hydrogen production from food waste for clean energy generation. *Process Safety and Environmental Protection*, 183, 555-567. <https://doi.org/10.1016/j.psep.2024.01.045>
- Khan, A. A., Partho, A. T., Arnab, M. H., Khyam, M. A., Kumar, N., & Tahir, M. (2024). Recent advances in Lanthanum-based photocatalysts with engineering aspects for photocatalytic hydrogen production: A critical review. *Materials Science in Semiconductor Processing*, 184, 108809. <https://doi.org/10.1016/j.mssp.2024.108809>
- Kossalbayev, B. D., Yilmaz, G., Sadvakasova, A. K., Zayadan, B. K., Belkozhaev, A. M., Kamshybayeva, G. K., ... & Allakhverdiev, S. I. (2024). Biotechnological production of hydrogen: Design features of photobioreactors and improvement of conditions for cultivating cyanobacteria. *International Journal of Hydrogen Energy*, 49, 413-432. <https://doi.org/10.1016/j.ijhydene.2023.09.001>
- Kumar, A., Mishra, B., & Singh, M. (2024). Threats, challenges and issues of large-scale cyanobacterial cultivation. *Pharmaceutical and Nutraceutical Potential of Cyanobacteria*, 245-275. [10.1007/978-3-031-45523-0_10](https://doi.org/10.1007/978-3-031-45523-0_10)
- Kumar, P., & Fiori, L. (2024). Thermochemical and biological routes for biohydrogen production: A review. *Energy Conversion and Management*, 278, 106659. <https://doi.org/10.1016/j.ecmx.2024.106659>
- Kumar, R. K., & Samuel, P. (2024). Designing a hydrogen generation system through PEM water electrolysis with the capability to adjust fast fluctuations in photovoltaic power. *International Journal of Hydrogen Energy*, 82, 1-10. <https://doi.org/10.1016/j.ijhydene.2024.07.376>
- Lachmann, M. T., Duan, Z., Rodríguez-Maciá, P., & Birrell, J. A. (2024). The missing pieces in the catalytic cycle of [FeFe] hydrogenases. *Chemical Science*, 15(35), 14062-14080. <https://doi.org/10.1039/D4SC04041D>
- Martínez-Fraile, C., Muñoz, R., Simorte, M. T., Sanz, I., & García-Depraect, O. (2024). Biohydrogen production by lactate-driven dark fermentation of real organic wastes derived from solid waste treatment plants. *Bioresource Technology*, 403, 130846. <https://doi.org/10.1016/j.biortech.2024.130846>
- Martins, F. P., Almaraz, S. D. L., Junior, A. B. B., Azzaro-Pantel, C., & Parikh, P. (2024). Hydrogen and the sustainable development goals: synergies and trade-offs. *Renewable and Sustainable Energy Reviews*, 204, 114796. <https://doi.org/10.1016/j.rser.2024.114796>
- Nemitallah, M. A., Alnazha, A. A., Ahmed, U., El-Adawy, M., & Habib, M. A. (2024). Review on techno-economics of hydrogen production using current and emerging processes: Status and perspectives. *Results in Engineering*, 21, 101890. <https://doi.org/10.1016/j.rineng.2024.101890>
- Nnabuife, S. G., Hamzat, A. K., Whidborne, J., Kuang, B., & Jenkins, K. W. (2024). Integration of renewable energy sources in tandem with electrolysis: A technology review for green hydrogen production. *International Journal of Hydrogen Energy*. <https://doi.org/10.1016/j.ijhydene.2024.06.342>

Converging Chemical and Biological Sciences for a Sustainable Era

- Ofélia de Queiroz, F. A., Morte, I. B. B., Borges, C. L., Morgado, C. R., & de Medeiros, J. L. (2024). Beyond clean and affordable transition pathways: A review of issues and strategies to sustainable energy supply. *International Journal of Electrical Power & Energy Systems*, 155, 109544. <https://doi.org/10.1016/j.ijepes.2023.109544>
- Perat, L., Escudié, R., Bernet, N., Richard, C., Jégoux, M., Juge, M., & Trably, E. (2024). New insights on waste mixing for enhanced fermentative hydrogen production. *Process Safety and Environmental Protection*, 188, 1326-1337. <https://doi.org/10.1016/j.psep.2024.06.006>
- Pereira, J., Souza, R., Oliveira, J., & Moita, A. (2024). Hydrogen production, transporting and storage processes—a brief review. *Clean Technologies*, 6(3), 1260-1313. <https://doi.org/10.3390/cleantechnol6030061>
- Rady, H. A., Ali, S. S., & El-Sheekh, M. M. (2024). Strategies to enhance biohydrogen production from microalgae: A comprehensive review. *Journal of Environmental Management*, 356, 120611. <https://doi.org/10.1016/j.jenvman.2024.120611>
- Ram, C., Rani, P., & Kumar, A. (2024). Recent developments in biohydrogen production from wastewater: A review. *Biocatalysis and Biotransformation*, 42(1), 1-18. [10.1080/10242422.2023.2181046](https://doi.org/10.1080/10242422.2023.2181046)
- Rathi, B. S., Kumar, P. S., Rangasamy, G., & Rajendran, S. (2024). A critical review on Biohydrogen generation from biomass. *International Journal of Hydrogen Energy*, 52, 115-138. <https://doi.org/10.1016/j.ijhydene.2022.10.182>
- Saha, P., Akash, F. A., Shovon, S. M., Monir, M. U., Ahmed, M. T., Khan, M. F. H., ... & Akter, R. (2024). Grey, blue, and green hydrogen: A comprehensive review of production methods and prospects for zero-emission energy. *International Journal of Green Energy*, 21(6), 1383-1397. [10.1080/15435075.2023.2244583](https://doi.org/10.1080/15435075.2023.2244583)
- Sarkar, O., Rova, U., Christakopoulos, P., & Matsakas, L. (2024). Continuous biohydrogen and volatile fatty acids production from cheese whey in a tubular biofilm reactor: Substrate flow rate variations and microbial dynamics. *International Journal of Hydrogen Energy*, 59, 1305-1316. <https://doi.org/10.1016/j.ijhydene.2024.02.041>
- Sebbahi, S., Assila, A., Belghiti, A. A., Laasri, S., Kaya, S., Hlil, E. K., ... & Hajjaji, A. (2024). A comprehensive review of recent advances in alkaline water electrolysis for hydrogen production. *International Journal of Hydrogen Energy*, 52, 583-599. <https://doi.org/10.1016/j.ijhydene.2024.07.428>
- Singla, M. K., Gupta, J., Beryozkina, S., Safaraliev, M., & Singh, M. (2024). The colorful economics of hydrogen: Assessing the costs and viability of different hydrogen production methods-A review. *International Journal of Hydrogen Energy*, 52, 664-677. <https://doi.org/10.1016/j.ijhydene.2024.02.255>
- Srinadh, R. V., & Neelancherry, R. (2024). Advancements in Hydrogen Production Technologies from Agricultural Waste. In *Agricultural Waste to Value-Added Products: Bioproducts and its Applications* (pp. 55-81). Singapore: Springer Nature Singapore. [10.1007/978-981-97-2535-9_3](https://doi.org/10.1007/978-981-97-2535-9_3)
- Srivastava, P., García-Quismondo, E., Palma, J., & González-Fernández, C. (2024). Coupling dark fermentation and microbial electrolysis cells for higher hydrogen yield: Technological competitiveness and challenges. *International Journal of Hydrogen Energy*, 52, 223-239. <https://doi.org/10.1016/j.ijhydene.2023.04.293>

Green Hydrogen Generation: Materials, Potential, and Challenges

- Swaminathan, P., Ghosh, A., Sunantha, G., Sivagami, K., Mohanakrishna, G., Aishwarya, S., ... & Prajapat, R. (2024). A Comprehensive Review of Microbial Electrolysis Cells Integrated with Wastewater Treatment for Hydrogen Generation. *Process Safety and Environmental Protection*. <https://doi.org/10.1016/j.psep.2024.08.032>
- Teke, G. M., Anye Cho, B., Bosman, C. E., Mapholi, Z., Zhang, D., & Pott, R. W. M. (2024). Towards industrial biological hydrogen production: a review. *World Journal of Microbiology and Biotechnology*, 40(1), 37. [10.1007/s11274-023-03845-4](https://doi.org/10.1007/s11274-023-03845-4)
- Tiwari, A., & Nakamura, K. (2024). Closing the loop on biohydrogen production: A critical review on the post-fermentation broth management techniques. *International Journal of Hydrogen Energy*, 81, 595-614. <https://doi.org/10.1016/j.ijhydene.2024.07.307>
- Tran, D. P. H., You, S. J., Bui, X. T., Wang, Y. F., & Ramos, A. (2024). Anaerobic membrane bioreactors for municipal wastewater: Progress in resource and energy recovery improvement approaches. *Journal of Environmental Management*, 366, 121855. <https://doi.org/10.1016/j.jenvman.2024.121855>
- Worku, A. K., Ayele, D. W., Deepak, D. B., Gebreyohannes, A. Y., Agegnehu, S. D., & Kolhe, M. L. (2024). Recent advances and challenges of hydrogen production technologies via renewable energy sources. *Advanced Energy and Sustainability Research*, 5(5), 2300273. <https://doi.org/10.1002/aesr.202300273>
- Zaiter, I., Ramadan, M., Bouabid, A., Mayyas, A., El-Fadel, M., & Mezher, T. (2024). Enabling industrial decarbonization: Framework for hydrogen integration in the industrial energy systems. *Renewable and Sustainable Energy Reviews*, 203, 114782. <https://doi.org/10.1016/j.rser.2024.114782>
- Zarei, Z., Malekshahi, P., Morowvat, M. H., & Trzcinski, A. P. (2024). A review of bioreactor configurations for hydrogen production by cyanobacteria and microalgae. *International Journal of Hydrogen Energy*, 49, 472-495. <https://doi.org/10.1016/j.ijhydene.2023.09.108>
- Zhang, J., Li, F., Liu, D., Liu, Q., & Song, H. (2024b). Engineering extracellular electron transfer pathways of electroactive microorganisms by synthetic biology for energy and chemicals production. *Chemical Society Reviews*, 53(3), 1375-1446. <https://doi.org/10.1039/D3CS00537B>
- Zhang, L., Jia, C., Bai, F., Wang, W., An, S., Zhao, K., ... & Sun, H. (2024a). A comprehensive review of the promising clean energy carrier: Hydrogen production, transportation, storage, and utilization (HPTSU) technologies. *Fuel*, 355, 129455. <https://doi.org/10.1016/j.fuel.2023.129455>
- Zhang, X. G., Abdul Raman, A. A., Jewaratnam, J., & Buthiyappan, A. (2024c). Sustainable carbon dioxide capture, storage, and utilization: review of current status and future direction. *International Journal of Environmental Science and Technology*, 1-36. <https://doi.org/10.1007/s13762-024-05908-x>

Dynamics of Micelle-Vesicle Interconversion: Mechanisms and Modulation

Shrabani Sen

Department of Chemistry, Rammohan College, Kolkata, West Bengal, India

Corresponding Author's E-mail: sen.shrabani@gmail.com

Abstract

The self-assembly of surfactant molecules in an aqueous medium not only produces micelles with polar head groups outside and nonpolar groups inside the core but can also assume the form of vesicles with closed bilayers. The vesicular and micellar structures of the fatty acid molecules can interconvert between themselves as $\text{Micelle} \rightleftharpoons \text{Vesicle}$ in a rhythmic fashion when they are coupled to a pH-oscillator. Based on a two-state model where the two states correspond to two different forms of the self-assembled system, this micelle-vesicle transition has been explored. The theoretical analysis of the numerical simulation of pH-oscillation induced hopping between the two states shows how the phase of chemical oscillation can be used to estimate directly the rate of transition between the two unmodulated states of the self-assembly.

Keywords: *Micelles; pH Oscillators; Surfactants; Vesicles*

Introduction

Surfactants are compounds that lower the surface tension of a liquid, allowing easier spreading and lowering of the interfacial tension between two liquids or between a liquid and a solid (Menger, 1979). Surfactant molecules having two moieties with antagonistic properties, a polar hydrophilic moiety and a nonpolar hydrophobic moiety self-assemble and form micelles beyond the critical micellization concentration (CMC) (Leng, Egelhaaf & Cates, 2003). Some surfactants self-assemble into closed bilayers to form vesicles (or liposomes when formed from phospholipids). There is evidence that at very low concentrations, surfactants start forming micelles that may turn into vesicles at higher concentrations (Ghosh *et al.*, 2013). The transition between the micellar and vesicular structures of surfactant molecules has been a major area of research in the last several years. Andelman, Kozlov and Helfrich (1994) have presented a model of phase transition between micelles and vesicles. Their model predicted a first-order transition between micelles and vesicles depending on the relative concentration of the two components. The phase transition boundaries were calculated as a function of the specific areas of the two components, their spontaneous curvatures and elastic moduli. Structural transitions between different forms of surfactant assembly are important in connection with drug targeting, which may be carried out using liposomes (vesicles) of phospholipid mixed with single-chain surfactants. Lagzi *et al.* (2010) have shown that the rhythmic interconversion of nanoscopic oleic acid (OA) vesicles and micelles can be controlled by a pH oscillator when coupled to a system of self-assembly of OA molecules. Their experiment reveals that the dynamic interconversion of

micellar and vesicular structures of OA molecules critically depends upon the pH of the methylene glycol-sulphite-gluconolactone (MGSG) oscillator system.

As the two forms of molecular self-assembly are the distinct thermodynamic equilibrium states characterised by definite free energies, it is worthwhile to understand the rate of transition between the two different states when they are unmodulated. The focus of the present paper is to construct a two-state model of interconversion of the two forms. In what follows, a two-state model has been considered corresponding to a double well potential, and based on a rate equation approach, examine the modulation of the activation barrier for the interconversion. The numerical simulation of the differential equations for the coupled dynamics of the pH oscillator (MGSG)-two-state (micelle-vesicle) system is carried out to estimate the rate from the phase of oscillation of micelle (or vesicle) concentration.

Micelle-Vesicle Transition and a Two-State Model

The methylene glycol-sulphite reaction is a hydroxide ion clock reaction in batch, and this reaction displays complex behaviour in a flow reaction. Kovacs *et al.* (2007) have demonstrated a coupling mechanism of this reaction with hydrolysis of gluconolactone to create an organic-based pH oscillator. In this oscillator model the pH oscillates between 7 and 10. The detailed reaction scheme for the various species is given in Table 1. The dynamics of the stock solutions for different molecular and ionic components are governed by the kinetic equations which are discussed in detail. Furthermore, the dynamics of the reactions in the flow reactor are followed according to the scheme, which also includes all the rate constants as referred to. The flow rate k_0 is used as a control parameter for the dynamics.

Following Lagzi *et al.* (2010) let us now couple the above-mentioned MGSG system to the self-assembly of OA molecules. The pH oscillation within the reactor has a time period of approximately 85 sec for the fixed flow rate $k_0 = 5.4 \times 10^{-3} \text{ sec}^{-1}$. When the oscillator is in the low pH range (e.g., pH=7-8.3), OA molecules form membrane vesicles (bilayer structures), burying the hydrophobic chain and presenting inner and outer hydrophilic surfaces with interspersed protonated and deprotonated carboxylic groups. When the oscillator is in the high pH range, e.g., around 9.4, the OAs become deprotonated and form unilamellar micelles presenting COO^- head groups. In other words, they interconvert between themselves following the kinetics $\text{micelle} \rightleftharpoons \text{vesicle}$.

Introduction of Mass Action Kinetics

In order to explore quantitatively this interconversion of the two forms, two rate equations have been introduced following mass action kinetics

$$\frac{dn_a}{dt} = -k_{mv}(H^+)n_a + k_{vm}(OH^-)n_b \quad (1)$$

$$\frac{dn_b}{dt} = -k_{vm}(OH^-)n_b + k_{mv}(H^+)n_a \quad (2)$$

where n_a and n_b are the concentrations of the micelle and vesicles, respectively, and k_{mv} and k_{vm} are the rate constants, which depend on the concentration of H^+ and OH^-

as shown (Sen, Riaz & Ray, 2008; Sen, Riaz & Ray, 2009).

The rationale behind such a choice of form of coefficients of n_a and n_b is as follows: Since the vesicle-micelle transition is assisted by H^+ or OH^- concentrations (controlled by the MSGG oscillator through dehydration of methylene glycol along with catalytic production of OH^- and hydrolysis of gluconolactone by OH^- , the autocatalytic species.) the scheme micelle \rightleftharpoons vesicle interconversion clearly suggests that the rate constants of Eq. 1 and Eq. 2 should be the functions of $[H^+]$ and $[OH^-]$ as the activation barrier is expected to be modulated by pH. This modulation is adiabatic in the sense that the rate of transition between the two states in the absence of modulation of the barrier is much faster than the modulation of the activation barrier. It is therefore assumed that very weak dependence of rate constants on H^+ and OH^- ion concentrations in the following form:

$$\begin{aligned} k_{mv}(H^+) &\sim \exp\left(\frac{-E_0 + \alpha[H^+]}{RT}\right) \\ &\sim k_{oa} + \alpha[H^+] \\ &\text{and} \\ k_{vm}(OH^-) &\sim \exp\left(\frac{-E_0 + \beta[OH^-]}{RT}\right) \\ &\sim k_{ob} + \beta[OH^-] \end{aligned}$$

Here E_0 and T refer to the activation barrier for the micelle-vesicle transition and the temperature, respectively. In the present problem the parameters k_{oa} , k_{ob} , α and β are adjusted in relation to the entries in Table I of Kovac *et al.* (Scot) and are set as $k_{oa} = 10^{-4} \text{ sec}^{-1}$, $k_{ob} = 10^{-4} \text{ sec}^{-1}$, $\alpha = 107 \text{ M}^{-1} \text{ sec}^{-1}$ and $\beta = 105 \text{ M}^{-1} \text{ sec}^{-1}$. The coupled dynamics of the MSGG oscillation, as well as the components in the flow reactor according to the scheme and the rate equations for the micelle-vesicle transition, are followed by numerical integration performed using the package XPPAUT. The method of integration was CVODE with a time step of 0.01 sec and the tolerance set at 1×10^{-7} . The results are shown in Figs 2 and 3 for the set of parameter values as mentioned. In Figure 1(a) it has been displayed the variation of pH as a function of time for the fixed flow rate $k_0 = 5.4 \times 10^{-3} \text{ sec}^{-1}$. It is found that after some induction period, pH settles down for sustained oscillation with a time period of ≈ 85 sec, which can be estimated from Figure 2(b). The steady oscillations of concentration of micelle (na) and vesicle (nb) are shown in Figs. 2(a) and 2(b), respectively, after the lapse of the initial period of induction.

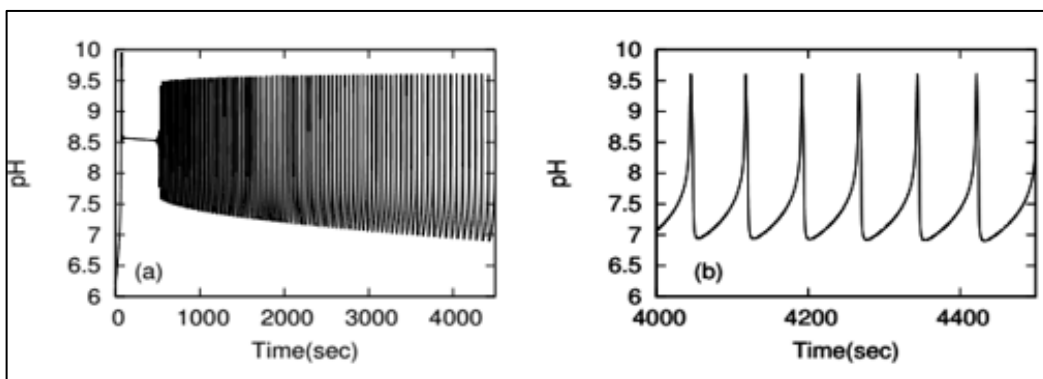


Figure 1: Oscillatory Variation of pH with Time (a) between $t=0$ to $t=4500$ sec, (b) between $t=4000$ sec to $t=4500$ sec for the Set of Parameter Values Mentioned in the Text and for the Flow Rate $k_0 = 5.4 \times 10^{-3}$

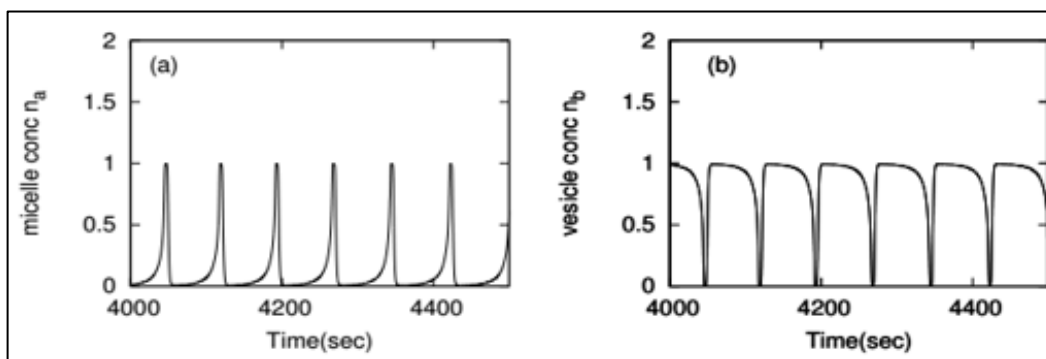


Figure 2: Variation of (a) Micelle Concentration n_a and (b) Vesicle Concentration n_b with Time for the Set of Parameter Values as Mentioned in the Text and for $k_0=5.4 \times 10^{-3} \text{ sec}^{-1}$

The dynamics of transition between the two states of molecular assembly are assisted by modulation of the pH oscillation of the MGSG oscillator. As the two states, i.e., the vesicle and micelle, are thermodynamically distinct, it is worthwhile exploring the unmodulated activation barrier and the associated Kramers rate. In the end, there has been a plan to make a theoretical analysis of the oscillation to estimate the rate of transition over the unmodulated activation barrier between the two states from the phase of the chemical oscillation.

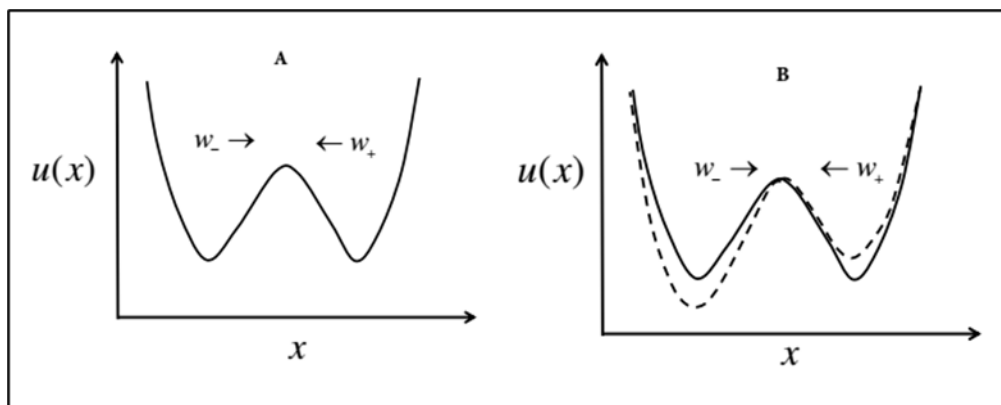


Figure 3: The Schematic Diagram of the Double Well in (a) Absence and (b) Presence of Periodic Modulation of the Barrier

Future Endeavours

There can be represented in a schematic diagram a double well potential with two minima separated by a barrier. Micelles and vesicles are in each of the two wells of the double well. A natural simplification of this continuum model is a discrete two-state system. This two-state model has been used in widely different contexts, e.g., stochastic resonance, resonance activation, and dynamic hysteresis in polymer gel to name a few. Introducing transition probabilities for jumping from one well to another and then applying a probabilistic approach, the rate of transition can be calculated. This will be analysed in upcoming issues.

Conclusion

In this chapter a pH oscillator is considered an oscillator in conjunction with a pH-sensitive molecular assembly which can assume micellar and vesicular forms depending on the pH of the solution. The micelle and the vesicle are the two distinct stable thermodynamic states of the molecular assembly separated by an activation barrier. The oscillation of pH modulates the activation barrier, which leads to oscillatory population changes of the two species. It has been numerically simulated the dynamics of the pH oscillator (MGSG) coupled to the molecular self-assembly (oleic acid) to follow the oscillation of the two states. The oscillatory profile of the concentration of micelle/vesicle is planned to be analysed in light of the theoretical scheme for the two-state model in the next issues.

Acknowledgment: The author gratefully acknowledges Prof Debshankar Ray for his valuable support and encouragement throughout the course of this work.

References

- Andelman, D., Kozlov, M. M., & Helfrich, W. (1994). Phase transitions between vesicles and micelles driven by competing curvatures. *Europhysics Letters*, 25(3), 231-236. <http://dx.doi.org/10.1209/0295-5075/25/3/013>
- Ghosh, S., Ghatak, C., Banerjee, C., Mandal, S., Kuchlyan, J., & Sarkar, N. (2013). Spontaneous transition of micelle-vesicle-micelle in a mixture of cationic surfactant and anionic surfactant-

Micelle-Vesicle Interconversion: Dynamics and Modulation

- like ionic liquid: a pure nonlipid small unilamellar vesicular template used for solvent and rotational relaxation study. *Langmuir*, 29(32), 10066-10076. <https://doi.org/10.1021/la402053a>
- Kovacs, K., McIlwaine, R. E., Scott, S. K., & Taylor, A. F. (2007). An organic-based pH oscillator. *The Journal of Physical Chemistry A*, 111(4), 549-551. <https://doi.org/10.1021/jp068534v>
- Lagzi, I., Wang, D., Kowalczyk, B., & Grzybowski, B. A. (2010). Vesicle-to-micelle oscillations and spatial patterns. *Langmuir*, 26(17), 13770-13772. <https://doi.org/10.1021/la102635w>
- Leng, J., Egelhaaf, S. U., & Cates, M. E. (2003). Kinetics of the micelle-to-vesicle transition: aqueous lecithin-bile salt mixtures. *Biophysical Journal*, 85(3), 1624-1646. [https://doi.org/10.1016/S0006-3495\(03\)74593-7](https://doi.org/10.1016/S0006-3495(03)74593-7)
- Menger, F. M. (1979). The structure of micelles. *Accounts of Chemical Research*, 12(4), 111-117. <https://doi.org/10.1021/ar50136a001>
- Sen, S., Riaz, S. S., & Ray, D. S. (2008). Temperature dependence and temperature compensation of kinetics of chemical oscillations; Belousov–Zhabotinskii reaction, glycolysis and circadian rhythms. *Journal of Theoretical Biology*, 250(1), 103-112. <https://doi.org/10.1016/j.jtbi.2007.08.029>
- Sen, S., Riaz, S. S., & Ray, D. S. (2009). Growth and decay of large fluctuations far from equilibrium. *Journal of Chemical Sciences*, 121, 905-911. <https://doi.org/10.1007/s12039-009-0107-7>

Breast Milk: A Free Radical Scavenger and Role of Mother's Diet

Pritha Mondal

Department of Zoology, Surendranath College, Kolkata, West Bengal, India

Corresponding Author's Email: prithagaria@gmail.com

Abstract

Breast milk is a vital source of antioxidants that play a crucial role in protecting infants against oxidative stress and supporting optimal growth and development. This review highlights the presence and significance of key antioxidant enzymes in breast milk, including catalase (CAT), superoxide dismutase (SOD), glutathione peroxidase (GPx), and lactoferrin (LF), which neutralise free radicals through enzymatic and non-enzymatic mechanisms. Malondialdehyde (MDA), a marker of lipid peroxidation, is shown to be the lowest in colostrum due to higher concentrations of these antioxidants, underscoring the importance of early breastfeeding. The antioxidant profile of breast milk is influenced by maternal diet, environmental factors, and lactation stage. Trace elements like zinc, copper, and iron, which serve as cofactors for antioxidant enzymes, also regulate oxidative balance through their interaction with binding proteins such as ceruloplasmin and ferritin. Additionally, maternal intake of polyphenols, carotenoids (lutein, zeaxanthin), and essential fatty acids affects breast milk composition, with evidence showing enhanced antioxidant capacity in women consuming plant-rich or fish-based diets. However, certain nutrients like taurine and vitamin B12 may be lower in vegan or vegetarian mothers, potentially influencing infant neurodevelopment. Overall, breast milk offers superior antioxidant protection compared to infant formulas and reflects maternal nutritional and lifestyle factors, emphasising the need for targeted dietary support during lactation.

Keywords: B12; CAT; GPx; LF; MDA; SOD

Introduction

Breast milk is very important for a newborn because it is easy to digest, readily available, and a low-cost natural food. It not only gives immunity, growth and development but also has other roles in the psychosocial growth of the mother and baby.

Besides giving high nutrition and immunity, it has its antioxidative properties. Reactive oxygen species (ROS) and reactive nitrogen species (RNS) in the breast milk destroy free radicals created by oxidative stress (Matos, Ribeiro & Guerra, 2015).

Cellular metabolism creates free radicals, oxidants and oxygen radicals, which cause harmful effects inside living organisms. Breast milk is more powerful at reducing free radical damage and structural changes of DNA in newborns than infant formulas. The enzymatic antioxidants like Superoxide dismutase (SOD) and Catalase (CAT) prevent the free radical formation of H_2O_2 and other peroxides (Yuksel *et al.*, 2015).

Breast Milk and Maternal Diet in Antioxidant Defense

Compared with formula milk, breast milk has an increased number of PUFAs (c20-c22) [long-chain polyunsaturated fatty acids], which are highly susceptible to lipid peroxidation and associated with increased oxidative injury. Antioxidants in human breast milk may protect long-chain polyunsaturated fattyacids in human milk against oxidation (Hanson *et al.*, 2016).

Overall growth and development of an infant is dependent on breast milk composition, which contains nutritive elements, antioxidants and micronutrients. Breast milk contains antioxidants, including superoxide dismutase (SOD), catalase (CAT), glutathione peroxidase (GPx), glutathione reductase and glutathione S-transferase. The relation between GPx, SOD and GST and the number of pregnancies was found. GST activity and BMI show an inverse relationship. Cu and catalase activity show a negative correlation with GPx and GST activity (Li *et al.*, 2009).

Breast milk is healthy and nutritious food for premature babies. When a mother is not capable (in a hospitalised condition), she cannot provide breast milk to her child, then donor milk is an ideal alternative to mother's milk. Premature babies do not have 1) an ample number of antioxidants at the time of birth and 2) the ability to synthesise antioxidants, so they become susceptible to different diseases like chronic lung disease, disease of the retina (Retinopathy), necrotising bowel disease and periventricularleukimalacia (PVL). So, it is crucial to make certain that premature babies get an ample amount of antioxidants through diet (Hanson *et al.*, 2016).

A hypothesis was made that preterm mothers' milk would have much better antioxidative protection than milk from the full-term mothers. In this regard, three experiments were designed to assess the power to resist the oxidative stress of breast milk and powdered formulas for both full-term and preterm infants and differences in resisting oxidative stress between milk from full-term and preterm infants. The experiments also examined factors that are responsible for increased resistance to oxidative stress in the mother's breast milk (Castillo-Castaneda *et al.*, 1980).

In this review, research will be made about the ability of breast milk to eliminate the free radicals from the bodies of the infants and the role of the mother's diet in enhancing different useful components in breast milk.

Different Antioxidants in Human Milk Which Act as Free Radical Scavenger

Vit-A: liposoluble compound, acts against ROS. Carotenoids, which are structurally similar to vitamin A, show antioxidative activity by quenching reactive oxygen, neutralising thiol radicals, and stabilising peroxy radicals to protect cells from peroxidative damage. The activity of enzymes involved in lipid peroxidation is suppressed by vitamin A and prevents oxidative disorders in cell membranes. Vitamin A is not transmitted through the placenta, so newborn babies are dependent on breast milk consumption (Matos, Ribeiro & Guerra, 2015).

Vit-E: Plasma membranes, fatty deposits and circulating lipoproteins contain vitamin E, which reacts with reactive oxygen species and molecular oxygen to protect PUFAs and

lipoproteins from peroxidation. Vitamin E is not transferred through the placenta, so breast milk is the main source of nutrition for infants.

Vit-C: Reacts with free radicals and has a low reduction potential. It plays a vital role in breast milk antioxidative properties and is associated with a reduced risk of atopy in high-risk infants.

Different Proteins and Enzymes in Breast Milk

B casein and the primary whey protein (α -lactalbumin), iron-binding glycoprotein (lactoferrin), IgA, serum albumin protein and protein hormones are moved to breast milk from plasma. These proteins and peptides show free radical scavenging activity and inhibit lipid peroxidation.

a) *Lactoferrin*: It is an anti-inflammatory compound as it takes up iron from the inflammatory compound. Its main mode of action is antimicrobial.

b) *Glutathione peroxidase*: Contains a selenium component in the form of selenocysteine. It provides protection against oxidative damage and protects lipids from oxidative stress.

c) *Enzymatic antioxidants*: Mn and copper/zinc superoxide dismutase (SOD) have been recognised in breast milk, which converts a superoxide anion to hydrogen peroxide.

d) *Ceruloplasmin*: Copper-containing multifunctional protein inhibits the formation of hydroxyl radicals through a chemical process (Fenton reaction) and lipid peroxidation. It prevents damage to DNA, proteins, and lipids.

e) *Coenzyme Q10 or ubiquinone*: Liposoluble vitamin, potent antioxidant and free radical scavenger.

f) *Melatonin*: A derivative of serotonin secreted by the pineal gland, a highly effective hormone (antioxidant) and free radical scavenger (Matos, Ribeiro & Guerra, 2015).

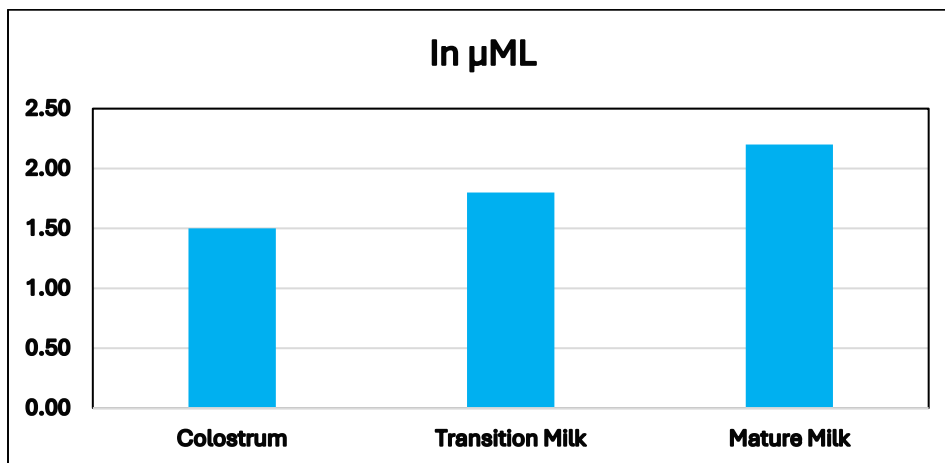


Figure 1: Malondialdehyde, (secondary products of lipid peroxidation). (MDA) levels in Colostrum, Transition Milk and Mature Milk [In µML]

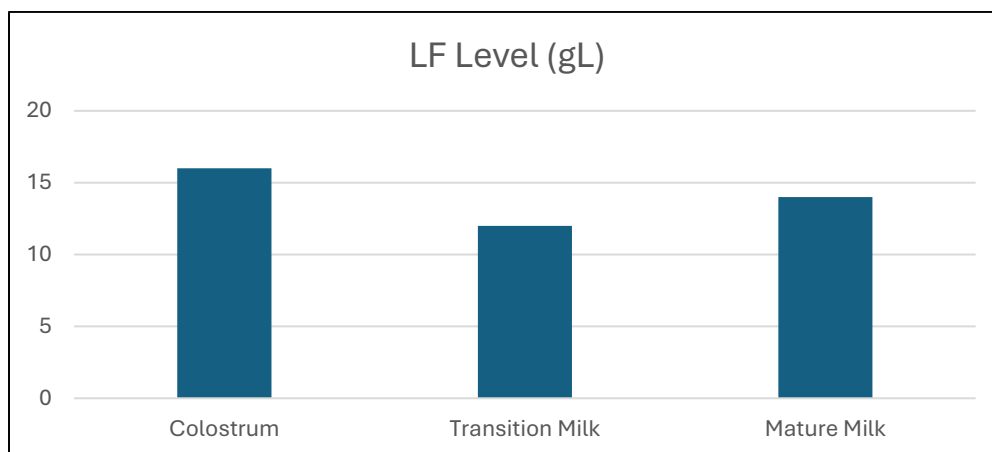


Figure 2: Lactoferrin (LF) levels in Colostrum, Transition milk, and Mature Milk [LF Level in g/L]

Phenolic compounds play a major role in anti-tumour activity. Phenolic compounds in breast milk reduce inflammation by inhibiting the transcription factor nuclear factor-B. When mothers consume a diet rich in phenolic compounds, their breast milk protects the newborn babies from diseases (Hanson *et al.*, 2016).

Infant health is dependent on nutritional status, antioxidant level and quality of mother's milk. Breast milk contains enzymatic antioxidants like superoxide dismutase (SOD), several vitamins like tocopherols, ascorbic acids, soy-based phytoestrogens and coenzyme-Q10, selenium, thiodoxin, etc. (Hanson *et al.*, 2016).

Relationship between Different Antioxidant Enzymes and Different Micronutrients Like Fe, Cu, and Zn in Breast Milk

1) *Role of Fe in BM:* Iron-containing glycoprotein (Lactoferrin) present in human milk helps in the cognitive development of babies.

2) *Role of Cu in BM:* Copper is essential in the formation of bone, myelin, collagen, neuropeptides, and haemoglobin and contributes to the electron transport chain.

3) *Role of Zn in BM:* Insufficient consumption of Zn by the infants may cause nervous system and growth defects.

In this study they have shown there is a correlation between antioxidant enzyme activity and number of pregnancies. Mothers who have more than 3 pregnancies show the highest Glutathione peroxidase activity. They also showed a correlation between enzymatic antioxidant activities and concentrations of copper, zinc, and iron by BMI value. Women who have a body mass index (BMI) < 25 show the highest GST activity. (Li *et al.*, 2009). The Glutathione peroxide (GPx) activity (0.08umg-1) was found in women with 3 or more pregnancies. Women whose body mass index is >25 and < 30 show significant differences. Zn, Cu and Fe concentrations did not differ with respect to the number of pregnancies and body mass index value (Li *et al.*, 2009).

Preterm babies are prone to oxidative stress as they lack adequate antioxidants at the time of birth, which leads to diseases like chronic lung disease (BPD), disease of the retina (ROP), necrotising bowel disease (NEC) and periventricular leukomalacia (PVL). So, dietary antioxidants are very essential in preterm babies. Samples of matured breast milk, donor milk and formula milk were analysed at the Biomarker Research Institute at the Harvard School of Public Health. samples were quantitated by high-performance liquid chromatography (HPLC). The result showed that breast milk contains higher levels of natural carotenoid pigments like β -cryptoxanthine (a precursor of vitamin A), lycopenes (effective antioxidants), Lutein + Zeaxanthene (natural carotenoid pigments), vitamin A, and different isoforms of vitamin E than donor milk. Premature babies who are formula-fed have lower levels of carotenoid pigments in the bloodstream than breastfed premature babies (Hanson *et al.*, 2016).

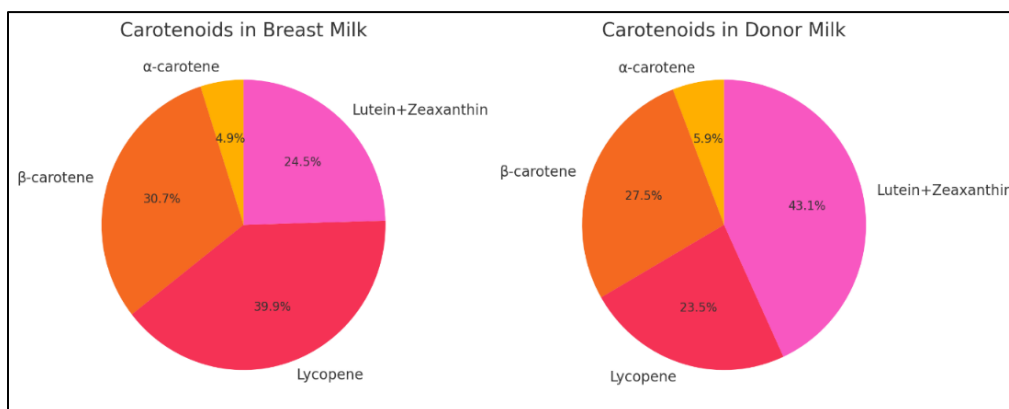


Figure 3: Percentage of α -carotene, β - carotene, Lycopene and Lutein + Zeaxanthin Breast Milk v/s Donor Milk Samples

Lycopene percentage is higher in mother's breast milk than donor milk. Research shows that Lutein + Zeaxanthin plays a major role in the vision, learning, thinking and understanding ability of the babies. Lutein +zeaxanthin concentration in different brain regions of preterm babies was remarkably lower compared to matured babies. infant in most of their brain regions. Because of the increased proportion of bioavailability of lutein concentration in breast milk, breastfed infants have more lutein concentration than formula-fed infants. Infant formula needs four times more Lutein than human milk to achieve similar serum lutein among breastfed and formula-fed infants (Hanson *et al.*, 2016).

Breast milk colostrum has the ability to reduce cytochrome - c spontaneously, depletes hydrogen peroxide produced by polymorphonuclear leukocytes, and protects the epithelial cells from polymorphonuclear leukocyte-mediated detachment.

Cow's milk is modified to formula milk, which is very similar to human milk. These powdered formula milks have increased radical trapping antioxidants in contrast with human milk. According to Goldman *et al.* antioxidants are absent or present in a very poor amount in

Breast Milk and Maternal Diet in Antioxidant Defense

cow's milk or other feedings. The premature babies fed with human milk had greater free radical trapping ability in vitro than formula-fed babies (Castillo-Castaneda *et al.*, 1980).

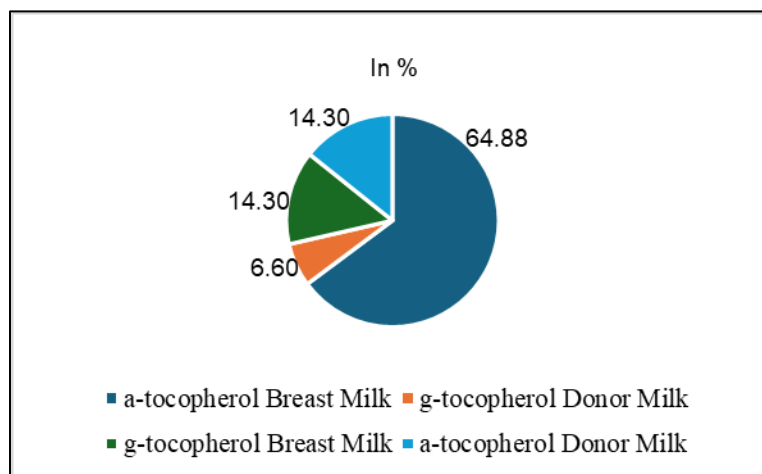


Figure 4: The Concentrations of α -tocopherol and γ -tocopherol in Maternal Breast Milk vs. Donor Milk Samples

Early feeding of human milk by premature babies reduces the occurrence of inflammatory bowel disease and disease of the retina (Retinopathy of prematurity). Due to some properties of human milk, which reduces the incidence of necrotising enterocolitis. Their experiments indicate that oxidative stress has very little impact on human milk compared to very effective formula milk. The report says the presence of GPx and SOD, CAT in human milk, plays a role in providing antioxidants in vitro. When formula milk is added with different enzymatic antioxidants like catalase, Superoxide dismutase, and Glutathione peroxidase it shows greater protection against oxidative stress and lipid damage. This indicates that formulas when added with these enzymatic antioxidants may help in reducing the damaging effects of excessive oxidative stress and inflammation caused by ROS (reactive oxygen species), which results in decreased symptoms, speedy recovery and normal development (Castillo-Castaneda *et al.*, 1980).

Breast milk of lactating women contains different polyphenols and their metabolic products like flavonoids, phenolic acids, ellagic acid and urolithin, which are plant-based natural compounds transferred to breast milk through the mother's blood circulation. The metabolic products of polyphenols in mother's milk undergo a new cycle of digestion when they are consumed by the newborn babies (Carregosa *et al.*, 2023).

Polyphenols get broken down into small molecular weight phenolics by gut microbiota by undergoing Phase-I and Phase-II metabolic reactions. All these compounds enter the liver and are transferred to circulation, where they may reach the mother's milk. Several studies indicate that breast milk contains phytoestrogens like daidzein and genistein when mothers consume diet isoflavone-rich foods like soya milk and roasted soybeans (Carregosa *et al.*, 2023).

Mother's diet has an impact on breast milk composition. When grapefruit juice is consumed by mothers, her breast milk shows flavanones. After consumption of red raspberry, breast milk shows different flavonoids, microbial metabolites and phenolics. According to Lu *et al.*, when mothers consume plant-based foods and polyphenols, it remarkably affects the phenolic composition of her breast milk.

Quercetin was the flavonol detected in the highest concentration in human breast milk, ranging from 0.05 to 0.15 μM . Zhang *et al.* (2018) showed that quercetin was more plentiful in breast milk and urine than in plasma of mothers.

Different studies have suggested polyphenols have a protective role against inflammation, oxidative damage and cardiometabolic stress. Vegetable consumption and antioxidative properties of polyphenols in breast milk are positively correlated. (Carregosa *et al.*, 2023).

The concentration of Arachidonic acid and docosahexanoic acid was studied by Kelishadi *et al.* (2012). They found that DHA content was low in comparison to other studies. DHA is important in infant brain development. According to WHO recommendation AA/DHA ratio should be 2:1 in colostrum, as DHA is important in brain development. In a well-developed country, this ratio varies from 5:1 to 15:1. In their study, the AA/DHA ratio was 2.6:1 higher than the WHO recommendation. It was shown that in the regions where fish consumption is high, the DHA content of breast milk is higher.

The antioxidant status of infants is closely influenced by the mother's antioxidant levels during pregnancy and breastfeeding. Human milk contains a variety of antioxidant substances—such as vitamins, enzymes, and trace elements – that work together to protect the infant from oxidative stress. The total antioxidant capacity (TAC) of breast milk is affected by the mother's diet, with healthy dietary patterns like the Mediterranean diet enhancing the presence of beneficial compounds like polyphenols. Since the body cannot synthesise certain antioxidants, they must be obtained from foods such as fruits, vegetables, and whole grains. Studies show that breast milk offers superior antioxidant protection compared to infant formulas, underlining the importance of maternal nutrition for infant health (Karbasi *et al.*, 2022).

Karcz and Królak-Olejek (2021) have shown in their review vegan, vegetarian and non-vegetarian mothers' breast milk is comparable in their nutritional value. Some differences are found in fatty acids and some microcomponents, primarily Vitamin B12. Their study suggests that vegetarian and vegan mothers produce milk of the same nutritional value, except some nutritional supplement is added to the mother's diet. An appropriately planned plant-based diet can contribute to the sustainable growth of infants. As vitamin B12 helps in the proper maintenance of the nervous system, lactovegetarian mothers are also advised to take B12 supplements regularly.

Discussion

Antioxidants like catalase, superoxide dismutase, Glutathione peroxidase and Lactoferrin present in the breast milk can eliminate reactive oxygen species by enzymatic and nonenzymatic reactions. MDA, which is a metabolite of lipid peroxides, acts as a measure for LPO. Research indicates that mothers' milk contains crucial protective mechanisms,

Breast Milk and Maternal Diet in Antioxidant Defense

which are absent in powdered formula or bovine milk. The current study shows that colostrum contains decreased levels of MDA compared to transition milk and mature milk because enzymatic antioxidants' (CAT, SOD, NO, and LF) levels were highest inside colostrum. The high oxidative stress requires high antioxidant levels from the 1st day of lactation (Yuksel *et al.*, 2015).

The major whey proteins lactalbumin and lactoglobulin, the iron-binding protein lactoferrin, serum albumin and immunoglobulins present in milk show antioxidant activity by ferrous ion-chelating abilities as well as by inhibitory effects on LPO.

High molecular weight milk catalase enzyme induces the decomposition of H_2O_2 . The current investigation shows that catalase activity markedly decreased as the lactation period began. Superoxide radicals are changed into H_2O and O_2 by superoxide dismutase, having an antitoxic effect against superoxide anion. (Yuksel *et al.*, 2015).

It has been reported that breast-fed infants have significantly lower oxidative stress than formula-fed infants. Granot *et al.* (1999) suggest that breastfed babies showed more oxidative injury compared with formula-fed babies having similar antioxidant capacity because of differences in fatty acids between mother's milk and formula milk.

Long-chain polyunsaturated fatty acids (PUFA) in breast milk may get protection against oxidative injury by the antioxidants present in it. Antioxidant composition varies among different racial groups of the same region. It has been found that Nigerian women's breast milk has a higher antioxidant content than the women of Nepal. Antioxidant levels decrease in smoker mothers and their passive smoker babies when compared with those of nonsmokers. During the freezing process and refrigeration, antioxidant activity notably decreased (Hanson *et al.*, 2016).

This has been found in this review that for the first six months of life, breast milk provides the infants with the best nourishment, which reduces the risk of morbidity in infant, and provides growth, development and immunity. Proteins, fatty acids, vitamins, antioxidants, and microelements such as zinc, copper, and iron contribute to the proper growth and development of the child. Metabolism, foreign chemicals (Xenobiotics) and the smoking of the mother produce free radicals and create oxidative damage in breast milk.

Free radicals (ROS) cause oxidative damage to DNA, proteins, Lipids and other substrates and also cause structural and functional damages to the nutrients in milk. Breast milk contains enzymatic and non-enzymatic antioxidants that provide infants' antioxidant defences and may protect nutrients in milk from oxidative damage.

The microelements zinc, iron, and vitamin C have an impact on copper absorption. In the current study shows that zinc concentration has a positive correlation with Cu content in breast milk. However, the Cu:Zn ratio can measure the oxidative stress as well as the immunological and nutritional condition.

Copper takes part in the Fenton reaction instead of iron. In this reaction Cu^{2+} changes to Cu^+ and reduces H_2O_2 to $OH\cdot$, a more reactive free radical. Breast milk contains ceruloplasmin, which transports copper. Copper, when bound with these proteins, which

decreases its accessibility to take part in the Fenton reaction, consequently, stops oxidative damage (Li *et al.*, 2009).

Level of free iron is decreased as it remains in a soluble, non-toxic form as ferritin, preventing oxidative reactions. The activity of enzymatic antioxidants like superoxide dismutase and Catalase is influenced by the concentration of Cu, Zn and Fe, which are cofactors of these enzymes. These microelements also influence (GPx, GST), by reducing their substrate (H_2O_2) availability or by intervening with their functional groups (Li *et al.*, 2009).

Research shows that Lutein + Zeaxanthin plays a major role in optical, learning, thinking and memory development. Lutein and zeaxanthin concentration was remarkably lower in premature babies in major brain areas compared to full-term babies. Because of the higher amount of lutein concentration in breast milk, breast infants have more lutein concentration than formula-fed infants (Hanson *et al.*, 2016).

The mother's diet plays an important role in enhancing the quality of breast milk. Metabolic products of polyphenols, mainly flavonoids, phenolic acids and ellagic acid, are found in the breast milk of lactating mothers. Studies indicate that isoflavone is present in breast milk when mothers take isoflavone-rich food like soyamilk and roasted soybeans. Flavonone is also detected in breast milk after grapefruit juice consumption (Castillo-Castaneda *et al.*, 1980).

Multiple studies indicate that polyphenols protect babies from inflammation and cardiometabolic stress. Antioxidative properties of breast milk are associated with a higher vegetable consumption by mothers (Castillo-Castaneda *et al.*, 1980).

During pregnancy DHA plays a very important role in infant brain development. It requires the mother's dietary intervention. DHA contents of breast milk become higher where fish consumption is high. Women having reproductive potential are recommended to consume food rich in fatty acids (Kelishadi *et al.*, 2012).

Baby's antioxidant level depends on the mother's antioxidant level throughout the entire gestation period. Infant synthesizes antioxidants through its endogenous component at the expense of exogenous component transmitted to him or her through breast milk. Vitamins A, E and C and different enzymes like (GPx, SOD) different chemicals like copper, Zinc, and Selenium act as antioxidants and neutralise free radicals. Among the most essential antioxidants are phenolic compounds and flavonoids, which are derived from plants and are powerful natural dietary antioxidants (Karbasi *et al.*, 2022).

The ratio of LA/ALA (Linoleic Acid and Alpha Linoleic Acid) was higher, whereas omega - 6 and omega-3 ratios are higher in the case of vegan mothers. The average percentage of alpha-linolenic acid in milk samples was 2.09% for vegan mothers, 1.55 % for vegetarian mothers and 1.19 % for omnivore mothers.

Bijur *et al.* and Debski *et al.* found no significant difference in particular dietary groups in terms of protein concentrations in human milk. According to them, the mean values in the case of lactovegetarians were 1.122 gm/dl, 1.221 gm/dl for occasional meat eaters and 1.216 for frequent meat eaters. From the above report, it indicates that a vegetarian or

Breast Milk and Maternal Diet in Antioxidant Defense

nonvegetarian diet does not have an impact on milk protein concentrations (Karcz & Królak-Olechnik, 2021).

Rana *et al.* in their experiment compared the taurine concentration in two different groups – one group of omnivores and another of vegans – and found that vegan milk samples contained significantly lower taurine concentration compared with omnivore as vegan mothers consumed less protein containing preformed taurine. In the human body, taurine acts as a neurotransmitter in the brain. Adults can synthesise taurine from cysteine and hypotaurine. It is present in high amounts in meat and fish (Karcz & Królak-Olechnik, 2021).

Patel and Lovelady (1998) reported that cobalamin, or Vitamin B12 is also low in vegetarian mothers. Women of India showed lower B12 concentrations than omnivore control groups. Specker *et al.* (1990) said that a vegetarian diet has an inverse correlation with breast milk B12 levels (P1/40.03). Finley *et al.* analysed that in the incase of minerals like Cu, Zn, Ca, Mg, K, and Na concentrations, there was no notable contrast in breast milk of vegetarian and nonvegetarian mothers.

Plant based vegan diet contains huge amounts of linoleic acid, omega-6 polyunsaturated fatty acids and monounsaturated oils. Vegetarian and vegan mothers' diets contain a good amount of omega-6 fatty acids, but lower omega-3 fatty acids compared to nonvegetarians (omnivores) (Karcz & Królak-Olechnik, 2021).

Conclusion

From the above discussion, it is clear that breast milk is the best source of antioxidants in newborn babies, as it contains a lot of antioxidants for reducing the free radicals. There are several microelements which are important. Breastmilk contains an essential defence mechanism to protect the newborn from free radicals, which is not present in formula or bovine milk. A mother's diet plays an important role in breastmilk composition. Vegan and vegetarian mothers' breast milk contains all the components, but omega-3 fatty acids, taurine (an essential amino acid), and vitamin B12 are in lower concentrations than in non-vegetarian or omnivorous mothers. Therefore, during the gestation period, vegan and vegetarian mothers need to regularly take a vitamin B12 (cobalamin) supplement to ensure the quality of their breast milk.

Acknowledgment

The author expresses sincere gratitude to the Department of Zoology, Surendranath College, India, for their unwavering support and encouragement throughout the course of this work. Their guidance and collaborative spirit have been invaluable in shaping this research.

References

Carregosa, D., Silva, I. P., Teixeira, C., Baltazar, M., García-Villalba, R., Vieira, F. S., ... & Santos, C. N. (2023). (Poly) phenols in Human Breast Milk and their health benefits for the newborn. *medRxiv*, 2023-03. <https://doi.org/10.1101/2023.03.27.23287781>

- Castillo-Castaneda, P. C., García-Gonzalez, A., Bencomo-Alvarez, A.E., Barros-Nunez, P., Gaxiola-Robles, R., Mendez-Rodriguez, L.C., & Zenteno-Savin, T. (1980). Micronutrient content and antioxidant enzyme activities. *The American Journal of Clinical Nutrition*, 33(2), 227-231. <https://doi.org/10.1016/j.jtemb.2018.09.008>
- Granot, E., Golan, D., Rivkin, L., & Kohen, R. (1999). Oxidative stress in healthy breast fed versus formula fed infants. *Nutrition Research*, 19(6), 869-879. [https://doi.org/10.1016/S0271-5317\(99\)00047-0](https://doi.org/10.1016/S0271-5317(99)00047-0)
- Hanson, C., Lyden, E., Furtado, J., Van Ormer, M., & Anderson-Berry, A. (2016). A comparison of nutritional antioxidant content in breast milk, donor milk, and infant formulas. *Nutrients*, 8(11), 681. <https://doi.org/10.3390/nu8110681>
- Karbasi, S., Bahrami, A., Asadi, Z., Shahbeiki, F., Naseri, M., Zarban, A., & Ferns, G. A. (2022). The association of maternal dietary quality and the antioxidant-proxidant balance of human milk. *International Breastfeeding Journal*, 17(1), 56. <https://doi.org/10.1186/s13006-022-00498-1>
- Karcz, K., & Królak-Olejnik, B. (2021). Vegan or vegetarian diet and breast milk composition—a systematic review. *Critical Reviews in Food Science and Nutrition*, 61(7), 1081-1098. <https://doi.org/10.1080/10408398.2020.1753650>
- Kelishadi, R., Hadi, B., Iranpour, R., Khosravi-Darani, K., Mirmoghtadaee, P., Farajian, S., & Poursafa, P. (2012). A study on lipid content and fatty acid of breast milk and its association with mother's diet composition. *Journal of Research in Medical Sciences: The Official Journal of Isfahan University of Medical Sciences*, 17(9), 824. Retrieved from: <https://pubmed.ncbi.nlm.nih.gov/articles/PMC3697205/>, Accessed on 6th December 2024.
- Li, W., Hosseini, F. S., Tsopmo, A., Friel, J. K., & Beta, T. (2009). Evaluation of antioxidant capacity and aroma quality of breast milk. *Nutrition*, 25(1), 105-114. <https://doi.org/10.1016/j.nut.2008.07.017>
- Matos, C., Ribeiro, M., & Guerra, A. (2015). Breastfeeding: Antioxidative properties of breast milk. *Journal of Applied Biomedicine*, 13(3), 169-180. <https://doi.org/10.1016/j.jab.2015.04.003>
- Patel, K. D., & Lovelady, C. A. (1998). Vitamin B12 status of east Indian vegetarian lactating women living in the United States. *Nutrition Research*, 18(11), 1839-1846. [https://doi.org/10.1016/S0271-5317\(98\)00153-5](https://doi.org/10.1016/S0271-5317(98)00153-5)
- Specker, B. L., Black, A., Allen, L., & Morrow, F. (1990). Vitamin B-12: low milk concentrations are related to low serum concentrations in vegetarian women and to methylmalonic aciduria in their infants. *The American Journal of Clinical Nutrition*, 52(6), 1073-1076. <https://doi.org/10.1093/ajcn/52.6.1073>
- Yuksel, S., Yigit, A. A., Cinar, M., Atmaca, N., & Onaran, Y. (2015). Oxidant and antioxidant status of human breast milk during lactation period. *Dairy Science & Technology*, 95, 295-302. <http://dx.doi.org/10.1007/s13594-015-0211-z>

Study of Synthesis, Crystal Structure, Magnetic Properties, EPR, Cyclic Voltammetric Analysis and Zigzag Chain Coordination of Polymer Prepared through Copper Catalysed Hemiacetal Synthesis

Piu Dhal

Department of Chemistry, Rammohan College, Kolkata, West Bengal, India

Corresponding Author's Email: piudhal@gmail.com

Abstract

A 1D polymeric complex $[\text{Cu}^{\text{II}}_2(\text{R})_2(\text{SCN})_2]_n$ (1) has been prepared by the reaction of picolinaldehyde with NaSCN. The complex 1 has been well characterised by UV-Vis, FT-IR, and elemental analysis. Structural study of Complex 1 exhibits a unique arrangement, where copper centres in tetrahedral and pentacoordinated geometries are interconnected in a chain-like pattern. This linkage is facilitated by single thiocyanato bridges and double alkoxido bridges, resulting in the formation of dimer complexes that repeat throughout the structure. Magnetic measurements at varying temperatures reveal a strong antiferromagnetic interaction between copper centres of the dimer, facilitated by the double alkoxido bridge. The exchange coupling constant (J) is determined to be -374 cm^{-1} . This strong antiferromagnetic interaction highlights the important role of the bridging ligands in mediating magnetic exchange between the metal centres.

Keywords: Alkoxo Bridges; Copper (II) Complexes; Magnetic Properties; Single Step Reaction

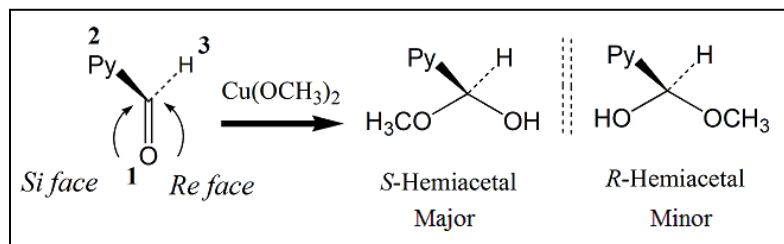
Introduction

Recent years have seen significant advancements in single step ligand synthesis, driven by its efficacy, ease of use, and eco-friendly nature. This approach has emerged as a potent tool in designing coordination complexes. Furthermore, decades of research have focused on one step metal/ligand reactions, aiming to uncover novel organic reactions, shed light on reaction mechanisms, and create unique compounds that cannot be synthesised directly (Chen & Tong, 2007; Zhang, 2005).

A wide range of single step ligand syntheses under hydro(solvo)thermal conditions have been documented, encompassing various reactions such as carbon-carbon bond formation (Blake *et al.*, 1997; Liu, Gao & Kou, 2001), hydroxylation (Zhang, Tong & Chen, 2002; Zhang *et al.*, 2002), and cycloaddition reactions (Xiong *et al.*, 2002; Xue *et al.*, 2002; Qu *et al.*, 2003; Zhang *et al.*, 2004). Other reported reactions include substitution of carboxyl with sulfonic groups (Xiong *et al.*, 2001), alkylation (Cheng *et al.*, 2004). Notably, the formation of polynuclear complexes often involves single step reactions between an organic ligand and a small molecule or solvent.

Copper-Catalysed Polymer: Structure and Magnetic Analysis

Here a novel synthetic route is described, wherein $\text{Cu}(\text{ClO}_4)_2 \cdot 6\text{H}_2\text{O}$ facilitates a single step reaction, enabling the addition of methanol as a nucleophile to aldehydes, resulting in the formation of hemiacetals within a methanolic medium (Scheme 1).



Scheme 1: Scheme Representation of Hemiacetal Synthesis through Single Step Reaction (Dhal *et al.*, 2014)

Magnetic properties of interest can be achieved by employing paramagnetic metal ions as connecting points, which are bridged by ligands that enable magnetic interactions between the metal centres, ultimately giving rise to unique magnetic behaviours (Tommasino *et al.*, 2012; Novitchi *et al.*, 2012). The magnetic properties of these synthesised complexes, which were prepared using a building block approach, have been thoroughly investigated through various experimental methods (Gatteschi *et al.*, 1991; Xue *et al.*, 2002; Kahn, 1993; Sasmal *et al.*, 2012; Sasmal *et al.*, 2013).

This study reports the preparation, crystal structure, EPR, magnetic properties and cyclic voltammetric study of the prepared $[\text{Cu}^{\text{II}}_2(\text{R})_2(\mu\text{-SCN})(\text{SCN})]_n$ (1) synthesised through the reaction of picolinaldehyde with Cu^{II} and NaSCN .

Synthesis of Complex $[\text{Cu}^{\text{II}}_2(\text{R})_2(\text{SCN})_2]_n$ (1)

Reaction of $\text{Cu}(\text{ClO}_4)_2 \cdot 6\text{H}_2\text{O}$ and Pyridine-2-carboxaldehyde was carried out in a methanolic medium with gentle heating; the reaction mixture was stirred. The mixture was then cooled, followed by the dropwise addition of an aqueous sodium thiocyanate solution, and subsequently stirred to ensure the reaction proceeded to completion. The final green solution was filtered and was set aside to undergo slow evaporation, resulting in the formation of needle-shaped green single crystals.

Results and Discussion

EPR study

The room-temperature EPR spectrum of compound 1, as shown in Figure 1, exhibits a tetragonal pattern characterised by two distinct g values, with the order $g_z > g_x = g_y > g_e$, indicative of its electronic structure and copper (II) ion environment.

The tetragonal EPR spectrum observed for compound 1 suggests a $\{dx^2-y^2\}^1$ ground state configuration (Sasmal *et al.*, 2013), consistent with the square planar and square pyramidal geometries present in compound 1, as supported by the g values obtained.

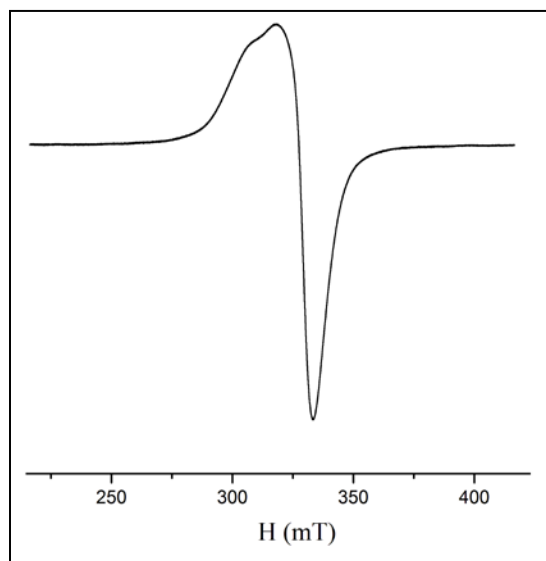


Figure 1: Room Temperature EPR Spectra of Complex 1 (Dhal et al., 2014)

Electrochemical Studies

Cyclic voltammetry measurements were performed on the complex in a solution of acetonitrile. Tetrabutylammonium perchlorate was used as a supporting electrolyte under a nitrogen atmosphere. The scan rate was 50 mV/s. Figure 2 exhibits two distinct cathodic signals in the cyclic voltammogram of the complex, appearing at potentials of -0.28 V and -0.96 V.

The first wave, which is quasi-reversible, is attributed to the reduction of $\text{Cu}^{\text{II}}\text{Cu}^{\text{II}}$ to $\text{Cu}^{\text{II}}\text{Cu}^{\text{I}}$, whereas the second wave, being fully irreversible, is assigned to the reduction of $\text{Cu}^{\text{II}}\text{Cu}^{\text{I}}$ to $\text{Cu}^{\text{I}}\text{Cu}^{\text{I}}$.

A subsequent dissolution process is observed, potentially triggered by the partial degradation of the complex liberating Cu^{I} ions following the two-step one-electron reduction. As the Cu^{I} is further reduced to Cu_0 , metallic copper accumulates on the electrode surface.

A sharp anodic peak at -0.25V signifies the dissolution of the deposited Cu_0 . This phenomenon implies that the $\text{Cu}^{\text{I}}(\mu\text{-O})_2\text{Cu}^{\text{I}}$ entity is unstable and prone to rapid decomposition. Notably, this electrochemical profile is similar to that of other dimeric copper complexes (Torelli et al., 2002; Torelli et al., 2000; Basak et al., 2010; Banerjee et al., 2009), likely due to the necessary structural rearrangements accompanying reduction. Furthermore, the anodic segment of the CV curve reveals an oxidation signal at 0.41V, which is provisionally attributed to the oxidation of the metal centre-bound ligand.

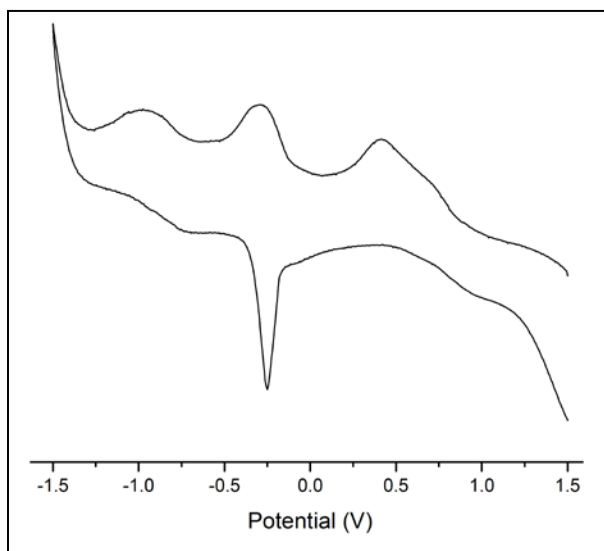


Figure 2: CV Curve of Complex 1 (Dhal et al., 2014)

Crystal Structure Description

Crystal Structure Analysis of $[\text{Cu}^{\text{II}}_2(\text{R})_2(\text{SCN})_2]_n$ (1)

Structural analysis of complex 1 reveals that the complex crystallises in the monoclinic P21/c space group. The crystal structure of the synthesised complex reveals a dinuclear entity, comprising two Cu atoms, two ligands (R), and two SCN moieties, which are linked by a double-alkoxido bridge, forming a $[\text{Cu}^{\text{II}}_2(\text{R})(\text{SCN})]_2$ core within the asymmetric unit (Figure 3). The chelating ligand R, identified as S-methoxy(pyridine-2) methanol, is generated in a single step through a copper-facilitated reaction, which is a crucial intermediate in the process.

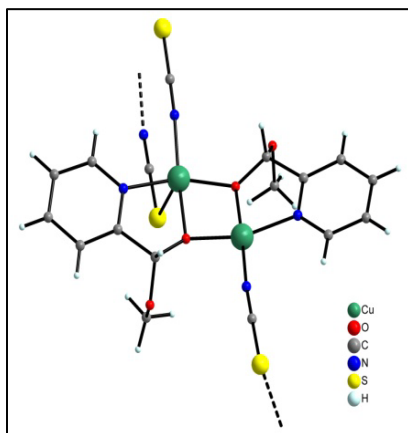


Figure 3: Perspective View of Asymmetric Unit of the Complex $[\text{Cu}^{\text{II}}_2(\text{R})_2(\text{SCN})_2]_n$ (Dhal et al., 2014)

The coordination environments around the two Cu^{II} ions within the dinuclear unit exhibit subtle differences. Specifically, the Cu2 centre adopts a distorted square-pyramidal geometry, characterised by an Addison parameter (Addison *et al.*, 1984) (τ) of 0.2158. It features an elongated axial Cu2-S23 bond (2.8286(8) Å) that semi-coordinates each Cu2 atom to the Cu1 atom of an adjacent dimer (Figure 4).

Cu1 adopts a more precise square planar coordination. As the axial Cu1-S28 distance of 3.243(8) Å exceeds the typical range for a covalent Cu-S bond with a notable interaction between copper and the sulphur centre. The basal plane of each copper atom is formed by one nitrogen atom from the pyridine ring and another from the thiocyanate moiety and two bridging η^2 -alkoxido oxygen atoms from the methoxy(pyridine-2) methanol ligand.

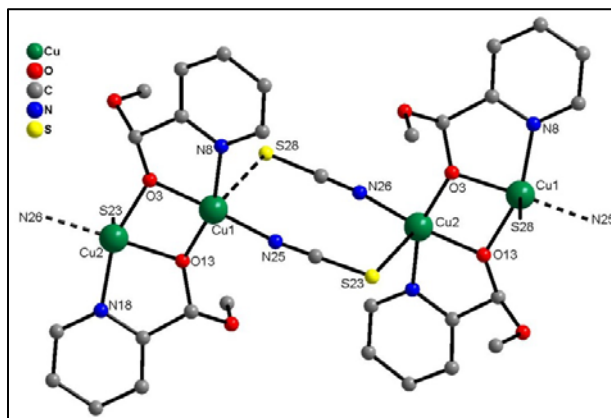


Figure 4: Representation of the Weak Cu...S Bonds in Compound 1 (Dhal *et al.*, 2014)

Each Cu2 atom is linked to the Cu1 atom of an adjacent dimer through the Cu2-S23 bond, resulting in a zigzag chain that propagates through the c-axis as shown in Figure 5. This one-dimensional polymer features an alternating arrangement of double methoxido and single thiocyanato bridges between Cu1 which is square planar, and Cu2 ions, which are square pyramidal in nature. The zigzag chains are spatially separated due to the significant steric hindrance imposed by the methoxy substituents.

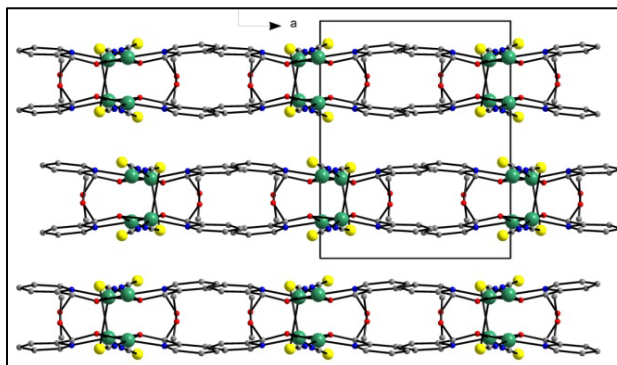


Figure 5: View of Complex 1 Along the ab Plane (Dhal *et al.*, 2014)

Cu...Cu intrachain separation is 2.968(4) Å, consistent with known dialkoxido-bridged copper complexes (Seppälä *et al.*, 2012). The Cu1(μ -O)₂Cu2 bridging unit exhibits a slight fold, with a dihedral angle of 15.11(8)° between Cu1-O3-O13-Cu2. Within the equatorial planes, Cu-N bond lengths (1.916-1.996 Å) are comparable to Cu-O bond lengths, which are around 1.919-1.935 Å and significantly shorter than the axial Cu-S distance of 2.8286(8) Å. The basal planes of Cu1 and Cu2 are oriented at an angle of 26.40° relative to each other.

Magnetic Studies

The room-temperature $\chi_m T$ value of compound **1** exhibits a value of approximately 0.40 cm³ K mol⁻¹, significantly lower than the expected value. As the temperature decreases, $\chi_m T$ steadily declines, eventually reaching a plateau at 0.03 cm³ K mol⁻¹ below around 80 K (Figure 6).

The structure of complex **1** feature alternating zigzag chains so the magnetic interaction along the lengthy axial Copper Sulphur bond is likely insignificant. Consequently, complex **1** can be magnetically treated as a Cu^{II} dimer connected by double methoxido bridges, disregarding the chain-like arrangement.

The magnetic properties were successfully modelled using the classical Bleaney-Bowers $S = 1/2$ dimer approach (Bleaney & Bowers, 2012). This approach accurately describes the magnetic behaviour of the complex across the entire temperature range, yielding best-fit parameters of $g = 2.150$, $J = -374$ cm⁻¹ and a 3.3 % paramagnetic impurity (with the Hamiltonian defined as $H = -JS_1S_2$, represented by the solid line in Figure 6). In the inset of Figure 6 the presence of this paramagnetic impurity is accounted for in the observed low-temperature divergence in the χ_m plot and the residual low-temperature $\chi_m T$ value is approximately 0.03 cm³ K mol⁻¹.

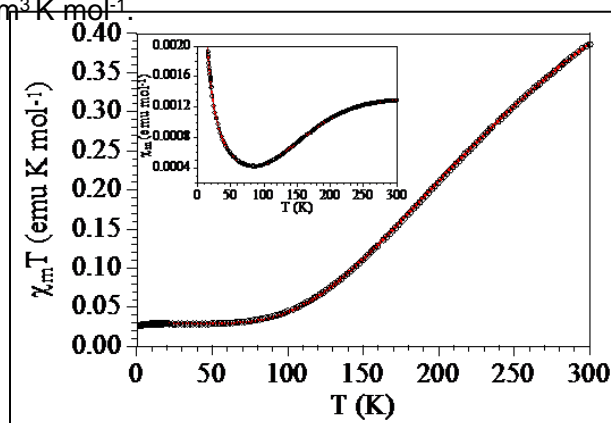


Figure 6: Temperature Dependence of the $\chi_m T$ Product Per Cu^{II} Dimer of Compound **1, Thermal Variation of χ_m is Shown in the Inset (Dhal *et al.*, 2014)**

The strong antiferromagnetic coupling can be readily rationalised based on established magneto-structural relationships for double alkoxido bridges occupying equatorial sites. These studies have identified the bond angles (α) between copper and oxygen as the key

factors influencing magnetic coupling, along with the angle between the Cu_2O_2 plane (τ) and the C-O bond of the alkoxido ligand. The slightly lower observed coupling of -374 cm^{-1} in **1** may be attributed to the non-planarity of the Cu_2O_2 unit, as evidenced by a dihedral angle of $15.11(8)^\circ$.

Conclusion

Here a polymeric copper (II) complex, $[\text{Cu}^{\text{II}}_2(\text{R})_2(\text{SCN})_2]_n$ has been reported. It is prepared via a single step reaction of picolinaldehyde in methanolic medium. The formation of this complex proceeds through the in-situ generation of the (S)-methoxy(pyridine-2) methanol ligand, which is produced via copper-catalysed hemiacetal formation resulting from the nucleophilic attack of methoxide on picolinaldehyde. The planar $[\text{Cu}^{\text{II}}_2(\text{R})_2(\text{SCN})_2]$ dimers exhibit strong antiferromagnetic coupling, consistent with established magneto-structural relationships observed in $\text{Cu}(\mu\text{-O})_2\text{Cu}$ dimers that have been structurally and magnetically characterised.

Acknowledgement

The author extends her sincere gratitude to Prof. Samiran Mitra for his mentorship and to Dr. Arup Mandal of Rammohan College for his valuable support and constant encouragement.

References

- Addison, A. W., Rao, T. N., Reedijk, J., van Rijn, J., & Verschoor, G. C. (1984). Synthesis, structure, and spectroscopic properties of copper (II) compounds containing nitrogen–sulphur donor ligands; the crystal and molecular structure of aqua [1, 7-bis (N-methylbenzimidazol-2'-yl)-2, 6-dithiaheptane] copper (II) perchlorate. *Journal of the Chemical Society, Dalton Transactions*, (7), 1349-1356. <https://doi.org/10.1039/DT9840001349>
- Banerjee, S., Sen, S., Chakraborty, J., Butcher, R. J., García, C. J. G., Puchta, R., & Mitra, S. (2009). A 'butterfly'-shaped water tetramer in a Cu_4 complex supported by a hydrazone ligand: Synthesis, crystal structure, magnetic properties, and quantum chemical study. *Australian Journal of Chemistry*, 62(12), 1614-1621. <https://doi.org/10.1071/CH09192>
- Basak, S., Sen, S., Roy, P., Gómez-García, C. J., Hughes, D. L., Butcher, R. J., ... & Mitra, S. (2010). Structural Variation and Magneto-Structural Correlation in Two New Dinuclear Bis (μ -2-Phenoxy)-Bridged Cu^{II} Schiff-Base Complexes: Catalytic Potential for the Peroxidative Oxidation of Cycloalkanes. *Australian Journal of Chemistry*, 63(3), 479-489. <https://doi.org/10.1071/CH09396>
- Blake, A. J., Champness, N. R., Chung, S. S., Li, W. S., & Schröder, M. (1997). In situ ligand synthesis and construction of an unprecedented three-dimensional array with silver (I): a new approach to inorganic crystal engineering. *Chemical Communications*, (17), 1675-1676. <https://doi.org/10.1039/A702972A>
- Bleaney, B., & Bowers, K. D. (1952). Anomalous paramagnetism of copper acetate. *Proceedings of the Royal Society of London. Series A. Mathematical and Physical Sciences*, 214(1119), 451-465. <https://doi.org/10.1098/rspa.1952.0181>

Copper-Catalysed Polymer: Structure and Magnetic Analysis

- Chen, X. M., & Tong, M. L. (2007). Solvothermal in situ metal/ligand reactions: a new bridge between coordination chemistry and organic synthetic chemistry. *Accounts of Chemical Research*, 40(2), 162-170. <https://doi.org/10.1021/ar068084p>
- Cheng, J. K., Yao, Y. G., Zhang, J., Li, Z. J., Cai, Z. W., Zhang, X. Y., ... & Wen, Y. H. (2004). A simultaneous redox, alkylation, self-assembly reaction under solvothermal conditions afforded a luminescent copper (I) chain polymer constructed of Cu₃I₄-and EtS-4-C₅H₄N⁺ Et components (Et= CH₃CH₂). *Journal of the American Chemical Society*, 126(25), 7796-7797. <https://doi.org/10.1021/ja048624i>
- Dhal, P., Sasmal, A., Gómez-García, C. J., Bauzá, A., Frontera, A., Pilet, G., & Mitra, S. (2014). Copper-Assisted Hemiacetal Synthesis: A Cull Chain Obtained by a One-Step in situ Reaction of Picolinaldehyde. *European Journal of Inorganic Chemistry*, 2014(20), 3271-3278. <https://doi.org/10.1002/ejic.201402176>
- Gatteschi, D., Kahn, O., Miller, J. S., & Palacio, F. (Eds.). (1991). *Magnetic Molecular Materials*. (Vol. 198). Springer Science & Business Media. <https://doi.org/10.1007/978-94-011-3254-1>
- Kahn, O. (1993). *Molecular Magnetism*. VCH Publishers: New York, 98(9), 1208. <https://doi.org/10.1002/bbpc.19940980935>
- Liu, C. M., Gao, S., & Kou, H. Z. (2001). Dehydrogenative coupling of phenanthroline under hydrothermal conditions: crystal structure of a novel layered vanadate complex constructed of 4, 8, 10-net sheets: [(2, 2'-biphen) Co] V₃O₈. 5. *Chemical Communications*, (17), 1670-1671. <https://doi.org/10.1039/B103304M>
- Novitchi, G., Pilet, G., Ungur, L., Moshchalkov, V. V., Wernsdorfer, W., Chibotaru, L. F., ... & Powell, A. K. (2012). Heterometallic Cu II/Dy III 1D chiral polymers: chirogenesis and exchange coupling of toroidal moments in trinuclear Dy 3 single molecule magnets. *Chemical Science*, 3(4), 1169-1176. <https://doi.org/10.1039/C2SC00728B>
- Qu, Z. R., Zhao, H., Wang, X. S., Li, Y. H., Song, Y. M., Liu, Y. J., ... & You, X. Z. (2003). Homochiral Zn and Cd coordination polymers containing amino acid- tetrazole ligands. *Inorganic Chemistry*, 42(24), 7710-7712. <https://doi.org/10.1021/ic034685q>
- Sasmal, A., Saha, S., Gómez-García, C. J., Desplanches, C., Garribba, E., Bauzá, A., ... & Mitra, S. (2013). Reversible switching of the electronic ground state in a pentacoordinated Cu (II) complex. *Chemical Communications*, 49(71), 7806-7808. <https://doi.org/10.1039/C3CC44276D>
- Sasmal, A., Shit, S., Rizzoli, C., Wang, H., Desplanches, C., & Mitra, S. (2012). Framework solids based on copper (II) halides (Cl/Br) and methylene-bridged bis (1-hydroxybenzotriazole): Synthesis, crystal structures, magneto-structural correlation, and density functional theory (DFT) studies. *Inorganic Chemistry*, 51(19), 10148-10157. <https://doi.org/10.1021/ic300629v>
- Seppälä, P., Colacio, E., Mota, A. J., & Sillanpää, R. (2012). Synthesis, crystal structures and magnetic properties of bis (μ-dialkoxo)-bridged linear trinuclear copper (ii) complexes with aminoalcohol ligands: a theoretical/experimental magneto-structural study. *Dalton Transactions*, 41(9), 2648-2658. <https://doi.org/10.1039/C2DT11628F>
- Tommasino, J. B., Chastanet, G., Le Guennic, B., Robert, V., & Pilet, G. (2012). A 1D coordination polymer built on asymmetric μ 1, 1, 3-azide bridge: from unusual topology to magnetic

- properties and Cu (ii)/Cu (i) redox reversibility. *New Journal of Chemistry*, 36(11), 2228-2235. <https://doi.org/10.1039/C2NJ40302A>
- Torelli, S., Belle, C., Gautier-Luneau, I., Pierre, J. L., Saint-Aman, E., Latour, J. M., ... & Luneau, D. (2000). pH-Controlled change of the metal coordination in a dicopper (II) complex of the ligand H- BPMP: Crystal structures, magnetic properties, and catecholase activity. *Inorganic Chemistry*, 39(16), 3526-3536. <https://doi.org/10.1021/ic991450z>
- Torelli, S., Belle, C., Hamman, S., Pierre, J. L., & Saint-Aman, E. (2002). Substrate binding in catechol oxidase activity: Biomimetic approach. *Inorganic Chemistry*, 41(15), 3983-3989. <https://doi.org/10.1021/ic025599d>
- Xiong, R. -G., Xue, X., Zhao, H., You, X. -Z., Abrahams, B. F., & Xue, Z. -L. (2002). Novel, Acentric Metal–Organic Coordination Polymers from Hydrothermal Reactions Involving in Situ Ligand Synthesis. *Angewandte Chemie*, 41(20), 3800-3803. [https://doi.org/10.1002/1521-3773\(20021018\)41:20<3800::AID-ANIE3800>3.0.CO;2-3](https://doi.org/10.1002/1521-3773(20021018)41:20<3800::AID-ANIE3800>3.0.CO;2-3)
- Xue, X., Wang, X. S., Wang, L. Z., Xiong, R. G., Abrahams, B. F., You, X. Z., ... & Che, C. M. (2002). Hydrothermal preparation of novel Cd (II) coordination polymers employing 5-(4-pyridyl) tetrazolate as a bridging ligand. *Inorganic Chemistry*, 41(25), 6544-6546. <http://dx.doi.org/10.1021/ic0257118>
- Xiong, R. G., Zhang, J., Chen, Z. F., You, X. Z., Che, C. M., & Fun, H. K. (2001). *In situ* ligand synthesis and the first crystallographically characterized lanthanide 3-D pillared networks containing benzene-1, 4-disulfonate as a building block. *Journal of the Chemical Society, Dalton Transactions*, (6), 780-782. <https://doi.org/10.1039/B009542G>
- Zhang, J. P., Zheng, S. L., Huang, X. C., & Chen, X. M. (2004). Two Unprecedented 3-Connected Three-Dimensional Networks of Copper (i) Triazoles: In Situ Formation of Ligands by Cycloaddition of Nitriles and Ammonia. *Angewandte Chemie International Edition*, 43(2), 206-209. <https://doi.org/10.1002/anie.200352627>
- Zhang, X. M. (2005). Hydro (solvo) thermal in situ ligand syntheses. *Coordination Chemistry Reviews*, 249(11-12), 1201-1219. <https://doi.org/10.1016/j.ccr.2005.01.004>
- Zhang, X. M., Tong, M. L., & Chen, X. M. (2002). Hydroxylation of N-Heterocycle Ligands Observed in Two Unusual Mixed-Valence CuI/CuII Complexes. *Angewandte Chemie International Edition*, 41(6), 1029-1031. [https://doi.org/10.1002/1521-3773\(20020315\)41:6%3C1029::AID-ANIE1029%3E3.0.CO;2-B](https://doi.org/10.1002/1521-3773(20020315)41:6%3C1029::AID-ANIE1029%3E3.0.CO;2-B)
- Zhang, X. M., Tong, M. L., Gong, M. L., Lee, H. K., Luo, L., Li, K. F., ... & Chen, X. M. (2002). Syntheses, Crystal Structures, and Physical Properties of Dinuclear Copper (i) and Tetranuclear Mixed-Valence Copper (i, ii) Complexes with Hydroxylated Bipyridyl-Like Ligands. *Chemistry—A European Journal*, 8(14), 3187-3194. [https://doi.org/10.1002/1521-3765\(20020715\)8:14%3C3187::AID-CHEM3187%3E3.0.CO;2-9](https://doi.org/10.1002/1521-3765(20020715)8:14%3C3187::AID-CHEM3187%3E3.0.CO;2-9)

KO^tBu Promoted Transformation of Nitriles to Amides

Ganesh Chandra Midya

Jogesh Chandra Chaudhuri College, Tollygunge, Kolkata, West Bengal, 700033 India

Corresponding Author's E-mail: gcmidya007@gmail.com

Abstract

The amide functional group is present in proteins and is essential for sustaining life. It is a synthetically versatile synthon distributed in several biologically active molecules. Although there are many synthetic methods, there is a need for the development of an ideal reaction condition, which can be performed at room temperature in a metal-free environment and be scalable for industrial applications. This chapter describes the hydration of nitriles using potassium tert-butoxide under anhydrous conditions. Potassium tert-butoxide acts as a nucleophilic oxygen source during the hydration of nitriles to give the corresponding amides under anhydrous conditions. This protocol does not need any transition-metal catalyst or any special experimental setup and is easily scalable to bulk-scale synthesis. A single-electron-transfer radical mechanism as well as an ionic mechanism are proposed for the hydration process. The reaction proceeds smoothly for a broad range of substrates under mild conditions, providing an efficient and economically affordable synthetic route to the amides in excellent yields.

Keywords: Amide; KO^tBu; Nitrile

Introduction

Amides form one of the most important functional groups in recent chemistry. They are present in numerous natural products and pharmaceutical molecules (Patai & Rappoport, 1970) In everyday life, some common medicines are taken by us, which contain amide units. Acetaminophen (paracetamol) is used as a common analgesic and antipyretic. Lidocaine and trimecaine are known as local anaesthetics. Piracetam is a nootropic in the racetams group, with a chemical name 2-oxo-1-pyrrolidine acetamide. The chemical name of levetiracetam, a single enantiomer, is (-)-(S)- α -ethyl-2-oxo-1-pyrrolidine acetamide. It is an antiepileptic drug. Pyrazinamide, the pyrazine analogue of nicotinamide, acts as an antitubercular agent. Atenolol is a selective β_1 receptor antagonist, a drug belonging to the group of beta blockers.

Temodar contains temozolomide, an imidazotetrazine derivative. Penicillin is a group of antibiotics. These are amide containing drugs and are widely used in the treatment of bacterial infections caused by susceptible, usually Gram-positive, organisms.

Atorvastatin and diltiazem are another two important drug molecules which contain amide bonds. Atorvastatin is considered the top selling drug worldwide since 2003, and it blocks the production of cholesterol. Diltiazem is used in the treatment of angina and hypertension.

KO^tBu -Mediated Nitrile to Amide Conversion

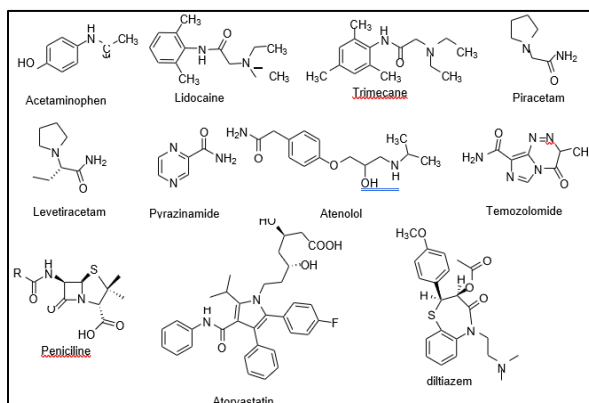


Figure 1: Amide Containing Pharmaceutical Molecules

Amide groups are present in biologically active standard amino acids like asparagines and glutamine, sphingolipids (N-acylated aminoalcohols sphingosines), nicotinamide (a vitamin, PPF) and amino sugars (all of them are N-acylated). Amides are present in linking amino acids to proteins such as enzymes. Aspartame is an amide containing compound, used as a sugar substitute in some foods and beverages. It is an artificial, non-saccharide sweetener.

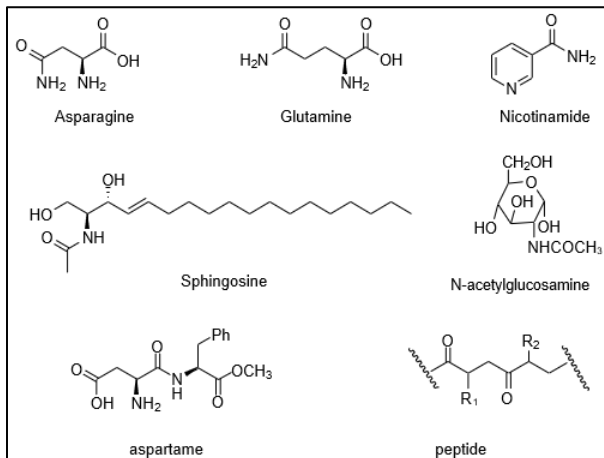
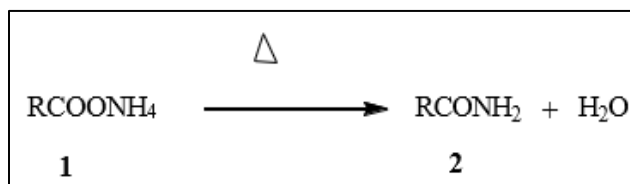


Figure 2: Amide Containing Biologically Active and Other Useful Molecules

Synthesis of Amides

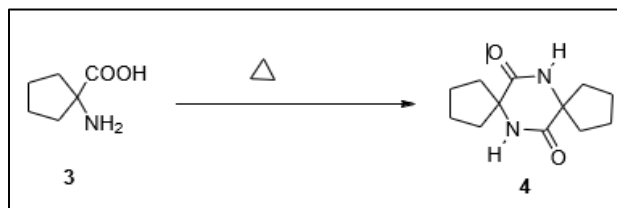
Pyrolysis of Amines and Carboxylic Acids

Heating a mixture of an amine and an acid is considered one of the common methods for preparation of amides. The salts formed by the reaction of carboxylic acids and amines lead to amide on strong heating, which is the case for the conversion of ammonium acetate 1 to acetamide 2 (Scheme 1) (Alvarado & Coleman, 1923, p.3).



Scheme 1: Formation of Amide by Heating of Ammonium Salt

Preparation of succinimide from heating ammonium succinate (Behr & Clarke, 1936, p.75) and preparation of benzanilide (Hurd & Webb, 1927, p.6) by heating benzoic acid with an excess of aniline are also known. An interesting method includes the formation of piperidinediones 4 by heating of α -amino acid (Scheme 2) (McElvain & Pryde 1949, p.326).



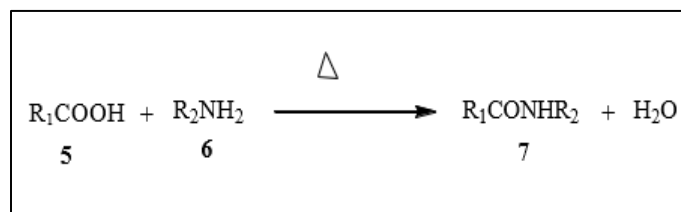
Scheme 2: Formation of Piperidinediones by Heating of A-Amino Acid

In 1931 Mitchell and co-workers (p.1879) reported that when ammonia gas is passed through an aliphatic carboxylic acid corresponding to aliphatic amide is formed. Temperature is maintained in such a way that the water formed is continually removed, and hence the equilibrium point of the reaction is shifted to the amide, side leading to a high yield. A drawback of this method is that the reaction is not suitable for carboxylic acids with a longer alkyl chain length than butyric acid. The rate of the reaction decreased considerably with increasing chain length of the carboxylic acid. On the other hand, as it requires high temperature to heat the acid, this high temperature leads dehydration of the longer chain amides to nitriles.

In 1993 Jursic and Zdravkovski (P. 2761) reported that a range of amides 7 can be synthesised by heating a mixture of different amines 5 and carboxylic acids 6 without any catalyst or coupling agent (Scheme 3). The optimum condition for the pyrolysis of amide-carboxylic acid mixture is heating at 160 - 180°C for 10-30 minutes. This method of preparing amides has so many advantages: it requires no catalysts or solvents; the procedure is simple, and the reaction times are short. On the other hand, there are several drawbacks to the method. Both the amines and carboxylic acids used should be thermally stable and should have a melting point below 200 °C. They should be non-volatile. Both the amine and acid have high boiling points. As the process

requires high temperature for completion, sometimes extreme heating can lead to tar formation. These reasons have limited this method from not to being a widely used general method for direct amide formation. This method is also not susceptible to small scale reactions and high value reactants.

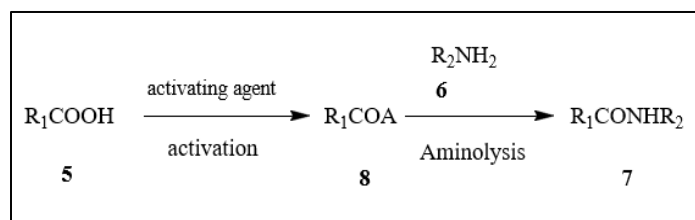
KO^tBu -Mediated Nitrile to Amide Conversion



Scheme 3: Formation of Amide by Direct Heating A Mixture of Acid and Amine

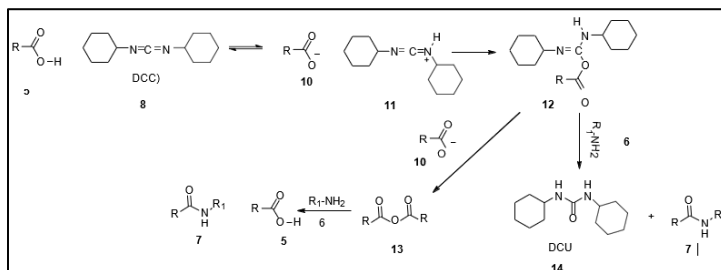
Amide Formation by Acid-amine Coupling

Typical methods of amide bond formation are reactions between amine and activated carboxylic acid derivatives such as acid chlorides (which are generally prepared from thionyl or oxalyl chloride), anhydrides, or by using the carboxylic acid directly with stoichiometric amounts of coupling reagents such as carbodiimides (Montalbetti & Falque, 2005, p.10827) (Scheme 4).



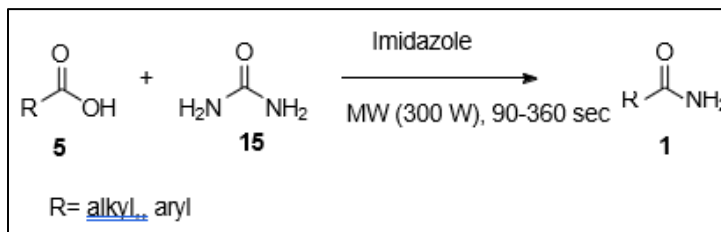
Scheme 4: Coupling Using Carbodiimides N,N'-Dicyclohexylcarbodiimide (DCC) 9

N,N'-Dicyclohexylcarbodiimide (DCC) 9 has been widely used as a coupling reagent since 1955 (Sheehan & Hess, 1955, p.1067). N,N'-Dicyclohexylcarbodiimide (DCC) 9 first reacts with carboxylic acid 5 to form the active species O-acyl urea 11. Then either direct coupling with the amine 6 leads the desired amide along with dicyclohexylurea (DCU) 14 as a by-product, or reaction of another acid unit leads carboxylic anhydride 13, which reacts with amine 5 to give amide 7. With DCC, oxazolone formation can take place after generation of the O-acylurea leading to epimerisation. Koenig and Geiger (1970, P.788) reported that in a coupling reaction with carbodiimides as coupling reagents, 1-hydroxy-1H-benzotriazole (HOBt) acts as an additive and reduces epimerisation.



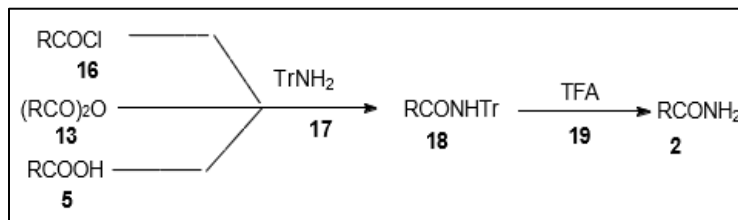
Scheme 5: Coupling of Acid and Amine in Presence of Coupling Agent DCC 9

In 2003 Khalafi-Nezhad, Mokhtari and Rad reported (p.7325) microwave assisted method for synthesising primary amides. Under microwave irradiation, carboxylic acid **5** reacts with urea **15** in the presence of imidazole to yield primary amide **2** (Scheme 6).



Scheme 6: Synthesis of Primary Amide Using Imidazole

In 2009 Theodorou *et al.* (p.277) developed another method of preparation of primary amides. Carboxylic acids **5** or its activated derivatives undergo acylation reactions to obtain N- tritylamides **18**, which undergo deprotection reactions with trifluoroacetic acid **19** at room temperature to the desired primary amides **2** (Scheme 7).



Scheme 7: Synthesis of Primary Amides Via Tritylamides Formation

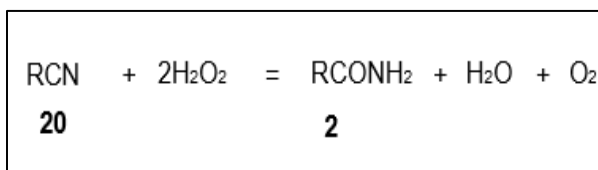
Hydrolysis of Nitrile to Amide

Though there are many methods for the synthesis of amides, the hydration of nitriles is a straightforward, atom-economical and classical transformation. Traditional processes are based on acid- or base-catalysed hydrolysis, which requires harsh conditions and gives low yield due to further hydrolysis of the amides to the carboxylic acids. Therefore, the limitation of acid- or base-catalysed hydrolysis demands sustainable methods. Subsequently, metalloenzyme (Drauz & Waldmann, 2002) and transition metal catalysts (Murahashi *et al.*, 1992, p.2521) were developed for the hydrolysis of nitriles.

Metal Free Hydrolysis of Nitrile to Amide

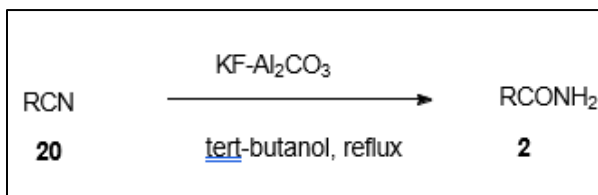
Although metal-catalysed reactions are efficient protocols for the synthesis of amides, the use of expensive and toxic metal catalysts limits the exploitation of these methods. Therefore, the development of a metal-free protocol is highly demanding in chemical research. Hydrogen peroxide was reported as a hydrolytic agent for converting nitriles **20** into amides **2** (Scheme 8) by McMaster and Langreck (1917). McMaster and Langreck (1917, p.103) found that the reaction took place more smoothly when a small amount of alkali was present and at a temperature of 40 °C.

KO^tBu -Mediated Nitrile to Amide Conversion



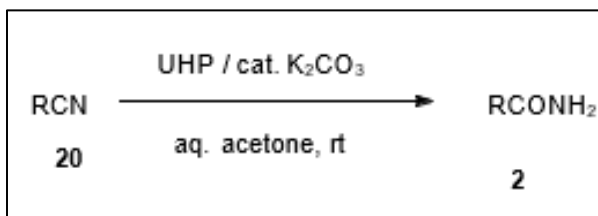
Scheme 8: Hydrogen Peroxide as Hydrolytic Agent for Conversion of Nitrile to Amide

In 1982 Rao (p. 177) described alumina coated potassium fluoride as useful catalyst for transformation of nitriles 20 to amides 2 in tert-butyl alcohol (Scheme 9).



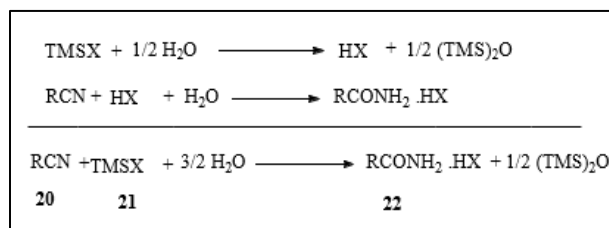
Scheme 9: Conversion of Nitriles to Amides by Alumina Coated Potassium Fluoride

In 1993, Balicki and Kaczmarek (P. 3149) developed a mild and efficient protocol where urea-hydrogen peroxide (UHP) adduct in combination with catalytic amount of K₂CO₃ easily hydrolyses a variety of aliphatic and aromatic nitriles 20 to amides 2 in aqueous acetone at room temperature (Scheme 10). This catalytic system is inexpensive, stable and easy to handle.



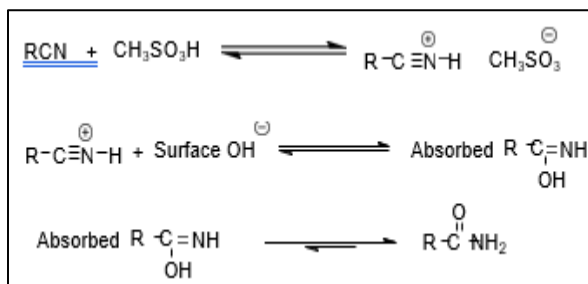
Scheme 10: Use of Urea-hydrogen Peroxide (UHP) Adduct and Potassium Carbonate

Basu and Luo, in 1998 (p.3005), reported that a variety of aliphatic and aromatic nitriles can smoothly be transformed to amides by hydrogen halide generated in situ by reaction of TMSX 21 and water at 0°C to 25°C for 2 to 4 h. They proposed that first the nitrile 20 gets protonated by HCl, generated in situ from TMSX 21 and half an equivalent of H₂O, the protonated nitrile then undergoes nucleophilic attack by another equivalent of H₂O to form the amide salt (Scheme 11).



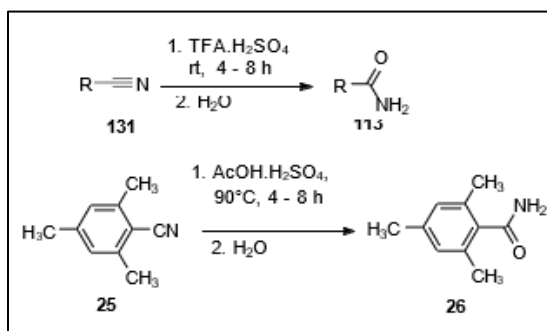
Scheme 11: Transformation of Nitriles to Amides Using in Situ Generated Hydrogen Halide

In 2003, Sharghi and Hosseini Sarvari reported (p. 207) that Al₂O₃/MeSO₃H (AMA) system can be used for the hydrolysis of nitriles to the amides. The reaction proceeded smoothly within 10–15 min when nitrile was heated at 120°C with AMA. The polar Al₂O₃ surface contains a layer of hydroxyl groups which serve as the source of water in the reaction (Scheme 12).



Scheme 12: Transformation of Nitriles to Amides by Al₂O₃/MeSO₃H

Later, Moorthy and Singhal (2005, p.1926) developed a reagent system consisting of TFA-H₂SO₄ mixture, which converts both aliphatic and aromatic nitriles 20 to the corresponding amides 2 (Scheme 13). Transformation of sterically hindered nitriles 25 needed higher temperatures (>90°C) and AcOH was used instead of TFA to obtain the corresponding amides 26 (Scheme 13).

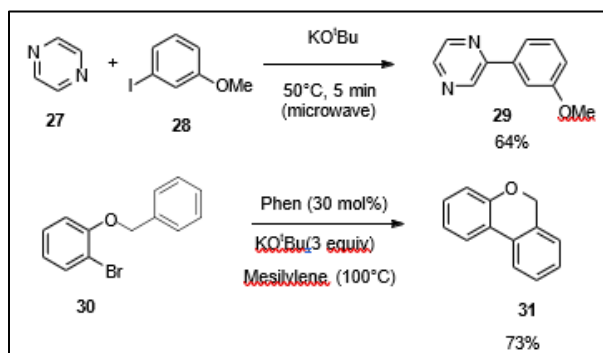


Scheme 13: Conversion of Nitriles to Amides Using TFA- H₂SO₄ or AcOH- H₂SO₄ Mixture

KO^tBu -Mediated Nitrile to Amide Conversion

Although these processes offer improved yields and selectivity, each of these protocols has its own set of disadvantages. There is a need for the development of an ideal reaction condition, which can be performed at room temperature in a metal-free environment and scalable for industrial applications.

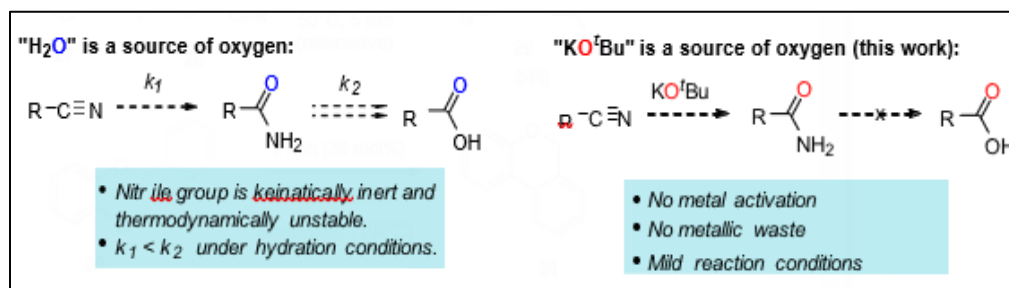
Recently the use of KO^tBu has attracted much more attention, which provides a cheap and green alternative to several metal-catalysed organic reactions. In 2008, Yanagisawa and co-workers (p. 4673) reported KO^tBu promoted synthesis of biaryls 29 by coupling reaction between electron- deficient arene 27 with aryl halide 28 (Scheme 14). Liu group (2010) independently reported KO^tBu mediated biaryl synthesis in 2010 (p.16737).



Scheme 14: Potassium tert-butoxide Promoted Synthesis of Biaryls

In 2011, a special role of KO^tBu was observed during iron-catalysed head-to-head dimerisation of terminal aryl alkynes to give the corresponding (E) selective conjugated enynes (Midya *et al.*, 2011, p.6698) These new modes of reactivity of KO^tBu raise concerns within the synthetic community. Therefore, the goal was to gain more mechanistic insights into the reactivity of KO^tBu. It has been reported by Kataoka and co-workers (2002, p. 5553) that the nitrile group can be activated via coordination with the potassium ion.

In this chapter we describe an efficient protocol for the hydrolysis of organonitriles to the corresponding amides using potassium tertiary butoxide (KO^tBu) as an oxygen source (Scheme 15).



Scheme 15: Potassium Tertiary Butoxide Promoted Transformation of Organonitriles to Amides

Converging Chemical and Biological Sciences for a Sustainable Era

Results and Discussion

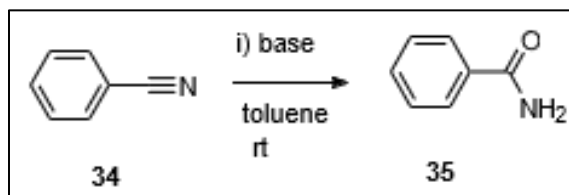
KO^tBu Promoted Transformation of Organonitriles to Amides Under Metal Free Condition

It was previously reported that the nitrile group can be activated via coordination of the nitrile group to the potassium ion (Liu *et al.*, 2010, p.16737). The possibility of nucleophilic addition of *tertiary* butoxide to the electrophilic carbon atom of the activated nitrile group was explored. When 50 mol% of KO^tBu was added to the solution of benzonitrile 34 in toluene under anhydrous conditions (Table 1, entry 1), 42% of the amide 35 was formed. This preliminary result inspires investigate this reaction in detail. Benzonitrile 34 was used as a model substrate to optimise the reaction conditions.

Optimisation of Bases

Improvement of the yield was observed when the amount of base was increased to 1.0 equivalent (entry 2, Table1). Using 2 equiv of base, the yield was further improved to 80% (entry 3, Table 1) and 91% benzamide 35 was obtained when 3.0 equivalent of KO^tBu was added and the reaction was stirred for 5 h at room temperature (entry 4).

Table 1: Screening of Bases for Hydrolysis Reaction of Benzonitrile 34 to Benzamide 35



Entry ^a	Base (eqv.)	Yield (%), time
1	KO ^t Bu (0.5)	42, 5 h
2	KO ^t Bu (1.0)	60, 5 h
3	KO ^t Bu (2.0)	80, 5 h
4	KO ^t Bu (3.0)	91, 5 h
5	KO ^t Bu (3.0)	96, 3 h ^b
6	KO ^t Bu (3.0)	89, 5 h ^c
7	NaO ^t Bu (3.0)	NR, 5 h
8	LiO ^t Bu (3.0)	NR, 5 h
9	K ₂ CO ₃ (3.0)	NR, 5 h ^d
10	Cs ₂ CO ₃ (3.0)	NR, 5 h
11	K ₃ PO ₄ (3.0)	NR, 5 h

^aall reaction were carried out under nitrogen atmosphere, ^bheating at 60 °C, ^cpurity of KO^tBu 99.99%, sigma-aldrich, ^dheating at 130 °C.

A slight improvement in yield (96%) as well as shorter reaction time (3 h) was noticed when it was carried out at 60 °C (entries 4-5). To avoid contamination from the glassware and reagents, hydration of benzonitrile 34 was performed using 99.99% pure KO^tBu (Sigma

KO^tBu -Mediated Nitrile to Amide Conversion

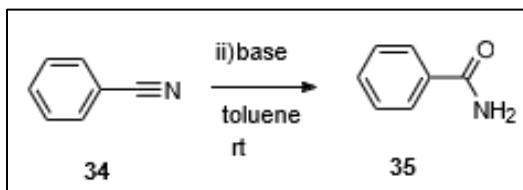
Aldrich) in thoroughly clean glassware. The benzamide was obtained in similar yield in toluene and ^tBuOH (entry 6, Table 1). To investigate the importance of the positive counter cation, sodium and lithium tertiary butoxide were used.

Surprisingly, no product formation was observed in the crude NMR analysis (entries 7-8). This experimental data proves that potassium cation plays an important role in this transformation. Next, several inorganic bases (K₂CO₃, Cs₂CO₃ & K₃PO₄) containing different counter anions were screened and none of these bases afforded the desired product (entries 9-11). Running the reaction in presence of K₂CO₃ at higher temperature did not improve the result after 5 h (Table 1, entry 9).

Optimisation of Solvents

Next, various solvents were screened to further improve the yield. At first, different aprotic solvents were used. Benzonitrile (34) yielded benzamide 35 in 91% yield, when it was treated with 3.0 equivalents of KO^tBu in toluene (Table 2, entry 1). While moderate yield (55%) of the amide 35 was obtained in both THF and xylene (entries 3-4).

Table 2: Screening of Solvent for Hydrolysis Reaction Benzonitrile 34 to Benzamide 35



Entry ^a	solvent	Yield (%), time
1	Toluene	91, 5 h
2	Toluene	15, 5 h ^b
3	Xylene	55, 5 h
4	THF	55, 5 h
5	Dioxane	27, 5 h
6	DMF	NR, 5 h
7	DMSO	NR, 5 h
8	DMAc	NR, 5 h
9	DCE	NR, 5 h
10	DCM	traces, 5 h
11	CHCl ₃	NR, 5 h
12	EtOH	65, 5 h
13	^t PrOH	75, 5 h
14	^t BuOH	>99, 4 h
15	^t BuOH	51, 4 h ^b

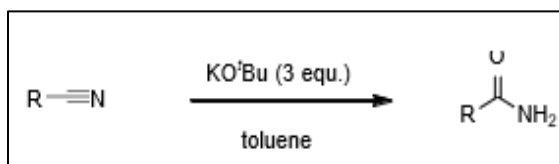
^aall reaction were carried out under nitrogen atmosphere, ^b 2% of H₂O (v/v) was added.

In case of polar aprotic solvents (DMF, DMSO and DMAc) no product formation was observed (entries 6-8). Halogenated solvents like dichloroethane (DCE) and chloroform failed to afford the desired amide 35 (entries 9 and 11) while dichloromethane (DCM) managed to give the desired amide 35 only in trace amounts (entry 10). When hydration was performed in polar protic solvents (entries 12-14), the desired product was obtained in 65%, 75%, and >99% yield in ethanol, isopropanol and tertiary butanol (^tBuOH) respectively. It might seem that air moisture is the source of the Oxygen atom in the amide. But in the presence of small amounts of water (2 % H₂O (v/v)) yield of the amide reduced significantly. The presence of 2 % H₂O (v/v) in toluene reduced the yield to 15%, and the same reduced the yield to 51 % in ^tBuOH (Table 2, entries 2 and 15). It implies that KO^tBu is the source of the Oxygen atom of the amide. Hence, 3 equivalent KO^tBu was proved to be the optimal base. The yield of each of these substrates was determined in both toluene (Table 3) and ^tBuOH (Table 4).

Generalisation of Reaction

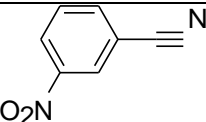
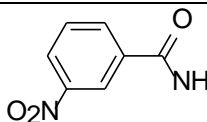
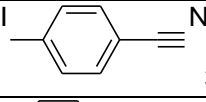
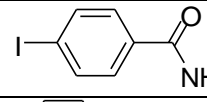
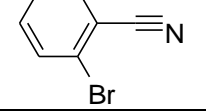
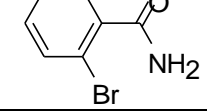
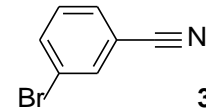
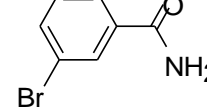
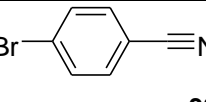
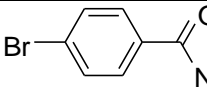
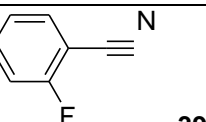
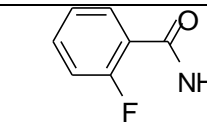
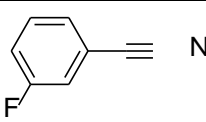
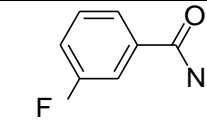
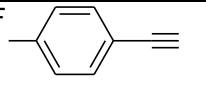
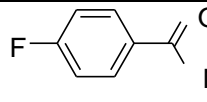
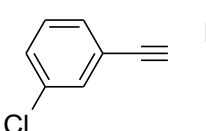
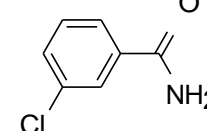
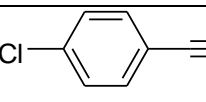
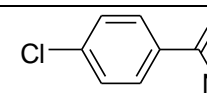
Having established optimal conditions for this reaction, expansion of the substrate scope was explored. Electron-deficient aromatic nitriles provided corresponding amides (36–41) in good to excellent yields (Table 3). Hydration of m-nitrobenzonitrile worked extremely well in ^tBuOH and the corresponding amide 36 was isolated in nearly quantitative yields (>99%). Reactivity of para-substituted halobenzonitriles is higher in both the solvents (^tBuOH and toluene) and the corresponding amides (37, 38c, 39c, 40b) were obtained in excellent yields (Table 3 & Table 4). On the other hand meta- and ortho-substituted halobenzonitriles reacted slowly in toluene (Table 3). The desired amides (38a, 38b, 39a, 39b, 40a, 41) are obtained in good to excellent yields when the hydration was carried out in ^tBuOH. Improved reactivity in ^tBuOH compared to toluene could be due to the strong hydrogen bonding ability of ^tBuOH with the heteroatom present in the aryl moiety. Para-substituted electron-rich aromatic nitriles afforded the corresponding amides (42c, 44, 45) in moderate to good yields in both toluene and ^tBuOH (Table 3 and Table 4).

Table 3: KO^tBu Promoted Hydrolysis of Nitriles to Amides in Toluene

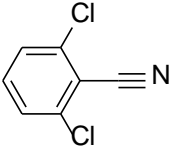
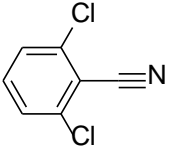
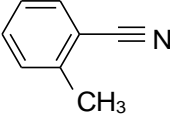
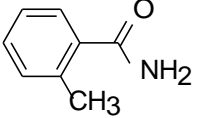
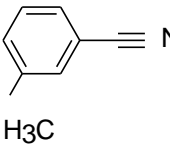
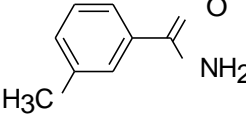
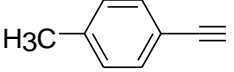
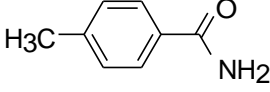
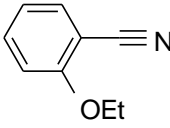
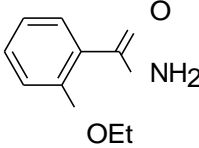
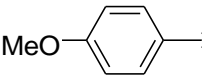
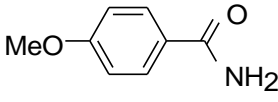
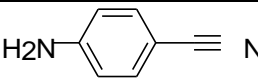
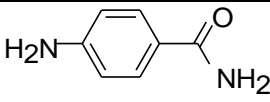
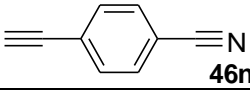
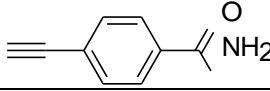
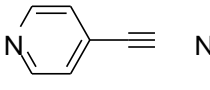
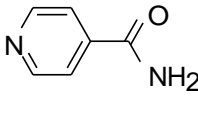
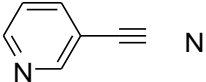
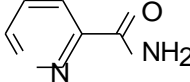


Entry	Substrate	Product	Time, Temperature, Yield
1	 34	 35	5 h, rt, 91%

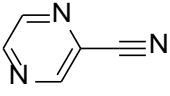
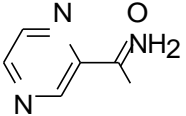
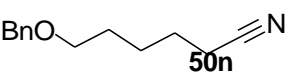
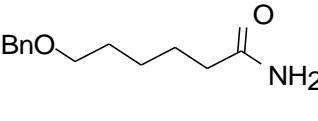
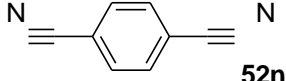
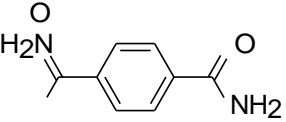
KO^tBu -Mediated Nitrile to Amide Conversion

2	 36n	 36	5 h, rt, no reaction
			5 h, 85 °C, 40%
3	 37n	 37	5 h, rt, 93%
4	 38an	 38a	9 h, rt, 80%
5	 38bn	 38b	9 h, rt, 85%
6	 38cn	 38c	9 h, rt, 90%
7	 39an	 39a	5 h, rt, 85%
8	 39bn	 39b	12 h, rt, 86%
9	 39cn	 39c	5 h, rt, 95%
10	 40an	 40a	12 h, rt, 79%
12	 40bn	 40b	5 h, rt, 84%

KO^tBu-Mediated Nitrile to Amide Conversion

13	 41n	 41	5 h, rt, 58%
14	 42an	 42a	9 h, rt, no reaction
			5 h, 60 °C, 45%
15	 42bn	 42b	9 h, rt, 45%
16	 42cn	 42c	9 h, rt, 79%
17	 43n	 43	5 h, rt, no reaction
			5 h, 60 °C, 95%
18	 44n	 44	9 h, rt, 71%
19	 45n	 45	5 h, 85 °C, 56%
20	 46n	 46	5 h, rt, 85%
21	 47n	 47	5 h, rt, 95%
22	 48n	 48	5 h, rt, 70%

KO^tBu -Mediated Nitrile to Amide Conversion

23	 49n	 49	9 h, rt, 50%
24	 50n	 50	5 h, 50 °C, no reaction
			3 h, 130 °C, 83%
25	 52n	 52	12 h, rt, 58%

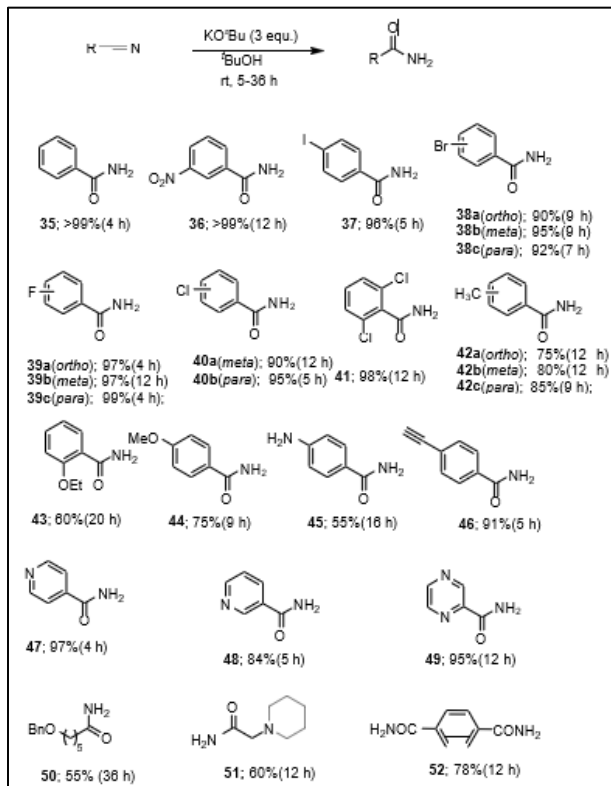
On the other hand, ortho substituted benzonitriles having electron-donating functional groups are less reactive under standard hydration conditions in toluene at rt (Table 3). These benzonitriles can be transformed into the corresponding hydration products (amides 42a and 43) in synthetically useful yields either by heating for a few hours or by performing the hydration reaction in ^tBuOH. The protocol is successfully applied for the hydration of para- and meta-cyano pyridine to give the corresponding amides (47, 48) in 97% and 84% yield, respectively. Antitubercular agent pyrazinamide 49 is prepared in 95% yield by hydration of the corresponding nitrile, protocol has been utilised by us. Meta-cyano pyridine and pyrazine nitrile show higher reactivity in ^tBuOH than toluene.

Higher reactivity can also be explained by hydrogen bonding model. As compared to aromatic nitriles, aliphatic nitriles seem to be less reactive under specific reaction conditions due to the absence of cation- π stabilisation (Scheme 16). Under optimised reaction conditions, amide 50 and 51 are obtained in 55% and 60% yield, when hydration is performed in ^tBuOH. Yield of amide 50 is improved significantly, when the reaction is performed in toluene at 130 °C. This reaction system can also be applied to 1,4-dicyanobenzene. It is delightful to observe the formation of the desired dicarboxamide product 52 as a single product in 78% yield.

These results indicate that the newly developed hydration methodology exhibits general substrate scope (electron-rich, electron-deficient aromatic, heteroaromatic, aliphatic and dicyano nitriles). These reactions can be performed in the air atmosphere without any change in yield of the amide products. The outcome of this protocol depends on both the electronic nature and sterics of the substrates.

In case of ortho- and meta- methylbenzonitriles, ortho-ethoxy benzonitrile and ortho-dichlorobenzonitrile, the hydration is less efficient in toluene at room temperature (Table 4, entries 13-15, 17) and carried out at higher temperature. But these substrates react efficiently in ^tBuOH at room temperature (Table 3) to give the corresponding amides.

Converging Chemical and Biological Sciences for a Sustainable Era

Table 4: KO^tBu Promoted Hydrolysis of Nitriles to Amides in ^tBuOH

The yields were enhanced from 58% (toluene) to 98% (^tBuOH) for the amide 41, 0% (toluene) to 75% (^tBuOH) for the amide 42a, 45% (toluene) to 80% (^tBuOH) for the amide 42b, 0% (toluene) to 60% (^tBuOH) for the amide 43. Similar enhancement of reactivity is also observed in case of meta- nitrobenzonitrile; the yield was enhanced from 0% (toluene) to >99% (^tBuOH) for the amide 36 at room temperature.

Mechanistic Study

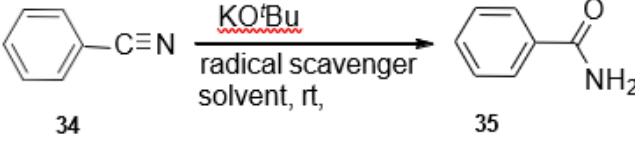
To gain further mechanistic information, radical quenching experiment was performed in both toluene and ^tBuOH, since most of the KO^tBu promoted reactions go through the radical process (Liu *et al.*, 2010, p.16737) (Table 5). When hydration of benzonitrile was performed in the presence of nucleophilic radical trap 2,2,6,6-tetramethylpiperidine (TEMPO), only 78% product formation was observed in toluene, while in the same reaction 82% product formation was observed in ^tBuOH. Furthermore, in both the solvents, around 30% inhibition of product formation was observed in presence of 1,1-diphenyl ethylene.

But in the presence of galvinoxyl as electrophilic radical trap, complete inhibition of nitrile hydration was observed in toluene (Table 5). In ^tBuOH, nearly 30% inhibition of product

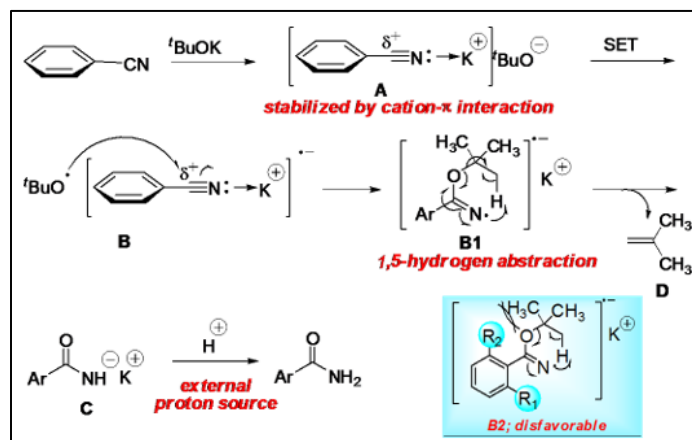
KO^tBu -Mediated Nitrile to Amide Conversion

formation was observed using galvinoxyl as the radical trap. Radical quenching experiments suggest the radical pathway of the hydration process.

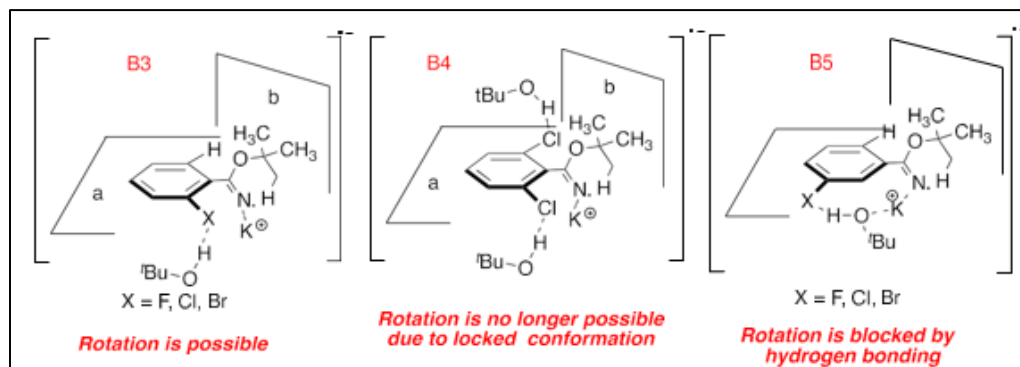
Table 5: Hydration of Nitriles in the Presence of Radical Scavengers

		
Radical Scavenger	Yield	
	<u>Toluene</u> (5 h)	<u>^tBuOH</u> (4 h)
none	91%	>99%
TEMPO	78%	82%
1,1-diphenyl ethylene	68%	70%
<i>galvinoxyl</i>	<i>trace</i>	<i>75%</i>

Based on this data, a single-electron transfer mechanism was proposed for the hydration of organonitriles (Scheme 16). Lewis basic nitrile will coordinate with potassium cation in the presence of KO^tBu. This kind of complexation was initially observed by Kataoka and co-workers (2002, p. 5553) Complex A can be further stabilised by intermolecular cation- π interaction as well as π - π^* stacking (Jonkheijm *et al.*, 2006, p.80) Next radical ion pair B will be generated via single electron transfer between the cationic complex A and tertiary butoxide anion. Nucleophilic addition of tert-butoxy radical to the electrophilic carbon atom of the nitrile would then form iminyl radical intermediate B1, which upon 1,5-hydrogen abstraction followed by elimination of isobutylene D would lead to the formation of potassium amidate C. Finally, protonation of C by any external proton source would lead to the formation of the amide. Based on this mechanism, working model B2 has been proposed to explain the lower yield in toluene in the case of ortho-substituted substrates. Formation of intermediate B1 is unfavourable due to the steric interaction between the ortho-substitution and 6 membered cyclic intermediate. As a result, hydration of ortho-substituted aryl nitriles does not undergo hydration at room temperature in toluene, these transformations occurred upon heating at 60 °C to give moderate yields of the corresponding products (Scheme 16).



However, in ^tBuOH hydrogen bonding partially locks the conformation (B3) (Figure 3), as a result, free rotation of C(aryl)-C(CN) is minimised and hence, hydration takes place at room temperature. But in the case of ortho-dichloro benzonitrile slightly better yield of the amide 41 is observed in toluene due to higher electrophilicity of the nitrile group. In ^tBuOH, intermolecular hydrogen bonding increases the effective steric bulk at the two ortho-positions hence conformation of B4 is locked (Figure3). As a result, hydration of ortho-dichloro benzonitrile proceeds through a lower energy transition state and provides amide 41 with nearly quantitative yield at room temperature. Similar trends were also observed during the formation of 38b, 39b, and 40a in ^tBuOH having hydrogen acceptor substituents at the meta-position. The involvement of intermediate B5 is anticipated in these cases (Figure 3). In the case of ortho- fluorebenzonitrile comparatively higher yield of the amide 39a was obtained due to the smaller size and strong electron withdrawing effect of the fluoro group (Table 3 & Table 4).



Conclusion

Classical hydration of nitriles is carried out under acid and base catalysed conditions. However, major limitations of these hydration protocols include a) the formation of corresponding acids by over-hydrolysis, b) the requirement of high temperature and pressure, c) poor functional group tolerance and narrow substrate scope and d) inability to hydrolyse substrates having more than one nitrile functional group. Moreover, organonitriles are the major industrial waste, which falls into the rivers and seas, causing a major environmental threat. So, potassium tertiary butoxide mediated hydration of organonitriles under mild reaction conditions is a suitable alternative to acids and base catalysed methods. Various electron-rich, electron-deficient nitriles as well as cyanopyridines have been transformed into amides in excellent yields. Ortho substituted substrates provide the corresponding amides in synthetically useful yields in *tert*-BuOH. Aliphatic nitriles work well under this reaction condition. None of these substrates underwent over-hydrolysis under this hydration condition. Very high selectivity is observed towards double hydration during hydrolysis of dicyanobenzene.

Acknowledgment

The author wishes to express sincere gratitude to the Organising Committee of Jogesh Chandra Chaudhuri College, Tollygunge, Kolkata, West Bengal, India, for their valuable support and cooperation throughout the course of this work.

References

- Alvarado, A. M., & Coleman, G. H. (1923). *Acetamide*. Organic Syntheses. <https://doi.org/10.15227/orgsyn.003.0003>
- Balicki, R., & Kaczmarek, Ł. (1993). Mild and efficient conversion of nitriles to amides with basic urea-hydrogen peroxide adduct. *Synthetic Communications*, 23(22), 3149-3155. <https://doi.org/10.1080/00397919308011173>
- Basu, M. K., & Luo, F. T. (1998). Efficient transformation of nitrile into amide under mild condition. *Tetrahedron Letters*, 39(19), 3005-3006. [https://doi.org/10.1016/S0040-4039\(98\)00444-4](https://doi.org/10.1016/S0040-4039(98)00444-4)
- Behr, L. D., & Clarke, H. T. (1936). *Succinimide*. Organic Syntheses. <https://doi.org/10.15227/orgsyn.016.0075>
- Drauz, K., & Waldmann, H. (2002). *Enzyme Catalysis in Organic Synthesis* (2nd ed.). VCH, Weinheim, <https://doi.org/10.1002/9783527618262.ch16b>
- Hurd, C. D., & Webb, C. N. (1927). *p*-Dimethylaminobenzophenone [*Benzophenone, p*-dimethylamino-]. Organic Syntheses. <https://doi.org/10.15227/orgsyn.007.0024>
- Jonkheijm, P., van der Schoot, P., Schenning, A. P., & Meijer, E. W. (2006). Probing the solvent-assisted nucleation pathway in chemical self-assembly. *Science*, 313(5783), 80-83. <https://doi.org/10.1126/science.1127884>

- Jursic, B. S., & Zdravkovski, Z. (1993). A simple preparation of amides from acids and amines by heating of their mixture. *Synthetic Communications*, 23(19), 2761-2770. <https://doi.org/10.1080/00397919308013807>
- Kataoka, N., Shelby, Q., Stambuli, J. P., & Hartwig, J. F. (2002). Air stable, sterically hindered ferrocenyl dialkylphosphines for palladium-catalyzed C–C, C–N, and C–O bond-forming cross-couplings. *The Journal of Organic Chemistry*, 67(16), 5553-5566. <https://doi.org/10.1021/jo025732j>
- Khalafi-Nezhad, A., Mokhtari, B., & Rad, M. N. S. (2003). Direct preparation of primary amides from carboxylic acids and urea using imidazole under microwave irradiation. *Tetrahedron Letters*, 44(39), 7325-7328. [https://doi.org/10.1016/S0040-4039\(03\)01866-5](https://doi.org/10.1016/S0040-4039(03)01866-5)
- König, W., & Geiger, R. (1970). Eine neue methode zur synthese von peptiden: aktivierung der carboxylgruppe mit dicyclohexylcarbodiimid unter zusatz von 1-hydroxy-benzotriazolen [A new method for peptide synthesis: activation of the carboxyl group with dicyclohexylcarbodiimide in the presence of 1-hydroxybenzotriazole]. *Chemische Berichte*, 103(3), 788-798. <https://doi.org/10.1002/cber.19701030319>
- Liu, W., Cao, H., Zhang, H., Zhang, H., Chung, K. H., He, C., ... & Lei, A. (2010). Organocatalysis in cross-coupling: DMEDA-catalyzed direct C–H arylation of unactivated benzene. *Journal of the American Chemical Society*, 132(47), 16737-16740. <https://doi.org/10.1021/ja103050x>
- McElvain, S. M., & Pryde, E. H. (1949, January 1). 2,2,5,5-Tetramethylpiperazine and Derivatives. *Journal of the American Chemical Society*, 71(1). <https://doi.org/10.1021/ja01169a092>
- McMaster, L., & Langreck, F. B. (1917, January 1). The Transformation of Nitrile into amide by hydrogen peroxide. *Journal of the American Chemical Society*, 39(1). <https://doi.org/10.1021/ja02246a012>
- Midya, G. C., Paladhi, S., Dhara, K., & Dash, J. (2011). Iron catalyzed highly regioselective dimerization of terminal aryl alkynes. *Chemical Communications*, 47(23), 6698-6700. <https://doi.org/10.1039/c1cc10346f>
- Mitchell, J. A., & Reid, E. E. (1931, May). The Preparation of Aliphatic Amides. *Journal of the American Chemical Society*, 53(5). <https://doi.org/10.1021/ja01356a037>
- Montalbetti, C. A., & Falque, V. (2005). Amide bond formation and peptide coupling. *Tetrahedron*, 61(46), 10827-10852. <https://doi.org/10.1016/j.tet.2005.08.031>
- Moorthy, J. N., & Singhal, N. (2005). Facile and highly selective conversion of nitriles to amides via indirect acid-catalyzed hydration using TFA or AcOH–H₂SO₄. *The Journal of Organic Chemistry*, 70(5), 1926-1929. <https://doi.org/10.1021/jo048240a>
- Murahashi, S., Sasao, S., Saito, E., & Naota, T. (1992). Ruthenium-catalyzed hydration of nitriles and transformation of delta.-keto nitriles to ene-lactams. *The Journal of Organic Chemistry*, 57(9), 2521-2523. <https://doi.org/10.1021/jo00035a003>
- Patai, S., & Rappoport, Z. (1970). *The Chemistry of Functional Groups*. The Chemistry of Cyano Group, Wiley, London.

KO^tBu -Mediated Nitrile to Amide Conversion

- Rao, C. G. (1982). Facile hydration of nitriles to amides using potassium fluoride on alumina. *Synthetic Communications*, 12(3), 177-181. <https://doi.org/10.1080/00397918208063674>
- Sharghi, H., & Hosseini Sarvari, M. (2003). A facile hydration of nitriles into amides by Al₂O₃/MeSO₃H (AMA). *Synthetic Communications*, 33(2), 207-212. <https://doi.org/10.1081/SCC-120015702>
- Sheehan, J. C., & Hess, G. P. (1955). A new method of forming peptide bonds. *Journal of the American Chemical Society*, 77(4), 1067-1068. <https://doi.org/10.1021/ja01609a099>
- Theodorou, V., Karkatsoulis, A., Kinigopoupou, M., Ragoussis, V., & Skobridis, K. (2009). Tritylamine as an ammonia synthetic equivalent: Preparation of primary amides. *Arkivoc*, 11, 277-87. <https://doi.org/10.3998/ark.5550190.0010.b25>
- Yanagisawa, S., Ueda, K., Taniguchi, T., & Itami, K. (2008). Potassium t-butoxide alone can promote the biaryl coupling of electron-deficient nitrogen heterocycles and haloarenes. *Organic Letters*, 10(20), 4673-4676. <https://doi.org/10.1021/ol8019764>

Association of Insect Fauna with the Flowers of the *Zea mays* (Sweet corn variety AKSH4) in Southern Part of West Bengal

Biswanath Bhowmik

Department of Zoology, Sree Chaitanya College, Habra 743268, West Bengal, India

Corresponding Author's E-mail: bbklec@gmail.com

Abstract

This particular variety of maize, AKSH4, is juicy and sweet compared to the native variety. Insects are more attracted to the crop, and hence this variety is more dependent on insects rather than wind for its pollination. This is a preliminary report on the association of different insect groups with the maize flowers as foragers and pollinators. Insects associated with this variety showing both foraging and pollinating activity at different time periods of the day belong to the orders Hymenoptera, Coleoptera, Orthoptera, and Hemiptera. Altogether, 18 species of four orders of insects were observed during this study. The study was conducted on agricultural land near Saratnagar (Lat: 22.634; Log: 88.395) of district North 24 Parganas of Southern part of West Bengal region, from December 15th to April 20th, 2022-2023. The plants were approx. 6-7 ft in height. The number of insect populations belonging to the order Coleoptera is reported to be the most abundant, efficient and active diurnal and nocturnal foragers/ pollinators whereas the order Hymenoptera was found to be the next active and efficient visitors/pollinators in this study. The total number of visitors/pollinators was highest at 6-10 am, followed by 11-03 pm, 3-8 pm and 9-12 pm. It is also evident from the study that this difference in the foraging and pollinating activity, along with other unique behaviour of different insect orders, varied because of the variation in temperature, relative humidity and photoperiod that affect the number of insects visiting the corn plant.

Keywords: AKSH4; Diurnal; Nocturnal Insect Foragers; Pollinators; *Zea mays*

Introduction

Zea mays, belonging to the family Poaceae, basically known as corn, is a monocotyledon flowering plant. *Zea mays* is a protandrous and monoecious species (Vincent, 2002) with a staminate inflorescence, also known as a tassel top (produces pollen (Fig.1)) of the plant and is a hermaphrodite or monoecious plant species. Its inflorescence is a staminate with one or more of the middle nodes with a pistillate inflorescence in the axil. Nielsen (2010) opined that the early developmental stage flowers are bisexual, and in the latter stage some gametic changeover occurs; the female gynoecia of the male flowers and the male components (stamens) of the female flowers were dissociated, resulting in tassel (male) and ear or cob (female) development. Each egg on the cob gives rise to silks, which are hairy elongated stigmas appearing near the top of the ear, identifying characteristics of this particular species. The quantity of pollen is a central factor in ensuring the efficiency of controlled pollinations, and the data obtained by comparing traditional varieties with modern

hybrids of maize showed that an increase in pollen production is determined by the increase in branching of the male inflorescence (Landoni *et al.*, 2024).

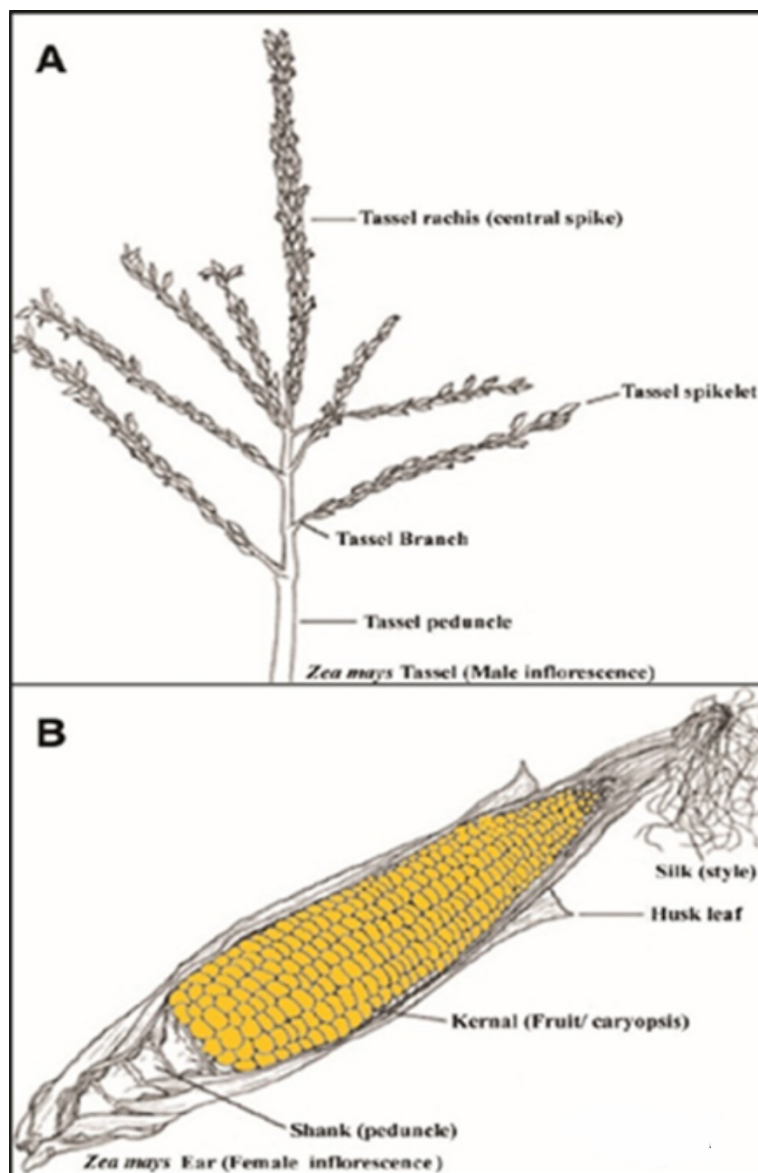


Figure 1: Male and Female Flower Part of Zea mays

According to Aldrich, Scott and Hoeft (1986) the tiny pollen grains of maize are carried by wind action to the silks (anemophilous), of the same plant or on a different plant. The pollen then travels down through the silk to fertilise an egg to form a kernel. Ollerton *et al.* (2019) and Asar, Ho and Sauquet (2022), who assessed during their premium research that, Pollination is a fundamental ecological process that influenced the diversification of many

Converging Chemical and Biological Sciences for a Sustainable Era

seed plant families throughout evolutionary history. However, the variety of maize under experiments, the variety of AKSH4 maize plant produces a juicier and sweeter variety than other native varieties, which attract more insects, which intended this variety to be more inclined to insect pollination rather than wind (entomophily). Maize thereby plays a diverse and dynamic role in global agri-food systems and food/nutrition security (Poole, Donovan & Erenstein, 2021).

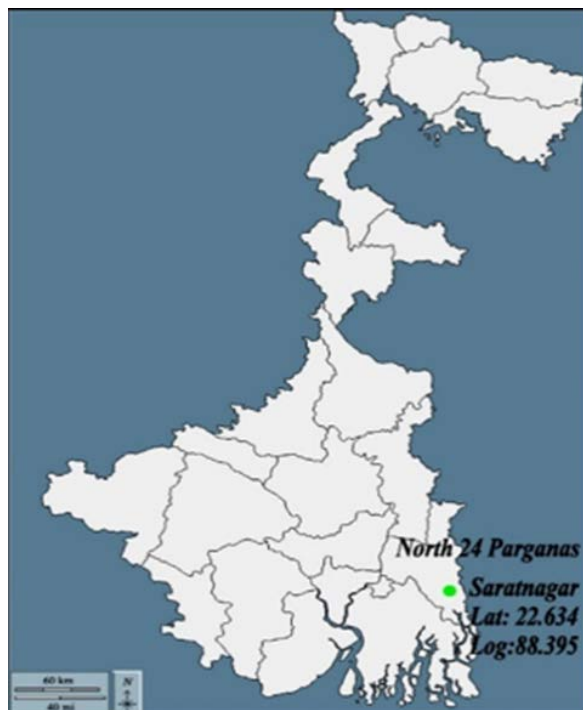


Figure 2: Location of the Area at North 24 Parganas of Southern Region of West Bengal

The present study describes the fact that both diurnal and nocturnal insects of various Orders play important roles in foraging (aggregation, collecting pollen, mating, predation), which in turn pollinates corn plants. This research is the pioneer to study the nocturnal floral visitors/pollinators of corn, *Zea mays*, in the Indian context and also to identify associated insects, those that act as foragers and pollinators. The extended study reveals the nature of those insects as diurnal and nocturnal pollinators, their behaviour along with their peak foraging period. The inference of this work also indicated that their behaviour varies with temperature, relative humidity and photoperiod. Altogether, 18 species of four orders of insects were collected as foragers and pollinators of *Zea mays* during this study (Tables 1 & 2).

Methodology

The study was conducted on agricultural land near Saratnagar (Lat: 22.634; Log: 88.395) of district North 24 Parganas of Southern part of West Bengal region (Figure 2), from December 15th to April 20th, 2022-2023. The plants were approx. 6-7 ft in height. The seeds of corn

Insect Fauna Associated with Zea mays Flowers in South Bengal

were very sweet and juicy. Variety AKSH4 was sown for seed production on December 1st, 2022, in three plots measuring each 35 m x 35 m. Sweep net of about 20 cm radius was used to collect visiting and pollinating insects at different time periods, viz. 6-7 am, 8-9 am, 10-11 am, 12-1 pm, 2-3 pm, 4-5 pm, 6-7 pm, 8-9 pm and 10-12 pm. Record of daily mean temperature and relative humidity were collected from the local meteorological laboratory (Avg. temperature 24°C, RH 50%). The methods for collection, killing, preservation, setting and pinning of the insects were adopted from the manual of the Zoological Survey of India (Jonathan, Tikader & Kulkarni, 1986). The collected specimens were identified from the Zoological Survey of India, Kolkata. The correlation coefficient of different species of various orders with temperature and relative humidity was calculated using the most widely used Pearson's correlation coefficient method. The correlation coefficient of different species of various orders with temperature and relative humidity was calculated using Pearson's correlation coefficient method.

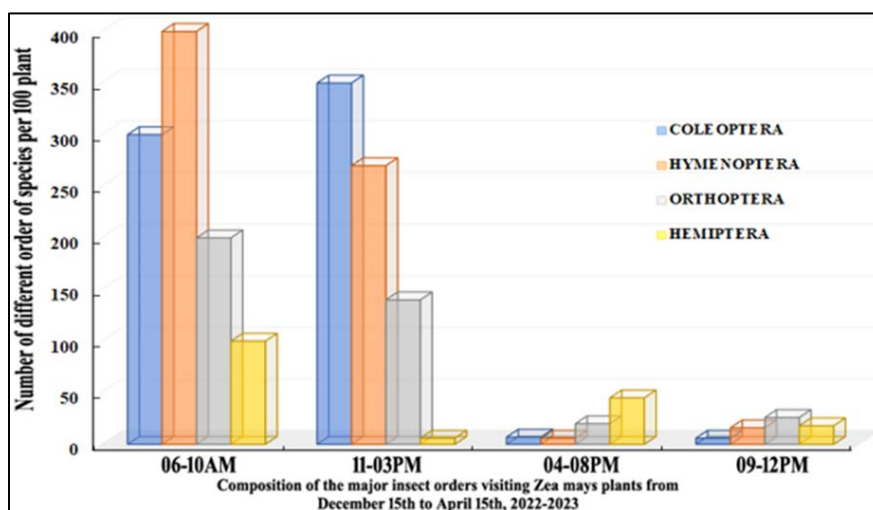


Figure 3: Composition of Different Insect Orders Visiting Maize Plant During Various Time Schedules

Results

In the present study, a total of 18 species under four Orders were observed to be associated with the flowers of maize crops (Table 1 & 2). The study reveals that most of the insects in relation to this crop pollinator activated condition are more active in daytime. Families Scarabaeidae, Elateridae and Coccinellidae of the order Coleoptera (one from each family) and family Tettigoniidae of the order Orthoptera (3 species) were found to be foragers of maize with nocturnal activity in *Zea mays*. Casual visitors like Two species of the family Pentatomidae and one species from the family Capsidae under the order Hemiptera were identified as pollinators of *Zea mays* (Fig.3). All these insects had been reported to show correlation with temperature and humidity. A representative correlation curve revealed a high correlation value, $r=0.75$, with temperature for order Coleoptera, and a high correlation

value, $r=0.94$ and 0.86 , for Hymenoptera and Orthoptera, respectively, with humidity. The other correlation values (r) were calculated (Figure 4).

The study identified beetles from different families, like Coccinellidae and Lycidae activated more during daytime, and Scarabaeidae and a species belonging to the order Elateridae during night, acting as visitors which also act as pollinators. It has also been observed that Coccinellidae, especially *Oenopia* sp. (~10-12/plant) and Lycidae (~3-4 /plant) preferred to visit between 6 am -3 pm. Their act of eating the pollen grains created aggregation of those insects on the tassels of the corn from the base to the tip. Insects of the family Lycidae aggregate for mating, observed during this study. They split open the bilobed anthers with their strong mandibles, thereby exposing the pollen grains.

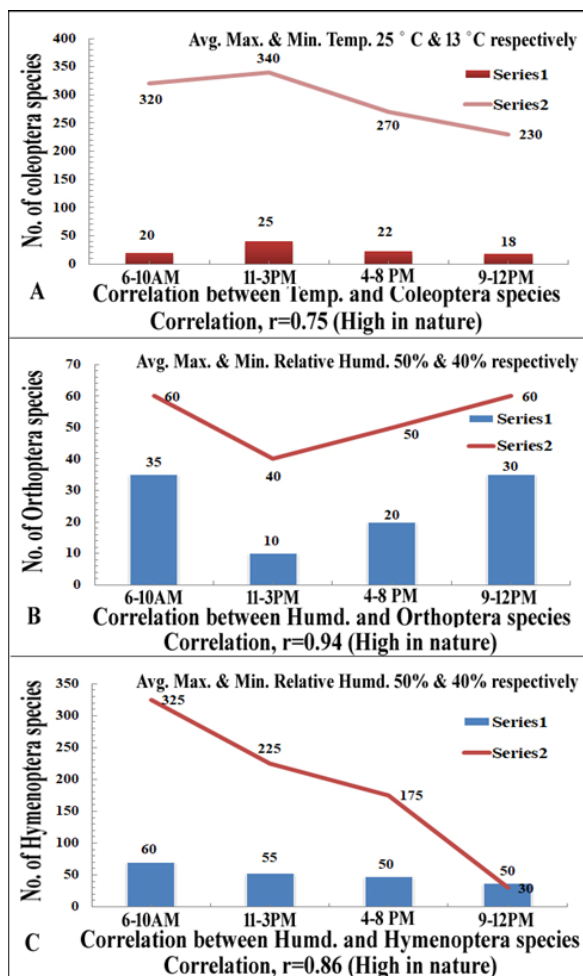


Figure 4: (A) Correlation between Temperature and Number of Species Under Order Coleoptera; (B) Correlation between Humidity and Number of Species Under Order Orthoptera; (C) Correlation between Humidity and Number of Species Under Order Hymenoptera

Insect Fauna Associated with Zea mays Flowers in South Bengal

During this activity their upper and lower surfaces of the body, the appendages, antennae and the mouth parts, to a large extent, get smeared with lots of pollen grains. It has also been observed that they usually spend at least 20-30 minutes on such condition.

The pollen grains as a result showered at a huge number from the tassels and dropped on the glossy and shiny silks of the same plant as well as nearby plants.

During the night from 6 to 10 pm, quite a number of coleopteran species from families Scarabaeidae (~3-4/plant) and Elateridae (~1-2/plant) were observed to visit the plants, which might be helping in pollination of this variety of maize. Honeybees were found to be effective pollinators. It was observed that their preferable time for foraging was 7am till 11am, and they spent at least 20-25 seconds per plant. Two different species of bees were observed; the bigger one, *Apis megapis dorsata* were more in number (~8-10/ plant) than the smaller one, *Apis cerana indica* (~6-7/plant). During their foraging activity pollen grains got deposited on the silks of the female part of the plant, and thus it helped in pollination, but honeybees, especially in this case, removed large quantities of pollen and deposited very little pollen on the stigmas because much of the amount of pollen grains got wasted. Their activities and population generally decreased after 12 noon till they again visited the field after 2.30pm and remained till 5pm.

Table 1: List of Diurnal Insect Foragers and Pollen Collectors on *Zea mays* in Saratnagar, West Bengal

Order	Family	Species	Time for foraging/pollination	Habit
Coleoptera	Coccinellidae	<i>Oenopia</i> sp.	7am-2pm	Diurnal
		<i>Harmonia arcuata</i>	7am-2pm	Diurnal
		<i>Coccinella septempunctata</i>	7am-2pm	Diurnal
		<i>Menochilus sexmaculatus</i>	7am-2pm	Diurnal
		<i>Chilocorus</i> sp.	7am-2pm	Diurnal
	Lycidae	Unidentified	7am-2pm	Diurnal
Hymenoptera	Apidae	<i>Apis megapis dorsata</i>	7am-11am	Diurnal
		<i>Apis cerana indica</i>	8am-11am	Diurnal
		<i>Apis mellifera</i>	7am-12pm	Diurnal
Hemiptera	Pentatomidae	<i>Nezara viridula</i>	9am-2pm	Diurnal
		<i>Agonoscelis nubile</i>	9am-2pm	Diurnal

A few diurnal species of bugs, viz. *Nazara viridula* and *Agonoscelis nubile* and the nocturnal species *Megacoelum stramineum* were also observed to visit for foraging, but no pollen grain was seen adhered to their bodies. From 3 pm onwards the activity of diurnal foragers and pollinators gradually decreased. After 4 pm some grasshoppers (~2-3/plant) of the family Tettigoniidae were found to visit the fields mainly for foraging. After 6 pm, their abundance increased (~3-4/plant). They were observed to be strong and powerful nocturnal visitors, though less abundant. They were observed to prefer a quiet, cool and dark ambience for foraging. They visited and sat on the tassels till late at night by hugging the thin, slender

tassels with the help of their strong fore and hind legs. With the help of their strong mandibles, they chewed and opened the anthers and thereby exposed the pollen grains. As a result, the pollen grains got dusted in large numbers on their thorax, forewings, ventral surface of the abdomen, the jointed appendages (specially the forelegs), the antennae and the mouth parts. The entire activity in each instance took about 15-20 minutes, and after that, they jumped/walked away to visit the nearby plants.

During the night from 7 pm onwards, it was observed quite often that the upper part of the maize plants bearing the dangling tassels got affected by a large number of aphids, where they probably came for foraging or for taking a rest. However, during daytime these aphids were less visible on the plants. It was observed that these aphids during the night attracted a large number of black ants (*Camponotus* sp.). These aphids were observed to excrete sugar-rich fluid for the ants and in return got protection from them against predators. This symbiotic association continued till 1-2 hrs. During this interaction these black ants got showered with large amounts of pollen grains, but their little active movement on the plants indicates them simply as visitors.

Table 2: List of Nocturnal Insect Foragers and Pollen Collectors on Zea mays in Saratnagar, West Bengal

Order	Family	Species	Time for foraging/pollination	Habit
Coleoptera	Elateridae	Unidentified	6am-10pm	Nocturnal
	Scarabaeidae	Unidentified	6am-10pm	Nocturnal
Hymenoptera	Formicidae	<i>Camponotus</i> sp.	7pm-10pm	Nocturnal
Hemiptera	Capsidae	<i>Megacoelum stramineum</i>	7pm-10pm	Nocturnal
Orthoptera	Tettigoniidae	<i>Ducetia japonica</i>	4pm - 10pm	Nocturnal
		<i>Atractomorpha</i> sp.	4pm - 10pm	Nocturnal
		<i>Euconocephalus</i> sp.	4pm - 10pm	Nocturnal

Discussion

In the case of maize plants, though anemophily is the most commonly reported phenomenon, the role played by the insect visitors in the pollen collection and pollination process needs to be looked into. The number of major insect Orders with respect to the time schedule, when they often visited the maize plant for foraging and pollination is shown (Table 1 & 2). It was reported by Fonseca *et al.* (2003) that although bees and other insects visit male tassels of maize plants for foraging, they have a small role in pollination because female flowers are little attractive for pollinating insects. It was even observed by Poehlman and Sleper (1995) that generally anthers will not open in cool and humid weather, thereby trapping the pollen within. Herrero and Johnson (1980) reported that prolonged exposure to temperatures above 32°C can even reduce pollen germination of many genotypes in maize to levels near zero. Hence, in such situations, pollination in maize by wind is not that

effective, and it has to depend on some biotic pollen dispersal agents like insects for effective pollination.

It has been observed that this special hybrid variety of maize crops (AKSH4) is more attracted by insect visitors than the native variety of maize. This may be due to its juicy and sweet qualities of corn and so the particular variety is more dependent on insect pollination rather than wind pollination. Beetles are considered reliable and specific pollinators of several plants in the tropics by many entomologists. Pollination by beetles has been observed in some wild flowering plants from Himachal Pradesh (Kritika & Jaimala, 2017). Mouthparts in most of the coleopterans are perpendicular to the body axis; this position limits the length of the mouthparts, and they are able to lick up nectar from open flat blossoms (Roubik, 1995), though in the present case it was the juicy anthers that were the main target. Diurnal visitors from the families Coccinellidae and Lycidae under order Coleoptera were found in large numbers as visitors on maize. Of them, *Oenopia* sp. and one unidentified species of the family Lycidae were found to show unique behaviour of aggregation and copulation, respectively. Hawkeswood (2002) reported that the lycids are generally nectar feeders and also reported as effective pollinators of some Heathland plants of Australia. The aggregation had a modifying effect due to sudden temperature changes. Two species of honeybees from the family Apidae were noticed abundantly. Though *Apis* sp. were abundant, they deposited little pollen on the stigmas and quite an amount of pollen got wasted.

Comparatively, Coccinellid beetles were observed to carry more pollen during the present study. Regarding the effectiveness of each species of pollinator, it seems that it depends chiefly on two factors: their relative abundance among the pollinator "pool" and the efficiency with which they remove and deposit pollen. Insects of the family Tettigoniidae were observed to visit during the late afternoon that continued till late night. During their visit to the plant, their body parts got dusted with lots of pollen grains, and they were often seen to walk from one plant to another carrying the pollen, spending time exploring the shiny stigma, which was again a clear indication of pollination by these species. A recent work by Suetsugu and Tanaka (2014) showed that though katydids are not regular floral visitors, the juvenile katydid, *Ducetia japonica*, regularly visited and consumed the pollinia and anther caps of *Habenaria* (Orchidaceae). Therefore, orthopterans may be considered as effective nocturnal pollinators of *Zea mays*.

Conclusion

The comparison among different insect orders clearly revealed that insect populations, specially from the family Coccinellidae of the order Coleoptera, showed the highest population diversity, relative abundance and high correlation values with temperature and humidity, respectively. They were the most efficient and effective foragers present at all four time periods, i.e., 6-10 am, 11-3 pm (maximum numbers), 4-8 pm and 9-12 pm (minimum numbers) (Fig. 3). Besides this, all the coccinellid beetles reported during this study were predatory in nature, and they visited every part of the plant for searching their prey. They may be the slow mover but had a chance to help in the pollination process of maize.

Their serrated antennae and ridged elytra helped them to carry pollen, which had been observed during this study. Even scarabaeid beetles were also reported to show pollination during the night.

Next to Coleoptera, it is the *Apis megapis dorsata* of order Hymenoptera that was reported to be the most abundant, but their distribution, unlike Coleoptera, was not that uniform. Their number decreased in the afternoon, and after 3:00 pm, their abundance again increased and ultimately lasted till 5 pm. Though the number of bees in maize plants was less but they also play a vital role in pollination as they are the recognised effective pollinators of other angiospermic plant species.

During this study, it had been observed that katydids with their strong mandibles chewed and opened the anthers and thereby exposed the pollen grains. Lastly, it can be concluded that this is the first attempt to make an inventory of insect pollinators of *Zea mays*, AKSH4, which will certainly help future workers as baseline data on pollinators and pollination of *Zea mays*.

Acknowledgement

The author gratefully acknowledges the Director, Zoological Survey of India, Kolkata, for helping in the identification of the insects. Also, the Principal of Sree Chaitanya College, Habra, is acknowledged for encouragement.

References

- Aldrich, S. R., Scott, W. O., & Hoeft, R. G. (1986). *How the Corn Plant Grows*. In *Modern Corn Production*. 3rd edition. A&L Publications.
- Asar, Y., Ho, S. Y., & Sauquet, H. (2022). Early diversifications of angiosperms and their insect pollinators: were they unlinked? *Trends in Plant Science*, 27(9), 858-869. <https://doi.org/10.1016/j.tplants.2022.04.004>
- Fonseca, A. E., Westgate, M. E., Grass, L., & Dornbos Jr, D. L. (2003). Tassel morphology as an indicator of potential pollen production in maize. *Crop Management*, 2(1), 1-15. <https://doi.org/10.1094/CM-2003-0804-01-RS>
- Hawkeswood., T. J. (2002). Observations on pollination of various Heahland Plants by *Metriorrhynchus rhipidius* (Macleay) (Coleoptera: Lycidae) in Eastern New South Wales, Australia, with a review of some feeding records for *Metriorrhynchus*. *Journal of Entomological Research Society*, 4(2), 1-6. Retrieved from:
- Herrero, M. P., & Johnson, R. R. (1980). High temperature stress and pollen viability of maize 1. *Crop Science*, 20(6), 796-800. <https://doi.org/10.2135/cropsci1980.0011183X002000060030x>
- Jonathan, J.K., Tikader, B.K., & Kulkarni, P.P. (1986). Manual: Collection, preservation and identification of insects and mites of economic importance. *Zoological Survey of India, Calcutta*, 307pp. Retrieved from: <https://archive.org/details/spb.zoological.spb.014>, Accessed on 15th November 2024.
- Kritika, T., & Jaimala, S. (2017). Diversity and ecology of Coleoptera in India: a review. *Journal of Entomology and Zoology Studies*, 5(2), 1422-1429. Retrieved from:

Insect Fauna Associated with Zea mays Flowers in South Bengal

- <https://www.entomoljournal.com/archives/2017/vol5issue2/PartS/5-2-143-945.pdf>. Accessed on 16th September 2024.
- Landoni, M., Sangiorgio, S., Ghidoli, M., Cassani, E., & Pilu, R. (2024). Study of Pollen Traits, Production, and Artificial Pollination Methods in Zea mays L. *Agriculture*, 14(10), 1791. <https://doi.org/10.3390/agriculture14101791>
- Nielsen, R.L. (2010). Tassel Emergence & Pollen Shed. Agronomy Department, Purdue University, West Lafayette, IN47907-2054. Retrieved from: <https://www.agry.purdue.edu/ext/corn/news/timeless/tassels.html>. Accessed on 15th November 2024.
- Ollerton, J., Liede-Schumann, S., Endress, M. E., Meve, U., Rech, A. R., Shuttleworth, A., ... & Quirino, Z. (2019). The diversity and evolution of pollination systems in large plant clades: Apocynaceae as a case study. *Annals of Botany*, 123(2), 311-325. <https://doi.org/10.1093/aob/mcy127>
- Poehlman, J.M. & Sleper, D.A. (1995). *Breeding Corn (Maize)*. In: Breeding Field Crops, 4th edition. Iowa State University Press. Retrieved from: <https://www.cabidigitallibrary.org/doi/full/10.5555/19951604586>. Accessed on 15th November 2024.
- Poole, N., Donovan, J., & Erenstein, O. (2021). Agri-nutrition research: revisiting the contribution of maize and wheat to human nutrition and health. *Food Policy*, 100. <https://doi.org/10.1016/j.foodpol.2020.101976>
- Roubik, D. W. (Ed.). (1995). *Pollination of cultivated plants in the tropics* (Vol. 118). Food & Agriculture Org. Retrieved from: <https://pmc.ncbi.nlm.nih.gov/articles/PMC1702377/>, Accessed on 15th November 2024.
- Suetsugu, K., & Tanaka, K. (2014). Consumption of Habenaria sagittifera pollinia by juveniles of the katydid Ducetia japonica. *Entomological Science*, 17(1), 122-124. <https://doi.org/10.1111/ens.12035>
- Vincent, P. L. D. (2002). Zea mays (Maize, Corn). e LS. <http://dx.doi.org/10.1038/npg.els.0003687>

Multireference Perturbation Based Quantum Chemical Investigation on Isomerization Alley of Diphosphorous Compounds

Suvonil Sinha Ray

Department of Chemistry, Ramananda College, Bishnupur, Bankura, West Bengal, 722122 India

Corresponding Author's E-mail: suvonil.sinharay@gmail.com

Abstract

Methodological advances and their mathematical applications are a progressive field of study in the area of electronic structure theory dominated by molecular systems having 'quasidegeneracy'. The recently proposed Improved Virtual Orbital State Specific Multi Reference Perturbation Theory (IVO-SSMRPT) has been progressively developed into an advantageous ab initio instrument for analysing electronic states with systems prone to static and dynamic electronic correlations. This method is an alluring substitute to the broadly used MRPT methodologies and it can dodge various challenges faced by the traditional MRPTs. Even at the twisted molecular levels, IVO- Brillouin-Wigner (BW)- MRPT provides a dependable picture of quasi-degeneracy among occupied and unoccupied orbitals. The competence of IVO-SSMRPT has been explored here using highly correlated electronic systems impending from isomerization of diphosphorous compounds. IVO-SSMRPT method mimics the findings of modern age state-of-the-art methods but with depreciated computational accomplishment.

Keywords: *Ab Initio Methods; Barrier Height; Improved Virtual Orbitals; Isomerization Energy; Multireference Theory*

Introduction

Theoretical study of molecular systems having two phosphorus atoms is an arduous assignment. Analysis of these molecular systems turns into an important subject due to the miscellaneous utilizations in material science. The reactivity of diphosphenes is always an appealing dispute for both the branches of experiment and theory. It calls attention to the synthetic chemists as they are responsive to a diverse spectrum of reagents (Geoffroy *et al.*, 1992; Binder *et al.*, 1996; Ito *et al.*, 1986; Shah *et al.*, 2000). Diphosphenes are more inclined to reduction process than olefins or other azo compounds (Ito & Nagase, 1986).

Unique photochemical behaviours shown by both diphosphines and diphosphenylidene are worth exploring in divergent field of organometallics (Pikies *et al.*, 2004). Even, PP bonded molecular systems have been efficiently used in chemical hydrogen storage (Matus *et al.*, 2007). The chemical isolation process of these species is a tricky job as they have tendencies to polymerization due to thermodynamic control (Shah *et al.*, 2000). Over the last few years, P=P compounds have been combined into their conjugated counterpart to make constituent elements of molecular electronics. It is worth mentioning that for

Converging Chemical and Biological Sciences for a Sustainable Era

diphosphene like systems, the PP bond distance remains in the range of 2.00 to 2.034 Å and it bears harmonic vibrational frequencies around 610 cm⁻¹. These signify the existence of a P=P double bond (Weber, 1992; Tokitoh, 2000; Hamaguchi *et al.*, 1984). Attempts have been made to study the diphosphene and diphosphinylidene class of compounds theoretically (Matus *et al.*, 2007; Ito & Nagase, 1986; Tongxiang *et al.*, 2009; Allen *et al.*, 1986; Lu *et al.*, 2010; Vogt-Gessie & Schaefer III, 2012; Allen *et al.*, 1990).

A depiction of the isomerization pathways of the quintessential P-P bonded compounds like diphosphinylidene (PPH₂) and diphosphene (HPPH) was extensively studied using IVO-SSMRPT formulation with minimal model space (Sinha Ray, 2020). Particular emphasis was granted to study both the transition states (TS) of two distinct isomerization pathways. The portrayal of electronic framework of TSs is usually tormented by quasidegeneracy, possessing various leading components in the total wave function. Thereby, the single reference method fails abruptly. The transition states highly need a MR study in a more notable pathway than the ground states. T₁ diagnostic test of Coupled cluster method (Lee & Taylor, 1987) shows a moderate MR character of *cis* and *trans* HPPH. Higher T₁ value of PPH₂ demonstrates higher MR nature. Maximum value of the T₁ diagnostic indicating highest MR character is due to TS between *trans* HPPH and planar PPH₂. Among the broadly applied MR methodologies, MRPT is at the arena of the techniques of selection (Chattopadhyay *et al.*, 2016). Complete Active Space Self Consistent Field (CASSCF) is an extensively used technique to build up the unperturbed basis function in MR-correlated computations like SSMRPT method as primarily introduced by Mukherjee and co-workers (Sinha Mahapatra, 1999; Evangelista *et al.*, 2009).

But CASSCF frequently attracts problems like convergence failure, multiple solution etc. A substitute to this problem has been developed as IVO-SSMRPT method (Sinha Ray *et al.*, 2016; Sinha Ray *et al.*, 2017) and it has been widely accepted in electronic structure theory. Study on *trans*- and *cis*-HPPH and planar PPH₂ systems with IVO-SSMRPT (Sinha Ray, 2020) is worth mentioning in this context. Results due to other *state-of-the-art* methods like State specific Multi Reference Coupled Cluster (SS-MRCC aka Mk-MRCC) (Mahapatra *et al.*, 1998; Evangelista *et al.*, 2006; Evangelista *et al.*, 2007), Coupled Cluster Single Double and perturbative Triple (CCSD(T)) and Multi Reference Configuration Interaction (MRCI) and values are available due to the work of Schaefer and co-workers (Tongxiang *et al.*, 2009; Allen *et al.*, 1986).

Results and Discussion

Correlation consistent quadruple zeta valence (cc-pVQZ) basis (Dunning Jr, 1989) has been used and have been implemented from the EMSL database (<https://bse.pnl.gov/bse>). CAS (m,n) expresses 'm' number of electrons, which are distributed in 'n' number of orbitals. For all IVO-SSMRPT cases, CAS(2,2) space has been utilised.

Trans-HPPH: Figure 1 reveals the optimized geometries of *trans* HPPH molecule. The structure is C_{2h} having ¹A_g symmetry. Due to the presence of bond between two phosphorous elements, its molecular framework like the P-P bond nature is appealing (Power, 2004). P-P bond length lies in the range of 2.024 Å to 2.054 Å. CAS(2,2) consists of

highest occupied molecular orbital (HOMO) and the lowest unoccupied molecular orbital (LUMO) having symmetries of a_u and b_g respectively [see Figure 4].

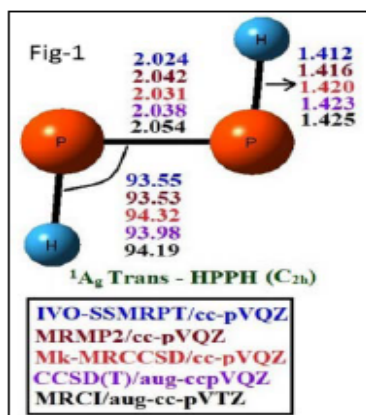


Figure 1: Geometrical Parameters of the Trans HPPH. Bond Lengths are in Angstroms (Å) and Angles are in Degrees (°) (Sinha Ray, 2020)

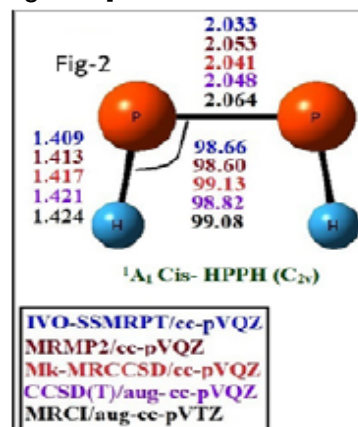


Figure 2: Geometrical Parameters of the Cis HPPH. Bond Lengths are in Angstroms (Å) and Angles are in Degrees (°) (Sinha Ray, 2020)

Cis-HPPH: Cis isomer of diphosphene has been optimized at A_1 symmetry of C_{2v} point group [see Figure 2]. The IVO-SSMRPT values are in well accord with the CCSD(T), MRMP2, Mk-MRCCSD and MRCI studies. The P-P bond length increases significantly from the trans isomer. Figure 4 describes the $2b_1$ (π) as HOMO and the $2a_2$ (π^*) as LUMO of the cis isomer.

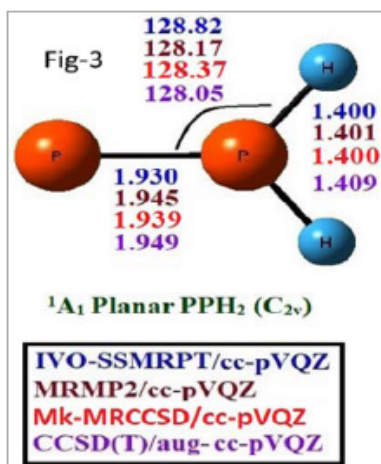


Figure 3: Geometrical Parameters of the Planar PPH₂. Bond Lengths are in Angstroms (Å) and Angles are in Degrees (°) (Sinha Ray, 2020)

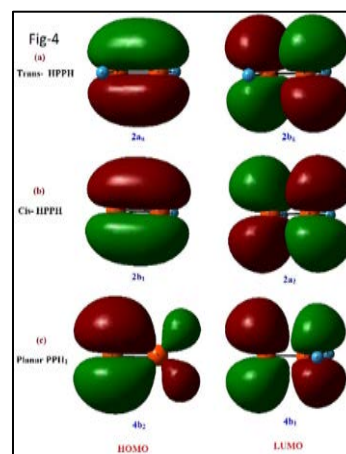


Figure 4: HOMO and LUMO of (a) Trans HPPH, (b) Cis HPPH and (c) Planar PPH₂ (Sinha Ray, 2020)

Diphosphenylidene (planar PPH₂): Another type of bonding pattern is shown in PPH₂ having ¹A₁ symmetry at planar C_{2v} structure [see in Figure 3]. Here the P-P bond length is much shorter than both the cis and trans diphosphene anticipating a strong double bond nature. This structure also displays a greater dipole moment than the cis counterpart. HOMO and LUMO are b₂ and b₁ respectively.

TS connecting trans HPPH and planar PPH₂: This TS is found to be of singlet in nature having C₁ symmetry [Figure 5]. Analogous molecular prototypes like NPH₂ and SCH₂ show prominent 1,2 hydrogen shift (Nguyen & Ha, 1989). In the TS, it is proposed that the migrating hydrogen atom behaves like a proton. The P₁P₂H₂ angle is calculated at 47.45 degree by IVO-SSMRPT which is almost half of the trans isomer (i.e, 93.55 degree) confirming the migration of the H atom (marked as H₂) over the P-P bond and also formation of a three-centered bond as also predicted by Schaefer III and co-workers (Tongxiang *et al.*, 2009).

TS connecting trans and cis HPPH: Trans-cis conversion of HPPH can be reached via two discrete pathways – torsional movement about P-P bond and the inversion via a linear P-P-H bond. First process is accepted due to the lower energy barrier. The TS is analysed to be in a singlet state with C₂ symmetry. The dihedral angle is found to be around 90 degree [see Figure 6] which indicates the halfway between trans and cis minima.

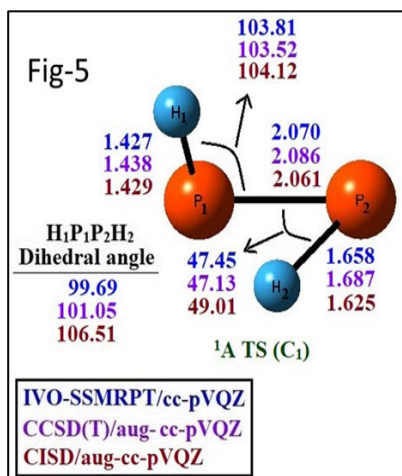


Figure 5: Geometrical Parameters of the TS between the Trans HPPH and Planar PPH₂ Isomers. Bond Lengths are in Angstroms (Å) and Angles are in Degrees (°) (Sinha Ray, 2020)

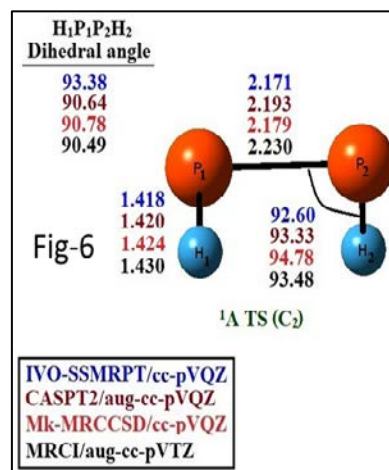


Figure 6: Geometrical Parameters of the TS between the Trans and Cis HPPH Isomers. Bond Lengths are in Angstroms (Å) and Angles are in Degrees (°) (Sinha Ray, 2020)

Relative energies and Barrier height: Geometrical optimization confirms that the trans HPPH has the lowest energy among all the isomers. In Table 1 the relative energies of other minima are represented. The ‘gold standard’ of quantum chemistry, CCSD(T) method indicates the geometrical isomerization energy to be 3.38 kcal/mol as compared to the 3.85 value of IVO-SSMRPT.

For structural isomerization alleyway between trans HPPH to planar PPH₂, the required energy is 24.89 which is in close proximity with the CCSD(T) estimate of 25.28 kcal/mol.

Table 1 : Relative Energies (in kcal/mol) of Different Local Minima as Compared to Global Minimum (trans-HPPH) Reflected by Different Level of Methods (Sinha Ray, 2020).

Method	Basis set	ΔE_{cis}	ΔE_{planar}
IVO-SSMRPT	cc-pVQZ	3.85	24.89
CCSD(T)	cc-pVQZ	3.38	25.28
Mk-MRCCSD	cc-pVQZ	3.32	---
MRCI	aug-cc-pVTZ	3.34	---

Table 2 : Energy Barriers (in kcal/mol) of Geometrical and Structural Isomerization Depicted Via Different Level of Methods (Sinha Ray, 2020)

Method	Basis set	TS between trans HPPH and Planar PPH ₂	TS between trans HPPH and cis HPPH
IVO-SSMRPT	cc-pVQZ	51.00	39.96
CCSD(T)	cc-pVQZ	50.50	35.19
Mk-MRCCSD	cc-pVQZ	---	35.19
MRCI	aug-cc-pVTZ	----	35.05

The energy barriers related to two disparate isomerization pathways are furnished in Table (2). Trans HPPH to planar PPH₂ has a potential barrier of around 50 kcal/mol whereas the energy barrier for HPPH to cis HPPH is predicted around 35 kcal/mol. The geometrical isomerization is assuredly more attainable having lower barrier height.

Conclusion

IVO-SSMRPT deals with the two distinct isomerization paths of molecules involving two phosphorus atoms. Isomerization energy and barrier height by IVO-SSMRPT have been computed and correlated with many other refined *ab initio* approaches. The work paves the way to the use of the very promising perturbative protocol i.e. IVO-SSMRPT with very low computational cost towards the simulation of isomerization pathways containing systems with arbitrary interplay of static and dynamic electron correlation effects.

Acknowledgment

The author expresses his gratitude to Professor Sudip Kumar Chattopadhyay (IEST, Shibpur, Howrah, India). The author is grateful to Ramananda College, Bishnupur, Bankura, West Bengal, India.

References

- Allen, T. L., Scheiner, A. C., & Schaefer III, H. F. (1990). Theoretical studies of diphosphene and diphosphinylidene. 2. Some unusual features of the radical cations and anions. *Journal of Physical Chemistry*, 94, 7780–7784. <https://doi.org/10.1021/j100383a008>

MRPT Analysis of Diphosphorous Isomers

- Allen, T. L., Scheiner, A. C., Yamaguchi, Y., & Schaefer III, H. F. (1986). Theoretical studies of diphosphene and diphosphinylidene in their closed-shell states, low-lying open-shell singlet and triplet states, and transition states. *Journal of the American Chemical Society*, *24*, 7579–7590. <https://doi.org/10.1021/ja00284a023>
- Binder, H., Riegel, B., Heckmann, G., Moscherosch, M., Kaim, W., von Schnering, H.-G., Honle, W., Flad, H. -J., & Savin, A. (1996). Generation and characterization of diphosphene and triphosphene radical anions. Computational studies on the structure and stability of P₃H₃⁻. *Inorganic Chemistry*, *35*, 2119–2126. <https://doi.org/10.1021/ic950661a>
- Chattopadhyay, S., Chaudhuri, R. K., Sinha Mahapatra, U., Ghosh, A., & Sinha Ray, S. (2016). State-specific multireference perturbation theory: Development and present status. *WIREs Computational Molecular Science*, *6*, 266–291. <https://doi.org/10.1002/wcms.1248>
- Dunning Jr., T. H. (1989). Gaussian basis sets for use in correlated molecular calculations. I. The atoms boron through neon and hydrogen. *Journal of Chemical Physics*, *90*, 1007–1023. <https://doi.org/10.1063/1.456153>
- Evangelista, F. A., Allen, W. D., & Schaefer III, H. F. (2006). High-order excitations in state-universal and state-specific multireference coupled cluster theories: model systems. *Journal of Chemical Physics*, *125*, 154113. <https://doi.org/10.1063/1.2335799>
- Evangelista, F. A., Allen, W. D., & Schaefer III, H. F. (2007). Coupling term derivation and general implementation of state-specific multireference coupled cluster theories. *Journal of Chemical Physics*, *127*, 024102. <https://doi.org/10.1063/1.2747742>
- Evangelista, F. A., Simmonett, A. C., Schaefer III, H. F., Mukherjee, D., & Allen, W. D. (2009). A companion perturbation theory for state-specific multireference coupled cluster methods. *Physical Chemistry Chemical Physics*, *11*, 4728–4741. <https://doi.org/10.1039/B822910D>
- Geoffroy, M., Jouaiti, A., Terron, G., Cattani-Lorente, M., & Ellinger, Y. (1992). Phosphaalkene radical anions: Electrochemical generation, ab initio predictions, and ESR study. *Journal of Physical Chemistry*, *96*, 8241–8245. <https://doi.org/10.1021/j100200a008>
- Hamaguchi, H., Tasumi, M., Yoshifuji, M., & Inamoto, N. (1984). The phosphorus-phosphorus double bond stretching frequency observed in the resonance Raman spectrum of bis(2,4,6-tri-tert-butylphenyl) diphosphene. *Journal of the American Chemical Society*, *106*, 508–509. <https://doi.org/10.1021/ja00315a006>
- Ito, K., & Nagase, S. (1986). Transition structures and barriers for the 1,2-H shifts in diphosphene (HP=PH), phosphazene (HP=NH), and diimide (HN=NH): A theoretical study of the singlet and triplet states. *Chemical Physics Letters*, *126*, 531–536. [https://doi.org/10.1016/S0009-2614\(86\)80169-5](https://doi.org/10.1016/S0009-2614(86)80169-5)
- Lee, T. J., & Taylor, P. R. (1989). A diagnostic for determining the quality of single-reference electron correlation methods. *International Journal of Quantum Chemistry, Quantum Chemistry Symposium*, *36*, 199–207. <https://doi.org/10.1002/qua.560360824>
- Lu, T., Hao, Q., Simmonett, A. C., Evangelista, F. A., Yamaguchi, Y., Fang, D.-C., & Schaefer III, H. F. (2010). Low-lying triplet states of diphosphene and diphosphinylidene. *Journal of Physical Chemistry A*, *114*, 10850–10856. <https://doi.org/10.1021/jp105281w>

- Mahapatra, U. S., Datta, B., & Mukherjee, D. (1998). A state-specific multi-reference coupled cluster formalism with molecular applications. *Molecular Physics*, 94, 157–171. <https://doi.org/10.1080/002689798168448>
- Matus, M. H., Nguyen, M. T., & Dixon, D. A. (2007). Heats of formation of diphosphene, phosphinophosphenidene, diphosphine, and their methyl derivatives, and mechanism of the borane-assisted hydrogen release. *Journal of Physical Chemistry A*, 111, 1726–1736. <https://doi.org/10.1021/jp067892v>
- Nguyen, M. T., & Ha, T. -K. (1989). 1,2 Hydrogen shifts in thioformaldehyde ($\text{H}_2\text{C}=\text{S}$), phosphazene ($\text{HN}=\text{PH}$), and diphosphene ($\text{HP}=\text{PH}$): in-plane versus out-of-plane migration. *Chemical Physics Letters*, 158, 135–141. [https://doi.org/10.1016/0009-2614\(89\)87307-5](https://doi.org/10.1016/0009-2614(89)87307-5)
- Pikies, J., Baum, E., Matern, E., Chojnacki, J., Grubba, R., & Robaszkiewicz, A. (2004). A new synthetic entry to phosphinophosphenidene complexes. Synthesis and structural characterisation of the first side-on bonded and the first terminally bonded phosphinophosphenidene zirconium complexes. *Chemical Communications*, 21, 2478–2479. <https://doi.org/10.1039/B409673H>
- Power, P. P. (2004). Some highlights from the development and use of bulky monodentate ligands. *Journal of Organometallic Chemistry*, 689, 3904–3919. <https://doi.org/10.1016/j.jorganchem.2004.06.010>
- Shah, S., Concolino, T., Rheingold, A. L., & Protasiewicz, J. D. (2000). Sterically encumbered systems for two low-coordinate phosphorus centers. *Inorganic Chemistry*, 39, 3860–3867. <https://doi.org/10.1021/ic0001558>
- Sinha Mahapatra, U., Datta, B., & Mukherjee, D. (1999). Molecular applications of a size-consistent state-specific multireference perturbation theory with relaxed model-space coefficients. *Journal of Physical Chemistry A*, 103, 1822–1830. <https://doi.org/10.1021/jp9832995>
- Sinha Ray, S. (2020). Ab initio diagnosis of isomerization pathway of diphosphene and diphosphenylidene. *Chemical Physics*, 529, 110555. <https://doi.org/10.1016/j.chemphys.2019.110555>
- Sinha Ray, S., Ghosh, A., & Chattopadhyay, S., Chaudhuri, R. K. (2016). Taming the electronic structure of diradicals through the window of computationally cost-effective multireference perturbation theory. *Journal of Physical Chemistry A*, 120, 5897–5916. <https://doi.org/10.1021/acs.jpca.6b03211>
- Sinha Ray, S., Ghosh, P., Chaudhuri, R. K., & Chattopadhyay, S. (2017). Improved virtual orbitals in state-specific multireference perturbation theory for prototypes of quasidegenerate electronic structure. *Journal of Chemical Physics*, 146, 064111. <https://doi.org/10.1063/1.4975322>
- Tokito, N. (2000). New aspects in the chemistry of low-coordinated inter-element compounds of heavier Group 15 elements. *Journal of Organometallic Chemistry*, 611, 217–227. [https://doi.org/10.1016/S0022-328X\(00\)00437-X](https://doi.org/10.1016/S0022-328X(00)00437-X)
- Tongxiang, L., Simmonett, A. C., Evangelista, F. A., Yamaguchi, Y., & Schaefer III, H. F. (2009). Diphosphene and diphosphenylidene. *Journal of Physical Chemistry A*, 113, 13227–13236. <https://doi.org/10.1021/jp904028a>

MRPT Analysis of Diphosphorous Isomers

Vogt-Geisse, S., & Schaefer III, H. F. (2012). Reducing and reversing the diphosphene-diphosphinylidene energy separation. *Journal of Chemical Theory and Computation*, 8, 1663–1670. <https://doi.org/10.1021/ct300221e>

Weber, L. (1992). The chemistry of diphosphenes and their heavy congeners: Synthesis, structure, and reactivity. *Chemical Reviews*, 92, 1839–1906. <https://doi.org/10.1021/cr00016a008>

Non-Adiabatic Escape Rate of a Quantum Dissipative System from a Rapidly Oscillating Periodic Potential

Anindita Shit

Department of Chemistry, Kandi Raj College, Kandi, Murshidabad 742137, West Bengal, India

Corresponding Author's E-mail: anindita.pchem@gmail.com

Abstract

Escape rate under the influence of a high-frequency field has appeared as a theme of topical interest in different variants of the kinetic model of chemical and biological phenomena over more than two decades. The escape rate of a quantum system modulated by a rapid, time-periodic external force is studied here in the presence of environmental dissipation with the effect of the foundational process of the intricate interplay of the temperature, field and the system parameters on the escape rate profile with the help of the modified Langevin equation obtained by systematically expanding in terms of $(1/\omega)$ via perturbative methods using the Kapitza–Landau time scale and quantum gauge transformation in the frame of the Floquet theorem. Present formalism, which is classical in appearance yet quantum in nature, provides the full time-independent activated escape rate that often plays a pivotal role in different processes and phenomena ranging from diffusion in condensed phases to biological and chemical reactions. This work, therefore, furnishes avenues of controlling such escape rates in realistic systems of arbitrary complexity and generality.

Keywords: *Effective Potential; Langevin Equation; Multiple Scale Perturbation Analysis; Path Integral Formalism; Quantum Dissipative Systems*

Introduction

In the field of physical, biological and chemical sciences, the system-reservoir model is a broadly acknowledged concept which is capable of explaining a plethora of phenomena. Thus, comprehending this model is inherently significant. The analysis of such systems becomes difficult due to the perturbation that varies over time. Usually when the system is driven by slow external perturbation, it remains in equilibrium with the potential with no time lag, but the situation becomes tricky when the external disturbance becomes periodic with higher field frequencies. A comprehensive methodology has not been established in existing studies to get insights into such dynamics (Jung 1993, Reichl & Kim 1996, Jülicher, Ajdari & Prost 1997, Doering & Gadoua 1992, Gammaitoni *et al.*, 1998, Reimann, Grifoni & Hänggi 1997, Reimann 2002). Thus, the investigation of responses of a system to rapid periodic external forces is crucial in the field of chemical dynamics in condensed matter. The dynamics of the non-equilibrium system are complex and varied, as substantial deviations from the Boltzmann distribution can arise, giving rise to effects that may appear partially counterintuitive. Generally, when a particle is exposed to an external time-dependent drive, its escape rate from a metastable state is also found to be time-dependent. Thus, one of the main challenges lies in determining the escape rate. Studying escape rate offers a

Converging Chemical and Biological Sciences for a Sustainable Era

deeper understanding of the system's overall dynamics as in an escape process where the system moves over its metastable state.

Literature Review

The most fundamental theory for studying such dynamical processes is the theory of the Brownian motion. The classical theory of Brownian motion which involves either Langevin equation (Coffey *et al.*, 2004) or Fokker–Planck equation (Risken 1989) is well-recognised but analysis for similar quantum systems are still absent as quantum dissipation involves a more intricate formulation compared to classical dissipation (Gammaitoni *et al.*, 1998, Coffey *et al.*, 2004, Coffey, Kalmykov & Waldron, 2004, Luchinsky, McClintock & Dykman, 1998, Weiss 2012, Hänggi, Talkner & Borkovec, 1990, Hänggi & Jung, 1995, Grabert, Schramm & Ingold, 1988, Hänggi & Ingold, 2005, Tanimura & Ishizaki, 2009, Coffey, Garanin & McCarthy, 2001, Coffey *et al.*, 2013). Recently, the quantum mechanics of systems driven by rapid external perturbations has gained attention where the driving force becomes nonadiabatic. In the regime of high-frequency external perturbations, the notion of eigenstate transitions for the unperturbed Hamiltonian ceases to be applicable. Several methodologies have been proposed to incorporate quantum effects in a diffusion equation (Machura *et al.*, 2004, Łuczka, Rudnicki & Hänggi, 2005, Ford & O'Connell, 2006, Tsekov, 1995, Tsekov 2007, Ankerhold, Pechukas & Grabert, 2001, Coffey *et al.*, 2007a, Banerjee *et al.*, 2002, Banerjee *et al.*, 2004, Ghosh, Barik & Ray, 2007, Bhattacharya, Chattopadhyay & Ray Chaudhuri, 2009, Ghosh *et al.*, 2010, Bhattacharya *et al.*, 2009, Dillenschneider & Lutz, 2009). The Wigner formulation is a valuable method for calculating quantum corrections to classical dissipation models (Leggett & Caldeira, 1983, Tanimura & Wolynes, 1991, Tanimura & Wolynes, 1992, Tanimura, 2006, and Tanaka & Tanimura, 2009, Tanaka & Tanimura, 2010, Sakurai & Tanimura, 2011, Tanimura, 2012, Coffey *et al.*, 2007a, Coffey *et al.*, 2007b, Coffey, Kalmykov & Titov, 2007, García-Palacios & Zueco, 2004, García-Palacios, 2004). The Wigner space formulation of the hierarchy equations of motion has been shown to offer a useful approach for exploring diverse phenomena in several significant areas (Tanimura & Wolynes, 1991; Tanimura & Wolynes; 1992, Tanimura, 2006; Tanaka & Tanimura, 2009; Tanaka & Tanimura, 2010; Sakurai & Tanimura, 2011; Tanimura, 2012). Among the various approaches to modelling dissipation, the path integral formulation of quantum mechanics stands out for its effectiveness (Grabert, Schramm & Ingold, 1987; Grabert, Schramm & Ingold, 1988; Ingold, 1997; Ingold, 2002). Ankerhold, Pechukas and Grabert (2001) proposed a quantum extension of the Smoluchowski equation, originating from the precise path-integral method to reduced dynamics. This formulation offers structural flexibility to include higher-order quantum corrections in the original quantum Smoluchowski equation and has been implemented to a broad range of problems, encompassing the systems both with and without external perturbation (Ankerhold, 2004; Machura *et al.*, 2006; Maier & Ankerhold, 2010). The chapter addresses the study of escape rates from a metastable potential well in the high-frequency modulation regime, where the frequency of modulation surpasses all other relevant system frequencies. Here multiple scale perturbation theory (MSPT) (Shit, Chattopadhyay & Ray Chaudhuri, 2013; Orszag & Bender, 1978) is used in the framework of the traditional path integral approach in order to handle non-Markovian and nonsecular quantum system-bath interplay. Path integral formulation is often used to study

decay from a metastable state of a quantum system modulated by rapid periodic oscillation. Periodic modulation is easier to understand conceptually regardless of the range of the frequency variation. However, as the system is no longer in thermal equilibrium, calculation of the escape rate is more complex. This work seeks to explore the underlying mechanisms of internal noise (resulting from SB coupling) and external driving, and to understand their mutual interaction. The outcomes of this work may prove useful in the context of modelling cold atom control through electromagnetic field interactions. In recent years, Shit *et al* have proposed a perturbative framework for examining the classical and quantum motion of particles influenced by high-frequency fields, particularly when the nature of the driving force shifts to nonadiabatic (Shit, Chattopadhyay & Ray Chaudhuri, 2011; Shit, Chattopadhyay & Chaudhuri, 2012). In this chapter, it has been shown that, on timescales longer than the perturbation period, the (Langevin) dynamics can be represented by replacing the periodic perturbation with an effective potential which does not have any explicit time dependence. Successful applications to different physical problems showcase the effectiveness of this method. Although there are results (Lehmann, Reimann & Hänggi, 2000; Kim *et al.*, 2010) that are precise when noise strength tends to zero, at elevated frequencies, the method fails to perform under fixed noise strength conditions. This regime is addressed in this chapter. It is crucial to recognise that many phenomena critically depend on activated escape, including diffusive processes in the solid-state materials and on their surfaces, as well as various chemical reactions. Consequently, finding methods to control escape rates is essential.

Discussion

The dynamics of quantum particles are studied here, which are acted upon by a fast-oscillating periodic force using the Kapitza time window (that involves separating the system's variables into slow and fast components). This development facilitates solving the problem in the presence of friction and random forces. Let us begin with considering a system-reservoir Hamiltonian in the proposal by Zwanzig (2001), where the reservoir is represented by a collection of harmonic oscillators characterised by frequencies, masses and the system is subjected to a high-frequency periodic field. The model can be expressed by the following Hamiltonian:

$$\begin{aligned}\hat{H} &= \hat{H}_S(\hat{x}, \hat{p}) + \hat{H}_B(\{\hat{q}_j\}, \{\hat{p}_j\}) + \hat{H}_{SB}(\hat{x}, \{\hat{q}_j\}) \\ &= \frac{\hat{p}^2}{2m} + \hat{V}_0(\hat{x}) + \hat{V}_1(\hat{x}, \omega t) + \sum_{j=1}^N \left\{ \frac{\hat{p}_j^2}{2m_j} + \frac{1}{2} m_j \omega_j^2 \left(\hat{q}_j - \frac{c_j \hat{x}}{m_j \omega_j^2} \right)^2 \right\}\end{aligned}\quad (1)$$

Here, \hat{x} and \hat{p} represent the position and momentum operators of the system, while $(\{\hat{q}_j\}, \{\hat{p}_j\})$ denote the sets of position and momentum operators for the bath oscillators. The confining potential is given by $\hat{V}_0(\hat{x})$ that the system would execute alone without any external drive, and \hat{V}_1 represents the potential due to the external driving with period T whose time average over one period is zero:

$$\hat{V}_1(\hat{x}, \omega(t + \tau)) = \hat{V}_1(\hat{x}, \omega t) \quad (2)$$

and

$$\frac{1}{T} \int_0^T dt \hat{V}_1(\hat{x}, \omega t) = 0$$

Following the customary approach of excluding the bath variables yields the quantum Langevin equation as

$$m\dot{\hat{x}} + \int_0^t dt' \gamma(t-t') \dot{\hat{x}}(t') + \frac{\partial \hat{V}(\hat{x}, \omega t)}{\partial \hat{x}} = \hat{\xi}(t) \quad (3)$$

$$\text{where } \hat{V} = \hat{V}_0 + \hat{V}_1 \quad (4)$$

$$\text{and the damping kernel } \gamma(t-t') = \frac{1}{\pi} \int_{-\infty}^{+\infty} d\omega [J(\omega)/\omega] \cos \omega(t-t') \quad (5)$$

The fluctuation operator, $\hat{\xi}(t)$ follows the fluctuation-dissipation relation. The bath's dual effects—fluctuation and dissipation—collaborate to uphold the system's thermal equilibrium in accordance with the fluctuation-dissipation theorem.

$$\langle \hat{\xi}(t) \hat{\xi}(t') + \hat{\xi}(t') \hat{\xi}(t) \rangle = \hbar \int_{-\infty}^{+\infty} \frac{d\omega}{\pi} J(\omega) \coth\left(\frac{\hbar\omega}{2k_B T}\right) \cos \omega(t-t') \quad (6)$$

Here the initial configuration of the bath degrees of freedom is used to compute the average. The friction coefficient γ clearly depicts that energy is irreversibly lost from the system to the environment. Here the Ohmic regime (i.e., strict Markovian limit) is considered with the spectral distribution function $J(\omega)$ $J(\omega) = m\gamma\omega$ which characterises the bath dynamics. In this context, γ reflects the correlation time of the bath-induced noise by characterising the spectral distribution width of the bath modes. It is to be mentioned here that the solutions of Eq. (3) are very complicated due to the involvement of time-dependent potential. It can typically be obtained numerically using various approximate methods. However, when the frequency of driving force is large and very large compared with all the other relevant system frequencies, a solution may be attainable, contingent on the type of problem being analysed. The force $\hat{F}(x, \omega t)$, due to the external time periodic field is given by:

$$\hat{F}(x, \omega t) = -\hat{V}'_1(x, \omega t) \text{ with } \omega \gg \frac{1}{T} \quad (7)$$

Here the oscillation of the particle induced by the external time periodic force is considered to be very small so that the particle lacks sufficient time to respond before the periodic force switches direction i.e., the acceleration over one period is barely affected by the periodic force. As a result, it is beneficial to separate the motion of the particle into "slow" and "fast" components. The Hamiltonian in Eq. (1) is time periodic, i.e., $[\hat{H}(t+T) = \hat{H}(t)]$. Thus, the dynamical analysis of such systems can be possible by using Floquet theorem which enables the simplification of the periodic or quasiperiodic time-dependent Schrödinger equation into a system of time-independent coupled equations or a Floquet matrix eigenvalue problem (Grifoni & Hänggi, 1998). The Schrödinger equation is as follows:

$$i\hbar \frac{\partial \psi}{\partial t} = \hat{H} \psi \quad (8)$$

The following Floquet states linked to their corresponding quasi-energies ε can be used to express solutions to Equation (8) as a linear combination:

$$\psi_\varepsilon = \left(\exp -\frac{i}{\hbar} \varepsilon t \right) \mathbb{U}_\varepsilon(x, \omega t) \quad (9)$$

$\mathbb{U}_\varepsilon(x, \omega t)$ denotes eigenstates of the Floquet Hamiltonian: $\hat{H}_F = -i\hbar \left(\frac{\partial}{\partial t} \right) + \hat{H}$. This reflects the key idea of the Bloch–Floquet theorem applied to time-dependent systems. Here, $\mathbb{U}_\varepsilon(x, \omega(t+T)) = \mathbb{U}_\varepsilon(x, \omega t)$ with $\omega = (2\pi/T)$. Floquet state has a “slow” part, $\left(\exp -\frac{i}{\hbar} \varepsilon t \right)$ (with the choice $0 \leq \varepsilon/\hbar \leq \omega$), which provides details regarding the quasienergies, and a “fast” part, $\mathbb{U}_\varepsilon(x, \omega t)$ that is solely dependent on the fast time $\tau = \omega t$. Thus, one can derive an equation of motion for the slow dynamics that encodes the system's quasienergies, with the necessary steps detailed as follows. Initially, a unitary gauge transformation $\exp(i\hat{T}(t))$, is aimed to be performed where $\hat{T}(t)$ is a Hermitian operator is periodic in time [$\hat{T}(t+T) = \hat{T}(t)$] with the same period as the Hamiltonian \hat{H} . This transformation removes the explicit time-dependence from the Hamiltonian making it time-independent in the new gauge. The transformed time independent Hamiltonian helps in deriving the equation of motion for the “slow” component. Eq. (8), expressed in the new gauge with $\chi = \exp(i\hat{T}(t))\psi$, is now written as

$$i\hbar \frac{\partial \chi}{\partial t} = \hat{H}_{eff} \chi \quad (10)$$

According to Floquet theory, χ has the same periodic behaviour as the Hamiltonian operator \hat{H} and the Hermitian operator \hat{T} . In the transformed gauge, χ represents a Floquet state characterised by the quasienergy ε . So, one may express the effective time-independent Hamiltonian as

$$\hat{H}_{eff} = \exp(i\hat{T}(t)) \hat{H} \exp(-i\hat{T}(t)) + i\hbar \left[\frac{\partial \exp(i\hat{T}(t))}{\partial t} \right] \exp(-i\hat{T}(t)) \quad (11)$$

The gauge transformation of Eq. (11) can be expressed in terms of fast time τ

$$\hat{H}_{eff} = \exp(i\hat{T}) \hat{H} \exp(-i\hat{T}) + i\hbar \omega \left[\frac{\partial \exp(i\hat{T})}{\partial \tau} \right] \exp(-i\hat{T}) \quad (12)$$

In the subsequent analysis, \hat{T} is treated as a perturbative term of order ω^{-1} in the high-frequency limit. Therefore, \hat{H}_{eff} and \hat{T} are expanded in powers of $1/\omega$ as

$$\hat{H}_{eff} = \sum_{n=0}^{\infty} \frac{1}{\omega^n} \hat{H}_n^e \quad (13)$$

$$\hat{T} = \sum_{n=0}^{\infty} \frac{1}{\omega^n} \hat{T}_n \quad (14)$$

The choice of \hat{T} ensures that \hat{H}_{eff} remains independent of time, order by order. Thus, \hat{H}_j^e is expressed in terms of $\hat{T}_1, \hat{T}_2, \dots, \hat{T}_{j+1}$, after which \hat{T}_{j+1} is selected such that \hat{H}_j^e is rendered time independent. Using the operator expressions to compute the terms in Eq. (11), one can get

$$\exp(i\hat{T}) \hat{H} \exp(-i\hat{T}) = \hat{H} + i[\hat{T}, \hat{H}] - \frac{1}{2!} [\hat{T}, [\hat{T}, \hat{H}]] - \frac{1}{3!} [\hat{T}, [\hat{T}, [\hat{T}, \hat{H}]]] + \dots \quad (15)$$

and

Non-Adiabatic Escape in Quantum Dissipative System

$$\frac{\partial \exp(i\hat{T})}{\partial \tau} \exp(-i\hat{T}) = i \frac{\partial \hat{T}}{\partial \tau} - \frac{1}{2!} \left[\hat{T}, \frac{\partial \hat{T}}{\partial \tau} \right] - \frac{1}{3!} \left[\hat{T}, \left[\hat{T}, \frac{\partial \hat{T}}{\partial \tau} \right] \right] + \dots \quad (16)$$

In the leading term, $O(\omega^0)$, \hat{H}_0^e is described by

$$\hat{H}_0^e = \frac{\hat{p}^2}{2m} + \hat{V}_0(\hat{x}) + \hat{H}_B + \hat{H}_{SB} + \hat{V}_1(\hat{x}, \tau) - \hbar \frac{\partial \hat{T}_1}{\partial \tau} \quad (17)$$

\hat{V}_0 , \hat{V}_1 , \hat{H}_B , and \hat{H}_{SB} do not depend on \hat{p} at all. For canceling the time dependence of \hat{H}_0^e , we choose

$$\hat{T}_1 = \frac{1}{\hbar} \int_0^\tau d\tau' \hat{V}_1(\hat{x}, \tau') \quad (18)$$

The integration constant is chosen as zero to get rid of the secular terms. Now, the substitution of Eq. (18) into Eq. (17) gives the leading order of the effective Hamiltonian

$$\hat{H}_0^e = \frac{\hat{p}^2}{2m} + \hat{V}_0(\hat{x}) + \hat{H}_B + \hat{H}_{SB} \quad (19)$$

Using Eq. (12) the effective Hamiltonian can be expressed in the order ω^{-1} as

$$\hat{H}_1^e = i[\hat{T}_1, \hat{H}] - \hbar \frac{\partial \hat{T}_2}{\partial \tau} - \frac{i\hbar}{2} \left[\hat{T}_1, \frac{\partial \hat{T}_1}{\partial \tau} \right] \quad (20)$$

As evident from Eq. (18), Since \hat{T}_1 is exclusively dependent on \hat{x} , so it will commute with its time derivative as well as with \hat{V}_0 , \hat{H}_B , and \hat{H}_{SB} . Thus, $\hat{H}_1^e = i[\hat{T}_1, (\hat{p}^2/2m)] - \hbar(\partial \hat{T}_2/\partial \tau)$. It is always possible to select \hat{T}_2 to be periodic such that $(\partial \hat{T}_2/\partial \tau) = i/\hbar[\hat{T}_1, (\hat{p}^2/2m)]$, leading to the vanishing of \hat{H}_1^e . Subsequently, \hat{T}_2 is determined using Equation (18) and the coordinate representation of the momentum operator \hat{p}

$$\hat{T}_2 = \frac{i}{2m} \int_0^\tau \partial \tau \int_0^\tau \partial \tau \hat{V}_1''(\hat{x}, \tau) + \frac{i}{m} \int_0^\tau \partial \tau \int_0^\tau \partial \tau \hat{V}_1'(\hat{x}, \tau) \frac{\partial}{\partial x} \quad (21)$$

With this choice, \hat{H}_1^e becomes zero. At the next order, ω^{-2} , \hat{H}_2^e can be calculated from

$$\hat{H}_2^e = i[\hat{T}_2, \hat{H}] - \frac{1}{2} [\hat{T}_1, [\hat{T}_1, \hat{H}]] - \hbar \frac{\partial \hat{T}_3}{\partial \tau} - \frac{i\hbar}{2} \left[\hat{T}_1, \frac{\partial \hat{T}_2}{\partial \tau} \right] - \frac{i\hbar}{2} \left[\hat{T}_2, \frac{\partial \hat{T}_1}{\partial \tau} \right] + \frac{\hbar}{6} \left[\hat{T}_1, \left[\hat{T}_1, \frac{\partial \hat{T}_1}{\partial \tau} \right] \right] \quad (22)$$

Using $\hat{H} = \hat{H}_0^e + \hbar(\partial \hat{T}_1/\partial \tau)$ and $(\partial \hat{T}_2/\partial \tau) = [\hat{T}_1, (\hat{p}^2/2m)] = [\hat{T}_1, \hat{H}]$, one obtains

$$\hat{H}_2^e = i[\hat{T}_2, \hat{H}_0^e] - \hbar \frac{\partial \hat{T}_3}{\partial \tau} + \frac{i\hbar}{2} \left[\hat{T}_2, \frac{\partial \hat{T}_1}{\partial \tau} \right] \quad (23)$$

Next, a periodic \hat{T}_3 is selected to counterbalance the time dependency of \hat{H}_2^e . It is found that \hat{H}_2^e contains a time-independent component given by $i\hbar/2[\hat{T}_2, (\partial \hat{T}_1/\partial \tau)]$. To ensure the periodicity of \hat{T}_2 , \hat{T}_3 is chosen so that

$$\frac{\partial \hat{T}_3}{\partial \tau} = \frac{i}{\hbar} [\hat{T}_2, \hat{H}_0^e] + \frac{i}{2} \left[\hat{T}_2, \frac{\partial \hat{T}_1}{\partial \tau} \right] - \frac{i}{2} \overline{\left[\hat{T}_2, \frac{\partial \hat{T}_1}{\partial \tau} \right]} \quad (24)$$

The overbar expresses the time average over one period. From Eqs. (18) and (21), \hat{T}_3 is found to be

$$\begin{aligned} \hat{T}_3 = & -\frac{\hbar}{m^2} \int_0^\tau \partial\tau \int_0^\tau \partial\tau \int_0^\tau \partial\tau \hat{V}_1''(\hat{x}, \tau) \frac{\partial^2}{\partial x^2} - \frac{\hbar}{m^2} \int_0^\tau \partial\tau \int_0^\tau \partial\tau \int_0^\tau \partial\tau \hat{V}_1'''(\hat{x}, \tau) \frac{\partial}{\partial x} - \\ & \frac{\hbar}{4m^2} \int_0^\tau \partial\tau \int_0^\tau \partial\tau \int_0^\tau \partial\tau \hat{V}_1^4(\hat{x}, \tau) - \frac{1}{m\hbar} \hat{V}_0'(\hat{x}) \int_0^\tau \partial\tau \int_0^\tau \partial\tau \int_0^\tau \partial\tau \hat{V}_1'(\hat{x}, \tau) + \frac{1}{2m\hbar} \int_0^\tau \partial\tau \hat{Q}(\hat{x}, \tau) + \hat{I}(\hat{x}, \hat{p}) \end{aligned} \quad (25)$$

where

$$\begin{aligned} \hat{Q}(\hat{x}, \tau) = & im\hbar \left[\hat{T}_2, \frac{\partial \hat{T}_1}{\partial \tau} \right] - im\hbar \left[\hat{T}_2, \frac{\partial \hat{T}_1}{\partial \tau} \right] = \overline{\hat{V}_1'(\hat{x}, \tau) \int_0^\tau \partial\tau \int_0^\tau \partial\tau \hat{V}_1'(\hat{x}, \tau)} - \\ & \hat{V}_1'(\hat{x}, \tau) \int_0^\tau \partial\tau \int_0^\tau \partial\tau \hat{V}_1'(\hat{x}, \tau) \end{aligned} \quad (26)$$

and $\hat{I}(\hat{x}, \hat{p})$ is the integration constant that is a Hermitian operator of \hat{x} and \hat{p} only. The determination of higher-order corrections necessitates understanding \hat{I} . Therefore, \hat{I} does not need to be evaluated in the leading-order correction. Substituting Equation (25) into Equation (23) yields time-independent \hat{H}_2^e :

$$\hat{H}_2^e = \frac{i\hbar}{2} \left[\hat{T}_2, \frac{\partial \hat{T}_1}{\partial \tau} \right] = \frac{1}{2m} \left[\int_0^\tau \partial\tau \hat{V}_1'(\hat{x}, \tau) \right]^2 \quad (27)$$

The resulting time-independent effective Hamiltonian, which includes the non-zero leading-order contribution:

$$\hat{H}_{eff} = \frac{\hat{p}^2}{2m} + \hat{V}_{eff} + \hat{H}_B + \hat{H}_{SB} \quad (28)$$

Here the effective time-independent potential, which depends on the driving frequency and amplitude influencing the slow motion, is expressed as follows

$$\hat{V}_{eff} = \hat{V}_0(\hat{x}) + \frac{1}{2m\omega^2} \left[\int_0^\tau \partial\tau \hat{V}_1'(\hat{x}, \tau) \right]^2 \quad (29)$$

Using the time-independent effective potential \hat{V}_{eff} , one can apply the established methodologies developed for such problems to address the original time-dependent issues. Thus, in the high-frequency regime, the slower dynamics are guided by the time-independent effective potential, which remains unaltered even in the presence of noise originating from the bath. The effective Hamiltonian can be interpreted as a quantum mechanical extension of the classical results by Kapitza (1986) and Landau and Lifshitz (1976), within the context of the SB model. Now the reduced Langevin equation expressing the slow variable becomes:

$$m\ddot{\hat{x}} + \int_0^t dt' \gamma(t-t')\dot{\hat{x}}(t') + \hat{V}_{eff}' = \xi(t) \quad (30)$$

Since Eq. (30) does not have explicit time dependence, its solution does not oscillate at the external frequency ω . The dynamics are governed by the nature of the effective potential (Fig. 1). Equations 29 and 30 stem from high-frequency perturbation theory, providing A method to convert a time-dependent problem into a time-independent framework approximately. This approach can be helpful in creating simplified models for condensed phase reactions.

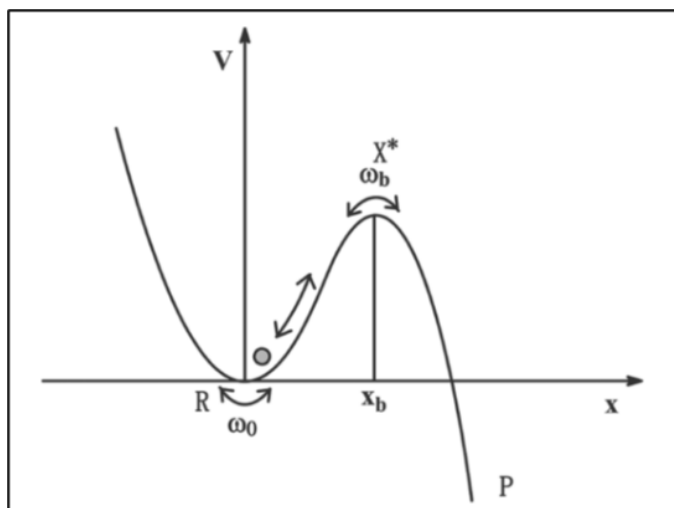


Figure 1: Graphical Representation of a Cubic Potential Where R Represents the Reactant State and P Denotes the Product State While X* Implies the Transition State (Shit, Chattopadhyay & Ray Chaudhuri, 2013)

To comprehend how the outcome from equation 30 may be applied to the stochastic dynamics of a system with periodic perturbations, it is helpful to analyse with a model. Consider a particle subject to an oscillating field ($V_0 = 0$),

$$V_1(x, \omega t) = Ae^{-\beta x^2} \sin(kx) \cos(\omega t + \phi) \quad (31)$$

Because the time-averaged potential energy cancels out, the influence of the oscillating field remains significant, even at elevated frequencies. As stated in equation 29, the slower component of the particle's motion can be roughly described as motion within an effective potential, which is governed by the ratio of the amplitude to the frequency of the external modulation.

$$V_{eff}(X) = \frac{A^2}{4m\omega^2} e^{-2\beta X^2} \omega [k \cos(kX) - 2\beta X \sin(kX)]^2 \quad (32)$$

$V_{eff}(X)$ is found to exhibit several local minima, two of these are more prominent in the parameters under consideration. Consequently, it can be concluded that a particle traversing such potential is likely to reside in one of these minima after an adequately extended period. As a result of dissipation, these minima are surrounded by basins of attraction. Therefore, when the friction dominates, the particle may become localised in one of the minima. Here the effective Hamiltonian does not have momentum-dependent couplings to the leading order (ω^{-2}) due to the very high frequency regime considered. This perspective makes quantum escape rate calculation easy and much less expensive. As per the earlier demonstration, some features of the time-dependent system may be captured by studying a suitable time-independent system governed by the Langevin equation (equation 30). It is now worth investigating whether both qualitative and quantitative results for the dissipation-driven escape from a metastable state can be obtained using a path-integral formulation

related to the Brownian motion (Ingold, 1997; Ingold, 2002) of quantum systems. In order to do so, a model system potential (say, a cubic potential, shown in Figure 1) is chosen so that an energy barrier of defined height separates the reactant and product states. Particles are initially confined in the well of state R by a large potential hump at X^* . They quickly reach thermal equilibrium within the well. However, due to the perturbation, a small number of particles may gain sufficient energy to overcome the barrier and enter region P, where return is not possible. The particle undergoes stochastic motion inside the well until a substantial perturbation drives it to overcome the potential barrier.

$$V_0 = \frac{A}{2}x^2 - \frac{B}{3}x^3 \quad (33)$$

A and B are positive constants. The position coordinate x has its values at $x = 0$ implying the reactant state and $x = x_b$ marking transition states. The finite potential barrier separating the transition state and the reactant state by is expressed as $(A^3/6B^2)$. Here, the system and environment's remaining degrees of freedom act as a heat bath at temperature T. Eq. (33) can be rewritten for examining the escape from a metastable state as

$$V_0(x) = \frac{1}{2}\omega^2x^2\left(1 - \frac{x}{x_0}\right) \quad (34)$$

A minima is located at $x = 0$ with with oscillations around this point having a frequency of ω_0 . A barrier appears at $x = (2/3)x_0$ with a potential barrier $V_b = (2/27)\omega_0^2x_0^2$. Assuming harmonic behaviour is close to the barrier leads to:

$$V(x) = V_b - \frac{1}{2}\omega_b^2x^2 \quad (35)$$

ω_b is the angular barrier frequency and V_b is the height of the potential barrier respectively located at x_b with $\omega_0 = \omega_b$. When the metastable state decays at a temperature T which is much higher than the crossover temperature, $T_0 [= (\hbar\omega_R/2\pi k_B)]$ where thermal activation becomes dominant, and accounting for memory effects, the dissipation of the metastable state leads to the following quantum escape rate:

$$k^Q = f_{cl}\omega c_{qm} \exp\left(\frac{V_b}{K_B T}\right) \quad (36)$$

Hence, the barrier crossing is boosted by quantum modifications due to the introduction of a further quantum "channel" when the temperature is in the quantum-classical crossover region. This increase is due to two key quantum occurrences: the mean energy in the well is raised by quantum fluctuations, and when the particle is subjected to thermal excitation near the top of the potential barrier, these fluctuations promote tunnelling through the residual small barrier.

These two effects reduce the barrier height. In the present model, when $T \gg T_0$, f_{cl} becomes the attempt frequency or classical pre-exponential factor and is calculated as

$$\omega_R f_{cl} = \frac{\omega_0 \omega_R}{2\pi \omega_b} \quad (37)$$

Non-Adiabatic Escape in Quantum Dissipative System

The frequency ω_R is a dissipation-renormalised quantity, determined by the largest positive solution of the equation: $\omega_R^2 + \omega_R \hat{\gamma}(\omega_R) = \omega_b^2$ and it corresponds to the well-known Kramers–Grote–Hynes frequency (Grote & Hynes, 1980; Hanggi & Mojtabai, 1982) described in the theory of non-Markovian rate processes. Renormalising the barrier frequency captures the influence of memory friction on the rate. Intriguingly, the renormalised frequency is the same as the one used to define the crossover temperature T_0 . The quantum correction factor c_{qm} has no dimension and it describes how quantum effects enhance the classical rate. It can lead to a significant rate enhancement, even at temperatures considerably above T_0 . As T approaches T_0 from above, the quantum correction factor exhibits a singularity. Using the standard functional integral approach (Grabert & Weiss, 1984), quantum mechanical correction factor can be expressed as:

$$c_{qm} = \prod_{n=1}^{\infty} \frac{\nu_n^2 + \omega_0^2 + \nu_n \hat{\gamma}(\nu_n)}{\nu_n^2 - \omega_b^2 + \nu_n \hat{\gamma}(\nu_n)} \quad (38)$$

Here $\hat{\gamma}(Z)$ is the Laplace transform of the damping kernel $\gamma(z)$ where ν_n 's are the Matsubara frequencies $[2\pi k_B T / \hbar]$. As the temperature approaches T_0 , i.e., the crossover temperature, c_{qm} approaches 1 and diverges exactly at T_0 . In the classical limit, where $T = T_0$ [i.e., $T/T_0 \rightarrow \infty$] the rate expression under intermediate-to-high damping conditions yields the correct classical result:

$$k_{IHD}^{cl} = \left(\frac{\omega_0 \omega_R}{2\pi \omega_b} \right) \exp \left(\frac{V_b}{k_B T} \right) \quad (39)$$

To extract leading quantum correction terms at elevated temperatures, Eq. (38) is reformulated as an exponential of a sum over logarithms, with each logarithm expanded in a power series of $k_B T / \hbar$.

$$c_{qm} = \exp \left[\frac{\hbar^2}{4\pi^2} (\omega_0^2 + \omega_b^2) \sum_{n=1}^{\infty} \frac{1}{n^2} \right] = \exp \left[\frac{\hbar^2}{4\pi^2} \left(\frac{\omega_0^2 + \omega_b^2}{(k_B T)^2} \right) \right] \quad (40)$$

Eq. 36, denoting the escape rate, may therefore be written as

$$k_{IHD}^Q = \left(\frac{\omega_0}{2\pi \omega_b} \right) \left(\sqrt{\frac{\gamma^2}{4} + \omega_b^2} - \frac{\gamma}{2} \right) \times \exp \left[\frac{\hbar^2}{4\pi^2} \left(\frac{\omega_0^2 + \omega_b^2}{(k_B T)^2} \right) \right] \exp \left(\frac{V_b}{k_B T} \right) \quad (41)$$

This expression is valid in The Kramers regime, i.e., moderate to strong damping regime and for $T > T_0$ where the primary mechanism for escape is not quantum tunnelling, yet it contributes notable quantum corrections to the classical activation rate. At strong friction $\gamma \gg \omega_0, \omega_b$ with $T \gg T_0$, the quantum correction can be given by

$$c_{qm} = \exp \left[\frac{\hbar(\omega_0^2 + \omega_b^2)}{2\pi k_B T} \left\{ \Psi \left(1 + \frac{\hbar \gamma}{2\pi k_B T} \right) - \Psi(1) \right\} \right] \quad (42)$$

where $\Psi(z)$ expresses digamma function. This simplified form, Eq. (42), is accurate only for systems with frequency-independent damping. The effective potential caused by external modulation is

$$V_{eff} = \frac{\tilde{A}}{2}x^2 - \frac{\tilde{B}}{3}x^3 \quad (44)$$

where

$$\tilde{A} = A + \frac{a^2}{2\omega^2} \quad (45)$$

It is clearly evident that the tuning of system parameters and the activation barrier height is influenced by external drive. Thus, the amplitude-to-frequency ratio of the driving modulation (a/ω) plays a crucial influence in determining the escape rate as well as the barrier height. The well and barrier are positioned at $x_0 = 0$ and $x_b = \tilde{A}/B$, respectively and leading to an effective potential barrier:

$$V_b^{eff} = \frac{\tilde{A}^3}{6B^2} \quad (46)$$

In the intermediate-to-high damping regime, where the energy dissipated per cycle far exceeds thermal energy, and assuming unit mass, the quantum Kramers rate for a rapid, periodically modulated particle can be expressed at times $t > 1/\omega$, when the dynamics effectively become time-independent, as:

$$k_{IHD}^Q = \left(\frac{\tilde{\omega}_0}{2\pi\tilde{\omega}_b} \right) \left(\sqrt{\frac{\gamma^2}{4} + \tilde{\omega}_b^2} - \frac{\gamma}{2} \right) \times \exp \left[\frac{\hbar^2}{4\pi^2} \left(\frac{\tilde{\omega}_0^2 + \tilde{\omega}_b^2}{(K_B T)^2} \right) \right] \exp \left(-\frac{V_b^{eff}}{K_B T} \right) \quad (47)$$

The classical counterpart of the rate can be written as:

$$k_{IHD}^{Cl} = \left(\frac{\tilde{\omega}_0}{2\pi\tilde{\omega}_b} \right) \left(\sqrt{\frac{\gamma^2}{4} + \tilde{\omega}_b^2} - \frac{\gamma}{2} \right) \exp \left(-\frac{V_b^{eff}}{K_B T} \right) \quad (48)$$

Here $\tilde{\omega}_0$ and $\tilde{\omega}_b$ are the frequency terms involved with the time-independent effective potential at the well and at the top of the barrier, respectively. Equation 47 contains both the exponents and the prefactors modified by the applied external field. When external perturbation is absent, this result agrees well with the well-known Kramers model. This is a clear indication of the accuracy of this model. Obtaining this result through path-integral techniques is a complex and challenging task. This analysis demonstrates the interplay between the fixed-temperature Intermediate-to-high-damping quantum Kramers rate and the semi-classical approach within the multiple-scale perturbation theory framework for Brownian motion in rapidly varying periodic potential. While the calculation of the rate of escape in a rapidly driven quantum system from a static metastable state might seem overwhelmingly dependent on time and far from adiabatic, this work offers a perspective through which the dynamics can be understood in terms of a time-independent modified potential. Theoretical calculation of the dissipation-induced escape rate from a metastable state subjected to a fast-oscillating external field reveals two main effects on the escape rate, arising from the high-frequency nature of the field relative to the particle's dynamics. First, environmental disturbances alter the kinetics near the energy barrier's peak, thereby influencing the stationary flux across it. Second, the equilibrium statistical distribution in the source well transitions to a steady-state form, incorporating the influence of energy injected by the external driving force. Taking into account these pronounced dynamic changes, a

Non-Adiabatic Escape in Quantum Dissipative System

generalised form of escape rate can be developed which reveals how external perturbation affects the rate. Equation (47) is subsequently rewritten as a function of a/ω :

$$k_{IHD}^Q = \underbrace{\frac{1}{2\pi} \left(\sqrt{\frac{\gamma^2}{4} + \left(A + \frac{a^2}{2\omega^2} \right)} - \frac{\gamma}{2} \right)}_I \times \underbrace{\exp \left[\frac{\hbar^2}{12} \left(\frac{A + \frac{a^2}{2\omega^2}}{(K_B T)^2} \right) \right]}_{II} \times \underbrace{\exp \left[- \frac{\left(A + \frac{a^2}{2\omega^2} \right)^3}{6B^2 K_B T} \right]}_{III} \quad (49)$$

Term II is found to be absent in k_{IHD}^{cl} . The effect of temperature and the parameter ratio a/ω on the escape dynamics can be examined by considering cubic potential and studying how $\ln k$ varies with $1/T$ for a Brownian particle in it, capturing both external field influences and quantum effects (as discussed elaborately in Ref. (Shit, Chattopadhyay & Ray Chaudhuri, 2013)). This analysis provides that in the low-temperature regime, dissipative quantum decay leads to a rise in the decay rate with temperature rise. The quantum correction effectively decreases the potential barrier, which increases the escape rate. The classical cases follow a linear trend, consistent with the Arrhenius law. However, at low temperatures (high $1/T$), the plot becomes nonlinear due to quantum effects, specifically the term II in equation 49, which is a key observation of this study. The quantum term is modulated by temperature as T^{-2} , contributing to the deviation from linearity. This highlights the quantum nature of the system. The escape process involves two processes—one is thermal activation which becomes dominant at elevated temperatures, and the other one is quantum tunnelling which plays a key role as the temperature decreases. Decay at extremely low temperatures arises purely from quantum mechanisms. As the temperature increases, the system displays linear trends, reflecting more classical behaviour. Since thermal energy remains well below the barrier height, external driving becomes essential for activation. When there is no external perturbation, the traditional Kramers plot is obtained. Observations reveal that periodic, space-dependent, high-frequency perturbations significantly increase the classical transition rate of Brownian particles relative to the unperturbed case.

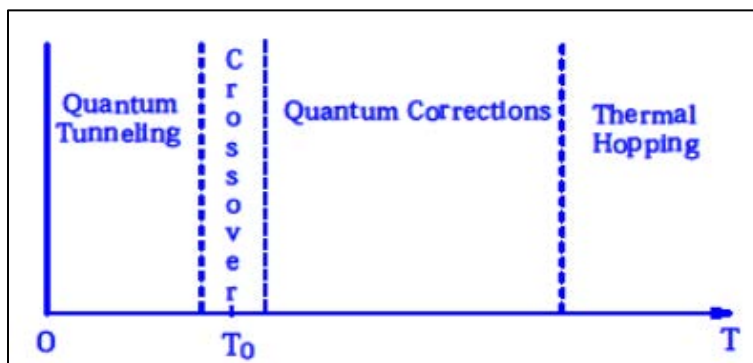


Figure 2: A Diagrammatic Representation Outlining the Temperature-Dependent Escape Dynamics Showing the Crossover Temperature T_0 , Below Which Quantum Tunnelling Dominates Over Thermal Escape (Shit, Chattopadhyay & Ray Chaudhuri, 2013)

The expression in Eq. (44) reveals that with an increase in the ratio a/ω , the barrier height increases, which in turn decreases the escape rate. This behaviour is demonstrated through the plots depicting analytical quantum (Eq. 47) and classical (Eq. 48) nonadiabatic escape rates, as functions of a/ω at different temperatures (Shit, Chattopadhyay & Ray Chaudhuri, 2013). Additionally, it is observed that tunnelling contributes to an increased escape rate through an effective decrease in barrier height. The findings suggest that with a rising a/ω ratio, the role of external driving overtakes that of quantum tunnelling. An increase in the ratio a/ω results in a higher barrier results a notable reduction in the stimulated escape rate causing the Brownian particle to take a longer time to transition into the more stable well. Thus, it is also noteworthy that tuning the ratio of the external drive's amplitude to its frequency allows control over the system's lifetime in a metastable state, either extending or reducing it. As temperature rises, the classical rate gets enhanced as expected, but the quantum escape rate behaves differently. For significantly elevated a/ω ratios, the quantum escapes rate rises with temperature, while in the low a/ω range, higher thermal energy paradoxically reduces the quantum escape rate. This counterintuitive finding reveals an unexpected mechanism for enhancing system stability under nonequilibrium conditions, in stark contrast to classical system behaviour. The subtle coupling between the driving field and the intrinsic system parameters causes this unusual temperature effect, offering valuable insights into dynamics away from thermal equilibrium. The physical basis for this unforeseen outcome can be explained using equation 49. It has been observed that term III controls the effect of temperature on k_{IHD}^{cl} and the classical escape rate gets enhanced with the elevation of temperature. But this is not the case for k_{IHD}^Q which includes two exponential components involving temperature, each with a different sign. The exponential components in equation 49 show that term II (stemming from field modulation) varies with T^{-1} , while term III (a pure quantum effect) shows a variation with T^{-2} . This asymmetric temperature dependence leads to the notable impact of temperature on k_{IHD}^Q as field parameters change. This analysis also illustrates how external perturbation influences the threshold or crossover temperature T_0 , which marks the transition between quantum tunnelling and thermal activation. The current theoretical framework is applicable for temperatures above this crossover point. As shown in Figure 2, a clear transition occurs at T_0 , where the dominant escape mechanism shifts from thermally activated hopping to quantum tunnelling. Since the dissipation mechanism dictates the magnitude of T_0 , the comparative extents of the quantum and classical regimes vary with dissipation strength. For $T < T_0$, escape is primarily governed by quantum tunnelling. Under high-temperature conditions ($T \gg T_0$), the decay is predominantly due to thermal activation induced barrier escape, with negligible quantum contributions. However, in the vicinity of the crossover temperature (i.e., just above T_0), quantum fluctuations start to significantly affect the escape rate, enhancing it beyond classical predictions. This quantum contribution becomes increasingly prominent as the temperature decreases. Within the framework of the present model, the revised crossover temperature \tilde{T}_0 may be expressed as:

$$\tilde{T}_0 = \frac{\hbar}{2\pi k_B T} \left[\sqrt{\left(\omega_0^2 + \frac{\gamma^2}{4} \right)} - \frac{\gamma}{2} \right] \quad (50)$$

As a result, it is clear that \tilde{T}_0 depends on the modulation parameters in addition to the dissipation mechanism. From the form of the crossover temperature expression, it is evident that as a result of external driving, the modified crossover temperature exceeds that of the unmodulated system. Therefore, a remarkable aspect of this work is the extension of the temperature range in which quantum effects become significant. Specifically, as spatial friction increases, the crossover temperature, marking the shift from quantum tunnelling to thermal activation, also rises and it makes the quantum effects relevant at higher temperatures.

Conclusion

Barrier-crossing processes are fundamental to a wide array of physical, chemical, and biological systems. Despite extensive studies and various strategies developed to control activation under external perturbations, the field remains active, with many open questions yet to be addressed. Periodically modulated systems, which are far from thermal equilibrium, form an important class of such systems. The present study is to analyse the escape dynamics of a quantum Brownian system in contact with an Ohmic bath, driven by a high-frequency periodic monochromatic driving field—conditions that create a far-from-equilibrium environment that presents theoretical challenges. Using the path-integral approach within the "Kapitza-Landau time window" framework for the interactions between the system and the environment, under high-frequency modulation, the quantum system's behaviour is well approximated by a static effective Hamiltonian or potential. As a consequence, the barrier height becomes renormalised, and the escape rate acquires a nontrivial prefactor that intricately depends on the system and external field characteristics. Therefore, the field alters the activation energy for escape. This formulation delivers a time-independent rate expression that holds for intermediate-to-high damping, for temperatures exceeding the crossover temperature, and in the high-frequency driving regime where ω surpasses all other related system frequencies. The structure of the time-independent modified potential-shaped by amplitude-to-frequency ratio a/ω plays a key role in determining the escape rate. Modifications arising from the applied perturbation and quantum mechanical contributions are also crucial in shaping the barrier-crossing dynamics. For a well-chosen set of field parameters, even a simplified static potential surface may see a substantial reduction in the net escape rate as the temperature increases. Therefore, the "extra dose" of external modulation does not always result in an increase in the rate of escape, which is a rare and paradoxical outcome. This stems from the subtle balance between dissipative forces and the applied modulation. While classical escape rates, such as those predicted by the Kramers model, generally rise with temperature under modulation, quantum escape rates display a much more nuanced and nontrivial temperature dependence. This study offers important understanding of how quantum mechanical effects modify reaction dynamics in condensed phases, especially in systems operating beyond equilibrium conditions.

Acknowledgement

The author expresses her gratitude to Professor Sudip Kumar Chattopadhyay and Professor Jyotipratim Ray Chaudhuri. She is thankful to Kandi Raj College, Kandi, Murshidabad, West Bengal, India.

References

- Ankerhold, J. (2004). Overdamped quantum phase diffusion and charging effects in Josephson junctions. *Europhysics Letters*, 67(2), 280. <https://doi.org/10.1209/epl/i2004-10067-y>
- Ankerhold, J., Pechukas, P., & Grabert, H. (2001). Strong friction limit in quantum mechanics: The quantum Smoluchowski equation. *Physical Review Letters*, 87, 086802 (1–4); Erratum: 2008, 101, 119903. <https://doi.org/10.1103/PhysRevLett.87.086802>
- Banerjee, D., Bag, B. C., Banik, S. K., & Ray, D. S. (2002). Approach to quantum Kramers' equation and barrier crossing dynamics. *Physical Review E*, 65, 021109 (1–13). <https://doi.org/10.1103/PhysRevE.65.021109>
- Banerjee, D., Bag, B. C., Banik, S. K., & Ray, D. S. (2004). Solution of quantum Langevin equation: Approximations, theoretical and numerical aspects. *Journal of Chemical Physics*, 120, 8960–8972. <https://doi.org/10.1063/1.1711593>
- Bhattacharya, S., Chattopadhyay, S., & Ray Chaudhuri, J. (2009). Investigation of noise-induced escape rate: A quantum mechanical approach. *Journal of Statistical Physics*, 136, 733–750. <https://doi.org/10.1007/s10955-009-9802-5>
- Bhattacharya, S., Chaudhury, P., Chattopadhyay, S., & Ray Chaudhuri, J. (2009). Quantum transport in a periodic symmetric potential of a driven quantum system. *Physical Review E*, 80, 041127(1–14). <https://doi.org/10.1103/PhysRevE.80.041127>
- Coffey, W. T., Garanin, D. A., & McCarthy, D. J. (2001). Crossover formulas in the Kramers theory of thermally activated escape rates—Application to spin systems. *Advances in Chemical Physics*, 117, 483–765. <https://doi.org/10.1002/9780470141779.ch5>
- Coffey, W. T., Kalmykov, Y. P., & Titov, S. V. (2007). Solution of the master equation for Wigner's quasiprobability distribution in phase space for the Brownian motion of a particle in a double well potential. *Journal of Chemical Physics*, 127, 074502(1–10). <https://doi.org/10.1063/1.2759486>
- Coffey, W. T., Kalmykov, Y. P., & Waldron, J. T. (2004). *The Langevin Equation* (2nd ed.). World Scientific: Singapore. <https://doi.org/10.1142/5343>
- Coffey, W. T., Kalmykov, Y. P., Titov, S. V., & Mulligan, B. P. (2007). Quantum master equation in phase space: Application to the Brownian motion in a periodic potential. *Europhysics Letters*, 77, 20011(1–6). <https://doi.org/10.1209/0295-5075/77/20011>
- Coffey, W. T., Kalmykov, Y. P., Titov, S. V., & Mulligan, B. P. (2007). Semiclassical master equation in Wigner's phase space applied to Brownian motion in a periodic potential. *Physical Review E*, 75, 041117. <https://doi.org/10.1103/PhysRevE.75.041117>
- Coffey, W. T., Kalmykov, Y. P., Titov, S. V., & Dowling, W. J. (2013). Longest relaxation time of relaxation processes for classical and quantum Brownian motion in a potential: Escape rate

Non-Adiabatic Escape in Quantum Dissipative System

- theory approach. *Advances in Chemical Physics*, 153, 111–309. <https://doi.org/10.1002/9781118571767.ch3>
- Coffey, W. T., Kalmykov, Y. P., Titovac, S. V., & Mulligan, B. P. (2007). Wigner function approach to the quantum Brownian motion of a particle in a potential. *Physical Chemistry Chemical Physics*, 9, 3361–3382. <https://doi.org/10.1039/b614554j>
- Dillenschneider, R., & Lutz, E. (2009). Quantum Smoluchowski equation for driven systems. *Physical Review E*, 80, 042101(1–4). <https://doi.org/10.1103/PhysRevE.80.042101>
- Doering, C. R., & Gadoua, J. C. (1992). Resonant activation over a fluctuating barrier. *Physical Review Letters*, 69, 2318–2321. <https://doi.org/10.1103/PhysRevLett.69.2318>
- Ford, G. W., & O'Connell, R. F. (2006). Anomalous diffusion in quantum Brownian motion with colored noise. *Physical Review A*, 73, 032103 (1–6). <https://doi.org/10.1103/PhysRevA.73.032103>
- Gammaitoni, L., Hänggi, P., Jung, P., & Marchesoni, F. (1998). Stochastic resonance. *Reviews of Modern Physics*, 70, 223–287. <https://doi.org/10.1103/RevModPhys.70.223>
- García-Palacios, J. L. (2004). Solving quantum master equations in phase space by continued-fraction methods. *Europhysics Letters*, 65, 735–741. <https://doi.org/10.1209/epl/i2003-10134-y>
- García-Palacios, J. L., & Zueco, D. (2004). The Caldeira–Leggett quantum master equation in Wigner phase space: Continued-fraction solution and application to Brownian motion in periodic potentials. *Journal of Physics A*, 37, 10735–10770. <https://doi.org/10.1088/0305-4470/37/45/003>
- Ghosh, P. K., Barik, D., & Ray, D. S. (2007). Inhomogeneous quantum diffusion and decay of a metastable state. *Physics Letters A*, 361, 201–211. <https://doi.org/10.1016/j.physleta.2006.08.090>
- Ghosh, P., Shit, A., Chattopadhyay, S., & Ray Chaudhuri, J. (2010). Escape of a driven particle from a metastable state: A semiclassical approach. *Journal of Chemical Physics*, 132, 244506(1–13). <https://doi.org/10.1063/1.3443774>
- Grabert, H., & Weiss, U. (1984). Crossover from thermal hopping to quantum tunneling. *Physical Review Letters*, 53, 1787–1790. <https://doi.org/10.1103/PhysRevLett.53.1787>
- Grabert, H., Schramm, P., & Ingold, G.-L. (1987). Localization and anomalous diffusion of a damped quantum particle. *Physical Review Letters*, 58, 1285–1288. <https://doi.org/10.1103/PhysRevLett.58.1285>
- Grabert, H., Schramm, P., & Ingold, G.-L. (1988). Quantum Brownian motion: The functional integral approach. *Physics Reports*, 168, 115–207. [https://doi.org/10.1016/0370-1573\(88\)90023-3](https://doi.org/10.1016/0370-1573(88)90023-3)
- Grifoni, M., & Hänggi, P. (1998). Driven quantum tunneling. *Physics Reports*, 304, 229–354. [https://doi.org/10.1016/S0370-1573\(98\)00022-2](https://doi.org/10.1016/S0370-1573(98)00022-2)
- Grote, R. F., & Hynes, J. T. (1980). The stable states picture of chemical reactions. II. Rate constants for condensed and gas phase reaction models. *Journal of Chemical Physics*, 73, 2715–2732. <https://doi.org/10.1063/1.440485>
- Hänggi, P., & Ingold, G. L. (2005). Fundamental aspects of quantum Brownian motion. *Chaos*, 15, 026105 (1–12). <https://doi.org/10.1063/1.1853631>

- Hänggi, P., & Jung, P. (1995). Colored noise in dynamical systems. *Advances in Chemical Physics*, 89, 239–326. <https://doi.org/10.1002/9780470141489.ch4>
- Hänggi, P., & Mojtabai, F. (1982). Thermally activated escape rate in presence of long-time memory. *Physical Review A*, 26, 1168–1170. <https://doi.org/10.1103/PhysRevA.26.1168>
- Hänggi, P., Talkner, P., & Borkovec, M. (1990). Reaction-rate theory: Fifty years after Kramers. *Reviews of Modern Physics*, 62, 251–341. And references therein. <https://doi.org/10.1103/RevModPhys.62.251>
- Ingold, G.-L. (1997). In Quantum fluctuations. In S. Reynaud, E. Giacobino, & J. Zinn-Justin (Eds.), *Quantum Fluctuations* (pp. 577–584). Elsevier: New York. <https://pubs.acs.org/doi/abs/10.1021/jp402565y>
- Ingold, G.-L. (2002). In Path integrals and their application to dissipative quantum systems. In A. Buchleitner & K. Hornberger (Eds.), *Lecture Notes in Physics* (Vol. 611, pp. 1–53). Springer: New York. https://doi.org/10.1007/3-540-45855-7_1
- Jülicher, F., Ajdari, A., & Prost, J. (1997). Modeling molecular motors. *Reviews of Modern Physics*, 69, 1269–1282. <https://doi.org/10.1103/RevModPhys.69.1269>
- Jung, P. (1993). Periodically driven stochastic systems. *Physics Reports*, 234, 175–295. [https://doi.org/10.1016/0370-1573\(93\)90022-6](https://doi.org/10.1016/0370-1573(93)90022-6)
- Kapitza, P. L. (1986). *Collected Papers of P. L. Kapitza* (Vol. 3, D. ter Haar, Ed.). Pergamon: New York.
- Kim, C., Talkner, P., Lee, E. K., & Hänggi, P. (2010). Rate description of Fokker-Planck processes with time-periodic parameters. *Chemical Physics*, 370, 277–289. <https://doi.org/10.1016/j.chemphys.2009.10.027>
- Landau, L. D., & Lifshitz, E. M. (1976). *Mechanics*. 3rd Edition. Pergamon: Oxford. Retrieved from: <https://cimec.org.ar/foswiki/pub/Main/Cimec/MecanicaRacional/84178116-Vol-1-Landau-Lifshitz-Mechanics-3Rd-Edition-197P.pdf>, Accessed on 21st December 2024.
- Leggett, A. J., & Caldeira, A. O. (1983). Statistical thermodynamics of fluid hydrogen at high energy density. *Physica A*, 121, 587–596. [https://doi.org/10.1016/0378-4371\(85\)90047-0](https://doi.org/10.1016/0378-4371(85)90047-0)
- Lehmann, J., Reimann, P., & Hänggi, P. (2000). Surmounting oscillating barriers. *Physical Review Letters*, 84, 1639–1642. <https://doi.org/10.1103/PhysRevLett.84.1639>
- Luchinsky, D. G., McClintock, P. V. E., & Dykman, M. I. (1998). Analogue studies of nonlinear systems. *Reports on Progress in Physics*, 61, 889–997. 10.1088/0034-4885/61/8/001
- Łuczka, J., Rudnicki, R., & Hänggi, P. (2005). The diffusion in the quantum Smoluchowski equation. *Physica A: Statistical Mechanics and its Applications*, 351, 60–68. <https://doi.org/10.1016/j.physa.2004.12.007>
- Machura, L., Kostur, M., Hänggi, P., Talkner, P., & Łuczka, J. (2004). Consistent description of quantum Brownian motors operating at strong friction. *Physical Review E*, 70, 031107 (1–5). <https://doi.org/10.1103/PhysRevE.70.031107>
- Machura, L., Kostur, M., Talkner, P., Łuczka, J., & Hänggi, P. (2006). Quantum diffusion in biased washboard potentials: Strong friction limit. *Physical Review E*, 73, 031105(1–7). <https://doi.org/10.1103/PhysRevE.73.031105>

Non-Adiabatic Escape in Quantum Dissipative System

- Maier, S. A., & Ankerhold, J. (2010). Quantum Smoluchowski equation: A systematic study. *Physical Review E*, 81, 021107(1–14). <https://doi.org/10.1103/PhysRevE.81.021107>
- Orszag, S., & Bender, C. M. (1978). *Advanced Mathematical Methods for Scientists and Engineers* (pp. xiv+593). New York, NY, USA: McGraw-Hill.
- Reduced hierarchy equations of motion approach to molecular vibrations. *Journal of Physical Chemistry A*, 115, 4009–4022. <https://doi.org/10.1021/jp1095618>
- Reichl, L. E., & Kim, S. (1996). Stochastic chaos and resonance in a bistable stochastic system. *Physical Review E*, 53, 3088–3095. <https://doi.org/10.1103/PhysRevE.53.3088>
- Reimann, P. (2002). Brownian motors: Noisy transport far from equilibrium. *Physics Reports*, 361, 57–265. [https://doi.org/10.1016/S0370-1573\(01\)00081-3](https://doi.org/10.1016/S0370-1573(01)00081-3)
- Reimann, P., Grifoni, M., & Hänggi, P. (1997). Quantum ratchets. *Physical Review Letters*, 79, 10–13. <https://doi.org/10.1103/PhysRevLett.79.10>
- Risken, H. (1989). *The Fokker–Planck equation*. Springer: Berlin. <https://doi.org/10.5772/9730>
- Sakurai, A., & Tanimura, Y. (2011). Does \hbar play a role in multidimensional spectroscopy?
- Shit, A., Chattopadhyay, S., & Chaudhuri, R. (2012). Quantum escape in the presence of a time-periodic oscillating force. *Europhysics Letters*, 97, 40006(1–5). <https://doi.org/10.1209/0295-5075/97/40006>
- Shit, A., Chattopadhyay, S., & Ray Chaudhuri, J. (2011). Effective quantum Brownian dynamics in presence of a rapidly oscillating space-dependent time-periodic field. *Physical Review E*, 83, 060101(R)(1–4). <https://doi.org/10.1103/PhysRevE.83.060101>
- Shit, A., Chattopadhyay, S., & Ray Chaudhuri, J. (2013). Quantum stochastic dynamics in the presence of a time-periodic rapidly oscillating potential: Nonadiabatic escape rate. *Journal of Physical Chemistry A*, 117, 8576–8590. <https://doi.org/10.1021/jp402565y>
- Tanaka, M., & Tanimura, Y. (2009). Quantum dissipative dynamics of electron transfer reaction system: Nonperturbative hierarchy equations approach. *Journal of the Physical Society of Japan*, 78, 073802(1–4). <https://doi.org/10.1143/JPSJ.78.073802>
- Tanaka, M., & Tanimura, Y. (2010). Multistate electron transfer dynamics in the condensed phase: Exact calculations from the reduced hierarchy equations of motion approach. *Journal of Chemical Physics*, 132, 214502(1–11). <https://doi.org/10.1063/1.3428674>
- Tanimura, Y. (2006). Stochastic Liouville, Langevin, Fokker–Planck, and master equation approaches to quantum dissipative systems. *Journal of the Physical Society of Japan*, 75, 082001(1–39). <https://doi.org/10.1143/JPSJ.75.082001>
- Tanimura, Y. (2012). Reduced hierarchy equations of motion approach with Drude plus Brownian spectral distribution: Probing electron transfer processes by means of two-dimensional correlation spectroscopy. *Journal of Chemical Physics*, 137, 22A550(1–9). <https://doi.org/10.1063/1.4766931>
- Tanimura, Y., & Ishizaki, A. (2009). Modeling, calculating, and analyzing multidimensional vibrational spectroscopies. *Accounts of Chemical Research*, 42, 1270–1279. <https://doi.org/10.1021/ar9000444>

- Tanimura, Y., & Wolynes, P. G. (1991). Quantum and classical Fokker-Planck equations for a Gaussian-Markovian noise bath. *Physical Review A*, 43, 4131–4142. <https://doi.org/10.1103/PhysRevA.43.4131>
- Tanimura, Y., & Wolynes, P. G. (1992). The interplay of tunneling, resonance, and dissipation in quantum barrier crossing: A numerical study. *Journal of Chemical Physics*, 96, 8485–8496. <https://doi.org/10.1063/1.462892>
- Tsekov, R. (1995). Dissipation in quantum systems. *Journal of Physics A: Mathematical and General*, 28, L557–L561. <https://doi.org/10.1088/0305-4470/28/21/007>
- Tsekov, R. (2007). Comment on ‘Semiclassical Klein–Kramers and Smoluchowski equations for the Brownian motion of a particle in an external potential’. *Journal of Physics A: Mathematical and Theoretical*, 40, 10945–10947. <https://doi.org/10.1088/1751-8113/40/35/N01>
- Weiss, U. (2012). *Quantum dissipative systems* (4th ed.). World Scientific Publishing Company: Singapore. <https://doi.org/10.1142/8334>
- Zwanzig, R. (2001). *Nonequilibrium Statistical Mechanics*. Oxford University Press: New York.

Exploring the Catalytic Potential of Ionanofluids in Green Chemistry

Prasenjit Mandal^{1*}, Aniruddha Mondal², Shib Shankar Biswas³, Amit Kumar Kundu⁴

¹Department of Chemistry, Santipur College, Nadia 741404, West Bengal, India

²Department of Chemistry, Harindanga High School, Harindanga, Falta 743504, West Bengal, India

³Department of Physics, Surendranath College, Mahatma Gandhi Road, Kolkata 700009, West Bengal, India

⁴Department of Chemistry, Sripat Singh College, Jiaganj, Murshidabad 742123, West Bengal, India

*Corresponding Author's E-mail: mandalprasenjit21@gmail.com

Abstract

Ionanofluids, a unique combination of ionic liquids and nanoparticles, have emerged as a promising class of advanced materials with remarkable potential for sustainable chemistry and catalytic processes. The synergy between ionic liquids' tunable physicochemical properties and nanoparticles' catalytic activity has unlocked numerous opportunities for green chemistry, offering environmentally benign alternatives to traditional solvents and catalysts. These hybrid systems exhibit exceptional thermal stability, low volatility, and high ionic conductivity, making them ideal for applications in energy-efficient reactions and renewable processes. In catalysis, ionanofluids have demonstrated enhanced reaction rates, selectivity, and recyclability in both homogeneous and heterogeneous systems. They have found applications across a diverse range of transformations, including organic synthesis, electrocatalysis, photocatalysis, and biocatalysis. By stabilising catalysts and improving their activity, ionanofluids contribute to reducing energy demands and minimising waste, aligning with the principles of green chemistry. Additionally, their ability to stabilise enzymes and facilitate biocatalytic reactions offers immense potential for industrial biotechnology. Despite their advantages, the widespread adoption of ionanofluids is limited by challenges such as the high cost of ionic liquids, toxicity concerns, and the stability of nanoparticles in the ionic liquid matrix. Addressing these issues through the development of cost-effective, biodegradable ionic liquids and robust nanoparticle systems is essential for broader implementation. Looking ahead, the integration of ionanofluids into renewable energy technologies, environmental remediation, and bio-based chemical processes offers an exciting frontier for research and innovation. This review provides a comprehensive overview of the synthesis, properties, and applications of ionanofluids, with an emphasis on their transformative role in sustainable chemistry and catalysis. It also highlights current challenges and proposes future directions for advancing this interdisciplinary field.

Keywords: *Catalysis; Green Chemistry; Ionanofluids; Nanotechnology; Sustainable Chemistry*

Converging Chemical and Biological Sciences for a Sustainable Era

Introduction

Ionanofluids, a hybrid material combining ionic liquids (ILs) and nanoparticles (NPs), represent a significant advancement in the field of nanotechnology and green chemistry (Alqahtani, 2024). Ionic liquids, characterised by their low volatility, high thermal stability, and remarkable ionic conductivity, provide an excellent medium for the dispersion and stabilisation of nanoparticles (Pereira, Souza & Moita, 2024). These nanoparticles, which may include metals, metal oxides, or other nanostructures, impart enhanced catalytic activity, thermal properties, and surface functionality to the composite system. The synergistic combination of these components in ionanofluids not only leverages the individual advantages of ILs and NPs but also results in unique physicochemical properties that surpass those of their individual constituents (Das *et al.*, 2021). This combination enables ionanofluids to serve as advanced materials for applications ranging from catalysis and energy storage to environmental remediation and biotechnology.

The significance of ionanofluids lies in their alignment with the principles of sustainable chemistry, offering innovative solutions to pressing environmental and economic challenges (Rahman *et al.*, 2024). Traditional chemical processes often rely on volatile organic solvents and energy-intensive conditions, resulting in significant environmental impacts. In contrast, ionanofluids serve as green alternatives that reduce energy consumption, minimise waste generation, and enhance reaction efficiency (Behera, Sangwai & Byun., 2025). Their high thermal and chemical stability allows them to operate under extreme conditions, while their tunable properties enable customisation for specific applications. Furthermore, the incorporation of nanoparticles provides additional functionality, such as improved catalytic activity and recyclability. This makes ionanofluids an ideal choice for achieving sustainability in industrial and academic research settings, particularly in catalytic processes where efficiency and selectivity are paramount (Madheswaran *et al.*, 2023).

This review aims to provide a comprehensive understanding of the synthesis, properties, and applications of ionanofluids, emphasizing their transformative role in green and catalytic chemistry. By examining the unique attributes of these materials, we will explore their use in processes ranging from organic synthesis and biocatalysis to electrocatalysis and photocatalysis. The ability of ionanofluids to stabilise catalysts, enhance reaction rates, and enable energy-efficient pathways positions them as a critical technology for addressing global challenges such as energy sustainability, environmental remediation, and resource efficiency. Additionally, the review will discuss the current challenges associated with ionanofluids, such as cost, toxicity, and scalability, and propose strategies to overcome these barriers.

The scope of this review encompasses a detailed analysis of the fundamental properties and synthesis techniques of ionanofluids, followed by an exploration of their applications in sustainable chemistry and catalytic processes. Particular attention will be given to their role as solvents and reaction media, as well as their integration into advanced catalytic systems. Furthermore, the review will highlight emerging trends and future directions, including the

development of eco-friendly ionic liquids, the design of multi-functional nanoparticle systems, and the application of ionanofluids in renewable energy technologies. By bridging the gap between material science, chemistry, and engineering, this review aims to provide a foundation for future research and innovation in the field of ionanofluids.

Properties and Synthesis of Ionanofluids

Physicochemical Properties

Ionanofluids are characterised by a unique set of physicochemical properties that make them valuable for a variety of applications in catalysis, energy storage, and sustainable chemistry (Das *et al.*, 2021). The properties of ionanofluids stem from the synergistic interaction between the ionic liquids (ILs) and the nanoparticles (NPs) suspended within them. Ionic conductivity, thermal stability, viscosity, and nanostructuring are key attributes that govern their performance in different processes (Figure 1).

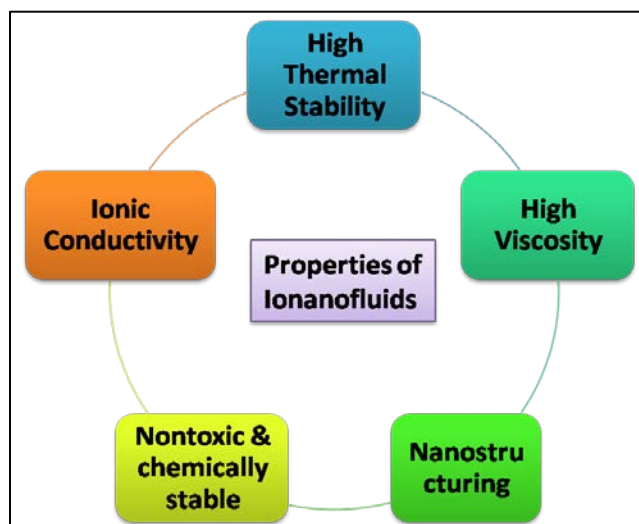


Figure 1: Represents the Various Properties of Ionanofluids

Ionic Conductivity: One of the most significant characteristics of ionanofluids is their high ionic conductivity, which is mainly attributed to the presence of ionic liquids (Joseph *et al.*, 2022). Ionic liquids, being composed entirely of ions, exhibit high ionic conductivity, which is advantageous in various electrochemical applications, including fuel cells and energy storage devices. When nanoparticles are incorporated into ionic liquids, the interaction between the IL and the NPs can affect the overall conductivity of the system. For instance, well-dispersed nanoparticles may enhance conductivity by facilitating ionic movement, while agglomeration of nanoparticles can hinder the flow of ions and decrease conductivity (Li, Mbonu & Akcora, 2025).

Thermal Stability: Ionic liquids are known for their exceptional thermal stability, typically operating in temperature ranges between -50°C to over 300°C without decomposing or evaporating (Wang *et al.*, 2024). This property makes them ideal for high-temperature

catalytic reactions and other industrial processes where conventional solvents would fail. The nanoparticles in ionanofluids can further enhance thermal conductivity, enabling better heat transfer and temperature management in processes that require precise control over temperature (Moulefera *et al.*, 2025). The overall thermal stability of ionanofluids is thus largely determined by the combination of the IL's inherent properties and the type and concentration of nanoparticles used.

Viscosity: The viscosity of ionanofluids plays a crucial role in determining their efficiency in various applications, particularly in catalytic processes and energy transfer (Moosavi, Torkzadeh & Akbarinezhad, 2024). While ionic liquids are generally more viscous than conventional organic solvents or water, the addition of nanoparticles can either increase or decrease the viscosity of the system depending on the size, concentration, and dispersion of the particles (Chen, Qiao & Liu, 2022). High viscosity can reduce the diffusion of reactants and hinder reaction rates, but it can also be advantageous in specific applications where stable and thick media are required, such as in lubrication or as heat transfer fluids.

Nanostructuring: The presence of nanoparticles in ionic liquids leads to the formation of nanostructured systems that exhibit unique behaviours not seen in pure ILs or conventional nanofluids (Bo *et al.*, 2022). These nanostructures, which can range from well-dispersed nanoparticles to aggregated clusters, can significantly alter the physical and chemical properties of the fluid. The interaction between the IL and the nanoparticle surface can lead to the formation of a structured interface, which can further influence properties like viscosity, surface tension, and electrochemical stability. The resulting nanostructuring is crucial in determining the catalytic and transport properties of ionanofluids in various reactions.

The relationship between ionic liquids and nanoparticles is complex and critical for the design of efficient ionanofluids (Lee *et al.*, 2025). The properties of the ILs can influence the dispersion, stability, and reactivity of nanoparticles, while their nature can modify the solvation and ionic characteristics of the ionic liquid. For instance, the functionalisation of nanoparticles with ligands or surfactants can improve their dispersion in the IL, thereby enhancing the overall performance of the ionanofluid. Conversely, the presence of nanoparticles can impact on the ionic liquid's viscosity, conductivity, and stability, highlighting the interdependence between the two components.

Synthesis Techniques

The synthesis of ionanofluids involves various methods that aim to combine ionic liquids effectively with nanoparticles while maintaining their individual properties (Zhang *et al.*, 2025). The two most common techniques for preparing ionanofluids are physical mixing and in situ synthesis. Each approach has its advantages and challenges, particularly in terms of scalability, reproducibility, and the final properties of the material.

Physical Mixing: Physical mixing is the simplest and most widely used method for synthesising ionanofluids (Duarte *et al.*, 2024). In this process, nanoparticles are directly added to the ionic liquid under controlled conditions. Typically, the nanoparticles are dispersed in the IL using mechanical stirring, sonication, or high shear mixing, ensuring a homogeneous distribution of the particles within the liquid (Figure 2). This method is highly

efficient and cost-effective, particularly when commercially available nanoparticles are used. However, achieving stable dispersion of nanoparticles in ionic liquids can be challenging due to the strong interactions between the IL and the particles, which can lead to aggregation or settling of nanoparticles over time (Kulshrestha, Kumar & Sharma, 2024). To overcome this, surfactants or stabilising agents are often added to improve the dispersion and stability of the nanoparticles.

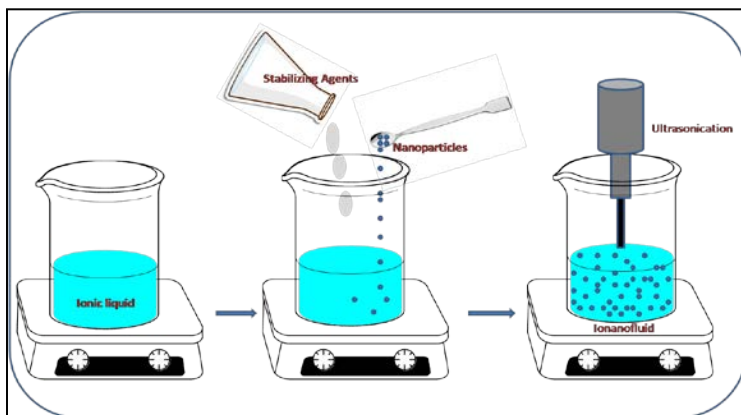


Figure 2: Schematic Representation of the Synthesis of Ionanofluid by Physical Mixing

In Situ Synthesis: In situ synthesis involves the formation of nanoparticles directly within the ionic liquid matrix. This approach typically involves the reduction or precipitation of metal or metal oxide nanoparticles from precursor salts or complexes (Yang *et al.*, 2025). By controlling the reaction conditions (e.g., temperature, time, and concentration of precursors), nanoparticles can be synthesised with precise control over their size, shape, and distribution within the ionic liquid. In situ synthesis often results in better nanoparticle-IL interactions and more stable dispersion, as the nanoparticles are formed within the IL environment. This method also eliminates the need for additional stabilisation agents, as the ionic liquid itself can act as a stabilising medium (Dupont *et al.*, 2024).

However, controlling the size and uniformity of the nanoparticles can be more challenging compared to physical mixing, especially for complex or highly reactive nanoparticles.

Stabilisation Mechanisms: A critical aspect of ionanofluid synthesis is ensuring the long-term stability and uniform dispersion of nanoparticles in ionic liquids (Urmi *et al.*, 2021). This is particularly important for catalytic applications, where the size, shape, and distribution of nanoparticles significantly impact the reactivity and efficiency of the system. Stabilisation mechanisms include electrostatic stabilisation, steric stabilisation, and hybrid approaches that combine both. Electrostatic stabilisation relies on the repulsive forces between charged nanoparticles and the ionic liquid ions to prevent aggregation (Khavani, Mehranfar & Mofrad, 2022).

Steric stabilisation, on the other hand, involves the use of surfactants or ligands to create a physical barrier around the nanoparticles and prevent their agglomeration. In some cases,

Ionanofluids as Green Catalysts

hybrid stabilisation methods are used to enhance both electrostatic and steric repulsion, ensuring long-term stability.

Challenges in Scalability and Reproducibility: While ionanofluids show great promise in various applications, scaling up their synthesis for industrial applications presents significant challenges. Achieving uniform dispersion of nanoparticles in large volumes of ionic liquids is difficult, as agglomeration tends to increase with the scale of the system (Hu *et al.*, 2023).

Additionally, the synthesis process often requires precise control of reaction conditions, which can be difficult to maintain in large-scale operations. Reproducibility is another challenge, as small variations in the synthesis procedure can result in significant differences in the properties of the final ionanofluid, affecting its performance in catalytic and other applications. Developing more efficient and scalable synthesis methods, such as continuous flow reactors or automated systems for nanoparticle functionalization, will be essential for the broader adoption of ionanofluids in industrial settings.

Comparison with Conventional Solvents and Nanofluids

Ionanofluids offer several advantages over conventional solvents and traditional nanofluids, particularly in the context of sustainability and catalytic efficiency (Paul *et al.*, 2021). When compared to water and organic solvents, ionanofluids demonstrate superior stability, higher thermal conductivity, and tunable properties that can be optimized for specific applications.

Advantages over Water and Organic Solvents: Water, although widely used as a solvent, has limitations in terms of its thermal stability and chemical reactivity (Mondal, Kundu & Mandal, 2024). Many chemical processes require solvents that can operate at high temperatures or under harsh conditions, where water would either boil off or undergo decomposition. Organic solvents, while more stable than water, often exhibit high volatility, toxicity, and environmental hazards, making them unsuitable for sustainable chemistry applications. In contrast, ionic liquids, which are non-volatile and thermally stable, offer a safer and more efficient alternative. Ionanofluids, by combining ionic liquids with nanoparticles, can further enhance the performance of these materials, enabling reactions to take place under more efficient and controlled conditions (Swapna *et al.*, 2024).

Additionally, ionic liquids are inherently less toxic and can be designed to be biodegradable, aligning with the principles of green chemistry.

Advantages over Traditional Nanofluids: Traditional nanofluids are typically composed of nanoparticles suspended in conventional liquids, such as water or oils. While these nanofluids exhibit enhanced thermal conductivity and catalytic properties compared to pure liquids, they suffer from issues like poor stability, aggregation of nanoparticles, and limited tunability of the solvent. In contrast, ionanofluids offer better stability due to the interaction between the nanoparticles and the ionic liquid medium, which reduces aggregation and ensures better long-term performance (Xu *et al.*, 2024). The ionic nature of the solvent also allows for greater control over the solvation environment, enhancing the dispersion and reactivity of nanoparticles.

Furthermore, ionanofluids can be tailored for specific applications by adjusting the ionic liquid's structure, which is not possible with traditional nanofluids.

Role of Ionanofluids in Sustainable Chemistry

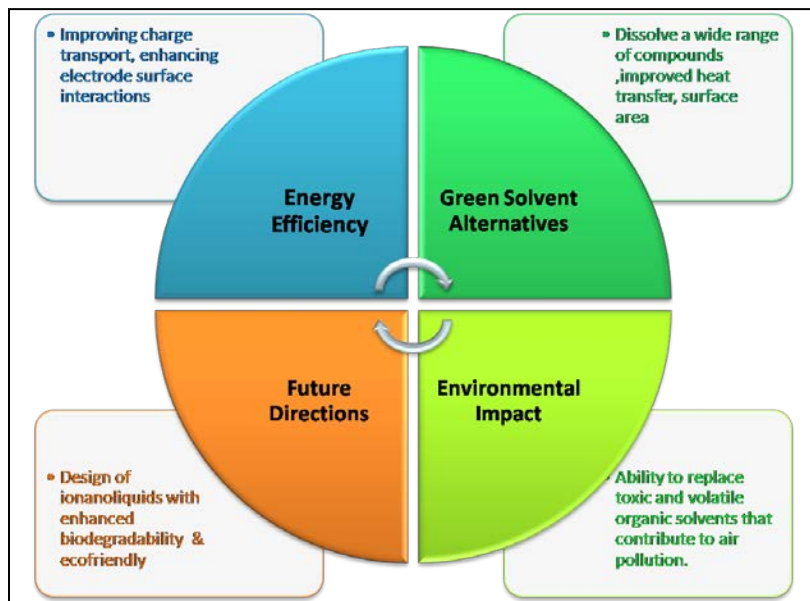


Figure 3: Represents the Various Roles of Ionanofluids in Sustainable Chemistry

Green Solvent Alternatives

The increasing global awareness of environmental issues and the need for sustainable chemical processes has driven the development of green solvents (Ullah, Haseeb & Tuzen, 2024). Traditional solvents, especially volatile organic compounds (VOCs), have significant environmental drawbacks, such as high toxicity, flammability, and the potential to cause air pollution and environmental contamination. The use of volatile solvents in various chemical processes contributes to the release of harmful emissions and poses challenges in waste disposal. In this context, ionanofluids, which combine ionic liquids (ILs) with nanoparticles, offer an effective alternative for sustainable solvent systems, addressing many of the issues associated with conventional solvents.

Ionic liquids are a class of solvents composed entirely of ions, which are characterized by their negligible vapor pressure, high thermal stability, and tunability of physicochemical properties (Vishwakarma *et al.*, 2025). The non-volatile nature of ionic liquids makes them ideal for processes that would otherwise rely on volatile organic solvents. By introducing nanoparticles into these ionic liquids, ionanofluids not only retain the favorable properties of ILs, such as their ability to dissolve a wide range of compounds, but also gain enhanced properties like improved heat transfer, increased surface area, and better catalytic behavior. As a result, ionanofluids can serve as effective green alternatives to volatile solvents, offering improved efficiency and environmental benefits (Figure 3).

A notable example of ionanofluids used in green extraction processes is their application in liquid-liquid extractions (Khan *et al.*, 2024). In the extraction of bioactive compounds from plant materials, ionanofluids have been successfully used as solvents for green extraction techniques, such as microwave-assisted and ultrasonic-assisted extraction. In these processes, the ionic liquids in the ionanofluids provide excellent solubility for a wide variety of polar and non-polar compounds, making them ideal for selectively extracting bioactive compounds without the need for toxic organic solvents. The addition of nanoparticles enhances the extraction process by providing additional surface area for solute interaction and improving the overall efficiency of the extraction (Khoramian *et al.*, 2024).

Furthermore, ionanofluids have been explored in the field of separation processes, such as the separation of rare-earth elements and precious metals. In traditional processes, organic solvents are often used for solvent extraction or precipitation, leading to the generation of toxic waste. Ionanofluids, due to their tunable properties and the possibility of adjusting the interaction between the ionic liquid and nanoparticles, can be optimized for specific separation processes, thus improving the selectivity and efficiency of separations while minimizing waste generation. Additionally, the recyclability of ionanofluids further enhances their sustainability, as they can often be reused multiple times without a significant loss in performance (Mao *et al.*, 2025).

Energy Efficiency

Ionanofluids have gained significant attention for their role in improving the energy efficiency of various processes, particularly in electrochemical reactions and energy storage applications. One of the major advantages of ionanofluids in sustainable chemistry is their ability to operate under lower energy demands, thus contributing to energy savings in industrial processes and reducing the overall environmental impact. This is especially relevant in processes that require precise temperature control or involve energy-intensive operations.

In electrochemical reactions, such as those used in batteries, fuel cells, and supercapacitors, energy efficiency is a critical concern (Raza *et al.*, 2024). Ionic liquids, due to their high ionic conductivity and thermal stability, have already demonstrated their potential to enhance the performance of electrochemical devices. When combined with nanoparticles to form ionanofluids, these systems can offer even greater advantages by improving charge transport, enhancing electrode surface interactions, and promoting better heat management. The addition of nanoparticles, particularly metal and metal oxide nanoparticles, can further improve the electrochemical performance by providing additional active sites for reactions, thereby enhancing the efficiency of energy conversion and storage (Pazhamalai *et al.*, 2024).

For instance, in fuel cells, ionanofluids have been employed as electrolytes or catalysts, replacing conventional organic electrolytes or acids, which are prone to corrosion and degradation over time. The high thermal conductivity of ionanofluids facilitates better heat management, ensuring that the system remains within optimal operating conditions and

reduces the energy required for cooling. In energy storage systems such as lithium-ion batteries, the use of ionanofluids as electrolytes can improve the cycling stability and efficiency of the battery, resulting in higher performance over longer periods (Joseph & Mathew, 2025). The addition of nanoparticles can also improve the conductivity of the electrolyte, allowing for faster charge and discharge cycles while maintaining stability and reducing energy losses.

In addition to electrochemical applications, ionanofluids have shown promise in reducing energy demands in various industrial processes, such as catalytic reactions and heat exchange systems. Their enhanced thermal conductivity, a result of the interaction between nanoparticles and the ionic liquid, allows for more efficient heat transfer, reducing the need for external heating or cooling sources. This leads to lower energy consumption and improved process efficiency, particularly in energy-intensive industries like petrochemicals, refining, and chemical manufacturing.

The incorporation of ionanofluids into sustainable energy systems holds immense potential for improving energy efficiency across various sectors, from industrial manufacturing to renewable energy applications (Hai *et al.*, 2024). By reducing the energy required for key processes, ionanofluids can contribute significantly to minimizing the environmental footprint of energy production and consumption.

Environmental Impact

The environmental impact of chemical processes is a central concern in the field of sustainable chemistry, and ionanofluids offer several advantages that contribute to reducing emissions, waste generation, and overall ecological harm (Razzaq *et al.*, 2025). Their unique properties, such as non-volatility, recyclability, and biodegradability, make them a promising solution for reducing the environmental footprint of industrial processes.

One of the primary benefits of ionanofluids in reducing environmental impact is their ability to replace toxic and volatile organic solvents that contribute to air pollution and hazardous waste generation. Conventional organic solvents are often harmful to both human health and the environment, and their disposal typically involves complex procedures to mitigate toxicity. Ionic liquids, on the other hand, are designed to be less toxic, non-volatile, and chemically stable, making them safer alternatives. The incorporation of nanoparticles into ionic liquids to form ionanofluids further enhances their environmental profile, as these systems are typically more stable and efficient, requiring less solvent and fewer chemical additives in processes (Mathew *et al.*, 2024).

Ionanofluids also contribute to reducing waste generation in catalytic processes. Traditional catalytic systems often require large amounts of solvent or produce significant amounts of waste products that must be carefully handled. The use of ionanofluids in catalytic reactions allows for better control over reaction conditions, leading to higher selectivity and reduced byproduct formation. Furthermore, ionanofluids can often be recycled and reused multiple times, minimizing waste and reducing the need for fresh solvents or reagents (Tomar & Jain, 2022). This aspect is particularly important in industrial applications, where minimizing waste

Ionanofluids as Green Catalysts

and recycling materials can significantly reduce operational expenses and environmental impact.

In addition to their role in reducing emissions and waste, ionanofluids are also being explored for their potential in sustainable energy applications. As mentioned earlier, the improved thermal conductivity and energy efficiency of ionanofluids can lead to reduced energy consumption in industrial processes, which in turn results in lower greenhouse gas emissions. By reducing the overall energy demand of chemical processes and energy storage systems, ionanofluids contribute to mitigating climate change and promoting the transition to cleaner, more sustainable energy sources.

Moreover, the environmental benefits of ionanofluids extend to their potential for biodegradability and recyclability (Gonçalves *et al.*, 2021). Many ionic liquids, particularly those based on biocompatible or renewable sources, can be designed to break down into non-toxic byproducts over time. This property is critical for ensuring that ionanofluids do not pose long-term risks to ecosystems or human health. Ongoing research is focused on developing new ionic liquids and ionanofluid systems that are not only effective in their applications but also environmentally benign and easily recyclable. The biodegradability of ionanofluids adds another layer of sustainability, ensuring that they contribute to a circular economy rather than becoming a source of persistent waste (Anadebe *et al.*, 2024).

Finally, the use of ionanofluids in environmental remediation processes, such as wastewater treatment and pollution control, further enhances their positive environmental impact. By improving the efficiency of water purification and pollutant removal, ionanofluids can help mitigate the environmental damage caused by industrial pollution and chemical contamination. The ability to tailor the properties of ionanofluids to specific contaminants allows for more targeted and efficient removal, reducing the need for harsh chemicals and minimizing the generation of secondary pollutants.

Future Directions in Sustainable Chemistry with Ionanofluids

Looking ahead, the potential for ionanofluids to play a transformative role in sustainable chemistry is vast. As the demand for more efficient, greener, and environmentally friendly chemical processes continues to rise, the development of ionanofluids will be central to achieving these goals (Mahian *et al.*, 2021). Future research will likely focus on optimizing the synthesis and properties of ionanofluids to enhance their performance in specific applications, particularly in catalysis, energy storage, and environmental remediation.

One promising area of research is the design of ionic liquids with enhanced biodegradability and minimal environmental impact. As more ionic liquids are derived from renewable resources, their environmental footprint can be reduced even further. In addition, the development of more efficient nanoparticle-ionic liquid interactions could lead to the creation of ionanofluids with improved performance in catalytic reactions, separations, and energy applications. Innovations in nanomaterials, such as functionalized nanoparticles and hybrid nanostructures, could further enhance the properties of ionanofluids, making them even more versatile and effective in sustainable chemistry (Karatrantos *et al.*, 2022).

Converging Chemical and Biological Sciences for a Sustainable Era

The integration of ionanofluids into existing industrial processes is also expected to grow. By replacing conventional solvents with ionanofluids, industries such as pharmaceuticals, petrochemicals, and bioenergy can reduce their environmental impact while improving process efficiency. The continued development of scalable and cost-effective synthesis methods for ionanofluids will be key to their widespread adoption in industrial settings.

Applications in Catalysis

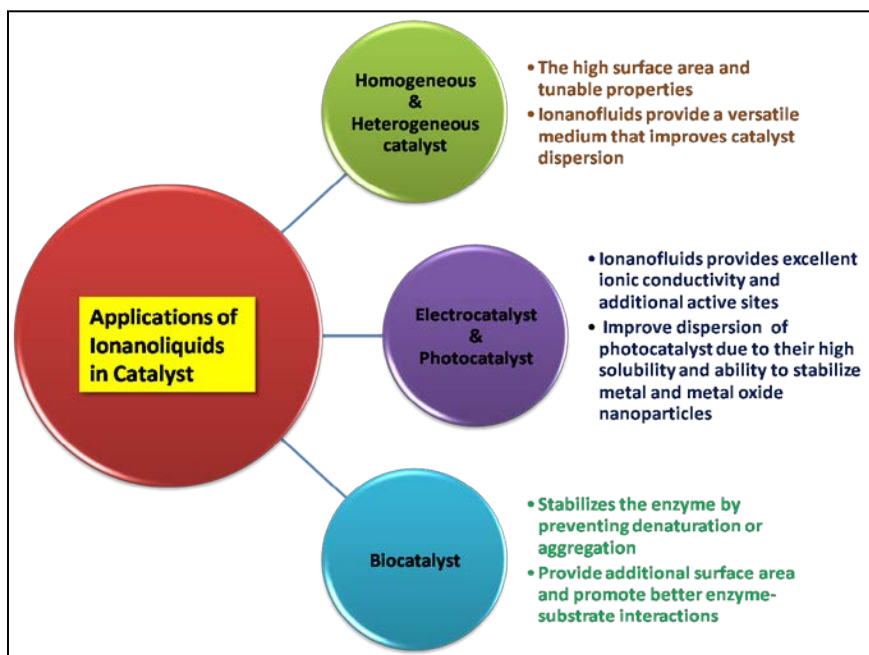


Figure 4: Represents the Different Catalytic Applications of Ionanofluids

Catalysis plays a crucial role in modern chemical industries, driving a wide range of reactions with higher selectivity and efficiency (Isahak & Al-Amiery, 2024). The integration of ionic liquids with nanoparticles to form ionanofluids offers exciting opportunities in the field of catalysis. These materials have been shown to enhance the performance of catalytic processes by improving reaction rates, selectivity, stability, and reusability. In this section, we explore the diverse applications of ionanofluids in catalytic systems, ranging from homogeneous and heterogeneous catalysis to electrocatalysis, photocatalysis, and biocatalysis (Figure 4). Additionally, we will examine their industrial applications and the advantages they offer in large-scale catalytic processes.

Homogeneous and Heterogeneous Catalysis

Ionanofluids have been found to significantly enhance both homogeneous and heterogeneous catalytic processes (Bashir *et al.*, 2024). Homogeneous catalysis typically involves a catalyst that is in the same phase as the reactants, often a liquid or solution, which enables efficient mixing and interaction with the reactants. In contrast, heterogeneous catalysis involves catalysts in a different phase, often solids, interacting with reactants in a

Ionanofluids as Green Catalysts

gas or liquid phase. The combination of ionic liquids and nanoparticles to form ionanofluids offers unique advantages in both types of catalytic systems, primarily by enhancing the reaction rates and improving the selectivity of reactions.

In homogeneous catalysis, the use of ionic liquids provides a stable environment for catalysts, often enabling reactions that are not possible or are inefficient in traditional organic solvents (Migowski, Lozano & Dupont, 2023). The incorporation of nanoparticles into the ionic liquid matrix results in the formation of ionanofluids, which further enhance the catalytic activity and stability. The high surface area and tunable properties of nanoparticles improve the interaction between the catalyst and the reactants, leading to enhanced reaction rates. Furthermore, the unique properties of ionic liquids, such as their non-volatility, low vapor pressure, and high thermal stability, make them ideal for carrying out high-temperature reactions, particularly those involving sensitive or volatile reactants.

For heterogeneous catalysis, ionanofluids provide a versatile medium that improves catalyst dispersion and enhances the efficiency of catalytic reactions (Shaari *et al.*, 2022). The nanoparticles within the ionic liquid environment allow for better interaction between the solid catalyst and reactants, promoting faster reactions and higher selectivity. Additionally, ionanofluids can be used to stabilize the catalyst, preventing deactivation or aggregation that is common in traditional solvents. The ability of ionanofluids to support both homogeneous and heterogeneous catalysis is an exciting feature, as it enables a broader range of reactions to be carried out under milder conditions, reducing the need for harsh solvents or extreme temperatures.

One key advantage of ionanofluids in catalysis is their reusability. Catalysts suspended in ionanofluids show improved stability and can be reused multiple times without significant loss in activity (Yadav, Gupta & Sharma, 2022). This capability is especially beneficial for industrial processes, where catalyst recycling can lead to reduced costs and improved sustainability. The ability to recover and reuse catalysts effectively makes ionanofluids a valuable tool for both academic research and industrial applications.

Electrocatalysis and Photocatalysis

Ionanofluids also play a critical role in electrocatalysis and photocatalysis, two important areas for energy production and environmental sustainability. Electrocatalysis involves the acceleration of electrochemical reactions, such as those used in fuel cells, batteries, and water splitting, while photocatalysis relies on light energy to drive chemical reactions, such as CO₂ reduction and water splitting (Ni *et al.*, 2023). Both fields benefit significantly from the use of ionanofluids due to the unique properties of ionic liquids and nanoparticles.

In electrocatalysis, ionanofluids are used to enhance the efficiency of reactions such as hydrogen evolution, oxygen reduction, and CO₂ reduction, all of which are vital for energy storage and renewable energy production. The ionic liquid component in ionanofluids provides excellent ionic conductivity, while the nanoparticles, often metal or metal oxide-based, enhance the electrochemical properties by providing additional active sites for reactions. For instance, ionanofluids have been used in fuel cells to improve the performance of the anode and cathode catalysts, leading to increased efficiency in energy conversion.

(Ghosh & Subudhi, 2022). The high thermal stability and low volatility of ionic liquids, combined with the conductivity-enhancing properties of nanoparticles, make ionanofluids highly effective in maintaining consistent performance in electrochemical devices.

A particularly promising application of ionanofluids is in water splitting for hydrogen production, an essential process for the development of clean hydrogen energy. Ionanofluids can facilitate both the oxygen evolution reaction (OER) and hydrogen evolution reaction (HER), which are key to efficient water splitting (Subramaniam *et al.*, 2024). The use of ionanofluids in this context enhances the reaction rates, stability, and durability of the electrocatalysts, making the process more efficient and cost-effective. The nanoparticles present in ionanofluids can improve the catalyst's surface area, while the ionic liquid can help stabilize the catalyst and prevent unwanted side reactions, leading to higher hydrogen production efficiency.

In photocatalysis, ionanofluids have been explored for their ability to enhance the dispersion and efficiency of photocatalysts (Malika & Sonawane, 2022). Photocatalysts, typically semiconductors such as titanium dioxide (TiO₂), are used in reactions like CO₂ reduction and water splitting under light irradiation. The dispersion of photocatalysts in a liquid medium is crucial for maximizing their efficiency, and ionic liquids help improve this dispersion due to their high solubility and ability to stabilize metal and metal oxide nanoparticles. Additionally, ionanofluids can be engineered to tune the properties of the photocatalyst, such as its bandgap, to improve light absorption and catalytic performance. These properties make ionanofluids an attractive medium for driving photocatalytic reactions, enabling more efficient energy conversion and environmental remediation.

Biocatalysis

Biocatalysis, the use of natural catalysts, such as enzymes, to carry out chemical reactions, is another area where ionanofluids are showing promise (Khan *et al.*, 2022). Enzymes are highly selective catalysts that operate under mild conditions, making them ideal for many industrial processes, especially those involving complex organic molecules. However, enzymes are often limited by their stability, solubility, and reusability, which can hinder their broader application in industrial catalysis. Ionanofluids offer a solution to these challenges by providing a stable and supportive environment for enzymes, thereby enhancing their performance and longevity.

In ionic liquid-nanoparticle systems, the ionic liquid stabilizes the enzyme by preventing denaturation or aggregation, while the nanoparticles provide additional surface area and promote better enzyme-substrate interactions. This results in enhanced catalytic efficiency and improved stability of the enzyme over extended use. Ionanofluids have been successfully used in various enzymatic reactions, such as the hydrolysis of polysaccharides and the synthesis of biofuels (Shahbaz *et al.*, 2022). The tunable properties of ionic liquids allow for the optimization of enzyme activity, as they can influence the polarity and viscosity of the medium, which in turn affects enzyme conformation and activity.

Case studies have demonstrated the effectiveness of ionanofluids in biotransformations. For example, in the production of biodiesel from triglycerides, enzyme-catalyzed reactions can

be enhanced by using ionanofluids as the medium (Ong *et al.*, 2021). The presence of nanoparticles can increase the surface area available for enzyme-substrate interactions, leading to faster reaction rates and improved conversion efficiencies. Additionally, the ability to recycle ionanofluids with minimal loss in activity makes them a viable option for large-scale industrial applications. This recyclability is a key advantage in reducing the overall cost of biocatalytic processes and ensuring their sustainability in the long term.

Industrial Applications

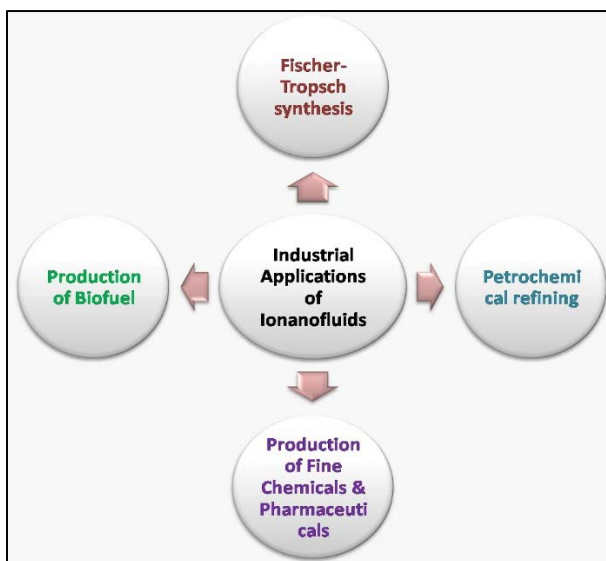


Figure 5: Represents the Various Industrial Applications

The use of ionanofluids in industrial catalysis is an exciting area of development, as they offer both economic and operational advantages in large-scale catalytic processes (Kumar *et al.*, 2022). One notable example is their application in Fischer-Tropsch synthesis, a process used to convert syngas (a mixture of carbon monoxide and hydrogen) into liquid hydrocarbons. This process is essential for producing synthetic fuels, particularly in regions where natural oil resources are limited. The use of ionanofluids in Fischer-Tropsch synthesis improves the efficiency of the reaction by enhancing the dispersion of the catalyst and providing better control over reaction conditions (Teimouri *et al.*, 2022). The high stability and non-volatility of ionic liquids also make them suitable for high-temperature catalytic processes, such as those involved in Fischer-Tropsch synthesis.

Another industrial application of ionanofluids is in petrochemical refining, where they are used to catalyze the cracking of large hydrocarbons into smaller, more valuable products (Figure 5). The presence of nanoparticles in ionanofluids improves catalyst activity and selectivity, which leads to higher yields of desired products and reduced byproduct formation. Ionanofluids also enhance heat transfer and reduce energy consumption in industrial processes, contributing to overall energy savings and improved sustainability (Elsaid *et al.*, 2021). Furthermore, the ability to recover and reuse ionanofluids multiple times

without significant loss in catalytic activity makes them cost-effective for large-scale operations.

Beyond these applications, ionanofluids have potential uses in other industrial catalytic processes, such as the production of fine chemicals, pharmaceuticals, and biofuels. In these industries, the ability to perform highly selective reactions under mild conditions is critical for improving product yields and reducing environmental impact. Ionanofluids offer a promising solution by providing a more efficient medium for catalytic reactions, reducing waste, and improving reaction efficiency (Obalalu *et al.*, 2023). Their tunable properties, high stability, and recyclability make them an attractive option for a wide range of industrial applications, helping companies reduce costs while meeting sustainability goals.

Challenges and Limitations

Despite the promising applications and benefits of ionanofluids in sustainable chemistry and catalysis, there are several challenges and limitations that need to be addressed before their widespread adoption in industrial and commercial applications (Ikeuba *et al.*, 2024). These challenges primarily include the high cost and complexity of ionic liquids, toxicity concerns, stability issues of nanoparticles within ionic liquid matrices, and scalability concerns for large-scale industrial processes. Addressing these challenges is critical for maximizing the potential of ionanofluids and ensuring their long-term viability in both research and industrial settings.

High Cost and Complexity of Ionic Liquids

One of the primary barriers to the widespread use of ionanofluids is the high cost associated with the synthesis of ionic liquids (Minea & Sohel Murshed, 2021). While ionic liquids offer exceptional properties such as low vapor pressure, high thermal stability, and tunable viscosity, the complex synthesis methods required to prepare them can be expensive. Many ionic liquids are synthesized from petrochemical feedstocks, which can drive up their production costs. Furthermore, the need for specialized equipment and precise control over reaction conditions can make the synthesis process even more costly. Although advancements in the development of more cost-effective ionic liquids are underway, the high production costs remain a significant challenge for their widespread use in industrial applications (Kaur *et al.*, 2025).

In addition to the cost of ionic liquids, the complexity of their synthesis can also limit the scalability of ionanofluids. Many ionic liquids require the use of rare or specialized chemicals, which may not be readily available in large quantities. The production of these materials in bulk at the industrial level can be difficult to achieve without significant modifications to existing manufacturing processes. To make ionanofluids a viable alternative to traditional solvents or catalytic systems, we must develop methods for producing ionic liquids on a larger scale in a cost-effective manner. Such development includes the identification of more abundant, cheaper raw materials and the optimization of synthetic routes to reduce time and cost. Without these advancements, the adoption of ionanofluids in large-scale applications will remain limited by their high production costs (Ali *et al.*, 2021).

Toxicity Concerns and Need for Greener Alternatives

Another challenge facing ionanofluids is the potential toxicity of ionic liquids. While ionic liquids are often touted as "green solvents" due to their non-volatile nature and ability to replace traditional organic solvents, some ionic liquids can be toxic or harmful to human health and the environment (Inman, Nlebedim & Prodius, 2022). The toxicity of ionic liquids depends on their chemical composition, and certain ionic liquids have been shown to exhibit adverse effects on aquatic life, soil microorganisms, and human cells. The long-term environmental impact of using ionic liquids in large-scale applications is not yet fully understood, and there is a growing concern regarding the potential for accumulation and persistence in the environment (de Jesus & Maciel Filho, 2022).

To address these concerns, research is needed to develop more environmentally benign ionic liquids that are both effective and safer for industrial use. This involves the design of ionic liquids that are biodegradable and have minimal toxicity to ecosystems. Recent efforts have focused on developing ionic liquids derived from renewable resources, such as amino acids or sugars, which may offer a more sustainable and less toxic alternative. Furthermore, the use of ionic liquids with lower toxicity profiles could enhance the environmental credentials of ionanofluids, making them more appealing for green chemistry applications (Wei *et al.*, 2021). Until safer and more eco-friendly ionic liquids are developed, the widespread adoption of ionanofluids will be hindered by these toxicity concerns.

Stability of Nanoparticles within Ionic Liquid Matrices and Scalability Issues

The stability of nanoparticles within ionic liquid matrices is another significant challenge for the practical application of ionanofluids (Hermida-Merino *et al.*, 2021). Nanoparticles play a critical role in enhancing the catalytic properties of ionanofluids by providing additional surface area and active sites for reactions. However, the long-term stability of nanoparticles in ionic liquid environments can be an issue. Nanoparticles have a tendency to agglomerate or aggregate over time, particularly in the presence of ionic liquids with high viscosity or strong solvation effects. This aggregation can lead to a decrease in the catalytic efficiency of ionanofluids, as the active surface area of the nanoparticles is reduced (Main *et al.*, 2021).

To address this challenge, researchers are exploring various stabilization techniques, such as functionalizing nanoparticles with surfactants or stabilizing agents to prevent aggregation. However, these methods can introduce additional complexities and may affect the overall performance of the ionanofluid. The development of more stable nanoparticle formulations, or the use of nanoparticles with inherent stability in ionic liquid matrices, will be essential for ensuring the long-term effectiveness of ionanofluids in catalytic processes (Ali *et al.*, 2024).

Finally, the scalability of ionanofluids for industrial applications remains a major limitation. While ionanofluids have shown promise in laboratory-scale reactions, their scalability for large-scale processes is not yet fully realized. Challenges related to the cost of production, stability of nanoparticles, and the synthesis of large quantities of suitable ionic liquids all contribute to the difficulties in scaling up ionanofluids for industrial applications. In addition, the need for specialized equipment to handle and process ionanofluids may further complicate their integration into existing industrial processes (Greer, Jacquemin & Hardacre,

2020). Overcoming these scalability issues will require the development of efficient and cost-effective manufacturing processes, as well as a better understanding of the behavior of ionanofluids in large-scale systems.

Future Perspectives

The future of ionanofluids is promising, with advancements in ionic liquid design poised to unlock new applications and optimize their performance in various fields. One area of focus is the development of ionic liquids tailored for specific applications through precision molecular engineering. By modifying the chemical structures of ionic liquids, researchers can enhance their compatibility with specific nanoparticles, improving the stability and efficiency of ionanofluids in catalysis, energy storage, or separation processes. For example, ionic liquids designed with functional groups that interact selectively with target molecules or nanoparticles could significantly enhance reaction rates and product selectivity. Additionally, there is growing interest in using renewable and bio-based resources, such as lignin derivatives or amino acids, as precursors for ionic liquid synthesis. This approach not only aligns with the principles of green chemistry but also offers a pathway to reduce the cost and environmental impact of ionic liquid production.

Integrating ionanofluids with renewable energy systems and bio-based resources represents another promising avenue for future research. In energy storage, ionanofluids can improve the efficiency of batteries, supercapacitors, and fuel cells by enhancing ion transport and reducing resistance at interfaces. Moreover, their unique properties make them well-suited for use in renewable energy processes such as solar energy harvesting, CO₂ capture, and conversion. Coupling ionanofluids with bio-based catalytic systems could open new possibilities for biotransformations in sustainable chemical production. For instance, using enzymes stabilized within ionanofluids can improve the efficiency of biomass conversion into biofuels or bioplastics. Furthermore, leveraging ionanofluids in processes such as electrochemical water splitting or CO₂ reduction could help mitigate environmental challenges by promoting the transition to a carbon-neutral economy.

Advances in computational modeling and broader applications in areas like environmental remediation and healthcare will also play a pivotal role in shaping the future of ionanofluids. Computational tools can aid in the design of tailored ionanofluid systems by predicting their physicochemical properties and interactions with specific substrates or nanoparticles. These models can significantly accelerate the development of optimized ionanofluid formulations for targeted applications, reducing reliance on trial-and-error methods in the laboratory. Additionally, ionanofluids have immense potential for broader applications beyond catalysis and sustainable chemistry. In environmental remediation, they could be employed for the extraction and recovery of heavy metals, oil spills, or persistent organic pollutants. Their ability to stabilize biological molecules in healthcare provides opportunities for drug delivery, biosensors, and advanced medical diagnostics. By focusing on these future directions, researchers can expand the applicability of ionanofluids while addressing global challenges in sustainability, energy, and healthcare.

Conclusion

Ionanofluids represent a transformative advancement in sustainable chemistry and catalysis, offering unparalleled versatility and efficiency through the synergistic integration of ionic liquids and nanoparticles. Their unique physicochemical properties, such as high thermal stability, tunable viscosity, and enhanced ionic conductivity, position them as superior alternatives to conventional solvents and catalytic systems. Ionanofluids have demonstrated remarkable potential across diverse applications, including green solvent systems, energy-efficient catalysis, and environmental remediation. By reducing emissions, minimizing waste, and supporting the transition to renewable resources, ionanofluids align with the core principles of green chemistry and sustainable industrial practices. Despite their promise, challenges such as high production costs, toxicity concerns, nanoparticle stability, and scalability hinder their broader adoption. Addressing these issues requires the development of cost-effective and eco-friendly ionic liquids, improved nanoparticle stabilization strategies, and innovative manufacturing techniques to scale up ionanofluid production. Additionally, the environmental impact and long-term safety of these materials must be thoroughly assessed to ensure their compatibility with sustainable development goals. The transformative potential of ionanofluids can only be realized through interdisciplinary research that bridges chemistry, materials science, engineering, and computational modeling. Collaborative efforts to design tailored ionanofluid systems for specific applications, integrate them with renewable energy technologies, and expand their applications in healthcare and environmental remediation will be crucial. As the field advances, ionanofluids have the potential to revolutionize catalytic processes, enhance energy efficiency, and address critical environmental challenges, paving the way for a more sustainable future. By leveraging their unique properties and addressing current limitations, ionanofluids could redefine the landscape of sustainable chemistry and catalysis, fostering innovation across industries and scientific disciplines.

Acknowledgement

The authors are thankful to all their departmental colleagues for their contribution and mental support. They also thank the Principal of the colleges for their continuous encouragement.

References

- Ali, N., Bahman, A. M., Aljuwayhel, N. F., Ebrahim, S. A., Mukherjee, S., & Alsayegh, A. (2021). Carbon-based nanofluids and their advances towards heat transfer applications – a review. *Nanomaterials*, 11(6), 1628. <https://doi.org/10.3390/nano11061628>
- Ali, S. A., Habib, K., Younas, M., Rahman, S., Das, L., Rubbi, F., ... & Reza kazemi, M. (2024). Advancements in Thermal Energy Storage: A Review of Material Innovations and Strategic Approaches for Phase Change Materials. *Energy & Fuels*, 38(20), 19336-19392. <https://doi.org/10.1021/acs.energyfuels.4c03634>
- Alqahtani, A. S. (2024). Indisputable roles of different ionic liquids, deep eutectic solvents and nanomaterials in green chemistry for sustainable organic synthesis. *Journal of Molecular Liquids*, 124469. <https://doi.org/10.1016/j.molliq.2024.124469>

- Anadebe, V. C., Chukwuike, V. I., Ebenso, E. E., & Barik, R. C. (2024). Trends and perspectives in waste-derived nanoparticles and circular economy. *Waste-Derived Nanoparticles*, 367-379. <https://doi.org/10.1016/B978-0-443-22337-2.00021-X>
- Bashir, S., Almanjahie, I. M., Ramzan, M., Cheema, A. N., Akhtar, M., & Alshahrani, F. (2024). Impact of induced magnetic field on Darcy–Forchheimer nanofluid flows comprising carbon nanotubes with homogeneous-heterogeneous reactions. *Heliyon*, 10(3). <https://doi.org/10.1016/j.heliyon.2024.e24718>
- Behera, U. S., Sangwai, J. S., & Byun, H. S. (2025). A comprehensive review on the recent advances in applications of nanofluids for effective utilization of renewable energy. *Renewable and Sustainable Energy Reviews*, 207, 114901. <https://doi.org/10.1016/j.rser.2024.114901>
- Bo, L., Zhang, X., Luo, Z., Saboori, T., Dehghan, M., Ghasemizadeh, M., ... & Mahian, O. (2022). An overview of the applications of ionic fluids and deep eutectic solvents enhanced by nanoparticles. *Journal of Thermal Analysis and Calorimetry*, 1-13. <https://doi.org/10.1007/s10973-021-11097-3>
- Chen, R., Qiao, X., & Liu, F. (2022). Ionic liquid-based magnetic nanoparticles for magnetic dispersive solid-phase extraction: A review. *Analytica Chimica Acta*, 1201. <https://doi.org/10.1016/j.aca.2022.339632>
- Das, L., Rubbi, F., Habib, K., Aslfattahi, N., Saidur, R., Saha, B. B., ... & Alqahtani, T. (2021). State-of-the-art ionic liquid & ionanofluids incorporated with advanced nanomaterials for solar energy applications. *Journal of Molecular Liquids*, 336. <https://doi.org/10.1016/j.molliq.2021.116563>
- de Jesus, S. S., & Maciel Filho, R. (2022). Are ionic liquids eco-friendly?. *Renewable and Sustainable Energy Reviews*, 157, 112039. <https://doi.org/10.1016/j.rser.2021.112039>
- Duarte, T. A., Pereira, R. F., Medronho, B., Maltseva, E. S., Krivoshapkina, E. F., Varela-Dopico, A., ... & de Zea Bermudez, V. (2024). A glance at novel ionanofluids incorporating silk-derived carbon dots. *Chemistry of Materials*, 36(3), 1136-1152. <https://doi.org/10.1021/acs.chemmater.3c01370>
- Dupont, J., Leal, B. C., Lozano, P., Monteiro, A. L., Migowski, P., & Scholten, J. D. (2024). Ionic liquids in metal, photo-, electro-, and (bio) catalysis. *Chemical Reviews*, 124(9), 5227-5420. <https://doi.org/10.1021/acs.chemrev.3c00379>
- Elsaid, K., Olabi, A. G., Wilberforce, T., Abdelkareem, M. A., & Sayed, E. T. (2021). Environmental impacts of nanofluids: A review. *Science of the Total Environment*, 763, 144202. <https://doi.org/10.1016/j.scitotenv.2020.144202>
- Ghosh, S., & Subudhi, S. (2022). Developments in fuel cells and electrochemical batteries using nanoparticles and nanofluids. *Energy Storage*, 4(3), e288. <https://doi.org/10.1002/est2.288>
- Gonçalves, A. R., Paredes, X., Cristino, A. F., Santos, F. J. V., & Queirós, C. S. (2021). Ionic liquids—A review of their toxicity to living organisms. *International Journal of Molecular Sciences*, 22(11), 5612. <https://doi.org/10.3390/ijms22115612>
- Greer, A. J., Jacquemin, J., & Hardacre, C. (2020). Industrial applications of ionic liquids. *Molecules*, 25(21), 5207. <https://doi.org/10.3390/molecules25215207>

Ionanofluids as Green Catalysts

- Hai, T., Basem, A., Alizadeh, A. A., Sharma, K., Jasim, D. J., Rajab, H., ... & Sawaran Singh, N. S. (2024). Integrating artificial neural networks, multi-objective metaheuristic optimization, and multi-criteria decision-making for improving MXene-based ionanofluids applicable in PV/T solar systems. *Scientific Reports*, 14(1).<https://doi.org/10.1038/s41598-024-81044-3>
- Hermida-Merino, C., Pardo, F., Zarca, G., Araújo, J. M., Urtiaga, A., Piñeiro, M. M., & Pereiro, A. B. (2021). Integration of stable ionic liquid-based nanofluids into polymer membranes. Part I: Membrane synthesis and characterization. *Nanomaterials*, 11(3), 607. <https://doi.org/10.3390/nano11030607>
- Hu, T., Zhang, J., Xia, J., Li, X., Tao, P., & Deng, T. (2023). A review on recent progress in preparation of medium-temperature solar-thermal nanofluids with stable dispersion. *Nanomaterials*, 13(8). <https://doi.org/10.3390/nano13081399>
- Ikeuba, A. I., Usibe, B. E., Sonde, C. U., Anozie, R. C., Edet, H. O., Obono, O. E., & Ita, B. I. (2024). Revisiting the advances on specific industrial applications of ionic liquids for a sustainable green future—a review. *Chemistry Africa*, 7(7), 3531-3548. <https://doi.org/10.1007/s42250-024-00953-y>
- Inman, G., Nlebedim, I. C., & Prodius, D. (2022). Application of ionic liquids for the recycling and recovery of technologically critical and valuable metals. *Energies*, 15(2), 628. <https://doi.org/10.3390/en15020628>
- Isahak, W. N. R. W., & Al-Amiery, A. (2024). Catalysts driving efficiency and innovation in thermal reactions: A comprehensive review. *Green Technologies and Sustainability*, 2(2), 100078.<https://doi.org/10.1016/j.grets.2024.100078>
- Joseph, A., & Mathew, S. (2025). Ionic Liquid-Based Redox Flow Batteries. In *Handbook of Energy Materials* (pp. 1-35). Singapore: Springer Nature Singapore. https://doi.org/10.1007/978-981-16-4480-1_10-1
- Joseph, A., Sobczak, J., Żyła, G., & Mathew, S. (2022). Ionic liquid and ionanofluid-based redox flow Batteries—A mini review. *Energies*, 15(13). <https://doi.org/10.3390/en15134545>
- Karatrantos, A. V., Mugemana, C., Bouhala, L., Clarke, N., & Kröger, M. (2022). From ionic nanoparticle organic hybrids to ionic nanocomposites: Structure, dynamics, and properties: A review. *Nanomaterials*, 13(1), 2. <https://doi.org/10.3390/nano13010002>
- Kaur, H., Thakur, A., Thakur, R. C., & Kumar, A. (2025). A Review on Multifaceted Role of Ionic Liquids in Modern Energy Storage Systems: From Electrochemical Performance to Environmental Sustainability. *Energy & Fuels*. <https://doi.org/10.1021/acs.energyfuels.4c05274>
- Khan, H. W., Reddy, A. V. B., Negash, B. M., Moniruzzaman, M., & Aminabhavi, T. M. (2024). Recent progress in ionic liquid-based green emulsion liquid membranes for separation of industrial discharges. *Chemical Engineering Journal*. <https://doi.org/10.1016/j.cej.2024.154309>
- Khan, R. A., Mohammed, H. A., Sulaiman, G. M., Subaiyel, A. A., Karuppaiah, A., Rahman, H., ... & Choonara, Y. E. (2022). Molecule (s) of Interest: I. Ionic Liquids—Gateway to Newer Nanotechnology Applications: Advanced Nanobiotechnical Uses', Current Status, Emerging Trends, Challenges, and Prospects. *International Journal of Molecular Sciences*, 23(22). <https://doi.org/10.3390/ijms232214346>

- Khavani, M., Mehranfar, A., & Mofrad, M. R. (2022). Effects of ionic liquids on the stabilization process of gold nanoparticles. *The Journal of Physical Chemistry B*, 126(46), 9617-9631. <https://doi.org/10.1021/acs.jpcc.2c05878>
- Khoramian, R., Issakhov, M., Pourafshary, P., Gabdullin, M., & Sharipova, A. (2024). Surface modification of nanoparticles for enhanced applicability of nanofluids in harsh reservoir conditions: A comprehensive review for improved oil recovery. *Advances in Colloid and Interface Science*, 333. <https://doi.org/10.1016/j.cis.2024.103296>
- Kulshrestha, A., Kumar, R., & Sharma, K. P. (2024). Efficient carbon capture and mineralization using porous liquids comprising hollow nanoparticles and enzymes dispersed in fatty acid-based ionic liquids. *ACS Sustainable Chemistry & Engineering*, 12(15), 5799-5808. <https://doi.org/10.1021/acssuschemeng.3c07182>
- Kumar, L. H., Kazi, S. N., Masjuki, H. H., & Zubir, M. N. M. (2022). A review of recent advances in green nanofluids and their application in thermal systems. *Chemical Engineering Journal*, 429. <https://doi.org/10.1016/j.cej.2021.132321>
- Lee, M., Kim, H., Hussain, Z., & Cho, H. (2025). Absorption and regeneration performance for waste refrigerant using [HMIM][Tf2N] ionic liquid and 0.5 wt% MWCNT-[HMIM][Tf2N] ionanofluid. *Applied Thermal Engineering*, 262. <https://doi.org/10.1016/j.applthermaleng.2024.125249>
- Li, R., Mbonu, C., & Akcora, P. (2025). Structure-Dependent Ionic Conductivity in Poly (Ionic Liquid)-b-Poly (methyl methacrylate)-Grafted Nanoparticles. *ACS Applied Polymer Materials*, 7(6), 3853-3862. <https://doi.org/10.1021/acsapm.5c00070>
- Madheswaran, D. K., Vengatesan, S., Varuvel, E. G., Praveenkumar, T., Jegadheeswaran, S., Pugazhendhi, A., & Arulmozhiwarman, J. (2023). Nanofluids as a coolant for polymer electrolyte membrane fuel cells: recent trends, challenges, and future perspectives. *Journal of Cleaner Production*, 424. <https://doi.org/10.1016/j.jclepro.2023.138763>
- Mahian, O., Bellos, E., Markides, C. N., Taylor, R. A., Alagumalai, A., Yang, L., ... & Wongwises, S. (2021). Recent advances in using nanofluids in renewable energy systems and the environmental implications of their uptake. *Nano Energy*, 86. <https://doi.org/10.1016/j.nanoen.2021.106069>
- Main, K. L., Eberl, B. K., McDaniel, D., Tikadar, A., Paul, T. C., & Khan, J. A. (2021). Nanoparticles size effect on thermophysical properties of ionic liquids based nanofluids. *Journal of Molecular Liquids*, 343. <https://doi.org/10.1016/j.molliq.2021.117609>
- Malika, M., & Sonawane, S. S. (2022). The sono-photocatalytic performance of a Fe₂O₃ coated TiO₂ based hybrid nanofluid under visible light via RSM. *Colloids and Surfaces A: Physicochemical and Engineering Aspects*, 641. <https://doi.org/10.1016/j.colsurfa.2022.128545>
- Mao, S. X., Huang, S. Y., Feng, T., Pang, J. Y., Dang, D. B., & Bai, Y. (2025). Enhanced oxidative desulfurization using carboxylic functionalized poly (ionic liquid)/polyoxomolybdates with double terminal oxygen active sites. *Separation and Purification Technology*, 362. <https://doi.org/10.1016/j.seppur.2025.131617>
- Mathew, H. T., Abhisek, K., Vhatkar, S. S., Kumar, A., & Oraon, R. (2024). Ionic Liquids as Green Solvents: Are Ionic Liquids Nontoxic and Biodegradable?. *Handbook of Ionic Liquids: Fundamentals, Applications, and Sustainability*, 69-96. <https://doi.org/10.1002/9783527839520.ch4>

Ionanofluids as Green Catalysts

- Migowski, P., Lozano, P., & Dupont, J. (2023). Imidazolium based ionic liquid-phase green catalytic reactions. *Green Chemistry*, 25(4), 1237-1260. <https://doi.org/10.1039/D2GC04749G>
- Minea, A. A., & Soheli Murshed, S. M. (2021). Ionic liquids-based nanocolloids—A review of progress and prospects in convective heat transfer applications. *Nanomaterials*, 11(4). <https://doi.org/10.3390/nano11041039>
- Mondal, A., Kundu, A. K., & Mandal, P. Applications of Green Solvents for the Development of Sustainable Chemical Process. <https://doi.org/10.31674/book.2024ecc.008>
- Moosavi, M., Torkzadeh, M., & Akbarinezhad, Z. (2024). Molecular dynamics investigation of ionanofluids (INFs): Towards a deeper understanding of their thermophysical, structural and dynamical properties. *Journal of Molecular Liquids*, 399. <https://doi.org/10.1016/j.molliq.2024.124355>
- Moulefera, I., Marín, J. D., Cascales, A., Montalbán, M. G., Alarcón, M., & Villora, G. (2025). Innovative application of graphene nanoplatelet-based ionanofluids as heat transfer fluid in hybrid photovoltaic-thermal solar collectors. *Scientific Reports*, 15(1). <https://doi.org/10.1038/s41598-025-91040-w>
- Ni, J., Wen, Y., Pan, D., Bai, J., Zhou, B., Zhao, S., ... & Zeng, Q. (2023). Light-driven simultaneous water purification and green energy production by photocatalytic fuel cell: A comprehensive review on current status, challenges, and perspectives. *Chemical Engineering Journal*, 473. <https://doi.org/10.1016/j.cej.2023.145162>
- Obalalu, A. M., Ahmad, H., Salawu, S. O., Olayemi, O. A., Odetunde, C. B., Ajala, A. O., & Abdulraheem, A. (2023). Improvement of mechanical energy using thermal efficiency of hybrid nanofluid on solar aircraft wings: an application of renewable, sustainable energy. *Waves in Random and Complex Media*, 1-30. <https://doi.org/10.1080/17455030.2023.2184642>
- Ong, H. C., Tiong, Y. W., Goh, B. H. H., Gan, Y. Y., Mofijur, M., Fattah, I. R., ... & Mahlia, T. M. I. (2021). Recent advances in biodiesel production from agricultural products and microalgae using ionic liquids: Opportunities and challenges. *Energy Conversion and Management*, 228. <https://doi.org/10.1016/j.enconman.2020.113647>
- Paul, T. C., Tikadar, A., Mahamud, R., Salman, A. S., Morshed, A. M., & Khan, J. A. (2021). A critical review on the development of ionic liquids-based nanofluids as heat transfer fluids for solar thermal energy. *Processes*, 9(5). <https://doi.org/10.3390/pr9050858>
- Pazhamalai, P., Krishnan, V., Mohamed Saleem, M. S., Kim, S. J., & Seo, H. W. (2024). Investigating composite electrode materials of metal oxides for advanced energy storage applications. *Nano Convergence*, 11(1), 30. <https://doi.org/10.1186/s40580-024-00437-2>
- Pereira, J., Souza, R., & Moita, A. (2024). A review of ionic liquids and their composites with nanoparticles for electrochemical applications. *Inorganics*, 12(7). <https://doi.org/10.3390/inorganics12070186>
- Rahman, M. A., Hasnain, S. M., Pandey, S., Tapalova, A., Akyzbekov, N., & Zairov, R. (2024). Review on nanofluids: preparation, properties, stability, and thermal performance augmentation in heat transfer applications. *Acs Omega*, 9(30), 32328-32349. <https://doi.org/10.1021/acsomega.4c03279>

- Raza, S., Hayat, A., Bashir, T., Chen, C., Shen, L., Orooji, Y., & Lin, H. (2024). Electrochemistry of 2D-materials for the remediation of environmental pollutants and alternative energy storage/conversion materials and devices, a comprehensive review. *Sustainable Materials and Technologies*.<https://doi.org/10.1016/j.susmat.2024.e00963>
- Razzaq, I., Xinhua, W., Rasool, G., Sun, T., Shflot, A. S., Malik, M. Y., ... & Ali, A. (2025). Nanofluids for advanced applications: a comprehensive review on preparation methods, properties, and environmental impact. *ACS Omega*, 10(6), 5251-5282.<https://doi.org/10.1021/acsomega.4c10143>
- Shaari, N., Ahmad, N. N. R., Bahru, R., & Leo, C. P. (2022). Ionic liquid-modified materials as polymer electrolyte membrane and electrocatalyst in fuel cell application: An update. *International Journal of Energy Research*, 46(3), 2166-2211. <https://doi.org/10.1002/er.7362>
- Shahbaz, A., Hussain, N., Saleem, M. Z., Saeed, M. U., Bilal, M., & Iqbal, H. M. (2022). Nanoparticles as stimulants for efficient generation of biofuels and renewables. *Fuel*, 319.<https://doi.org/10.1016/j.fuel.2022.123724>
- Subramaniam, T., Idris, M. B., Suganthi, K. S., Rajan, K. S., & Devaraj, S. (2024). Mitigating hydrogen evolution reaction and corrosion of zinc in electrically rechargeable zinc-air batteries using nanofluid electrolytes. *Journal of Energy Storage*, 81. <https://doi.org/10.1016/j.est.2024.110457>
- Swapna, M. N. S., Tripon, C., Farcas, A., Dadarlat, D. N., Korte, D., & Sankararaman, S. I. (2024). Tuning the Dynamic Thermal Parameters of Nanocarbon Ionanofluids: A Photopyroelectric Study. *C*, 10(2), 40.<https://doi.org/10.3390/c10020040>
- Teimouri, Z., Borugadda, V. B., Dalai, A. K., & Abatzoglou, N. (2022). Application of computational fluid dynamics for modeling of Fischer-Tropsch synthesis as a sustainable energy resource in different reactor configurations: A review. *Renewable and Sustainable Energy Reviews*, 160. <https://doi.org/10.1016/j.rser.2022.112287>
- Tomar, P., & Jain, D. (2022). A review of green solvent IONIC liquids: as a future solvent. *Journal of Advanced Scientific Research*, 13(06), 1-16. <https://doi.org/10.55218/JASR.202213601>
- Ullah, N., Haseeb, A., & Tuzen, M. (2024). Application of recently used green solvents in sample preparation techniques: A comprehensive review of existing trends, challenges, and future opportunities. *Critical reviews in analytical chemistry*, 54(8), 2714-2733. <https://doi.org/10.1080/10408347.2023.2197495>
- Urmi, W. T., Rahman, M. M., Kadirgama, K., Ramasamy, D., & Maleque, M. A. (2021). An overview on synthesis, stability, opportunities and challenges of nanofluids. *Materials Today: Proceedings*, 41, 30-37.<https://doi.org/10.1016/j.matpr.2020.10.998>
- Vishwakarma, R., Kumar, A., Behera, K., & Trivedi, S. (2025). Novel and innovative ionic liquid-based electrolytes and their applications. In *Deep Eutectic Solvents* (pp. 199-214). Elsevier.<https://doi.org/10.1016/B978-0-443-21962-7.00007-9>
- Wang, Y., Wei, Z., Ji, T., Bai, R., & Zhu, H. (2024). Highly Ionic Conductive, Stretchable, and Tough Ionogel for Flexible Solid-State Supercapacitor. *Small*, 20(20).<https://doi.org/10.1002/smll.202307019>

Ionanofluids as Green Catalysts

- Wei, P., Pan, X., Chen, C. Y., Li, H. Y., Yan, X., Li, C., ... & Yan, B. (2021). Emerging impacts of ionic liquids on eco-environmental safety and human health. *Chemical Society Reviews*, 50(24), 13609-13627. <https://doi.org/10.1039/D1CS00946J>
- Xu, X., Weng, K., Lu, X., Zhang, Y., Zhu, S., & Zou, D. (2024). Functional thermal fluids and their applications in battery thermal management: A comprehensive review. *Journal of Energy Chemistry*. <https://doi.org/10.1016/j.jechem.2024.02.054>
- Yadav, P., Gupta, S. M., & Sharma, S. K. (2022). A review on stabilization of carbon nanotube nanofluid. *Journal of Thermal Analysis and Calorimetry*, 147(12), 6537-6561. <https://doi.org/10.1007/s10973-021-10999-6>
- Yang, L., He, R., Chai, J., Qi, X., Xue, Q., Bi, X., ... & Cabot, A. (2025). Synthesis Strategies for High Entropy Nanoparticles. *Advanced Materials*, 37(1). <https://doi.org/10.1002/adma.202412337>
- Zhang, X., Zhang, J., Yin, J., Liu, X., Qiu, W., He, J., ... & Li, H. (2025). Mo-MOF-based ionanofluids for highly efficient extraction coupled catalytic oxidative desulfurization. *Separation and Purification Technology*, 353. <https://doi.org/10.1016/j.seppur.2024.128289>

Review on Spectroscopic Studies of the Binding Interactions between Serum Albumins and Quercetin

Sugata Samanta

Department of Chemistry, The Bhawanipur Education Society College, Kolkata 700020, West Bengal, India

Corresponding Author's E-mail: sugata.samanta@thebges.edu.in

Abstract

Quercetin is known as a prevalent bioactive flavonoid derived from plants. It is recognised for its anti-tumour and anti-cancer properties, along with other important therapeutic effects. The interaction between serum albumins and quercetin was explored, and association constants were calculated by monitoring the absorption spectra of quercetin. The effect on the emission intensities of serum albumins with the addition of quercetin was examined. Time-resolved emission studies of serum albumins with the addition of quercetin indicate a reduction in average lifetime, which suggests quercetin may bind with tryptophan and the potential for energy transfer from tryptophan to quercetin in the excited state.

Keywords: *Energy Transfer; Serum Albumin; Tryptophan; Quercetin*

Introduction

Plants of higher genera contain flavonoids, a significant class of naturally occurring bioactive polyphenolics (Wu *et al.*, 2023). Flavonoids have recently attracted a lot of attention due to two main factors: Their biological and pertinent therapeutic uses, such as against cancer, tumours, and AIDS. Allergies, inflammation, etc., are the first intriguing features (Scalia & Mezzena, 2009). Numerous studies have examined flavonoids' antioxidative properties. Quercetin (3, 3', 4', 5, 7- Pentahydroxy flavone), one of the most prevalent naturally occurring flavonoids, has been shown to suppress the actions of DNA topoisomerases, phosphorylase kinase, tyrosine, and phosphatidylinositol 3-kinase (Russo *et al.*, 2014; Das, Majumder & Saha, 2017). Unusual fluorescence emission properties of quercetin, along with their dual emission nature, broad Stokes shifts, and reactivity of different emission parameters towards the surrounding medium (like pH, temperature, hydrogen bond, polarity etc.), constitute their many intriguing features (Waychunas 2014; Ding, Peng & Peng, 2016; Munoz *et al.*, 2016).

Often referred to as transport proteins, serum albumins are widely distributed in blood plasma (Steinhardt, Krijn & Leidy, 1971). They serve as carriers for a variety of endogenous and foreign substances and are repeatedly circulated throughout the body. HSA (Human serum albumin) and BSA (Bovine serum albumin) are the two most often researched albumins. Very strong conformational flexibility to a wide range of ligands is possessed by both HAS and BSA (Siddiqui *et al.*, 2021). In ligand protein binding studies and the in vivo effects of drug and other metabolite binding to serum albumins, three primary methods have been used: absorption, fluorescence, and time-resolved emission studies (Kumar &

Buranaprapuk, 1999; Abaskharon & Gai, 2016; Mishra *et al.*, 2005). These investigations have led to the molecular-level reporting of data on the binding mechanism of numerous exogenous ligands, including metals, amino acids, bilirubin, long-chain fatty acids etc (Bertoza *et al.*, 2018; Chen *et al.*, 2007). Moreover, it was suggested that this type of binding can make ligands more soluble and that certain ligands become less toxic when they connect to albumins (Sengupta & Sengupta, 2002).

Low tryptophan and high cystine levels are typical characteristics of albumins. Tryptophan content is the primary difference between HSA and BSA. Human serum albumin has one tryptophan group at position 214, whereas bovine serum albumin has two tryptophan groups at sites 134 and 212 (Steinhardt, Krijn & Leidy, 1971; Siddiqui *et al.*, 2021). In this review, the binding constants for quercetin associated with HSA and BSA have been investigated utilising the energy transfer and fluorescence quenching experiments and determining the most likely location for quercetin binding with proteins.

Methodology

Steady State Absorption and Emission Studies

The steady-state absorption and emission spectra of free serum albumins, with varying concentrations of quercetin added, have been analysed (Rehman *et al.*, 2015). Using tryptophan as a reference, the quantum yields for both the HSA and BSA were calculated (Ameen *et al.*, 2020). All protein solutions were excited at the wavelength 290 nm while keeping the absorbance nearly constant, and the steady-state emission spectra were drawn from the wavelength 300 nm to 500 nm.

Time Resolved Emission Studies

Fluorescence lifetime measurements have been conducted for both the albumins with and without the addition of quercetin (Berezin *et al.*, 2008). The time-resolved emission decays were found to be multi-exponential, assessed using reduced χ^2 values and randomly distributed residuals among the various data channels.

Results and Discussion

There was a noticeable red shift in the quercetin absorption spectra when either HSA or BSA was present (Zsila, Bikádi & Simonyi, 2003). The spectroscopic changes suggest the forming of a complex between quercetin and albumins according to the given equation (Equation 1).



The binding constant (K) is calculated using Equation 2.

$$K = \frac{[\text{complex}]}{[\text{SA}][\text{quercetin}]^n}. \quad (2)$$

Here, [SA] is the concentration of serum albumin, and n represents binding sites in the complex of quercetin and albumins. The changes in absorbance value (ΔA) were monitored at various quercetin strengths and plotted using the Scatchard Equation 3 at the wavelength where the absorbance of unbound quercetin and albumins is at its lowest and the absorbance changes the most upon binding. As a result, ΔA for HSA and BSA were measured at 425 nm, and 406 nm respectively.

$$\frac{1}{\Delta A} = \frac{1}{n\Delta\epsilon[\text{SA}]} + \frac{1}{n\Delta\epsilon K[\text{SA}][\text{quercetin}]} \quad (3)$$

Here, [SA] is the concentration of serum albumins, and $\Delta\epsilon$ represents the molar extinction coefficient for quercetin forming complexes with HSA and BSA at 425nm and 406nm respectively.

Accordingly, the binding sites (n) and binding constant (K) for quercetin's binding to HSA were found to be $3.1 \times 10^4 \text{ M}^{-1}$, and 1.1 respectively. Similar experiments were carried out for BSA also and the binding constant (K) was found to be $3.5 \times 10^4 \text{ M}^{-1}$ and n was 1.0. The extinction coefficients were obtained as $1.6 \times 10^4 \text{ M}^{-1}\text{cm}^{-1}$ and $1.01 \times 10^4 \text{ M}^{-1}\text{cm}^{-1}$ for quercetin bound HSA, and BSA at 406 nm respectively (Mishra *et al.*, 2005). These values were utilised in all subsequent computations.

The fluorescence quantum yields were calculated to be 0.053 and 0.101 for HSA and BSA, respectively. As BSA has two tryptophan groups, its fluorescence quantum yield is almost doubled. The protein fluorescence was decreased in the presence of quercetin and the binding constant (K) was estimated using this fluorescence quenching. Solutions containing 2.5 to 20 mM quercetin and 30 mM serum albumin at pH 7.5 were stimulated at the wavelength 290 nm for these studies, and emission spectra were recorded in the range of 300-500 nm. It was predicted that a portion of light is directly absorbed by quercetin at concentrations above 20 mM because it has own absorption at around 290 nm. As a result, the excited states of the albumins were less populated, which decreases the fluorescence intensity of proteins. Therefore, measurement of binding constants did not use the data above 20 mM. The fluorescence measurement of Human serum albumin (HSA) with varying strengths of quercetin was carried out. The emission intensity of HSA at around 345 nm lowers when quercetin is added. Monitoring this quenching of fluorescence intensity at 345 nm, binding sites (n) and binding constant (K) were calculated using the following Equation 4 (Mohammadi *et al.*, 2009).

$$\log\left(\frac{F_0 - F}{F}\right) = \log K + n \log[\text{quercetin}] \quad (4)$$

Here, F_0 and F are the fluorescence intensities of albumin, without and with the presence of varying strengths of quercetin, respectively. When $\log (F_0 - F)/F$ vs. $\log(\text{quercetin})$ was plotted, it was found to be linear in nature (He *et al.*, 2008). Based on this, K and n were calculated for both the proteins using equation 4. For HSA the K value was $2.3 \times 10^4 \text{ M}^{-1}$, and n was 1.10, whereas in the case of BSA the results changed to $4.9 \times 10^4 \text{ M}^{-1}$ and 1.19, respectively. According to this observation, quercetin attaches in a single location to both the HSA and BSA. Although they differ significantly from those for BSA, the binding constant

found above using both the absorption and fluorescence techniques matches closely for HSA.

This is because BSA contains two tryptophan moieties. When quercetin is attached to BSA, it quenches one of the two tryptophan's emission, and the other one remains undisturbed. This results in mistakes when estimating the binding constant for BSA using the fluorescence approach. Such errors are not anticipated in the case of HSA because there is only one tryptophan molecule present, and the fluorescence quenching is indicative of binding close to tryptophan alone. Further research was carried out on the potential for excited state energy transfer from tryptophan to quercetin (Sengupta & Sengupta, 2002).

Because the fluorescence spectra of tryptophan of human serum albumin significantly overlaps with absorption spectra of quercetin, the reduction in tryptophan emission might be attributed to either the inner filter effect or the static quenching of tryptophan's emission by quercetin. The possible energy transfer precisely from the tryptophan moiety to quercetin in the excited state could not be ruled out (dynamic quenching) (Siddiqui *et al.*, 2019).

Time resolved fluorescence studies were performed to confirm this observation. Both HSA and BSA were subjected to time resolved fluorescence lifetime studies with and without quercetin. 30 mM protein solutions were prepared for this experiment. All the solutions were stimulated at the wavelength of 290 nm, and the emission intensities were measured at 345 nm. Time resolved emission decays for both the HSA and BSA were found to fit multi exponential function. HSA exhibits a biexponential fit with an average lifetime (τ_0) of 4.76 ns [6.33 ns (61.0%), and 2.34 ns (39.0%)], while BSA shows triple exponential decay with τ_0 value 5.95 ns [7.21 ns (65.0%), 3.84 ns (32.5%), and 0.13 ns (2.5%)].

The fluorescence lifetime (τ_0) for both the albumins was decreased after the addition of 30 mM quercetin. The average lifetime of HSA decreases to 3.745 ns [5.87 ns (44.6%), and 2.02 ns (55.4%)] after addition of quercetin (Mishra *et al.*, 2005). It is evident that both the components decrease, and the decay stays biexponential. These results indicate that quercetin binds closely to the tryptophan and the potential for excited state energy transfer between tryptophan and quercetin.

Conclusion

The binding sites (n) and binding constant (K) for the interaction between quercetin and both the proteins were ascertained by means of absorption and fluorescence spectroscopy. For both the systems, single binding sites and binding constants in the order of 10^4 M^{-1} were determined. The elevated K values indicate that quercetin ties up with bioactive sites of proteins. For HSA, there is a good agreement between the results obtained from the absorption and fluorescence studies, but for BSA, as two tryptophan are there, the values diverge by an order of magnitude. In the presence of quercetin, the average lifetimes (τ_0) decrease, and the protein fluorescence exhibits multi exponential decay, according to the time resolved fluorescence lifetime experiments. Based on these findings, it is proposed that the single tryptophan is the most likely location for quercetin to bind in HSA.

Acknowledgement

The author would like to express his deepest gratitude to the supervisor, late Prof. Sanjib Ghosh, for his guidance and inspiration and special thanks to the management of The Bhawanipur Education Society College, Kolkata, India, for providing the research facilities.

References

- Abaskharon, R. M., & Gai, F. (2016). Direct measurement of the tryptophan-mediated photocleavage kinetics of a protein disulfide bond. *Physical Chemistry Chemical Physics*, 18(14), 9602-9607. <https://doi.org/10.1039/C6CP00865H>
- Ameen, F., Siddiqui, S., Jahan, I., Nayeem, S. M., ur Rehman, S., & Tabish, M. (2020). A detailed insight into the interaction of memantine with bovine serum albumin: A spectroscopic and computational approach. *Journal of Molecular Liquids*, 303, 112671. <https://doi.org/10.1016/j.molliq.2020.112671>
- Berezin, M. Y., Lee, H., Akers, W., Nikiforovich, G., & Achilefu, S. (2008, February). Fluorescent lifetime of near infrared dyes for structural analysis of serum albumin. In *Molecular Probes for Biomedical Applications II* (Vol. 6867, pp. 257-267). SPIE. <https://doi.org/10.1117/12.769262>
- Bertoza, L. D. C., Tavares Neto, E., Oliveira, L. C. D., & Ximenes, V. F. (2018). Oxidative alteration of Trp-214 and Lys-199 in human serum albumin increases binding affinity with phenylbutazone: A combined experimental and computational investigation. *International Journal of Molecular Sciences*, 19(10), 2868. <https://doi.org/10.3390/ijms19102868>
- Chen, J., Song, G., He, Y., & Yan, Q. (2007). Spectroscopic analysis of the interaction between bilirubin and bovine serum albumin. *Microchimica Acta*, 159, 79-85. <https://doi.org/10.1007/s00604-007-0736-9>
- Das, A., Majumder, D., & Saha, C. (2017). Correlation of binding efficacies of DNA to flavonoids and their induced cellular damage. *Journal of Photochemistry and Photobiology B: Biology*, 170, 256-262. <https://doi.org/10.1016/j.jphotobiol.2017.04.019>
- Ding, F., Peng, W., & Peng, Y. K. (2016). Biophysical exploration of protein–flavonol recognition: effects of molecular properties and conformational flexibility. *Physical Chemistry Chemical Physics*, 18(17), 11959-11971. <https://doi.org/10.1039/C5CP07754K>
- He, Y., Wang, Y., Tang, L., Liu, H., Chen, W., Zheng, Z., & Zou, G. (2008). Binding of puerarin to human serum albumin: a spectroscopic analysis and molecular docking. *Journal of Fluorescence*, 18(2), 433-442. <https://doi.org/10.1007/s10895-007-0283-0>
- Kumar, C. V., & Buranaprapuk, A. (1999). Tuning the selectivity of protein photocleavage: spectroscopic and photochemical studies. *Journal of the American Chemical Society*, 121(17), 4262-4270. <https://pubs.acs.org/doi/abs/10.1021/ja9844377>
- Mishra, B., Barik, A., Priyadarsini, K. I., & Mohan, H. (2005). Fluorescence spectroscopic studies on binding of a flavonoid antioxidant quercetin to serum albumins. *Journal of Chemical Sciences*, 117, 641-647. <https://doi.org/10.1007/BF02708293>
- Mohammadi, F., Bordbar, A. K., Divsalar, A., Mohammadi, K., & Saboury, A. A. (2009). Analysis of binding interaction of curcumin and diacetylcurcumin with human and bovine serum albumin using fluorescence and circular dichroism spectroscopy. *The Protein Journal*, 28, 189-196. <https://doi.org/10.1007/s10930-009-9184-1>

Serum Albumin–Quercetin Binding Review

- Munoz, V. A., Ferrari, G. V., Sancho, M. I., & Montaña, M. P. (2016). Spectroscopic and thermodynamic study of chrysin and quercetin complexes with Cu (II). *Journal of Chemical & Engineering Data*, 61(2), 987-995. <https://doi.org/10.1021/acs.jced.5b00837>
- Rehman, S. U., Sarwar, T., Husain, M. A., Ishqi, H. M., & Tabish, M. (2015). Studying non-covalent drug–DNA interactions. *Archives of Biochemistry and Biophysics*, 576, 49-60. <https://doi.org/10.1016/j.abb.2015.03.024>
- Russo, G. L., Russo, M., Spagnuolo, C., Tedesco, I., Bilotto, S., Iannitti, R., & Palumbo, R. (2014). Quercetin: a pleiotropic kinase inhibitor against cancer. *Advances in Nutrition and Cancer*, 185-205. https://doi.org/10.1007/978-3-642-38007-5_11
- Scalia, S., & Mezzena, M. (2009). Incorporation of quercetin in lipid microparticles: Effect on photo- and chemical-stability. *Journal of Pharmaceutical and Biomedical Analysis*, 49(1), 90-94. <https://doi.org/10.1016/j.jpba.2008.10.011>
- Sengupta, B., & Sengupta, P. K. (2002). The interaction of quercetin with human serum albumin: a fluorescence spectroscopic study. *Biochemical and Biophysical Research Communications*, 299(3), 400-403. [https://doi.org/10.1016/S0006-291X\(02\)02667-0](https://doi.org/10.1016/S0006-291X(02)02667-0)
- Siddiqui, S., Ameen, F., Jahan, I., Nayeem, S. M., & Tabish, M. (2019). A comprehensive spectroscopic and computational investigation on the binding of the anti-asthmatic drug triamcinolone with serum albumin. *New Journal of Chemistry*, 43(10), 4137-4151. <https://doi.org/10.1039/C8NJ05486J>
- Siddiqui, S., Ameen, F., ur Rehman, S., Sarwar, T., & Tabish, M. (2021). Studying the interaction of drug/ligand with serum albumin. *Journal of Molecular Liquids*, 336, 116200. <https://doi.org/10.1016/j.molliq.2021.116200>
- Steinhardt, J., Krijn, J., & Leidy, J. G. (1971). Differences between bovine and human serum albumins. Binding isotherms, optical rotatory dispersion, viscosity, hydrogen ion titration, and fluorescence effects. *Biochemistry*, 10(22), 4005-4015. <https://pubs.acs.org/doi/pdf/10.1021/bi00798a001>
- Waychunas, G. A. (2014). Luminescence spectroscopy. *Reviews in Mineralogy and Geochemistry*, 78(1), 175-217. <https://doi.org/10.2138/rmg.2014.78.5>
- Wu, J., Lv, S., Zhao, L., Gao, T., Yu, C., Hu, J., & Ma, F. (2023). Advances in the study of the function and mechanism of the action of flavonoids in plants under environmental stresses. *Planta*, 257(6), 108. <https://doi.org/10.1007/s00425-023-04136-w>
- Zsila, F., Bikádi, Z., & Simonyi, M. (2003). Probing the binding of the flavonoid, quercetin to human serum albumin by circular dichroism, electronic absorption spectroscopy and molecular modelling methods. *Biochemical Pharmacology*, 65(3), 447-456. [https://doi.org/10.1016/S0006-2952\(02\)01521-6](https://doi.org/10.1016/S0006-2952(02)01521-6)

From Fossil Fuels to Blue-Green Energy: A New Era for Sustainability

Suchandra Chatterjee

Department of Chemistry, Surendranath College, Kolkata 700009, West Bengal, India

Corresponding Author's E-mail: chatterjeesuchandra01@gmail.com

Abstract

The accelerating global demand for sustainable energy has spurred substantial research into low- and zero-carbon energy carriers. Among these, green hydrogen, produced through water electrolysis powered by renewable energy, and blue ammonia, synthesised from hydrogen with Carbon Capture and Storage (CCS), have emerged as promising candidates. This review paper examines the current state of technology, recent advancements, economic benefits, policy support, and future outlook for these two energy vectors. The first half of the paper analyses green hydrogen's production methods, integration with renewables, and prospective applications in sectors ranging from transportation to industrial processes. The second section delves into blue ammonia, focusing on its production processes, benefits as an energy carrier, and comparative advantages over conventional fuels. In addition, a section dedicated to a comparative analysis discusses the trade-offs between the two systems regarding cost, scalability, environmental impacts, and infrastructure requirements. Finally, challenges, policy frameworks, and avenues for future research are discussed, providing a holistic view of the potential role of blue ammonia and green hydrogen in decarbonised energy systems. By synthesising the recent literature and development trends, the review outlines the crucial steps needed to transition from experimental research to commercially viable, sustainable energy solutions.

Keywords: *Blue Ammonia; Decarbonisation; Green Hydrogen; Sustainable Energy*

Introduction

Global energy systems have long relied on fossil fuels, which present significant challenges related to environmental degradation, economic instability, and geopolitical tensions. Considering these challenges, policymakers, researchers, and industry leaders are increasingly turning their attention to renewable and sustainable alternatives. Within this context, low-carbon energy carriers such as green hydrogen and blue ammonia offer promising pathways for achieving decarbonisation. Green hydrogen, produced through the electrolysis of water using renewable sources such as solar or wind power, represents a versatile energy vector that can substitute traditional fossil fuels in multiple sectors. At the same time, blue ammonia, a compound derived from hydrogen and nitrogen, where hydrogen is produced with CCS to minimise carbon emissions, provides an alternative mode of energy storage and transportation. Both technologies have captured widespread attention due to their dual potential: they not only offer solutions for energy storage and grid balancing but also hold promise for use in hard-to-decarbonise sectors, including heavy industry and transportation (Ahmed *et al.*, 2024).

Converging Chemical and Biological Sciences for a Sustainable Era

Transitioning to Blue-Green Energy: A Sustainable Future

The present review critically assesses the technological advancements, practical applications, economic implications, and policy measures concerning green hydrogen and blue ammonia. Although both are viewed as complementary solutions in the broader hydrogen economy, each comes with distinctive advantages and challenges.

The review is structured as follows. Section 2 discusses the fundamentals and recent developments in green hydrogen production and applications. Section 3 addresses blue ammonia, detailing its production processes and emerging applications. Section 4 provides a comparative analysis of the two approaches. Section 5 explores the economic benefits and policy support for these technologies, while Section 6 highlights the key challenges, research gaps, and future perspectives. Finally, Section 7 offers concluding remarks and recommendations for moving forward with renewable energy integration. This detailed investigation is intended to serve as a resource for policymakers, industry stakeholders, and researchers who are navigating the transition from fossil-based systems to a more sustainable, renewable energy landscape (Adeli *et al.*, 2023).

Green Hydrogen: Production, Advancements and Applications

Background and Definition

Green hydrogen refers to hydrogen gas produced via the electrolysis of water where the electricity required in the process is sourced entirely from renewable energy, such as wind, solar, or hydropower. Unlike conventional hydrogen production from natural gas (steam methane reforming) or coal gasification, which releases significant amounts of carbon dioxide. Green hydrogen offers a near-zero-emission pathway to production, provided that the renewable energy input is truly sustainable. Hydrogen as an energy vector is characterised by its high gravimetric energy density and its versatility in end-use applications.

However, its storability, transportability, and current cost remain challenges. In overcoming these barriers, the technology surrounding water electrolysis has steadily improved, making green hydrogen more attractive for large-scale deployment (Franco & Giovannini, 2023).

Electrolysis Technologies and Advancements

1. Alkaline and Proton Exchange Membrane (PEM) Electrolysis

The two most mature electrolysis technologies used for green hydrogen production are alkaline electrolysis and proton exchange membrane (PEM) electrolysis (Franco & Giovannini, 2023).

Alkaline Electrolysis: It has traditionally been the most established method, relying on a liquid alkaline electrolyte to facilitate the reaction. While it offers robustness and lower costs on a scale, its efficiency and dynamic response to renewable energy intermittency can sometimes lag behind newer methods.

PEM Electrolysis: It employs a solid polymer membrane, allowing for faster start-up times and better performance with fluctuating energy inputs, making it particularly suited when integrated with variable renewable energy sources. Recent research has focused on

Converging Chemical and Biological Sciences for a Sustainable Era

developing catalysts that reduce the overall energy consumption of these systems and increase durability during continuous operations.

2. Solid Oxide Electrolyser Cells (SOEC) and Photo Electrochemical (PEC) Water Splitting

Innovative technologies beyond conventional systems have also emerged. Solid Oxide Electrolyser Cells (SOEC) operate at high temperatures, theoretically offering higher conversion efficiencies by utilising the waste heat available in industrial processes. Additionally, photoelectrochemical (PEC) water splitting directly uses solar energy to produce hydrogen, integrating collection and conversion into a single device.

Although still largely in the laboratory or pilot stage, PEC systems represent a futuristic approach where solar energy is harnessed more directly than through conventional photovoltaics (Aslam *et al.*, 2024).

3. Scaling Up and Cost Reduction Initiatives

A significant area of recent advancement is the scaling up of electrolysis technologies. Researchers and industrial consortia are investing in large-scale demonstration projects that integrate electrolyzers with renewable power plants. Such integrated systems contribute not only to levelling the cost of green hydrogen but also to demonstrating consistent and reliable operation in real-world conditions. Collaborative efforts across governments and private sectors have led to pilot projects that span from regional microgrids to national-scale deployments, all aimed at proving the commercial viability of green hydrogen plants (Franco & Giovannini, 2023).

Integration with Renewable Energy

One significant advancement that makes green hydrogen particularly attractive is its compatibility with the renewable energy landscape. Renewable energy sources such as solar and wind are inherently intermittent, leading to periods of over-generation and under-generation. By using surplus energy to produce hydrogen, these sources can achieve a higher level of reliability. This concept, often referred to as "power to gas," allows green hydrogen to act as an energy storage medium, converting electrical surpluses into a storable chemical form that can later be converted back to electricity or used in industrial processes (Franco & Giovannini, 2023).

Furthermore, green hydrogen plays a vital role in grid stability. In regions with a high penetration of renewables, the ability to store excess energy and release it mitigates challenges associated with energy intermittency. Ongoing research has also focused on optimising the temporal matching between renewable energy generation and hydrogen production, reducing energy losses and improving overall system efficiency.

Applications of Green Hydrogen

1. Industrial Uses

Green hydrogen is finding increasing applicability in industrial processes where Fossil Fuels to Blue-Green Energy traditional fossil-based hydrogen has been used. For example, the

steel industry is experimenting with replacing coke with hydrogen in direct reduction processes. Similarly, the chemical industry is exploring the use of green hydrogen to produce ammonia and methanol in low-carbon processes. The substitution of fossil hydrogen with green hydrogen in these sectors not only reduces greenhouse gas emissions but also aligns with evolving regulatory and consumer expectations for sustainability (Behrendt, 2025).

2. Transportation and Mobility

The realm of transportation represents one of the most promising applications of green hydrogen. Hydrogen fuel cell electric vehicles (FCEVs) are already in commercial deployment in several regions. These vehicles offer quick refuelling times, long driving ranges, and the potential for zero emissions. Beyond road transport, green hydrogen is also under investigation for marine and aviation applications, where batteries may not presently offer a competitive energy density. The potential to develop hydrogen-powered trains further underlines the wide-ranging role of hydrogen in the future of transport (Behrendt, 2025).

3. Energy Storage and Grid Balancing

The intermittency of renewable energy sources creates a significant storage challenge that green hydrogen helps address. When renewable generation exceeds demand, surplus electricity can be routed to electrolyzers that produce hydrogen. This hydrogen can be stored in large quantities, either as a compressed gas or in liquid form, and later converted back to electricity through fuel cells or turbines during periods of high demand. Such applications are not only limited to stabilising the grid but also extend to seasonal storage solutions where hydrogen serves as a long-term energy reserve (Maka & Mehmood, 2024).

4. Synthetic Fuels and Industrial Feedstock

Green hydrogen is also critical in the formulation of synthetic fuels. By combining hydrogen with captured carbon dioxide, industries can produce synthetic methane, diesel, or other fuels that mimic the performance characteristics of fossil fuels but with a considerably reduced carbon footprint. This approach holds transformational potential for sectors that are deeply entrenched in conventional fuel usage and where decarbonisation alternatives are limited (Yang *et al.*, 2023).

5. Summary of Recent Research Directions

Recent advancements in green hydrogen research have focused on several key areas:

Catalyst Optimisation: Research into non-precious metal catalysts for water splitting has the potential to drastically reduce the cost of both PEM and alkaline electrolyzers.

Durability and Efficiency Improvements: Innovations in cell design and materials science target increased lifetime and lower degradation rates in electrolyser stacks.

Hybrid System Integration: Projects integrating renewable energy sources directly with electrolysis systems are being evaluated to improve system-wide efficiency, including the combination of wind, solar, and even geothermal sources.

Economic Feasibility Studies: Life cycle assessments, along with techno-economic studies, provide insights into scalability and commercial deployment, driving policy and investment decisions.

The multifaceted research landscape ensures that green hydrogen is not merely a theoretical promise but is actively progressing towards competitive industrial adoption (Yang *et al.*, 2023)

Global Investments and Projects on Green Hydrogen

China: With a cumulative capacity of 780 MW in 2023 and more than 9 GW in advanced stages of development, China leads in the addition of electrolyser capacity (Athia, Pandey & Saxena, 2024).

The European Union: In February 2023, the European Union approved two delegated acts with rules to define renewable hydrogen. In 2024, the European Hydrogen Bank launched two auctions for a total of EUR 1.9 billion (USD 2 billion) and approved funding for four waves of hydrogen-related Important Projects of Common European Interest, with funding already provided to some project developers (Athia, Pandey & Saxena, 2024).

India: In January 2023 India approved the National Green Energy Mission with the aim of producing 5 Mt of renewable hydrogen by 2030. As part of that, the Strategic Interventions for Green Hydrogen Transition (SIGHT) program is a major financial measure to promote domestic manufacturing of electrolyzers and the production of renewable hydrogen (Athia, Pandey & Saxena, 2024).

The United Kingdom: In July 2022 the UK released its Low-Carbon Hydrogen Standard, and in February 2023 it launched a consultation for a certification scheme. The first and second Electrolytic Allocation Rounds were launched with the goal of supporting 1,000 MW of capacity in projects that use electrolysis to produce hydrogen (Athia, Pandey & Saxena, 2024).

The United States: As a part of the Industrial Demonstration Program, the United States of America approved USD 1.7 billion for six projects. In early 2025, the final rules for the Inflation Reduction Act (IRA) clean hydrogen production tax credit were released (Athia, Pandey & Saxena, 2024).

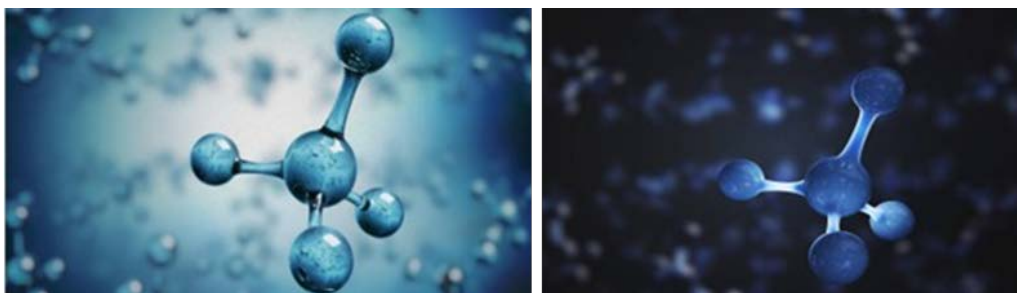
Mauritania: In 2023 it released its Hydrogen Strategy, joining South Africa, Kenya and Namibia as the only sub-Saharan countries that have adopted a hydrogen strategy, plus the Economic Community of West African States (ECOWAS) (Athia, Pandey & Saxena, 2024).

Blue Ammonia: Production Methods, Advances, and Applications

Overview and Definition

Blue ammonia is an emerging energy carrier that leverages the well-known synthesis process of ammonia but introduces a significant environmental upgrade, with a significant reduction in carbon emissions through the incorporation of carbon capture and storage (CCS). In essence, blue ammonia is produced by synthesising ammonia from hydrogen (typically derived through steam methane reforming or water electrolysis) and nitrogen,

where the carbon dioxide by-product is captured and stored or repurposed. When hydrogen is sourced with low carbon intensity, the resulting ammonia can serve as a low-carbon fuel and as a chemical feedstock for fertiliser production in agriculture. The interest in blue ammonia is driven by its capacity to be stored and transported with relative ease compared to hydrogen, offering a more energy-dense alternative. Its liquid form at moderate pressures means that existing infrastructure, such as port facilities and pipelines, can be repurposed, accelerating its acceptance as part of the new energy economy (Del Pozo & Cloete, 2022).



Source: <https://www.istockphoto.com/photos/blue-ammonia>

Figure 1: A Symbolic Picture of Blue Ammonia

Production Processes and Technological Advancements

1. Conventional Ammonia Synthesis and its Carbon Footprint

Traditionally, the Haber-Bosch process has been the cornerstone of ammonia production. This process combines hydrogen and nitrogen under high pressure and temperature in the presence of an iron-based catalyst. Although highly efficient from a chemical standpoint, the conventional route is energy intensive and typically relies on hydrogen produced via natural gas reforming—a method known as “grey ammonia” production. The carbon emissions associated with grey ammonia are considerable, making it incompatible with rigorous carbon reduction targets.

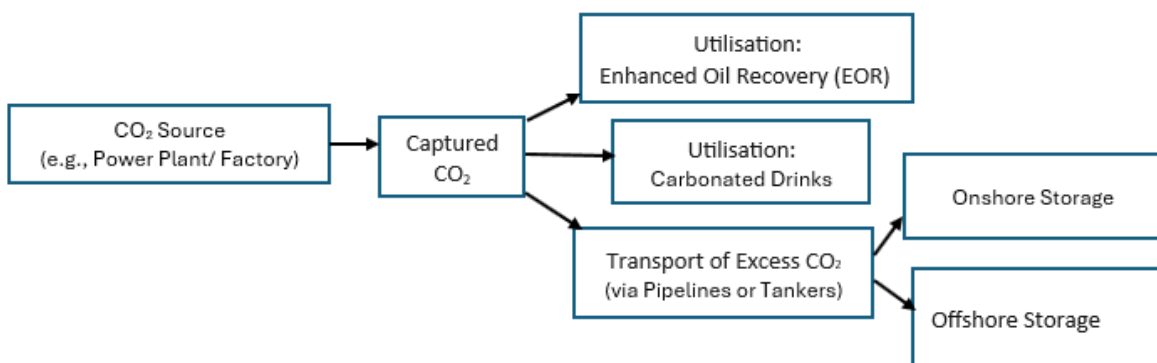


Figure 2: Carbon Capture Utilisation and Storage Operations

(Based on Ministry of Energy and Energy Industries)

Converging Chemical and Biological Sciences for a Sustainable Era

2. Integrating Carbon Capture and Storage (CCS)

Blue ammonia distinguishes itself by incorporating CCS into the hydrogen production process. When hydrogen is produced via Steam Methane Reforming (SMR), the associated CO₂ emissions can be captured using various CCS technologies. Recent technological advances have improved the capture efficiency and reduced the cost of those processes, making blue ammonia a more financially feasible proposition. Innovations include better absorption solvents, membrane-based capture technologies, and novel adsorbent materials that offer the dual benefits of higher capture rates and lower energy penalties. Furthermore, improvements in logistics and storage of CO₂ make the integration of CCS more streamlined in industrial settings (Park *et al.*, 2023).

2. Alternative Production Approaches

Beyond SMR-based production with CCS, researchers have also explored routes that combine renewable energy sources with ammonia synthesis. One promising strategy is the integration of electrolysis-based hydrogen production (essentially green hydrogen) with the Haber-Bosch process. Although technically challenging due to the dynamic nature of renewable energy inputs, such systems have the potential to further reduce the carbon footprint of ammonia production. Advances in reactor design and process control are addressing these intermittencies, indicating a future where hybrid systems could bridge the gap between blue and green ammonia (Park *et al.*, 2023).

Advantages and Applications of Blue Ammonia

1. Energy Density and Storage

One of the key advantages of blue ammonia is its high energy density relative to hydrogen gas. Because ammonia is easier to liquefy and store at moderate conditions, it is considered an attractive carrier for transporting energy over long distances. Existing global ammonia logistics networks—developed over decades for fertiliser distribution—can potentially be repurposed for energy transport, reducing the need for entirely new infrastructures.

2. Role in Decarbonizing Hard-to-Abate Sectors

Blue ammonia offers a route to decarbonise sectors where switching to pure electrification is difficult. In maritime transport, for instance, ammonia-fuelled engines are being developed as alternatives to fossil fuels. In the industrial domain, ammonia not only functions as a feedstock for various chemicals but can also be used directly as a combustion fuel for power generation. Such versatility means that blue ammonia could play a critical role in achieving deep decarbonisation in sectors such as shipping, heavy industry, and remote power supply (Tanzeem & Al-Thubaiti, 2023).

3. Industrial Integration and Economic Sensitivity

In addition to its energy carrier role, blue ammonia aligns with existing industrial ecosystems. The transition from grey to blue ammonia does not necessitate a complete overhaul of the industrial process; rather, it involves retrofitting with CCS technology and process optimisation. This incremental transition lowers the economic risk associated with the shift,

Transitioning to Blue-Green Energy: A Sustainable Future

thereby attracting investments from both government and private sectors. Studies indicate that once CCS technology reaches further maturity, the cost differential between blue ammonia and fossil-based ammonia will narrow significantly (Park *et al.*, 2023).

Recent Research and Development Trends

Recent academic and industrial research has resulted in significant progress in the areas of process integration, catalyst development, and operational efficiency in blue ammonia production (Park *et al.*, 2023). The key research topics include:

Enhanced CCS Techniques: Researchers are working on lowering the energy penalty of CCS, increasing capture rates, and developing modular CCS systems that can be retrofitted into existing ammonia plants.

Hybrid Production Systems: Pilot projects integrating renewable-based electrolysis with traditional ammonia synthesis (augmented by CCS) are under development, with early results indicating promising cost and emissions performance.

Materials Innovation: Advances in materials science have led to the development of improved catalysts for the Haber-Bosch process, which can operate under milder conditions, thereby reducing the overall energy input.

Life Cycle and Techno-Economic Assessments: Detailed studies are increasingly available that model the full-cycle emissions of blue ammonia. These assessments provide a roadmap for industrial adoption by comparing blue ammonia's carbon footprint to that of grey and green ammonia.

Overall, the focus on optimising production processes and integrating CCS into the ammonia synthesis value chain suggests that blue ammonia will become a cornerstone in the decarbonisation of the chemical and energy sectors (Park *et al.*, 2023).

Global Investments and Projects on Blue Ammonia

Japan: Leading the charge with large-scale pilot programs for shipping fuel. South Korea: Investing in power plants adapting to ammonia co-firing.

Saudi Arabia: Engaging in partnerships between energy companies and governments to promote blue ammonia.

United States: Also leading with significant investments and projects in blue ammonia.

These countries are pioneering efforts to integrate blue ammonia into their energy systems, demonstrating its potential as a viable and scalable solution for decarbonisation (Park *et al.*, 2023).

Comparative Analysis: Blue Ammonia vs. Green Hydrogen

Technical and Operational Considerations

When comparing blue ammonia and green hydrogen, several technical parameters are critical: energy density, storage, transport, and end-use flexibility (Mersch *et al.*, 2024).

Converging Chemical and Biological Sciences for a Sustainable Era

Energy Density and Storage

Green hydrogen, although having an exceptionally high energy content per unit mass, suffers in volumetric density. Its storage requires either high-pressure tanks or cryogenic systems, both of which incur additional infrastructural costs and technical challenges. Conversely, blue ammonia offers a higher volumetric energy density and benefits from established storage and transport systems used in the chemical industry. Such characteristics grant blue ammonia an edge in scenarios where long-distance transportation or large-scale storage is key (Mersch *et al.*, 2024).

Production and Process Efficiency

Green hydrogen production is primarily dependent on the availability of renewable energy and the efficiency of electrolyser systems, which have improved over recent years but are still subject to economies of scale. Blue ammonia production, by its reliance on the established Haber-Bosch process integrated with CCS, can leverage decades of industrial experience. However, blue ammonia's overall carbon footprint is contingent on the efficiency of its CCS systems and the source of its hydrogen. In a context where renewable integration is robust, green hydrogen may present a more sustainable solution; yet during the transitional period, blue ammonia serves as a cost-competitive alternative (Mersch *et al.*, 2024).

Operational Flexibility

Both energy carriers cater to distinct operational constraints. Green hydrogen is suitable for applications that require high purity and fast response times—such as fuel cells and precision industrial applications—whereas blue ammonia's strength lies in bulk energy storage and transportation. The choice between the two is often dictated by the specific logistical and operational requirements of the end user (Mersch *et al.*, 2024).

Economic and Market Considerations

Cost Trajectories and Economies of Scale

The economic viability of both green hydrogen and blue ammonia is evolving as technologies mature and scale up. Green hydrogen's cost largely depends on the capital expenditure associated with electrolyser systems and the cost trajectory of renewable energy. Continuous improvements are driving costs down, and economies of scale are anticipated to further bolster its market competitiveness. Blue ammonia, while benefiting from existing industrial practices, faces additional costs associated with CCS. Economic analyses suggest that in regions with favourable CCS economics and established ammonia infrastructures, blue ammonia may reach cost parity with—or even outperform—green hydrogen in the near term. However, policy incentives and carbon pricing mechanisms are pivotal in tilting the economic scales in either direction (Mayer *et al.*, 2023).

Infrastructure and Supply Chain Integration

A key advantage of blue ammonia lies in its ready compatibility with current ammonia transportation and storage infrastructures. In contrast, green hydrogen requires the

Transitioning to Blue-Green Energy: A Sustainable Future

development of specialised high-pressure pipelines, cryogenic storage solutions, or conversion systems (such as ammonia synthesis) for easier handling. The transformation of these supply chains represents a significant upfront investment, yet it is critical for pushing green hydrogen toward larger markets (Mayer *et al.*, 2023).

Market Adoption and Investment Trends

Investment trends in both technologies reflect the growing interest in decarbonisation. Government subsidies, industrial partnerships, and private capital are increasingly directed toward pilot projects, research grants, and infrastructure development. Both blue ammonia and green hydrogen are receiving targeted policy support in many regions, particularly within the European Union and Asia, where aggressive climate policies are in place. While blue ammonia can transition more seamlessly into existing markets, green hydrogen is poised to capture long-term value in sectors where sustainability metrics are critical (Mayer *et al.*, 2023).

Environmental Considerations

Carbon Emissions and Lifecycle Analysis

Environmental impact is the decisive factor when evaluating sustainable energy carriers. Green hydrogen, when paired with renewable energy, offers near-zero direct emissions. Its lifecycle emissions are predominantly tied to the production of renewable energy infrastructure. Blue ammonia's lifecycle emissions depend on the efficiency of its CCS. While blue ammonia can achieve significant carbon reductions compared to grey ammonia, any imperfections in capture or leakage can pose environmental risks that green hydrogen can, by design, avoid (Mayer *et al.*, 2023).

Safety and Handling Concerns

Both green hydrogen and blue ammonia involve handling flammable substances, but their safety profiles differ. Green hydrogen requires careful management due to its low ignition energy and high diffusivity, necessitating robust safety protocols in storage and transportation. Blue ammonia, while less flammable than pure hydrogen, must be managed for its toxicity and potential environmental hazards in the event of spills. Advances in safety standards, process automation, and monitoring technologies are crucial in mitigating these hazards for both processes (Mayer *et al.*, 2023).

Summary of Comparative Insights

The comparative analysis reveals that both energy carriers offer distinct advantages within the renewable energy portfolio. Green hydrogen excels in applications requiring pure, high-quality hydrogen and benefits from never having been fundamentally reliant on fossil fuels. Blue ammonia, by contrast, offers a pragmatic transitional pathway by leveraging existing industrial assets and infrastructure. The synthesis of these technologies in a hybrid model may even be the optimal strategy for a multi-faceted, resilient low-carbon energy future (Mayer *et al.*, 2023).

Economic Benefits and Policy Frameworks

Economic Advantages of the Hydrogen Economy

The economic benefits of shifting toward green hydrogen and blue ammonia extend well beyond the direct reduction in greenhouse gas emissions (Samylingam *et al.*, 2024). These technologies foster:

Industrial Decarbonisation: Transitioning to hydrogen-based processes can help avoid anticipated carbon pricing penalties and open up new market opportunities.

Job Creation: The scaling of hydrogen production necessitates the development of new infrastructure, from electrolyser manufacturing to transportation systems, creating a diverse spectrum of skilled jobs.

Energy Security: By reducing dependence on imported fossil fuels, countries can enhance their energy sovereignty, promoting stability in the energy markets.

Cost Competitiveness: As renewable energy costs continue to decline and electrolyser efficiencies improve, green hydrogen is rapidly approaching cost parity with hydrogen produced via fossil-fuel routes. In parallel, blue ammonia investments are being supported by retrofitting existing infrastructures, unlocking further economic efficiencies.

These economic drivers underscore the role of hydrogen as not only a sustainable alternative but also an engine for economic growth and innovation (Samylingam *et al.*, 2024).

Policy Initiatives and Governmental Support

Government policy is a critical catalyst for the rapid deployment of green hydrogen and blue ammonia technologies. Several key initiatives include:

1. National and Regional Strategies

Many countries have launched ambitious hydrogen strategies aimed at scaling up production and integrating these technologies into the energy mix. For example:

Hydrogen Missions: National missions dedicated to clean hydrogen production provide substantial funding, research support, and public-private partnerships aimed at developing viable hydrogen supply chains (Behrendt, 2025).

Regional Subsidies and Incentives: Certain regions and states provide targeted subsidies, tax breaks, and low-interest loans to industries that invest in hydrogen and CCS technologies. These measures help offset initial capital outlays and mitigate the financial risks of transitioning from conventional to low-carbon processes.

2. International Collaborations

Global collaborations and long-term strategic partnerships have further accelerated the hydrogen revolution. The European Union, for instance, has adopted directives that foster cross-border hydrogen infrastructures and joint research programmes. Collaborative projects in Asia are similarly designed to pool resources and expertise, ensuring that both

green hydrogen and blue ammonia remain competitive on the international stage (Behrendt, 2025).

3. Carbon Pricing and Regulatory Frameworks

The imposition of carbon pricing mechanisms is gradually tilting the economic balance in favour of low-carbon energy carriers. By establishing clear regulatory frameworks that penalise emissions and reward sustainability, governments create a market environment where blue ammonia and green hydrogen can thrive. Rigorous lifecycle analyses and clear emissions metrics are now integral to the policy discourse, ensuring transparency and accountability in the transition process.

Investment Trends and Market Dynamics

Recent investment trends highlight substantial capital flows into hydrogen projects across both green and blue pathways. Strategic investors, including national oil companies and new entrants in the renewable sector, are increasingly forming joint ventures to capture the emerging market potential. Modern techno-economic assessments indicate that, in the long term, the combination of scale, technological improvements, and supportive policy measures will drive down production costs, making both green hydrogen and blue ammonia economically competitive with fossil fuels. The market dynamics in this space are evolving rapidly. For instance, private sector investment in advanced electrolyser technology and modular CCS systems has seen double-digit growth rates in recent years. Industry conferences, technical workshops, and policy roundtables are increasingly focusing on de-risking projects and standardising operational protocols—moves that are essential for mainstream market adoption (Harichandan & Kar, 2023).

Challenges, Research Gaps, and Future Perspectives

Technological Challenges

Despite enormous progress, several technological challenges remain (Noussan *et al.*, 2021)

Efficiency and Durability: Both green hydrogen and blue ammonia production depend on system components (electrolysers, catalysts, CCS units) that require further improvements to achieve higher efficiency and extended operational lifetimes. Research is ongoing to develop new materials with superior catalytic properties and lower degradation rates.

Integration with Renewable Energy: Capturing the intermittent nature of renewable energy remains a technical hurdle. Enhancing the dynamic response of electrolysis systems and optimising process controls to handle variability are critical areas for further innovation.

Storage and Transportation: For green hydrogen, developing cost-effective, safe storage systems is paramount. This includes overcoming challenges related to compression, liquefaction, and leak prevention. Blue ammonia, while leveraging existing infrastructures, still necessitates enhancements in safety protocols and handling procedures.

Economic and Scale-Up Barriers

Several economic and infrastructural barriers continue to affect the pace of commercialisation:

Capital Intensive Infrastructure: The upfront capital investment required for building large-scale electrolyser plants, CCS facilities, and associated transportation networks remains high, potentially slowing economic viability until economies of scale are achieved (Harichandan & Kar, 2023).

Market Readiness and Transition: The gradual integration of these technologies into mature industrial sectors can face resistance due to entrenched processes and significant transformation costs. Policy incentives are required to mitigate these transitional costs and encourage rapid deployment (Harichandan & Kar, 2023).

Cost Uncertainties: While predictions point toward a downward trend in costs as technology matures, uncertainties remain regarding the pace of cost reductions. Continued R&D efforts, pilot projects, and cross-sector collaboration are essential to validate economic models and demonstrate commercial competitiveness (Harichandan & Kar, 2023).

Regulatory and Safety Concerns

As both green hydrogen and blue ammonia move closer to widespread adoption, ensuring robust regulatory frameworks and safety standards is critical (Anilkumar, 2022).

Standardisation: The development of uniform standards for production, storage, and transportation is essential. This includes harmonising safety protocols across different jurisdictions and industrial sectors.

Risk Management: Robust risk assessments and emergency response frameworks are necessary to address potential hazards, ranging from hydrogen leaks to ammonia spills. Implementing advanced monitoring and control systems can preemptively mitigate risks and protect both personnel and the environment.

Environmental Monitoring: Continuous environmental monitoring, including lifecycle analysis of emissions and performance assessments of CCS technologies, is vital to ensure that the intended carbon reduction benefits are fully realised in practice.

Future Research Directions

Looking ahead, several key research directions can help unlock the full potential of blue ammonia and green hydrogen (Elçiçek, 2024):

Next-Generation Catalysis: Developing robust, non-precious metal catalysts will reduce dependency on expensive materials and improve the overall sustainability of electrolysis systems.

Integrated Renewable Systems: Research on integrated systems that couple renewable energy generation directly to hydrogen production—and even further to ammonia synthesis—could revolutionise system efficiency and reliability. Pilot projects exploring

hybrid operational models, such as coupling solar and wind with modular electrolyzers or CCS units, are on the horizon.

Digitalisation and Process Optimisation: The integration of advanced data analytics, artificial intelligence, and process automation presents opportunities for real-time optimisation of production processes. Digital twin models of hydrogen and ammonia production plants can simulate various operating conditions and predict maintenance needs, thereby reducing downtime and operational expenses.

Cross-Sector Collaboration: Partnerships between academia, industry, and government agencies must continue to blossom. Multidisciplinary collaboration can accelerate breakthroughs in key areas such as materials science, energy storage, and process engineering.

Lifecycle and Systemic Studies: Comprehensive environmental and economic lifecycle assessments will continue to be indispensable. These studies should incorporate broader societal impacts, such as job creation, resource utilisation, and energy security, alongside traditional emission metrics.

By aligning research priorities with industry needs and policy trends, the challenges can be transformed into opportunities, paving the way for a truly sustainable and integrated low-carbon energy system (Elçiçek, 2024).

Conclusion

Green Hydrogen and Blue Ammonia are key players in the shift to clean energy. Green hydrogen offers near-zero emissions and flexibility, while blue ammonia leverages existing infrastructure with carbon capture. Despite challenges in storage, transport, and scalability, both technologies can complement each other in a diversified hydrogen-based economy.

Economic growth, energy security, and job creation further highlight their value, with policy support driving adoption. Continued research, innovation, and collaboration will be crucial in overcoming hurdles and unlocking their full potential. Together, they represent a significant step toward a sustainable, low-carbon and green future.

Acknowledgement

The author is deeply thankful to all her departmental colleagues and college administration for fostering a collaborative and supportive environment that has enabled her to thrive.

References

- Adeli, K., Nachtane, M., Faik, A., Saifaoui, D., & Boulezhar, A. (2023). How green hydrogen and ammonia are revolutionizing the future of energy production: a comprehensive review of the latest developments and future prospects. *Applied Sciences*, 13(15), 8711. <https://doi.org/10.3390/app13158711>
- Ahmed, H. S., Yahya, Z., Ali Khan, W., & Faraz, A. (2024). Sustainable pathways to ammonia: a comprehensive review of green production approaches. *Clean Energy*, 8(2), 60-72. <https://doi.org/10.1093/ce/zkae002>

- Anilkumar, A. A. (2022). Safety standards and norms for green hydrogen, green ammonia, and green methanol. *TUV India Report*. Retrieved from: https://energyforum.in/fileadmin/india/media_elements/Presentations/20221129_Webinar_Safety_GH2/1_TUV.pdf. Accessed on 15th December 2024.
- Aslam, S., Awais, M., Ahmed, S., Safdar, M., Buksh, A. A., & Haroone, M. S. (2024). Photoelectrochemical water splitting by using nanomaterials: a review. *Journal of Electronic Materials*, 53(1), 1-15. <https://doi.org/10.1007/s11664-023-10794-z>
- Athia, N., Pandey, M., & Saxena, S. (2024). Evaluating the effectiveness of national green hydrogen mission in India. *Environment, Development and Sustainability*, 1-23. <https://doi.org/10.1007/s10668-024-05829-2>
- Behrendt, F. (2025). The future of industrial hydrogen: renewable sources and applications for the next 15 years. *Clean Energy*, 9(1), 3-8. <https://doi.org/10.1093/ce/zkae103>
- Del Pozo, C. A., & Cloete, S. (2022). Techno-economic assessment of blue and green ammonia as energy carriers in a low-carbon future. *Energy Conversion and Management*, 255. <https://doi.org/10.1016/j.enconman.2022.115312>
- Elçiçek, H. (2024). Bibliometric analysis on hydrogen and ammonia: A comparative evaluation for achieving IMO's decarbonization targets. *International Journal of Environmental Science and Technology*, 21, 7039–7060. <https://doi.org/10.1007/s13762-023-05450-2>
- Franco, A., & Giovannini, C. (2023). Recent and future advances in water electrolysis for green hydrogen generation: Critical analysis and perspectives. *Sustainability*, 15(24), 16917. <https://doi.org/10.3390/su152416917>
- Harichandan, S., & Kar, S. K. (2023). Financing the hydrogen industry: exploring demand and supply chain dynamics. *Environmental Science and Pollution Research*, 1-18. <https://doi.org/10.1007/s11356-023-30262-9>
- Maka, A. O., & Mehmood, M. (2024). Green hydrogen energy production: current status and potential. *Clean Energy*, 8(2), 1-7. <https://doi.org/10.1093/ce/zkae012>
- Mayer, P., Ramirez, A., Pezzella, G., Winter, B., Sarathy, S. M., Gascon, J., & Bardow, A. (2023). Blue and green ammonia production: A techno-economic and life cycle assessment perspective. *IScience*, 26(8). <https://doi.org/10.1016/j.isci.2023.107389>
- Mersch, M., Sunny, N., Dejan, R., Ku, A. Y., Wilson, G., O'Reilly, S., ... & MacDowell, N. (2024). A comparative techno-economic assessment of blue, green, and hybrid ammonia production in the United States. *Sustainable Energy & Fuels*, 8(7), 1495-1508. <https://doi.org/10.1039/D3SE01421E>
- Ministry of Energy and Energy Industries. (n.d.). *Carbon Capture Utilization and Storage (CCUS)*. Government of the Republic of Trinidad and Tobago. Retrieved from: <https://www.energy.gov.tt/our-business/carbon-capture-utilization-and-storage-ccus/>. Accessed on 15th February 2025.
- Noussan, M., Raimondi, P. P., Scita, R., & Hafner, M. (2020). The role of green and blue hydrogen in the energy transition—A technological and geopolitical perspective. *Sustainability*, 13(1), 298. <https://doi.org/10.3390/su13010298>

Transitioning to Blue-Green Energy: A Sustainable Future

- Park, S., Shin, Y., Jeong, E., & Han, M. (2023). Techno-economic analysis of green and blue hybrid processes for ammonia production. *Korean Journal of Chemical Engineering*, 40(1), 2657-2670. <https://doi.org/10.1007/s1814-023-1520-1>
- Samylingam, L., Aslfattahi, N., Kok, C. K., Kadirgama, K., Schmirler, M., Yusaf, T., ... & Ghazali, M. F. (2024). Underlying developments in hydrogen production technologies: economic aspects and existent challenges. *Korean Journal of Chemical Engineering*, 41(1), 2961- 2984. <https://doi.org/10.1007/s1814-024-00264-5>
- Tanzeem, M. A. T., & Morshed, M. M. (2023). Blue ammonia: an attractive pathway to decarbonize conventional ammonia plants. *World Journal of Advanced Engineering Technology and Sciences*, 9(1), 19-126. <https://doi.org/10.30574/wjaets.2023.9.1.0121>
- Yang, M., Hunger, R., Berrettoni, S., Sprecher, B., & Wang, B. (2023). A review of hydrogen storage and transport technologies. *Clean Energy*, 7(1), 190-216. <https://doi.org/10.1093/ce/zkad021>

Converging Chemical and Biological Sciences for a Sustainable Era

Mnemonic of Carbohydrates Structure with Proper Stereochemistry

Sisir Debnath

Department of Chemistry, Serampore College, Affiliated to University of Calcutta, Hooghly 712201, West Bengal, India

Corresponding Author's E-mail: dn.sisir@gmail.com

Abstract

There are sixteen structures possible for aldohexose since it contains four unlike chiral centres ($2^4 = 16$). Thus, eight pairs of enantiomers are possible, all of which are optically active. If the bottom chiral centre (C-5) is taken as naturally occurring D-isomer, still eight isomers are possible. So, it is a very difficult task for the students to remember the names of all the naturally occurring aldohexoses as well as their structures with appropriate stereochemistry. Most of the students lost their interest in organic chemistry while memorising the names and structures of these enormous numbers of molecules. Thus, writing the structure of aldohexoses on paper within a short period of time with proper stereochemistry is a challenging task for all the students. Currently, the students are memorising the structures of hexoses by starting from the structure of tetroses and pentoses. Also, the calculation by this process needs a very long time. Moreover, these memorised structures are very quickly lost after a few days of the evaluation since they are not using a proper mnemonic. Instead of directly memorising the structure of a complex molecule, mnemonics has been recognised to be much more effective in long-term memorisation. In this chapter a new and simple mnemonic will be described to write the structure of all the D-aldohexoses in Fischer projection formula within a few seconds. The mnemonic will be extended for the naturally occurring aldopentose as well.

Keywords: Aldohexose; Carbohydrates; Fischer Projection; Mnemonic; Stereochemistry

Introduction

Most students find enormous difficulties when they try to memorise the name and structure of larger organic molecules. It has been found that a vast majority of students lost their interest in organic chemistry during memorising the names and, in some cases, the stereochemistry of a huge number of biomolecules. But anyhow, if they memorise it, all their effort goes to vain after a few days since the memorised names and stereochemistry are quickly forgotten. In this case, mnemonics offer great help to the student since these tools help students to memorise complex organic structures with proper stereochemistry for a much longer time (Levin & Levin, 1990). Mezl (2001) demonstrated how a rhyme can be used to aid in memorising the structural properties of amino acids. Sailakshmi et al. (2013) showed that the phrase 'Oh My Such Good Apple Pie' (OMSGAP) helps us to remember the name and structure of dicarboxylic acids. If the molecule contains multiple chiral centres, writing the structure with proper stereochemistry becomes a nightmare for a large section of students. In this connection it is to be noted that the structure of different carbohydrate

Converging Chemical and Biological Sciences for a Sustainable Era

Memorizing Carbohydrate Structure and Stereochemistry

molecules plays an important role in the biological system (Su, Hendrikse & Meijer, 2022; Scherbinina & Toukach, 2020; Morgan & Baraban, 2024). For that type of molecule, some tricks need to be adopted to write on paper with proper stereochemistry. E.g., Leary (1955) reported that the name and the structures of the monosaccharides can be memorised by numbering the carbons and also remembering the position of the hydroxyl group on the right and left sides in the Fischer projection formula. In this process a lot of numbers need to be remembered, which limits the goal of the tools.

Another version for the nomenclature of the carbohydrates is done by binary numbering, which needs a lot of calculations to find a carbohydrate structure with stereochemistry (Klein, 1980). Ronald Starkey (2000) has shown how a student can remember the absolute configuration of all the chiral centres of glucose from the term SOS (Same–Opposite–Same), where 'S' denotes same configuration, 'O' denotes opposite configuration and again 'S' denotes same configuration of the chiral centres from C-2 to C-4 carbon, respectively, to the reference chiral centre C-5, which may be 'D' or 'L' configuration. The major drawback of this process is that the stereochemistry of the chiral centres of only glucose molecules can be memorised. Belhomme, Castex and Haudrechy (2019) recently reported a complex process of sugar mapping to find out the stereochemical relationship among the carbohydrates. Writing the structures of eight naturally occurring D-aldohexoses with proper stereochemistry is a huge challenge for undergraduate and postgraduate students because they need to remember the structure and stereochemistry of the pentoses first. Then, with the help of the structure of pentose, the student can write a structure of hexose after doing some calculations. For the whole process, the student needs a very long time, which sometimes becomes very difficult to manage, especially in the comparative examination. Here, an easy trick has been developed by which the structure of any aldohexose can be written directly within a few seconds without taking any help from the structure of pentoses.

Discussion

First, the popular phrase 'All Altruists Gladly Make Gum In Gallon Tanks' is used to know the name of eight aldohexose Allose, Altrose, Glucose, Mannose, Gulose, Idose and Galactose respectively (Parish, 1961). Thus, four pairs of hexoses are obtained in the category of naturally occurring aldohexose. Now, for a given aldohexose, the position of it is found out using this phrase. In every pair, the first member is termed as A, and second member is termed as B. So, the numbering of the molecules will be as follows (Figure 1).

All	Altruists	Gladly	Make	Gum	In	Gallon	Tanks
1A	1B	2A	2B	3A	3B	4A	4B
Pair 1		Pair 2		Pair 3		Pair 4	

Figure 1: Division of Eight Aldoexose into Four Pairs

Since all are aldohexoses, the top carbon will remain as -CHO and the bottom carbon as -CH₂OH. Also, in the bottom chiral centre (C5), the -OH group remains at the right-hand side in the Fischer projection formula since all are D-aldohexoses. Therefore, the common structure of all the D-aldohexoses is as follows (Figure 2).

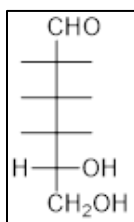


Figure 2: Common Fischer Projection Structural Formula of D-hexose

Now, all the -OH groups on the right-hand side in the Fischer projection formula are assumed to be the standard structure, i.e., the structure of allose is the standard structure, and changes come from the pair number and A, B. In every pair, A and B denote the orientation of the -OH group at the top chiral centre. A means the -OH group at the top chiral centre remains at the right-hand side, and B means the -OH group at the top chiral centre remains at the left-hand side in the Fischer projection formula. For the first pair of hexoses, the changes come only at the top chiral centre. For the second pair of hexoses, keeping the -OH group of the second chiral centre at the left-hand side, the top chiral centre will be changed according to A and B.

Similarly, for the third pair of hexoses, keeping the -OH group of the third chiral centre at the left-hand side, the top chiral centre will be changed according to A and B. For the fourth pair of hexose, keeping the -OH group of both the second and third chiral centres on the left-hand side, the top chiral centre will be changed according to A and B. For the fourth pair, since the -OH group of the fourth chiral centre cannot be changed, both the second and third chiral centres need to be changed. Now every individual structure can be written within a few seconds by following this instruction without taking any help from the structure of pentoses. E.g., if someone has been asked to write the structure of D-Gulose, first, the position of gulose in the phrase 'All Altruists Gladly Make Gum In Gallon Tanks' is found out. It is observed to be 3A (third pair first compound).

Therefore, during writing on paper, the -OH group of the third chiral centre will go to the left-hand side, and at the top chiral centre, the -OH group will go to the right-hand side since it is A. There will be no change in the position of the second chiral centre, i.e., it remains on the right-hand side like allose. So, the structure of Gulose will be as follows (Figure 3). Similarly, the Fischer projection of D-Idose can easily be drawn.

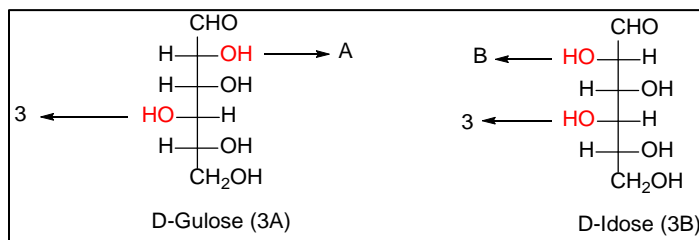


Figure 3: Fischer Projection Structural Formula of D-gulose and D- Idose

Memorizing Carbohydrate Structure and Stereochemistry

Similarly, if someone is asked to write the structure of D-mannose, within a few seconds it is found first that mannose is positioned 2B (second pair, second compound) in the aforementioned phrase. Therefore, during writing on paper, the -OH group of the second chiral centre will go at the left-hand side, and at the top chiral centre, the -OH group will also go at the left-hand side since it is B. So, the structure of mannose will be as follows (Figure 4). Similarly, the Fischer projection of D-glucose can easily be drawn.

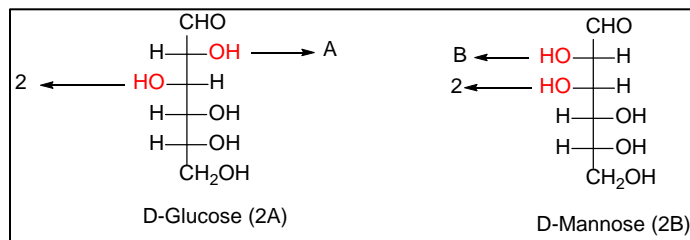


Figure 4: Fischer Projection Structural Formula of D-Glucose and D-mannose

Again, if the structure of galactose is asked to be written in Fischer projection formula, first the position of galactose is found to be 4A (fourth pair first compound) in the aforementioned phrase. Therefore, during writing on paper, the -OH group of both the second and third chiral centres will go to the left-hand side, and at the top chiral centre, the -OH group will go to the right-hand side since it is A. So, the structure of galactose will be as follows (Figure 5). Similarly, the Fischer projection of D-talose can easily be drawn.

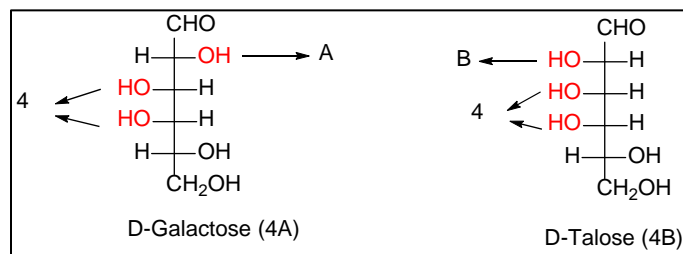


Figure 5: Fischer Projection Structural Formula of D-galactose and D-Talose

The name and structure of an aldopentose with proper stereochemistry can also be found out by the similar concept. The name of the pentose sugar can be memorised by the phrase 'Ring All Xylophones Loudly', where the words in the phrase stand for Ribose, Arabinose, Xylose and Lyxose, respectively. Now, for a given aldopentose, the position in the phrase was found out. In every pair, the first member is considered as A and the second member is B. So, the numbering of the molecules will be as follows (Figure 6).

Ring	All	Xylophone	Loudly
1A	1B	2A	2B
Pair 1		Pair 2	

Figure 6: Division of Four Aldopentose into Two Pairs

All aldopentoses contain -CHO and -CH₂OH groups at the top and bottom positions, respectively. Also, in the Fischer projection formula, the -OH group at the bottom chiral centre (C-4) remains at the right-hand side since all are D-aldopentose. Therefore, the common structure of all the D-aldopentoses is as follows (Figure 7).

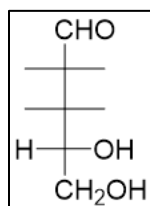


Figure 7: Common Fischer Projection Structural Formula of D-pentose

In the standard structure, all the -OH groups are taken at the right-hand side in the Fischer projection formula. i.e., the structure of Ribose is the standard structure, and changes in the structure come from the pair number and A, B. In every pair, A means the -OH group at the top chiral centre remains at the right-hand side, and B means the -OH group at the top chiral centre remains at the left-hand side in the Fischer projection formula. In the first pair of pentose (1A and 1B), the changes come only at the top chiral centre. The numbering of the second pair of pentose comes as 2A and 2B.

Thus, keeping the -OH group of the second chiral centre at the left-hand side, the top chiral centre will be changed according to A and B. For example, if the structure of Xylose is asked to be drawn, first, the position of Xylose in the phrase 'Ring All Xylophone Loudly' is found to be 2A (second pair first compound). Therefore, during writing on paper, the -OH group of the second chiral centre from the top will go to the left-hand side, and at the top chiral centre, the -OH group will go to the right-hand side since it is A. So, the structure of Xylose will be as follows (Figure 8). Similarly, the Fischer projection of D-Lyxose can be drawn based on the structure of molecule 2B.

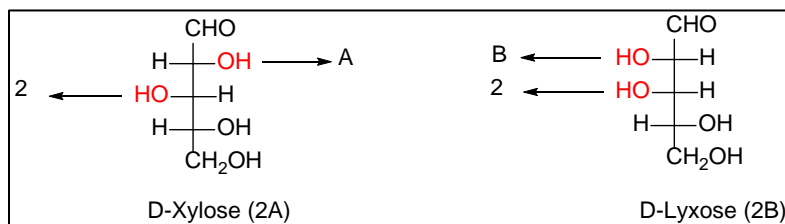


Figure 8: Fischer Projection Structural Formula of D-Xylose and D-Lyxose

Conclusion

An efficient way has been described by which a student can write the structure of any aldohexose and aldopentose with proper stereochemistry within a few seconds. The students do not need to memorise the structure of any aldoses. Therefore, the students will benefit enormously if they use this simple mnemonic.

Acknowledgment

The author expresses sincere gratitude to Serampore College, affiliated with the University of Calcutta, Serampore, Hooghly, West Bengal, India, for their valuable support.

References

- Belhomme, M. C., Castex, S., & Haudrechy, A. (2019). *Journal of Chemical Education*, 96 (11), 2643–2648. <https://doi.org/10.1021/acs.jchemed.8b00723>
- Klein, H. A. (1980). A Simplified Carbohydrate Nomenclature. *Journal of Chemical Information and Computer Sciences*, 20 (1), 15–18. <https://doi.org/10.1021/ci60021a006>
- Leary, R. H. (1955). A mnemonic for monosaccharides. *Journal of Chemical Education*, 32(8), 409. <https://doi.org/10.1021/ed032p409>
- Levin, M. E., & Levin, J. R. (1990). Scientific mnemonics: Methods for maximizing more than memory. *American Educational Research Journal*, 27(2), 301-321. <https://doi.org/10.2307/1163011>
- Mezl, V. A. (2001). The AAAmino acid list a mnemonic derivation of the structures and Morgan, K. M., & Baraban, J. H. (2024). Thermochemical Studies of Small Carbohydrates. *The Journal of Organic Chemistry*, 89 (3), 1769–1776. <https://doi.org/10.1021/acs.joc.3c02465>
- Parish, L. C. (1961). The Carbohydrates. *JAMA*, 175 (6), 532-533. <https://doi.org/10.1001/jama.1961.03040060106045>
- Sailakshmi, G., Mitra, T., Chatterjee, S., & Gnanamani, A. (2013). Engineering chitosan using α , ω -dicarboxylic acids—an approach to improve the mechanical strength and thermal stability.” *Journal of Biomaterials and Nanobiotechnology*, 4(2), 151-164. 10.4236/jbnb.2013.42021
- Scherbinina, S. I., & Toukach, P. V. (2020). Three-Dimensional Structures of Carbohydrates and Where to Find Them. *International Journal of Molecular Science*, 21(20). <https://doi.org/10.3390/ijms21207702>
- Starkey, R. (2000). SOS: A Mnemonic for the Stereochemistry of Glucose. *Journal of Chemical Education*, 77 (6), 734. <https://doi.org/10.1021/ed077p734>
- Su, L., Hendrikse, S. I. S., & Meijer, E. W. (2022). Supramolecular glycopolymers: How carbohydrates matter in structure, dynamics, and function. *Current Opinion in Chemical Biology*, 69, 102171. <https://doi.org/10.1016/j.cbpa.2022.102171>

A Brief Review on Recent Developments in C(sp²)-H and C(sp³)-H Activation Protocols through Cobalt-catalysis

Rupankar Paira

Department of Chemistry, Maharaja Manindra Chandra College, Ramkanto Bose Street, Kolkata 700003, India

Corresponding Author's E-mail: rpaira@mmccollege.ac.in

Abstract

Cobalt (Co) is presently of greater interest to researchers exploring C-H functionalisation than noble metals like Pd, Rh, and Ir due to its accessibility, cost, and low toxicity. In this way, during the past few decades, the number of instances of co-catalysed functionalisation has grown dramatically. This review work focuses on the latest advancements in C(sp²)-H and C(sp³)-H co-catalysed functionalisations, including some recent applications on enantioselective transformations.

Keywords: Alkynes; Allenes; Arene; C-H Activation; Cobalt-Catalysis

Introduction

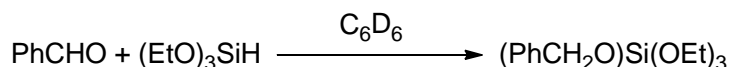
Chemistry has always had a significant influence on how we see the world and is frequently regarded as the foundational science. From comprehending the complex mechanistic pathways of biological processes to building new, novel materials with unparalleled functions, chemical science is one of the most vital topics in scientific research and technological advancement. This brief overview article will look at the latest advancements and state-of-the-art techniques in organometallic chemistry by using Co-catalysis to activate carbon chains in quinolone and pyridine-based nitrogen heterocycles using a range of C-H activation techniques. Direct functionalisation of a C-H bond is made possible by transition metal catalysis, which is beneficial because it does not require the traditional functional group manipulation technique. Because it enables the direct functionalisation of a C-H bond without depending on the traditional manipulation of the functional group approach, research on Co-catalysed C-H activation has expanded in the field of organic chemistry during the past few decades (Baccalini *et al.*, 2019).

A number of important, bioactive, and naturally occurring chemicals could be synthesised atom-by-atom and step-efficiently by identifying and functionalising a specific carbon-hydrogen bond inside a given molecule. Palladium, rhodium, ruthenium, and iridium were the 4d and 5d transition metals that dominated the area early in the history of C-H activation chemistry. As an alternative, creative techniques using inexpensive, widely available 3d metals have gained more popularity lately. They enable distinct patterns of selectivity and reactivity, which makes this idea intriguing from an environmental and financial standpoint. This notion is significant not only because of their peculiar electrical characteristics. Notwithstanding these advantages, there is still much to discover about novel first-row transition metal-based C-H activation techniques.

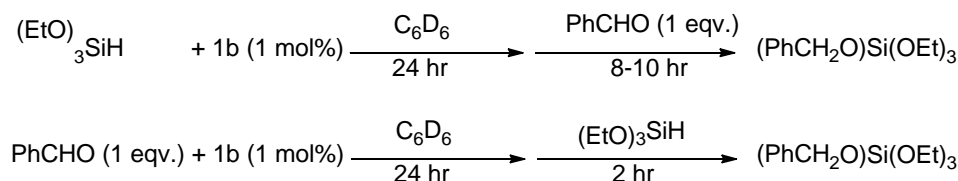
Converging Chemical and Biological Sciences for a Sustainable Era

Recent Developments

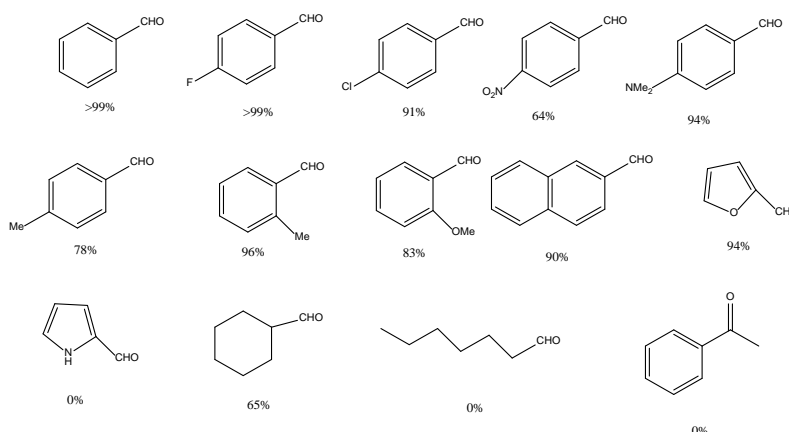
I. Catalytic activity for Hydrosilylation of aldehyde

**Figure 1: Catalytic Activity for Hydrosilylation of Aldehyde**

A more detailed examination of the open-system reaction at 50°C revealed that the hydrosilylation process (Figure 1) was completed in just 10 hours. The same conditions for substituting PhSiH₃ for (EtO)₃SiH resulted in a somewhat quicker catalytic reaction, converting PhCHO into several PhCH₂O-containing products in 8 hours. Despite the 24-hour duration of the hydrosilylation reaction, Ph₂SiH₂ was shown to be a successful silane for reducing PhCHO. However, with Et₃SiH, no hydrosilylation product was observed even after 48 hours (Li, Krause & Guan, 2018).

Proposed Reaction Mechanism**Figure 2: Mechanistic Considerations**

To find out which reactant-initiated catalyst activation, the author mixed 1b (cobalt POCOP pincer complex) with one reactant first (Figure 2) and let the mixture "age" for 24 hours under catalytic conditions before adding the second reactant. The time required to totally eradicate PhCHO was shown to be influenced by the additional sequence. The silane-first process took 8–10 hours to finish, which is comparable to the standard methodology that first mixes PhCHO and (EtO)₃SiH with catalyst 1b.

**Figure 3: Substrate Scope**

Cobalt-Catalyzed C(sp²)-H and C(sp³)-H Activation

In comparison, the aldehyde-first technique shortened the reaction time to two hours. By preactivating the catalyst, PhCHO preserved catalytic efficiency while enabling the hydrosilylation step to be finished in a closed system. Furthermore, we found that it only took two hours to fully decrease PhCHO and that refilling PhCHO and (EtO)₃SiH restarted the catalytic activity after the hydrosilylation reaction was completed. After repeating this process, the conversion rate rose to over 99% in less than two hours, yielding a 300 total turnover figure.

The authors also studied the substrate scope and obtained different yields in various products, which are shown in Figure 3.

II. C-H Activation by Insoluble Cationic (Bisphosphin) Cobalt (iii) mealocycle

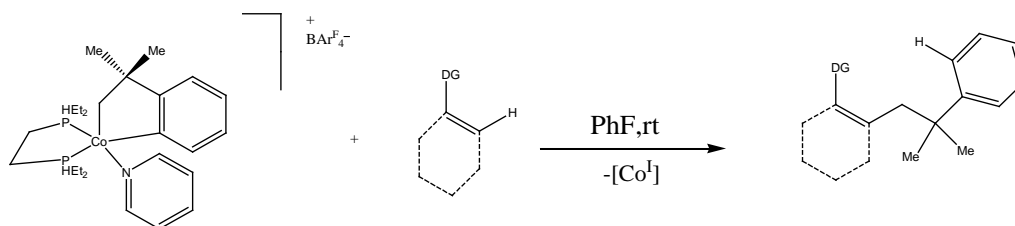


Figure 4: C-H Activation by Insoluble Cationic (Bisphosphin) Cobalt (iii) mealocycle

A variety of substrates with distinct coordinating groups and substitution patterns were used in the study (Figure 4) to investigate metallacycle-mediated C-H activation. Significant directed C(sp²)-H alkylation was typically the outcome of the reactions, which were carried out in fluorobenzene at room temperature. While 2'-bromoacetophenone demonstrated chemo selectivity favouring ortho-C-H over ortho-bromide, a ketone group quantitatively produced ortho-alkylated compounds.

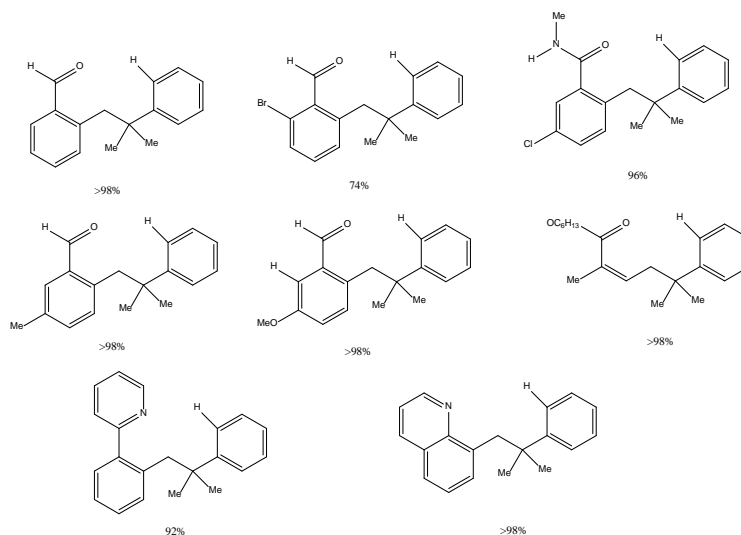


Figure 5: Substrate Scopes

Cobalt-Catalyzed C(sp²)-H and C(sp³)-H Activation

Steric issues regulated the site-selectivity of 3-chloro-N-methylbenzamide and 3-chloromethylacetophenone, favouring less hindered sites. The 6-position was where 3'-Methoxyacetophenone interacted most frequently, with just slight activation at the 2-position. Z-selective compounds were generated in great yield by hexyl methacrylate, which was consistent with known catalytic characteristics. Quinoline functionalised at the 8-position, suggesting compatibility with smaller chelate rings, and N-heterocycle-directed activation with 2-phenylpyridine and quinoline also showed efficacy. (Whitehurst *et al.*, 2022). Additionally, the authors examined the range of substrates and produced a variety of products with varying yields, as illustrated in Figure 5.

III. Regioselective C(sp³)-H Alkenylation of Thiamides

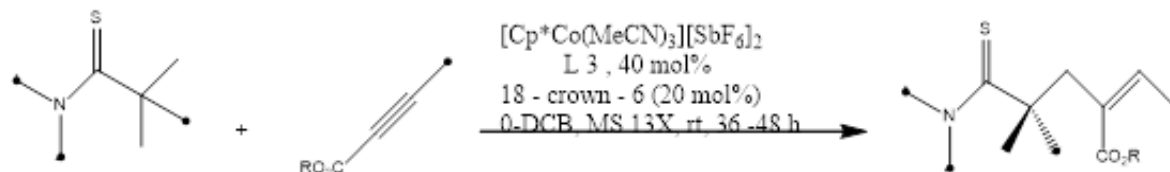


Figure 6: Regioselective C(sp³)-H Alkenylation of Thiamides

Under cobalt catalysis, the author investigated various coupling partners for C(sp³)-H activation (Figure 6) and discovered that methyl but-2-ynoate interacted well with thioamide 1a. Benzoic acid helped this reaction create alkenylated thioamide in a 63% yield with remarkable regioselectivity. We tested Fmoc-protected amino acids, such as alanine and trityl-protected asparagine, to achieve enantioselectivity, and the findings were encouraging, albeit small. Enantioselectivity was enhanced by subsequent testing using several amino acid derivatives, particularly L-alanine and L-tert-leucine-based catalysts; the most successful of these was L-tert-leucine derivative. The goal of additional optimisation was to improve these outcomes (Staronova *et al.*, 2023). Further, Figure 7 displays the various yields that the authors achieved from their investigation of the substrate scope.

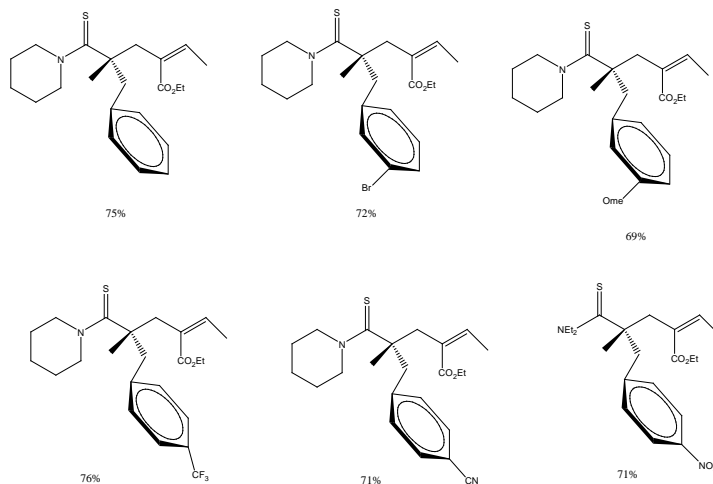
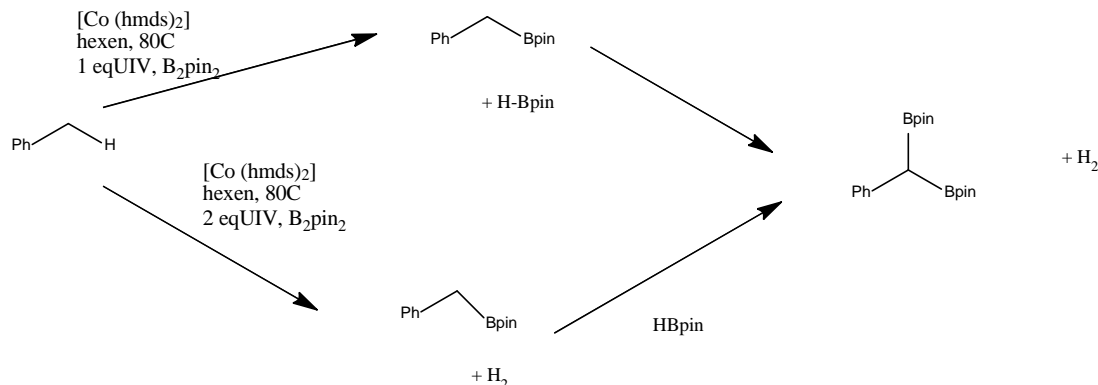
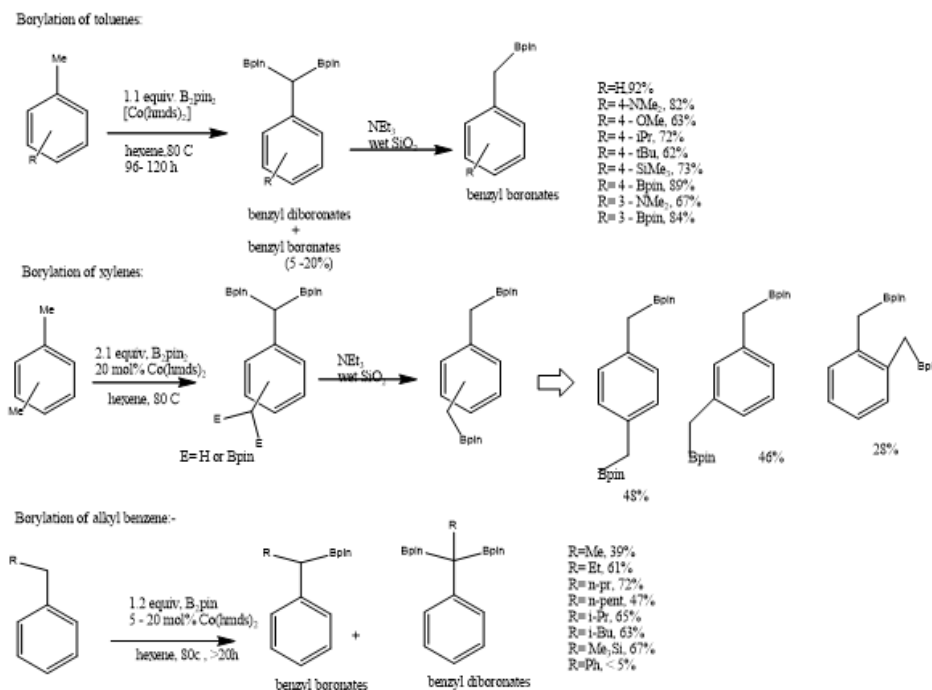


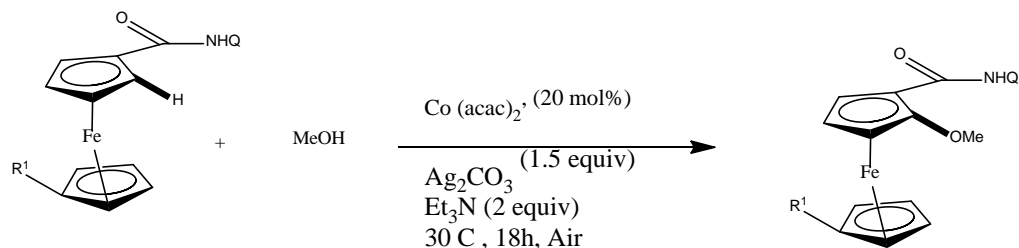
Figure 7: Substrate Scopes

Converging Chemical and Biological Sciences for a Sustainable Era

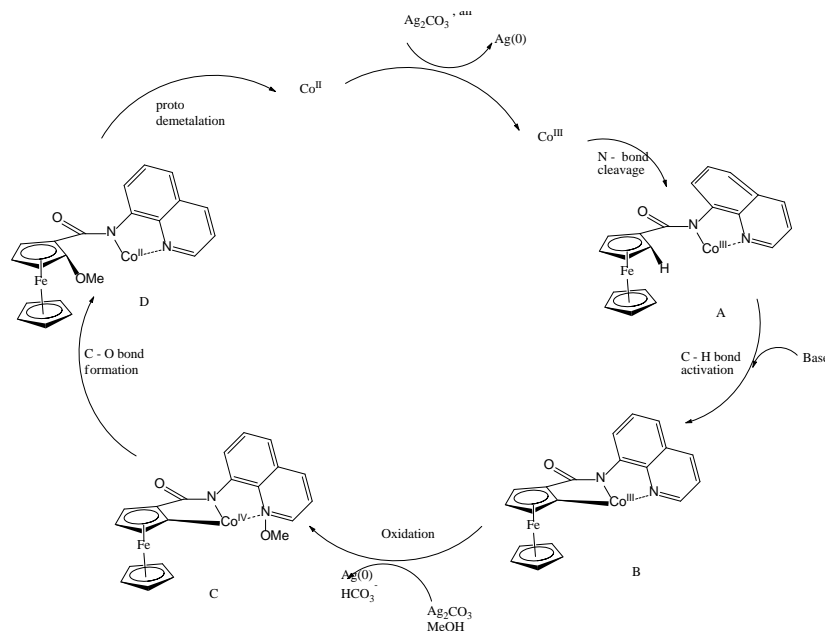
IV. Selective Benzylic C-H Borylation by Tandem Cobalt Catalysis:**Figure 8: Selective Benzylic C-H Borylation by Tandem Cobalt Catalysis**

The author used 5 mol% Co(hmnds)₂ to evaluate the reaction (Figure 8) between toluene and bis(pinacolato)diboron (B₂pin₂). This produced benzyl diboronate in n-hexane at 80°C with good conversion and great specificity for benzylic CH-borylation. Cobalt catalysts without the hmnds ligand were inactive, and Fe(hmnds)₂ produced results that were mild. Without the catalyst, no goods were produced (Ghosh *et al.*, 2021). Additionally, the different yields that the authors obtained from their examination of the substrate scope are shown in figure 9.

**Figure 9: Substrate Scopes**

V. Cobalt Catalysed C-H Alkoxylation:**Figure 10: Cobalt Catalysed C-H Alkoxylation**

With N-(quinolin-8-yl)ferrocene-1-carboxamide and MeOH, the reaction conditions (Figure 10) are optimised by employing Co(acac)₂ as a catalyst, Ag₂O as an oxidant, and NaHCO₃ as a base in MeOH at 40 °C. The yield from this original configuration was sixteen percent. After testing various bases, Et₃N turned out to be the most effective, raising the yield to 39%. After screening for several oxidants, Ag₂CO₃ increased the yield to 60%. The result was further enhanced to 66% by the use of methenamine. Et₃N was replaced by methenamine, which produced a 44% yield, suggesting that it might also be used as a base. The yield increased to 75% when the temperature was lowered to 30 °C. Other catalysts such as Ni(OAc)₂, Cu(OAc)₂, Co(PPh₃)Cl, and Co(OAc)₂·4H₂O did not work. Under these circumstances, other bidentate coordinating groups were unable to produce the intended results (Zhang *et al.*, 2021).

Proposed Reaction Mechanism**Figure 11: Mechanistic Constitutions**

Cobalt-Catalyzed C(sp²)-H and C(sp³)-H Activation

A Co(III)/Co(IV)/Co(II) mechanism for cobalt-catalysed C-H alkoxylation has been proposed by researchers (Figure 11). Ag₂CO₃ first oxidises Co(II) to Co(III), which subsequently interacts with ferrocene to activate the C-H bond via an irreversible CMD route, generating intermediate B. With the help of Ag₂CO₃, an alkyloxygen radical attacks Co(III), producing intermediate C. Following this, protodemetalation and the creation of C-O bonds result in the product formation and the regeneration of Co(II). Selective C-H alkoxylation of ferrocenes is made possible by the technique, which tolerates a variety of functional groups. According to mechanistic studies, the rate-limiting step is C-H bond activation, which most likely involves a Co(III)/Co(IV)/Co(II) cycle (Zhang *et al.*, 2021).

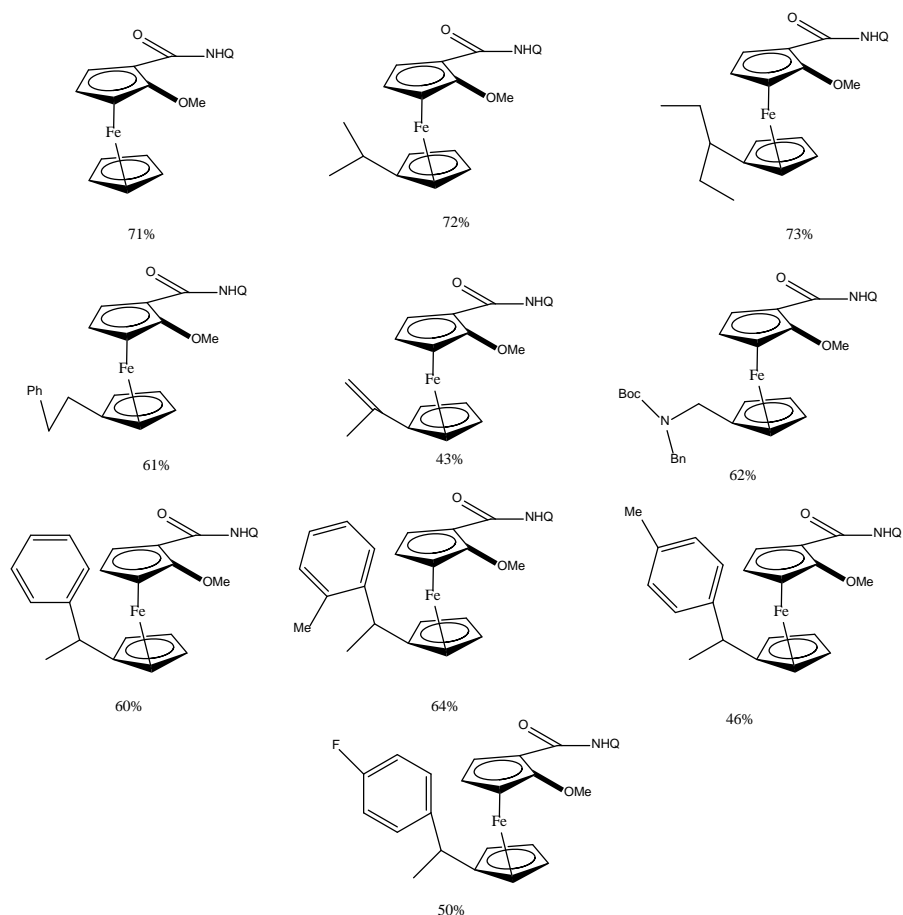
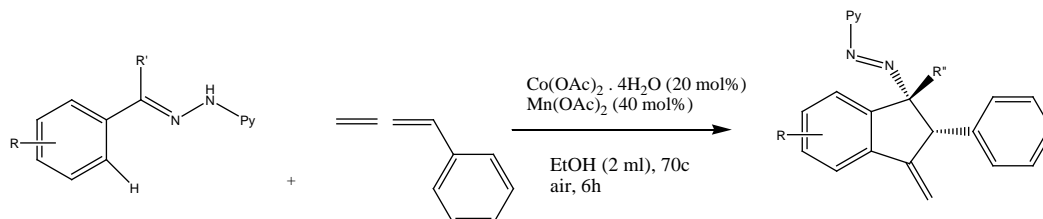
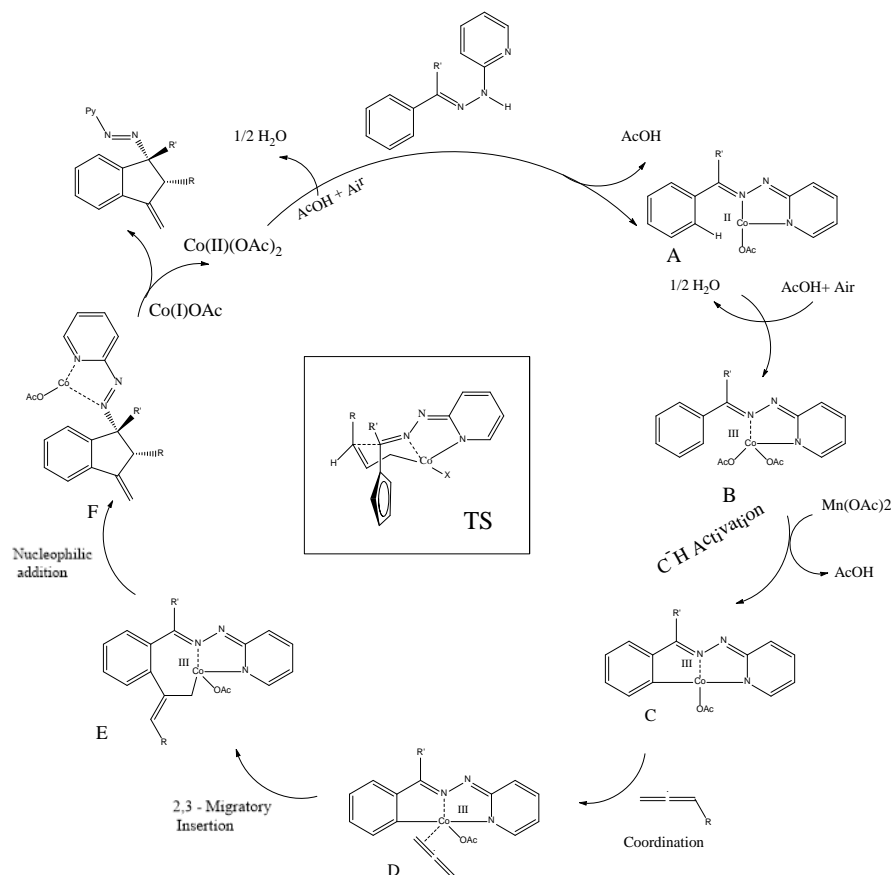


Figure 12: Substrates Scopes

Furthermore, figure 12 displays the various yields that the scientists were able to derive from their analysis of the substrate scope.

VI. Annulation with Allenes**Figure 13: Annulation with Allenes****Proposed Reaction Mechanism****Figure 14: Mechanistic Constituents**

The authors (Dey & Volla, 2021) screened the process by reacting phenyl allene with several substituted hydrazones (Figure 13). Consequently, indane derivatives with moderate to good yields were produced. The hydrazone derivative combines with a Co(II) catalyst to generate intermediate A, which initiates the suggested pathway (Figure 14).

Cobalt-Catalyzed C(sp²)-H and C(sp³)-H Activation

Complex C is the product of oxidation and a coordinated metalation deprotonation (CMD) process aided by Mn(OAc)₂. The allyl cobalt intermediate E, a σ-allyl complex, is produced by coordination with the allene and selective 2,3-migratory insertion of the less-substituted double bond. Using a six-membered cyclic transition state, this intermediate is intramolecularly nucleophilically added to the imine carbon to form intermediate F. Decomplexation yields the end product, and the catalytic cycle is completed by oxidising the Co(I) produced back to Co(II).

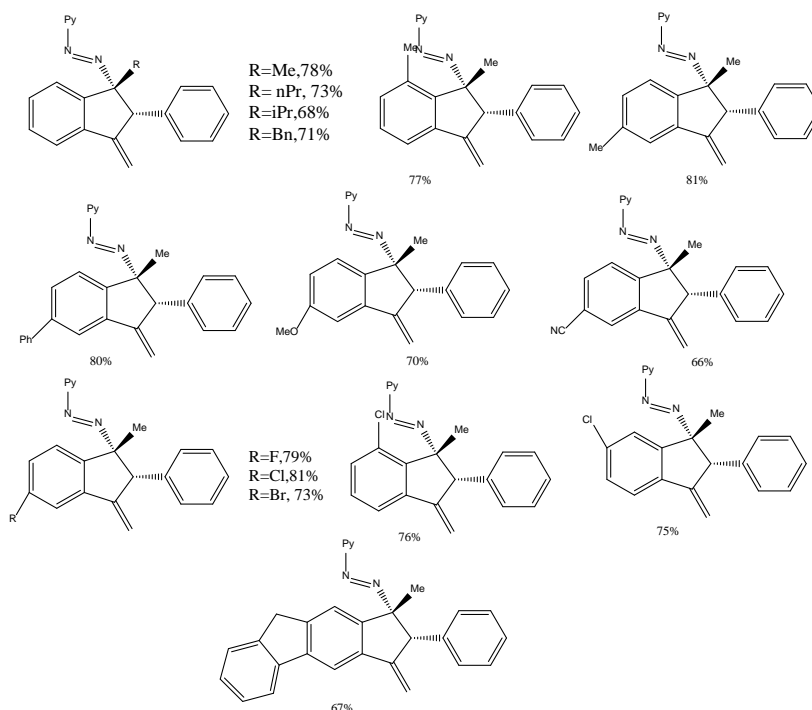


Figure 15: Substrates Scope

The authors experimented with the substrate shown in Figure 15 and obtained a range of yields.

VII. High Valent Cobalt Catalysed C-H Functionalisation

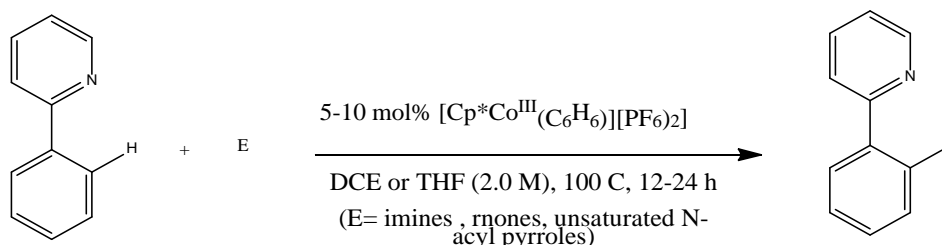


Figure 16: High Valent Cobalt Catalysed C-H Functionalisation

Converging Chemical and Biological Sciences for a Sustainable Era

Cobalt-Catalyzed C(sp²)-H and C(sp³)-H Activation

In 2013, scientists (Yoshino *et al.*, 2013) discovered a cationic compound, [Cp*CoIII(C₆H₆)](PF₆)₂ (Figure 16). With the help of this combination, 2-arylpyridines can be added nucleophilically to N-sulfonylimines and enones as polar electrophiles without the use of extraneous chemicals. Other Co(III) complexes with less packed or sterically more hindered groups on the cyclopentadiene ring were found to be less effective.

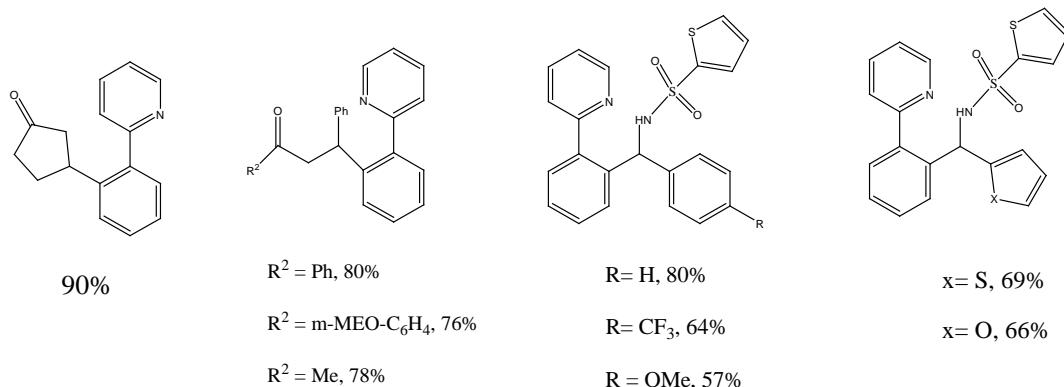


Figure 17: Substrates Scopes

Under the ideal circumstances, moderate to high yields were attained with good compatibility across functional groups, such as ether, amino, acetyl, and halogen groups. Additionally, α , β -unsaturated N-acyl pyrroles were used as ester and amide surrogates to generate Michael adducts. The C-H functionalisation is most likely to take place by electrophilic aromatic substitution or a CMD process in order to create the Cp*Co(III) intermediate. Electrophile coordination and insertion lead to protodemetalation, which regenerates cyclo-metalated Co(III) and produces the equivalent product (Yoshino *et al.*, 2013). The authors experimented with the substrate shown in Figure 17 and obtained a range of yields.

VIII. Asymmetric C-H Amidation of Ferrocenes

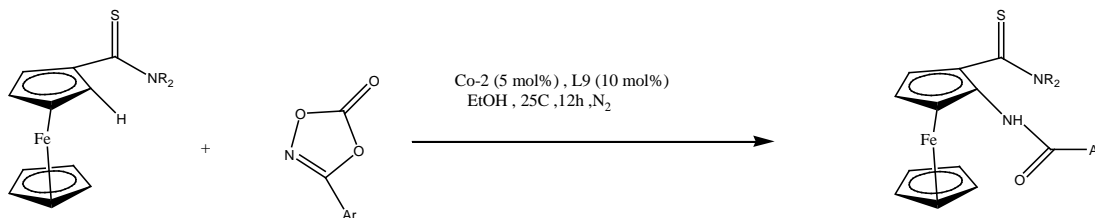


Figure 18: Asymmetric C-H Amidation of Ferrocenes

Planarly chiral ferrocene derivatives have been preferred as ligands or catalysts in asymmetric catalysis (Figure 18). In 2019, the Shi group created a new chiral monoprotected amino acid (MPAA) ligand to achieve the asymmetric amine modification of ferrocene thioamides with dioxazolones. The planar chiral amidated compounds showed moderate enantioselectivity (36%–55% ee) and good yields (48%–97%). Additionally, the

Cobalt-Catalyzed C(sp²)-H and C(sp³)-H Activation

enantiomeric purity could be raised to >99% ee with a single crystallisation (Zheng *et al.*, 2022).

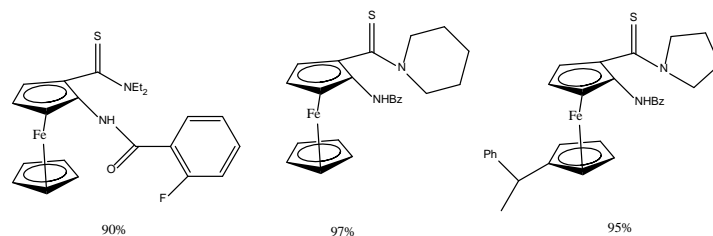


Figure 19: Substrate Scopes

Using different substrates, the authors experimented and got a variety of products with high yields, as depicted in Figure 19.

IX. Chiral Carboxylic Acid Assisted Enantioselective C-H Activation

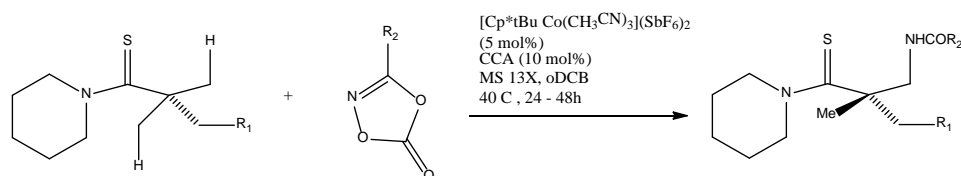


Figure 20: Chiral Carboxylic Acid Assisted Enantioselective C-H Activation

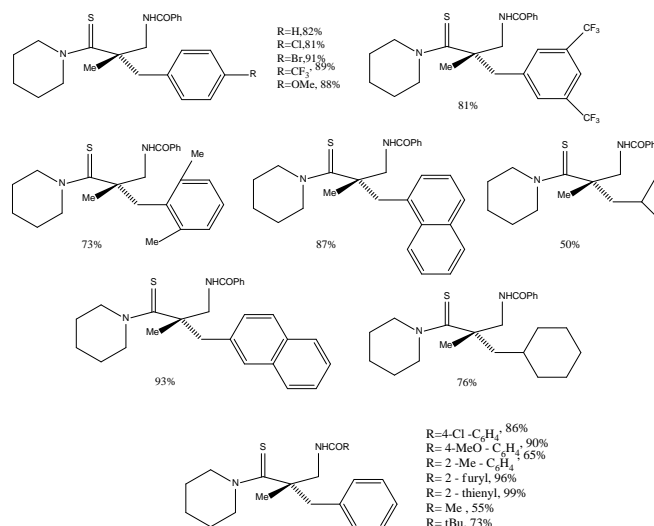


Figure 21: Substrate Scopes

An enantioselective C(sp³)-H amidation of thioamides is described (Figure 20) using the Cp*^tBu-Co(III) catalyst and amino acid ligands. Imide-protected α-amino acids were chosen because they are simple to synthesise and function well as ligands for transition-metal catalysts. The enantioselectivity was greatly enhanced by the sterically hindered imide

Cobalt-Catalyzed C(sp²)-H and C(sp³)-H Activation

moiety, which provided steric bulk without connecting to the metal centre. The optimal choice was determined to be C, with a maximum chiral ligand ratio of 94:6. By producing amines, amides, and aldehydes from their byproducts, gram-scale reactions demonstrated potential for practical synthetic uses (Yoshino & Matsunaga, 2021). The authors also studied many substrates as described in the above substrate scope (Figure 21) and obtained the products with decent yields.

X. Cobalt (III) Catalysed C-H Activation

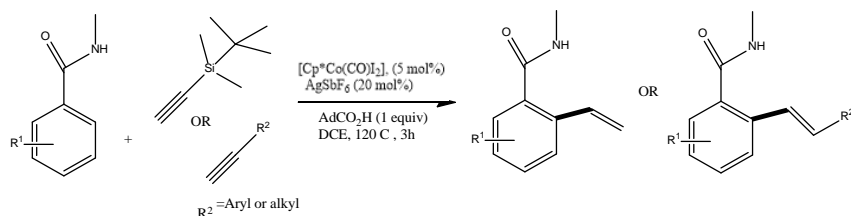


Figure 22: Cobalt (III) Catalysed C-H Activation

In 2018, Muniraj and Prabhu synthesised vinylated products from various 4-Me, 3-Me, and 4-OMe substituted N-methyl benzamides by reacting benzamides with alkynes and silyl-alkynes (Figure 22). Vinylation only occurred at the ortho position for 3-Me-substituted benzamide. Additionally, three compounds (with yields ranging from 50% to 56%) were extracted from halogenated N-methylbenzamides. Additionally, a 53% yield of N-methyl-4-vinyl benzamide was generated. Ortho-substituted benzamide produced a trace amount of product due to steric hindrance. Additionally, the yields of the amide made from thiophene were low (36%). Unreacted N-methyl benzamide was recovered in every instance. Even terminal alkynes, such as 1-pentyne and phenylacetylene, produced alkenylated compounds with yields of 60% to 68% (Muniraj & Prabhu, 2018).

Proposed Reaction Mechanism

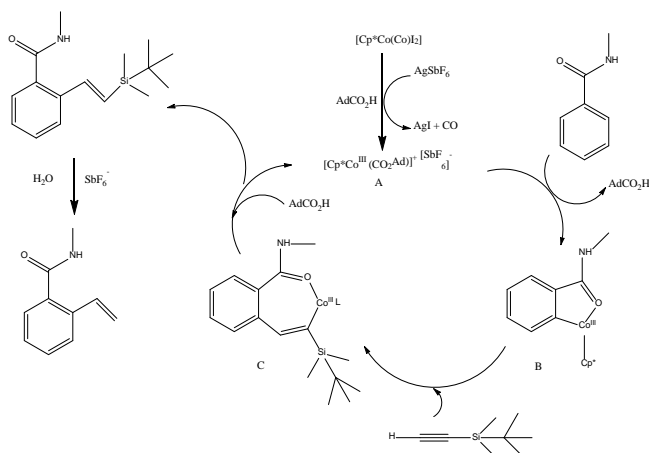


Figure 23: Mechanistic Constituents

Cobalt-Catalyzed C(sp²)-H and C(sp³)-H Activation

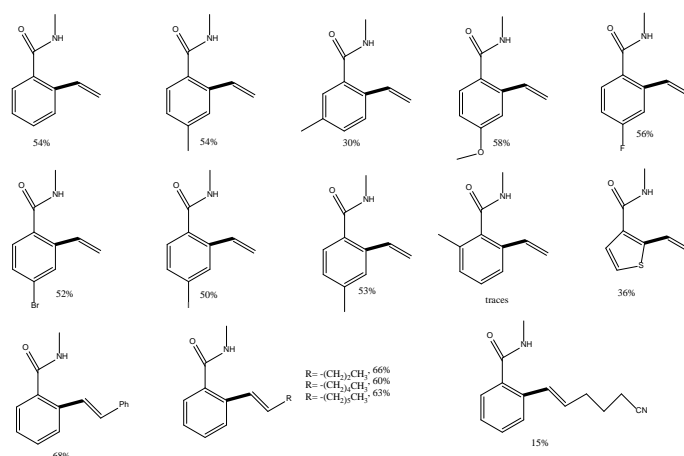


Figure 24: Substrate Scopes

Based on previous studies and control trials, a proposed procedure (Figure 23) is depicted for the production of catalytically active species-A. A interacts with the amide to form cobaltacycle-B. After that, intermediate C is created by inserting the alkyne. AdCO₂H promoted the protodemetalization of C, which yielded vinylsilane and regenerated catalyst A. When SbF₆ is present, desilylation eventually yielded the final product. The authors' research yielded varied results using the substrate shown in Figure 24.

XI. Functionalisation Catalysed by Simple, Low Valent Co Complex

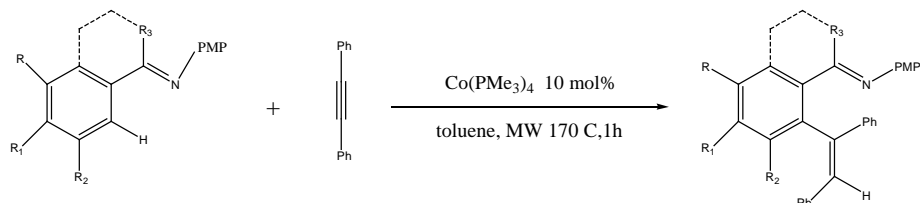


Figure 25: Functionalisation Catalysed by Simple, Low Valent Co Complex

Fallon and coworkers (2015) investigated the hydroarylation process using diphenylacetylene and a variety of imines in this work (Figure 25). With para-substituted imines, the reaction demonstrated high yields while tolerating neutral, electron-withdrawing, and electron-donating (like OMe) groups. Standard yields were replicated by gram-scale synthesis. Because of a secondary directing effect seen in cobalt, ruthenium, and iridium catalysis, substrates with methoxy, fluoro, and cyano groups favoured the more hindered ortho position, whereas substrates with meta-methyl substitutions selected the less hindered ortho position. Notably, imines made from tetralone, propiophenone, and 2-acetonaphthone also successfully produced the required molecules (Fallon *et al.*, 2015).

For both catalysts, the catalytic cycle shown in Figure 26 entails ligand exchange to create intermediate (I), which is then followed by a hydrogen transfer to create intermediate (II). Intermediate (III) is formed by subsequent reductive elimination, and the observed anti-

Cobalt-Catalyzed C(sp²)-H and C(sp³)-H Activation

selectivity is explained by isomerisation. The importance of cobalt in double bond isomerisation is demonstrated by the reported iridium-catalysed ketone addition, which results in 55% isomerisation to the anti-product. However, because ketones have weaker anchoring effects than imines, this process is less effective.

Proposed Reaction Mechanism

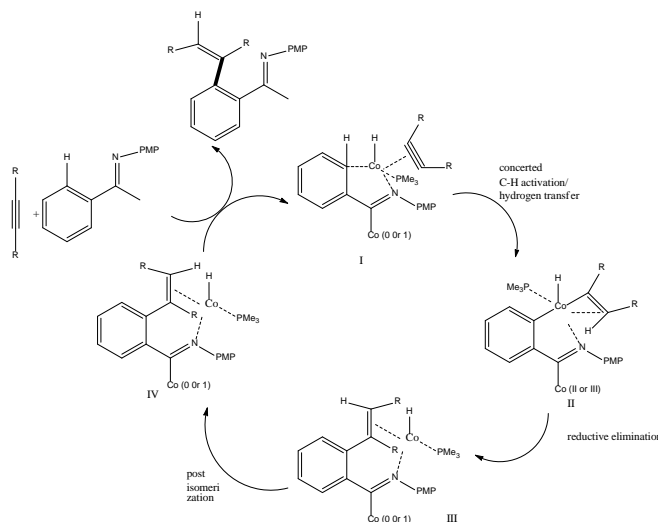


Figure 26: Mechanistic Constitutions

Conclusion

By emphasising the transformative impacts of co-catalysis on society and its numerous applications in C-H bond activation processes, this book chapter provides an insight into the most recent advancements in organometallic chemistry. These results may undoubtedly be applied to other heterocycle derivatives to promote further investigation and collaboration, which will deepen our grasp of the myriad possibilities in cobalt chemistry. This might be accomplished by looking at the developments of the past decade as well as the future paths of a number of sub-disciplines.

Acknowledgment

The teacher-in-charge of Maharaja Manindra Chandra College, who provided office space and internet access, is acknowledged by the author. The author also thanks his coworkers in the Maharaja Manindra Chandra College Chemistry Department for their unwavering support.

References

Baccalini, A., Vergura, S., Dolui, P., Zandoni, G., & Maiti, D. (2019). Recent advances in cobalt-catalysed C-H functionalizations. *Organic & Biomolecular Chemistry*, 17(48), 10119–10141. <https://doi.org/10.1039/c9ob01994d>

Cobalt-Catalyzed C(sp²)-H and C(sp³)-H Activation

- Dey, A., & Volla, C. M. R. (2021). Cobalt-Catalyzed C–H Activation and [3 + 2] Annulation with Allenes: Diastereoselective Synthesis of Indane Derivatives. *Organic Letters*, 23(13), 5018–5023. <https://doi.org/10.1021/acs.orglett.1c01521>
- Fallon, B. J., Derat, E., Amatore, M., Aubert, C., Chemla, F., Ferreira, F., Perez-Luna, A., & Petit, M. (2015). C–H Activation/Functionalization Catalyzed by Simple, Well-Defined Low-Valent Cobalt Complexes. *Journal of the American Chemical Society*, 137(7), 2448–2451. <https://doi.org/10.1021/ja512728f>
- Ghosh, P., Schoch, R., Bauer, M., & Von Wangelin, A. J. (2021). Selective Benzylic CH-Borylations by Tandem Cobalt Catalysis. *Angewandte Chemie*, 61(1). <https://doi.org/10.1002/anie.202110821>
- Li, Y., Krause, J. A., & Guan, H. (2018). Cobalt POCOP Pincer Complexes via Ligand C–H Bond Activation with Co₂(CO)₈: Catalytic Activity for Hydrosilylation of Aldehydes in an Open vs a Closed System. *Organometallics*, 37(13), 2147–2158. <https://doi.org/10.1021/acs.organomet.8b00273>
- Muniraj, N., & Prabhu, K. R. (2018). Cobalt(III)-Catalyzed C–H Activation: Counter Anion Triggered Desilylative Direct ortho-Vinylation of Secondary Benzamides. *Advanced Synthesis & Catalysis*, 360(18), 3579–3584. <https://doi.org/10.1002/adsc.201800649>
- Staronova, L., Yamazaki, K., Xu, X., Shi, H., Bickelhaupt, F. M., Hamlin, T. A., & Dixon, D. J. (2023). Cobalt-Catalyzed Enantio- and Regioselective C(sp³)-H Alkenylation of Thioamides. *Angewandte Chemie*. <https://doi.org/10.1002/ange.202316021>
- Whitehurst, W. G., Kim, J., Koenig, S. G., & Chirik, P. J. (2022). C–H Activation by Isolable Cationic Bis(phosphine) Cobalt(III) Metallacycles. *Journal of the American Chemical Society*, 144(41), 19186–19195. <https://doi.org/10.1021/jacs.2c08865>
- Yoshino, T., & Matsunaga, S. (2021). Chiral Carboxylic Acid Assisted Enantioselective C–H Activation with Achiral CpxM^{III} (M = Co, Rh, Ir) Catalysts. *ACS Catalysis*, 11(11), 6455–6466. <https://doi.org/10.1021/acscatal.1c01351>
- Yoshino, T., Ikemoto, H., Matsunaga, S., & Kanai, M. (2013). CP*CO_{III}-Catalyzed C2-Selective addition of indoles to imines. *Chemistry - a European Journal*, 19(28), 9142–9146. <https://doi.org/10.1002/chem.201301505>
- Zhang, Z., Cheng, J., Yao, Q., Yue, Q., & Zhou, G. (2021). Cobalt-Catalyzed C–H Alkoxylation of Ferrocenes with Alcohols under Mild Conditions. *Advanced Synthesis & Catalysis*, 363(16), 3946–3951. <https://doi.org/10.1002/adsc.202100423>
- Zheng, Y., Zheng, C., Gu, Q., & You, S. L. (2022). Enantioselective C–H functionalization reactions enabled by cobalt catalysis. *Chem Catalysis*, 2(11), 2965–2985. <https://doi.org/10.1016/j.checat.2022.08.020>

Published by :



ISO 9001:2015 Certified

e ISBN 978-967-2819-49-3



ISBN 978-967-2819-48-6



www.lucp.net